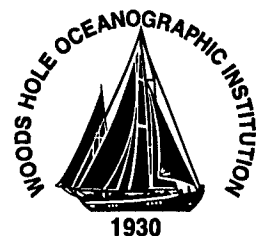


**Massachusetts Institute of Technology
Woods Hole Oceanographic Institution**



**Joint Program
in Oceanography/
Applied Ocean Science
and Engineering**



DOCTORAL DISSERTATION

Chemical Characterization of
Dissolved Organic Matter (DOM) in Seawater:
Structure, Cycling, and the Role of Biology

by

Tracy M. Quan

February 2005

DISTRIBUTION STATEMENT A
Approved for Public Release
Distribution Unlimited

20050627 089

MIT/WHOI

2005-05

**Chemical Characterization of Dissolved Organic Matter (DOM) in Seawater:
Structure, Cycling, and the Role of Biology**

by

Tracy M. Quan

Massachusetts Institute of Technology
Cambridge, Massachusetts 02139

and

Woods Hole Oceanographic Institution
Woods Hole, Massachusetts 02543

February 2005


DOCTORAL DISSERTATION

Funding was provided by the National Science Foundation (OCE-9818654) and the Department of Energy (DEFG0200ERG62999). Support was also provided by a National Science Foundation Graduate Student Fellowship.

Reproduction in whole or in part is permitted for any purpose of the United States Government. This thesis should be cited as: Tracy M. Quan, 2004. Chemical Characterization of Dissolved Organic Matter (DOM) in Seawater: Structure, Cycling, and the Role of Biology. Ph.D. Thesis. MIT/WHOI, 2005-05.

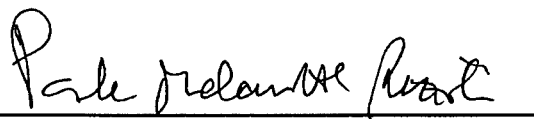
Approved for publication; distribution unlimited.

Approved for Distribution:

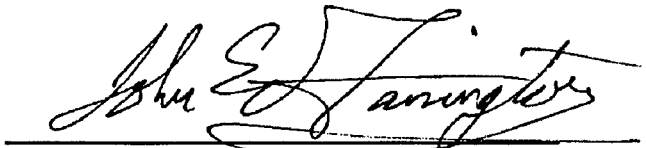


Ken O. Buesseler, Chair

Department of Marine Chemistry and Geochemistry



Paola Malanotte-Rizzoli
MIT Director of Joint Program



John W. Farrington
WHOI Dean of Graduate Studies

**Chemical Characterization of Dissolved Organic Matter (DOM) in Seawater:
Structure, Cycling, and the Role of Biology**

by

Tracy M. Quan

B. S. Chemistry with a Specialization in Earth Science,
University of California, San Diego
(1999)


submitted in partial fulfillment of the requirements for the degree of
Doctor of Philosophy

at the
MASSACHUSETTS INSTITUTE OF TECHNOLOGY
and the
WOODS HOLE OCEANOGRAPHIC INSTITUTION

February, 2005

© Tracy M. Quan, 2005. All rights reserved.

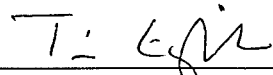
The author hereby grants to MIT and WHOI permission to reproduce paper and electronic copies of this thesis in whole or in part and to distribute them publicly.

Signature of Author: 

Department of Earth, Atmosphere and Planetary Sciences,
Massachusetts Institute of Technology and the Joint Program
in Oceanography, Massachusetts Institute of Technology/Woods
Hole Oceanographic Institution, January 28, 2004.

Certified by 

Daniel J. Repeta
Thesis Supervisor

Accepted by 

Timothy I. Eglinton
Chairman, Joint Committee for Chemical Oceanography,
Massachusetts Institute of Technology/Woods Hole
Oceanographic Institution

Chemical Characterization of Dissolved Organic Matter (DOM) in Seawater: Structure, Cycling, and the Role of Biology

By

Tracy M. Quan

Submitted to the MIT/WHOI Joint Program in Oceanography on January 28, 2005, in partial fulfillment of the requirements for the degree of Doctor of Philosophy in the field of Chemical Oceanography

Abstract

The goal of this thesis is to investigate three different areas relating to the characterization of dissolved organic matter (DOM): further determination of the chemical compounds present in high molecular weight DOM (HMWDOM), the cycling of individual compounds within the HMWDOM pool, and the biological controls on DOM release.

The first section of this thesis provided additional molecular level characterization of HMWDOM. While some individual components have been identified, the total yield of compounds isolated is much smaller than the amount expected by spectroscopic analysis by nuclear magnetic resonance (NMR) spectroscopy. Since the majority of the as-yet unidentified carbon was inferred to be carbohydrate, periodate over-oxidation was used to analyze this fraction. Analysis of both surface and deep water HMWDOM samples indicated that the majority of the carbon present was periodate over-oxidizable, including 70% of the aliphatic NMR signal. Comparison of the periodate demand for HMWDOM versus that for linear glucopolysaccharide standards indicated that HMWDOM had a greater degree of branching. Based on the changes in the ^1H NMR spectra during the reaction, it was concluded that 6-deoxysugars were the primary compounds in the unidentified fraction of HMWDOM.

Compound specific radiocarbon analysis can provide information about the cycling and relative ages for individual HMWDOM components. In the second section of this thesis, a new method was presented for the purification of individual underivatized amino acids hydrolyzed from HMWDOM. This new separation protocol utilized various chromatographic techniques, including cation exchange chromatography and high-pressure liquid chromatography (HPLC) using C18 and strong cation exchange (SCX) columns. Six amino acids were isolated from a HMWDOM sample with sufficient purity and quantity for radiocarbon analysis. These amino acids had a range of $\Delta^{14}\text{C}$ values, from 121‰ to -454‰.

The final section investigates biological controls on the dissolved organic nitrogen (DON) pool. Total hydrolyzable amino acids (THAA), and nucleic acids were measured for four incubations: a control incubation, a grazer added incubation, a zero virus incubation, and a 10 times virus incubation. Comparison to the control showed THAA and nucleic acid release were influenced by viruses but not grazers.

Thesis Supervisor: Daniel J. Repeta

Acknowledgements

Nothing exists except atoms and empty space; everything else is opinion.
– Democritus of Abdera

What it takes is time and perseverance,
With a little luck along the way...
The art of making art
Is putting it together.
– Stephen Sondheim

This thesis is not only a summation of my research, but a testament to all of the help and encouragement I have received from so many people. My most fervent thanks go to my thesis advisor, Dan Repeta, without whose support, chemical intuition, and firm encouragement this thesis would never have been finished. I would also like to thank my thesis committee members Tim Eglinton and Phil Gschwend for their input into this thesis and their confidence that it would turn out well. I am also grateful to Jeff Seewald, for chairing my defense.

I received chemical and instrumental assistance from so many people, most especially Carl Johnson, Daniel Montluçon, Chris Reddy, Jim Moffett, Lucinda Gathercole, Emma Teuten, Ben Van Mooy, Bruce Tripp, and Ann McNichol and the entire NOSAMS group. Thanks also go to the DOMINOS experiment collaborators, especially Deborah Bronk, Deborah Steinberg, Eric Wommack, and Craig Carlson. I am grateful to all of the students, post-docs, scientists and staff I have met and interacted with over the years, as they have taught me so much about science and life in general. Extra special thanks go to Linda Kalnejais, Helen White, Rachel Wisniewski, Rachel Stanley, Nick Drenzek, Gesine Mollenhauer, Sheri Simmons, Astri Kvassnes, Anna Cruse, and Ana Lima, for all of the laughs, tears, and chocolate cravings. I am also indebted to the MIT/WHOI Joint Program and the Academic Programs Office, for doing all of the little and big things to make the graduate school experience easier.

Lots of thanks also go to my best friend, Lauren Fischer Merlo, whose encouragement and emotional support spanned the many miles between us, and who never got mad at me for my tardiness in answering emails. Finally, I would like to thank my family for all of their love and faith in me, especially my parents and my sister Erin, who handled all crises with patience, understanding, and good humor, and who were always willing to lend a hand despite the distance.

I would like to dedicate this thesis to my late grandfathers, William Dea and Wilbur Quan, who always wanted a doctor in the family.

Funding for this research was provided by the National Science Foundation (OCE-9818654) and the Department of Energy (DEFG0200ERG62999). Student support was also provided by a National Science Foundation Graduate Student Fellowship.

TABLE OF CONTENTS

TABLE OF FIGURES	8
TABLE OF TABLES.....	11
1. INTRODUCTION.....	13
1.1 BACKGROUND INFORMATION.....	13
1.2 THE COMPOSITION OF HMWDOM.....	16
1.3 HMWDOM CYCLING VIA COMPOUND SPECIFIC RADIOCARBON MEASUREMENTS	19
1.4 DYNAMICS OF NITROGEN IN A BIOLOGICALLY COMPLEX SYSTEM	23
1.5 THE GOALS OF THE THESIS	26
1.6 REFERENCES	27
2. CHARACTERIZATION OF HIGH MOLECULAR WEIGHT DISSOLVED ORGANIC MATTER USING PERIODATE OVER-OXIDATION.....	33
2.1 INTRODUCTION	33
2.2.1 <i>Background</i>	33
2.2.2 <i>Characterization of the Unknown Fraction of HMWDOM Using NMR Spectroscopy</i>	34
2.2.3 <i>Introduction to Periodate Over-Oxidation</i>	38
2.2 MATERIALS AND METHODS.....	41
2.2.1 <i>Sample Location and Collection</i>	41
2.2.2 <i>Analyses</i>	42
2.2.3 <i>Periodate Over-Oxidation</i>	43
2.2.3.1 Standards and Samples	44
2.2.3.2 Periodate Over-Oxidation Method	44
2.2.4 <i>Molecular Analyses</i>	47
2.2.4.1 Monosaccharide Analysis.....	47
2.2.4.2 Lipid Analysis.....	48
2.3 RESULTS.....	48
2.3.1 <i>Ancillary Data</i>	48
2.3.2 <i>Periodate Over-Oxidation Data</i>	50
2.3.2.1 Carbohydrate and Amino Acid Standards	50
2.3.2.2 HMWDOM Data	52
2.3.2.3 Lipid Analysis	60
2.3.2.4 Octyl- β -glucopyranoside Oxidation.....	61
2.4 DISCUSSION	61
2.5 CONCLUSION.....	75
2.6 REFERENCES	77
3. RADIOCARBON ANALYSIS OF INDIVIDUAL AMINO ACIDS ISOLATED FROM MARINE HIGH MOLECULAR WEIGHT DISSOLVED ORGANIC MATTER.....	81
3.1 INTRODUCTION	81
3.2 MATERIALS AND METHODS.....	86
3.2.1 <i>Sample Location and Collection</i>	86
3.2.2 <i>Analytical Protocols</i>	87
3.2.1 <i>Standards</i>	87
3.2.2 <i>Amino Acid Isolation and Purification</i>	88
3.2.2.1 Hydrolysis and Column Chromatography	88
3.2.2.2 OPA Analysis.....	90
3.2.2.3 C18 HPLC Separation	91
3.2.2.4 Strong Cation Exchange HPLC Separation	92
3.2.2.5 Radiocarbon Sample Preparation	93
3.2.2.6 Accelerator Mass Spectrometry (AMS).....	98
3.3 RESULTS.....	99
3.3.1 <i>Ancillary Data</i>	99
3.3.2 <i>Hydrolysis and Resin Column Results</i>	101
3.3.3 <i>C18 HPLC results</i>	104

3.3.4	<i>SCX HPLC Results</i>	111
3.3.5	<i>Radiocarbon Analyses</i>	124
3.4	DISCUSSION	130
3.5	CONCLUSION	142
3.6	REFERENCES	146
4.	THE INFLUENCE OF VIRUSES AND GRAZERS ON AMINO ACID AND NUCLEIC ACID RELEASE	151
4.1	INTRODUCTION	151
4.2	METHODS	156
4.2.1	<i>Sample Collection and Incubation</i>	156
4.2.2	<i>Amino Acid Analysis</i>	158
4.2.3	<i>Nucleic Acid Analysis</i>	161
4.3	RESULTS AND DISCUSSION	165
4.3.1	<i>Ancillary Data</i>	165
4.3.2	<i>Amino Acid Results</i>	172
4.3.3	<i>Nucleic Acid Measurements</i>	186
4.4	CONCLUSIONS	193
4.5	REFERENCES	195
5.	CONCLUSIONS	201
5.1	GENERAL CONCLUSIONS	201
5.2	FUTURE RESEARCH DIRECTIONS	204
5.3	REFERENCES	211

TABLE OF FIGURES

Chapter 1

Figure 1.1 DOC concentration with depth for the Eastern North Pacific Ocean. Data reported by Loh and Bauer, 2000. 14

Figure 1.2 ^1H NMR (A) and ^{13}C NMR (B) spectra for surface HMWDOM, showing the presence of carbohydrate, acetate, and aliphatic functional groups 17

Figure 1.3 $\Delta^{14}\text{C}$ values for DIC (solid circles), DOC (solid diamonds), HMWDOC (open triangles) and neutral sugars isolated from HMWDOC (open squares). All samples were obtained from the North Central Pacific except for the neutral sugars, which were collected from the Mid-Atlantic Bight. DOC and DIC data reported by Druffel et al, 1992; HMWDOC data by Loh et al., 2004, and neutral sugars by Aluwihare et al., 2002. 20

Chapter 2

Figure 2.1 Mathematical analysis of the unknown fraction of HMWDOM, starting with the total solid state ^{13}C NMR spectra of surface seawater HMWDOM(A). The peak areas were translated to a normalized histogram (B), and the previously isolated molecular components were sequentially subtracted. The histograms represent the carbon remaining after subtraction of monosaccharides (C), acetate (D), hexoseamines (E), and amino acids (F). The remaining peak areas in part F represent the as yet unidentified fraction. 35

Figure 2.2 The reaction mechanism for periodate oxidation of a glucose monomer (A) and for the over-oxidation of a polysaccharide (B). The activated hydrogen circled in part B step 2 is converted for the $-\text{OH}$ functional group marked by a square. 39

Figure 2.3 Solid state ^{13}C NMR for surface water H0200 HMWDOM sample. The functional group assignments for each peak are also marked. 54

Figure 2.4 Series of ^1H NMR spectra of the periodate over-oxidation of H0200D surface HMWDOM. The initial spectrum (A) was taken before the addition of periodate. The other spectra were taken from subsamples of the oxidation reaction after 1 hour (B), 2 days (C), and after 10 days (D). 56

Figure 2.5 Excerpts from the ^1H NMR spectra of the periodate over-oxidation of H995200 deep water HMWDOM. The initial spectrum (A) was taken before the addition of periodate. Spectrum B was taken after 9 days of oxidation. 57

Figure 2.6 Histograms of the change in ^1H functional group peak areas over the course of the H0200D oxidation (A) and the H995200 oxidation (B). 58

Figure 2.7 Percent change relative to the initial values for the functional groups present in H0200D (A) and H995200 (B) during the course of periodate oxidation.59

Figure 2.8 The ^1H NMR of the methylene chloride extracted fraction of the H0200D sample reaction solution after the completion of the over-oxidation reaction.60

Chapter 3

Figure 3.1 Schematic representation of the purification protocol used to isolate amino acids for radiocarbon analysis.89

Figure 3.2 Proton NMR spectra for the unhydrolyzed H0200 sample (A), the hydrolyzed sample (B) and the hydrolyzed amino acid fraction collected from the AG-50W cation exchange resin (C). In all spectra, the water peak is at 4.8 ppm.103

Figure 3.3 Chromatograms for the C18 HPLC procedure for A: 15 amino acid standard, B: H0200 amino acid fraction. The amino acids are labeled in part A. The 12 collected fractions are marked on both chromatograms.105

Figure 3.4 Proton NMR spectrum of C18 HPLC collected vial 12 from H0200 sample (A) and a standard phenylalanine spectrum (B). The peak at 4.8 ppm in both spectra is assigned to water, and the peak at 2.0 ppm in part A is acetonitrile. Small shifts in H0200 peaks relative to the standard are due to the fact that the H0200 sample was not neutralized prior to NMR acquisition.107

Figure 3.5 ^1H NMR spectra of the amino acid fractions collected during the C18 purification of H0200 HMWDOM. With the exception of fraction 4, none of the subsamples were neutralized prior to NMR spectroscopy, which results in the shifting of some peaks relative to standard spectra. Peak at 4.8 ppm in all spectra is assigned to water.108

Figure 3.6 SCX HPLC chromatogram for a phenylalanine standard (A), and the H0200 C18 vial 12 (B). Previous NMR spectra of fraction 12 showed the presence of phenylalanine (shaded area) along with some contamination. The peaks at 5 min and 12 min in the fraction 12 chromatogram are solvent peaks.113

Figure 3.7 Proton NMR spectrum of the phenylalanine peak collected from the SCX HPLC column (A), and the phenylalanine standard spectrum (B). The peak at 4.8 ppm corresponds to water, while the peaks at 3.2 ppm and 1.9 ppm in A correspond to methanol and acetonitrile, respectively.115

Figure 3.8 ^1H NMR spectra for the collected peaks from the SCX HPLC procedure. Collected fractions that did not contain any functional groups other than water and methanol are not included in this figure. Small shifts in peaks relative to amino acid standards may be seen due to the presence of SCX buffer salts in the samples. In all

spectra, the water peak is at 4.8 ppm, and methanol present at 3.2 ppm. A list of the NMR spectra shown can be found in Table 3.4.....117

Figure 3.9 $\Delta^{14}\text{C}$ versus $\delta^{13}\text{C}$ for the albumin bulk and amino acid samples. Leucine samples are replicate CO_2 submissions of a sample split before combustion.....128

Figure 3.10 $\Delta^{14}\text{C}$ versus $\delta^{13}\text{C}$ for the H0200 bulk and amino acid samples. Leucine samples are replicate CO_2 submissions of a sample split before combustion.....129

Chapter 4

Figure 4.1 Production measurements ($\text{pmol } ^3\text{H leu/L/hr}$) for the control (open diamonds), 0 virus (0V; solid squares), grazers added (solid triangles) and 10 times virus (10V; solid circles). Values were the average for the A and B duplicate carboys for each treatment. Measurements made by Aubrey Cano/Craig Carlson, UCSB.....169

Figure 4.2 Chlorophyll *a* concentrations in $\mu\text{g/L}$ for the control (open diamond), 0 virus (0V; solid squares), grazers added (solid triangles) and 10 times virus (10V; solid circles) culture treatments. Data measured by Grace Henderson/Deborah Steinberg, VIMS.....170

Figure 4.3 Bacterial abundance counts (cells/mL) for the control (open diamonds), 0 virus (0V; solid squares), grazers added (solid triangles) and 10 times virus (10V; solid circles) incubation treatments. All measurements were averages of A and B duplicate carboys for each treatment. Data measured by Aubrey Cano/Craig Carlson, UCSB.....171

Figure 4.4 Total hydrolyzable amino acid concentration for control (open diamonds), 0 virus (0V; solid squares), grazers added (solid triangles) and 10 times virus (10V; solid circles). Values were averages of duplicate measurements for both A and B replicate carboy treatments.....173

Figure 4.5 DNA and RNA concentrations for the control (A), 0 virus (B), grazer added (C), and 10 times virus (D) culture treatments.....189

TABLE OF TABLES

Chapter 2

Table 2.1 Elemental data and monosaccharide distribution for the HMWDOM samples. For monosaccharides, R=rhamnose, F=fucose, A=arabinose, X=xylose, M=mannose, Gal=galactose, Glu=glucose, GluA=glucosamine, GalA=galactosamine, N.D.=not measured..... 49

Table 2.2 The periodate:glucose and periodate:amino acid stoichiometric ratios calculated for the glucose, polysaccharide, and albumin standards, along with the periodate demand per glucose or amino acid carbon..... 51

Table 2.3 Data from the periodate over-oxidation of H0100C, H0200D and H995200 HMWDOM samples. The calculations for μmol glucose in sample are based on the percent carbohydrate of the total carbon from the ^{13}C NMR analysis: 70% for H0100C, 75% for H0200D and 45% for H995200..... 53

Table 2.4 Evaluation of three different possible source structures for the aliphatic carbon present in the HMWDOM sample based on the criteria from the results of periodate over-oxidation experiments..... 71

Chapter 3

Table 3.1 Hydrolyzable amino acid distribution (mole percent of total) for HMWDOM sample H0200 compared to two literature sources of HAA distribution for HMWDOM. The Aluwihare 1999 values are an average of replicates from a coastal HMWDOM sample from Woods Hole, MA. The McCarthy et al., 1996 values are an average of surface water HMWDOM values from the N. Pacific, Sargasso Sea, and Gulf of Mexico. 100

Table 3.2 Basic elemental and recovery data for albumin and H0200 samples..... 101

Table 3.3 Average mass of each amino acid as calculated from the C18 chromatograms for albumin and H0200 samples, along with the percent standard deviation. The vial number each amino acid peak was collected in is also noted. Percent standard deviation is determined from the mass calculated from all of the individual injections..... 106

Table 3.4 List of ^1H NMR spectra from SCX collected fractions with the amino acid content of each fraction. This table lists the collection time for each fraction, along with an estimate of the amino acid purity based on the NMR spectra. The identifiable contaminants or functional groups are also listed..... 116

Table 3.5 The results for the albumin and H0200 samples submitted for $\delta^{13}\text{C}$ and $\Delta^{14}\text{C}$ analysis. The H0200 ser/gly C18 sample was re-cleaned using the C18 column after the SCX procedure..... 125

Chapter 4

Table 4.1 HPLC buffer gradient for amino acid analysis via OPA derivatives.....	160
Table 4.2 Agilent autoinjector injection program for the OPA-amino acid derivitization reaction.	160
Table 4.3 NH_4 and urea concentrations for the control, 0 virus (0V), grazer added, and 10 times virus (10V) incubations at 7 timepoints. Measurements were performed by Deborah Bronk, VIMS.....	166
Table 4.4 Dissolved organic carbon (DOC) and total nitrogen (TDN) concentrations for the control, 0 virus (0V), grazer added, and 10 times virus (10V) incubations. All concentrations are in μM C for DOC and μM N for the TDN measurements, and are averages of the A and B duplicate carboys for each incubation. Measurements were performed by Aubrey Cano/Craig Carlson, UCSB.....	167
Table 4.5 Hydrolyzable amino acid concentrations for the control (part A), 0 virus (part B), grazer added (part C), and 10 times virus (part D) incubations. The concentrations for each timepoint were averaged from duplicate measurements of both A and B replicate incubation treatments.....	175
Table 4.6 Amino acids as percent of DOC and TDN for the control, 0 virus (0V), grazer added and 10 times virus (10V) culture treatments. DOC and TDN measurements obtained from Aubrey Cano/Craig Carlson, UCSB.....	179
Table 4.7 Mole fraction of individual hydrolyzed amino acids for the control (A), 0 virus (0V; B), grazer added (C), and 10 times virus (10V; D) incubation treatments. The sum of the mole fraction for all amino acids at each timepoint was 1.....	182
Table 4.8 DNA and RNA concentrations for the control (A), 0 virus (B), grazer added (C), and 10 times virus (D) incubation treatments. Calculation of nucleic acids in μM was based on an average DNA base molecular weight of 325 g/mol, and an average RNA base molecular weight of 340 g/mol. It was also assumed that both DNA and RNA contained an equal distribution of nucleic acid base molecules.....	187

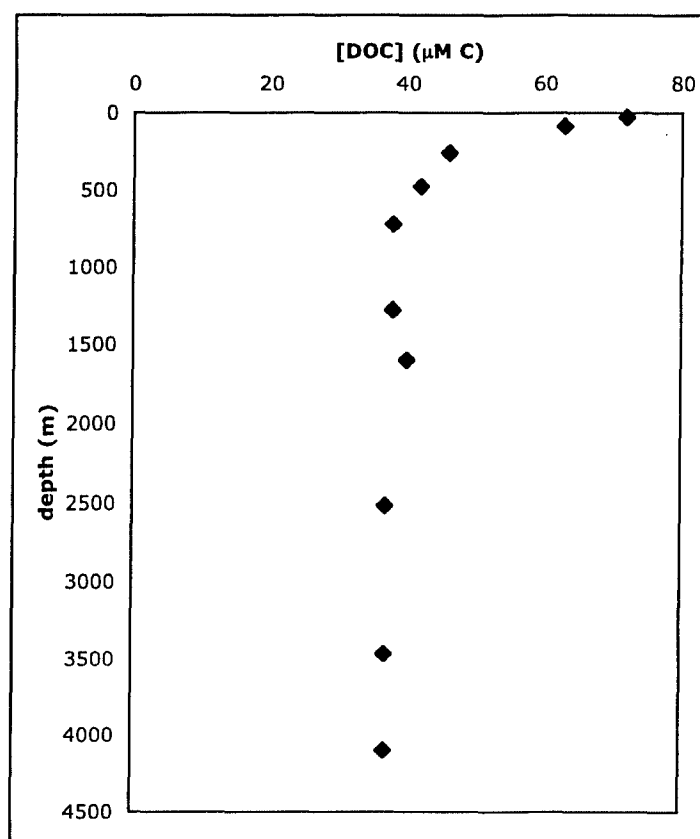
1. Introduction

1.1 Background Information

Dissolved organic matter (DOM) is the major organic carbon reservoir in the ocean, both in terms of size and importance to the global carbon cycle, and is second in size only to the dissolved inorganic carbon (DIC) pool. This carbon pool is operationally defined here as the fraction of total organic carbon that passes through a 0.2 μm filter. The total size of the dissolved pool in the ocean is approximately 680 Gt of carbon, which is similar in size to the land plant organic carbon and the total atmospheric CO_2 reservoirs (Hedges, 1992; Hansell and Carlson, 1998). The high molecular weight portion of DOM (HMWDOM), also known as colloidal DOM, can be isolated by ultrafiltration, and is defined in this thesis as the size fraction that passes through a 0.2 μm filter but is retained by a 1000 Da ultrafiltration membrane. The HMWDOM fraction constitutes approximately 20-30% of the total dissolved organic carbon (McCarthy et al., 1996; Aluwihare, 1999).

Dissolved organic carbon (DOC) has a characteristic concentration profile with depth, with a maximum concentration at the surface in the open ocean ranging from 60-80 μM C (Figure 1.1) (Druffel et al., 1992; Carlson et al., 1994; Guo et al., 1995; Bates and Hansell, 1999; Loh and Bauer, 2000). Concentration of DOC in surface water can vary with seasonal phytoplankton blooms and water stratification, and also tends to be higher in coastal waters (Guo et al., 1993; Carlson et al., 1994; Guo et al., 1995; Bates and Hansell, 1999). The concentration drops exponentially through the mesopelagic

Figure 1.1: DOC concentration with depth for the Eastern North Pacific Ocean. Data reported by Loh and Bauer, 2000.



ocean, down to a concentration of approximately 40 μM below 900 m (Druffel et al., 1992; Peltzer and Hayward, 1996; Hansell and Carlson, 1998; Carlson et al., 2000). The surface DOC concentration is higher near the coast than the open ocean, with some seasonal variations, but the deep ocean DOC concentration drops approximately 30% over the global conveyor belt from the Greenland Sea to the North Pacific Ocean (Peltzer and Hayward, 1996; Carlson et al., 2000). Recoveries of the HMWDOM fraction are generally higher (30%) in the surface ocean than at depth (20%) (McCarthy et al., 1996; Aluwihare, 1999). Particulate organic carbon (POC), defined as the size fraction greater than 0.2 μm , has a similar depth profile in the ocean, but with generally lower concentrations (3-10 μM in the surface to less than 0.1 μM below 900m) and with larger

seasonal surface variations (Druffel et al., 1992; Carlson et al., 2000; Daly et al., 2001). The partitioning between POC and DOC concentrations varies with seasonality and location, ranging from 90% POC/10% DOC in the surface Ross Sea to less than 10% POC/90% DOC in the surface Sargasso Sea, North Pacific, and Southern Ocean (Carlson et al., 2000; Loh and Bauer, 2000).

Measured C/N ratios of oceanic DOM range from 10-20, lower than those normally found for terrestrially-derived organic carbon and slightly higher than the C/N ratio of marine phytoplankton and bacteria (Aluwihare, 1999; Loh and Bauer, 2000; Aluwihare et al., 2002). Similarly, DOM $\delta^{13}\text{C}$ values are isotopically heavier (-22 ‰) than terrestrial C3 plant values (-27 ‰), indicating a marine source, though the potential impact of C4 plants cannot be eliminated (Guo and Santschi, 1997). Gradients in $\delta^{13}\text{C}$ from rivers to estuaries to the open ocean show an increase in $\delta^{13}\text{C}$ values as the influence of terrestrial inputs decreases (Guo and Santschi, 1997; Raymond and Bauer, 2001). These characteristics suggest that oceanic DOM is autochthonous in origin, and does not incorporate significant amounts of terrestrial organic carbon.

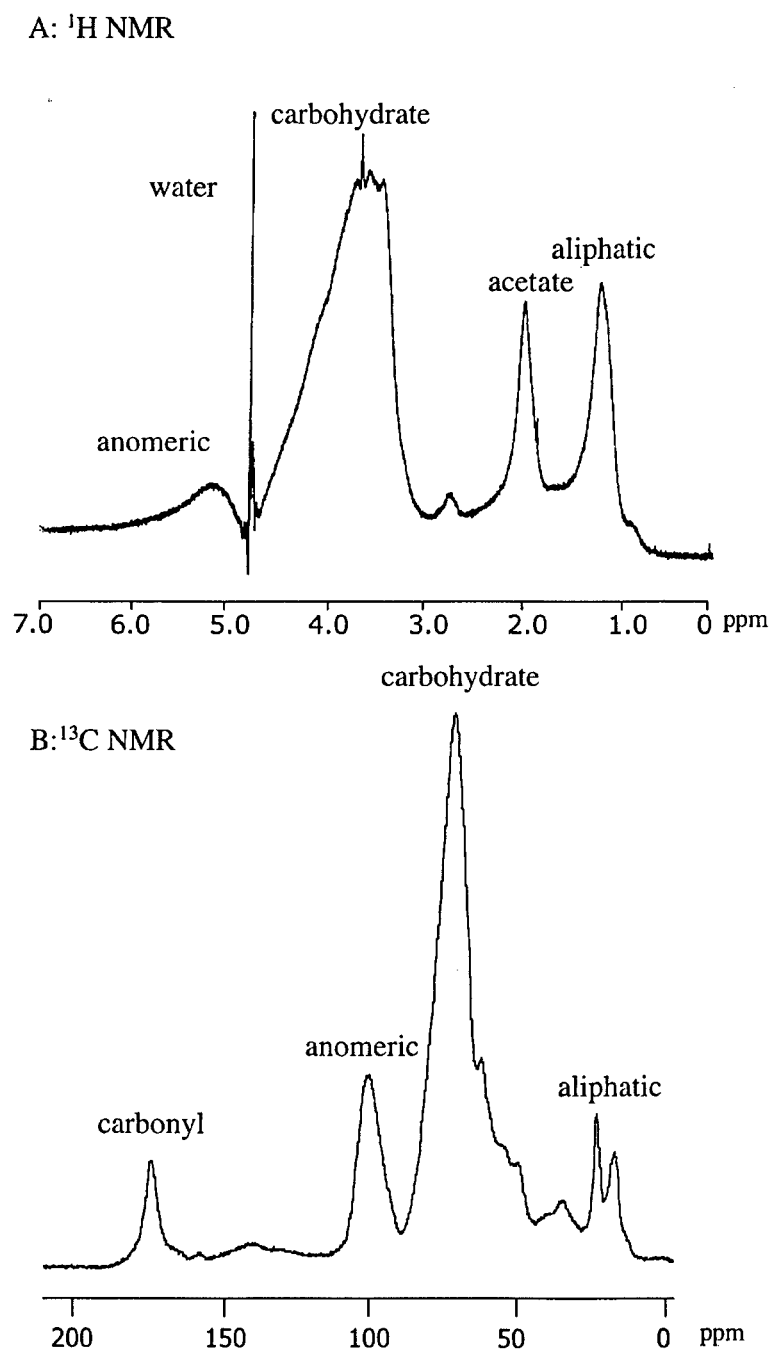
For all of the research done on the subject of DOM, there are still many questions left unanswered. While we have gained some knowledge about the chemical makeup of DOM, and particularly HMWDOM, the complete molecular composition and structure remains unknown. The lability and cycling of individual DOM compounds and the role they play in elemental carbon and nitrogen budgets has yet to be determined. The dynamics of DOM formation and uptake by marine organisms is also not fully understood. This thesis describes the results from three different experimental studies, each focusing on a different aspect of DOM and its cycling.

1.2 The Composition of HMWDOM

Due to the dissolved state, complexity, low concentrations, and interference from salt, molecular compositional analyses of oceanic DOM have proved challenging. The development of large volume ultrafiltration equipment has allowed the isolation of the high molecular weight fraction in a solid form, making it easier to analyze using molecular and spectroscopic methods. Nuclear magnetic resonance (NMR) spectroscopy can be used to gain a picture of the different chemical functional groups within HMWDOM. Proton NMR spectra (Figure 1.2 A) show the presence of four different types of hydrogen, with peaks corresponding to OCOH (5.0-4.8 ppm), HCOH (4.5-3.5 ppm), CH_3COOH (2.0 ppm) and CH_x (1.7-1.0 ppm) type hydrogens, indicating the presence of carbohydrate, acetate and aliphatic components in a characteristic $80\pm 4:10\pm 1:9\pm 4$ ratio (Aluwihare et al., 1997; Aluwihare, 1999). Similarly, ^{13}C NMR (Figure 1.2 B) shows the presence of carbohydrate, acetate and aliphatic types of carbon (McCarthy et al., 1996; Aluwihare, 1999). The ^{15}N NMR spectrum of HMWDOM contains a major peak at 260 ppm, indicating that the majority of the nitrogen in HMWDOM is present in the amide form (McCarthy et al., 1997). Spectra from all three types of NMR show little variation between samples from different ocean basins and water depths, indicating that the general chemical composition of HMWDOM is relatively homogenous, and contains only a few different types of functional groups.

The characterization of HMWDOM as consisting of a mixture of carbohydrates, acetate and lipids can be confirmed on a molecular level. A suite of seven neutral monosaccharides consisting of glucose, rhamnose, xylose, galactose, mannose, arabinose,

Figure 1.2: ^1H NMR (A) and ^{13}C NMR (B) spectra for surface water HMWDOM, showing the presence of carbohydrate, acetate, and aliphatic functional groups.



and fucose, has been isolated from the high molecular weight fraction in specific molar fractions (Sakugawa and Handa, 1985; McCarthy et al., 1996; Aluwihare et al., 1997; Borch and Kirchman, 1997; Biersmith and Benner, 1998). The relative distribution of

these seven monosaccharides with respect to each other appears to be consistent between oceans and at all depths. In surface waters the concentration of the total hydrolysable carbohydrate fraction is 10-20% of the total HMWDOC (3-6% of the total bulk DOC), but the concentration of identifiable monosaccharides decreases with depth. Fewer analyses have been done on the aliphatic portion of HMWDOM, but in general fatty acids and other lipids have been found to be a very minor fraction of the total organic carbon (Aluwihare, 1999; Mannino and Harvey, 1999; Wakeham et al., 2003).

Organic nitrogen compounds have also been isolated from HMWDOM, including amino acids and hexosamines (McCarthy et al., 1997; McCarthy et al., 1998; Aluwihare, 1999; Benner and Kaiser, 2003). Dissolved hydrolysable amino acids are the largest known contributor to the HMWDOM organic nitrogen pool, but only account for 10-20% of total dissolved organic nitrogen and 4-5% of the total organic carbon with little variation in depth (McCarthy et al., 1996; McCarthy et al., 1997; Aluwihare, 1999). Analysis of amino acid enantiomers has identified the presence of significant D-enantiomers for four amino acids, alanine, aspartic acid, glutamic acid and serine, leading to the hypothesis that these amino acids are derived from bacterially produced proteins (McCarthy et al., 1998; Dittmar et al., 2001; Perez et al., 2003). Isolations of complete proteins from HMWDOM using gel electrophoresis techniques has identified the presence of other bacterially derived proteins, including glycoproteins, porin homologues and outer membrane proteins (Tanoue, 1995; Yamada et al., 2000; Yamada and Tanoue, 2003). Glucosamine and galactosamine are present in similar concentrations to the neutral monosaccharides, accounting for approximately 3% of the total organic carbon

and 7% of the total organic nitrogen (Benner and Kaiser, 2003). The chemical character of the remaining fraction of amide nitrogen has not been determined.

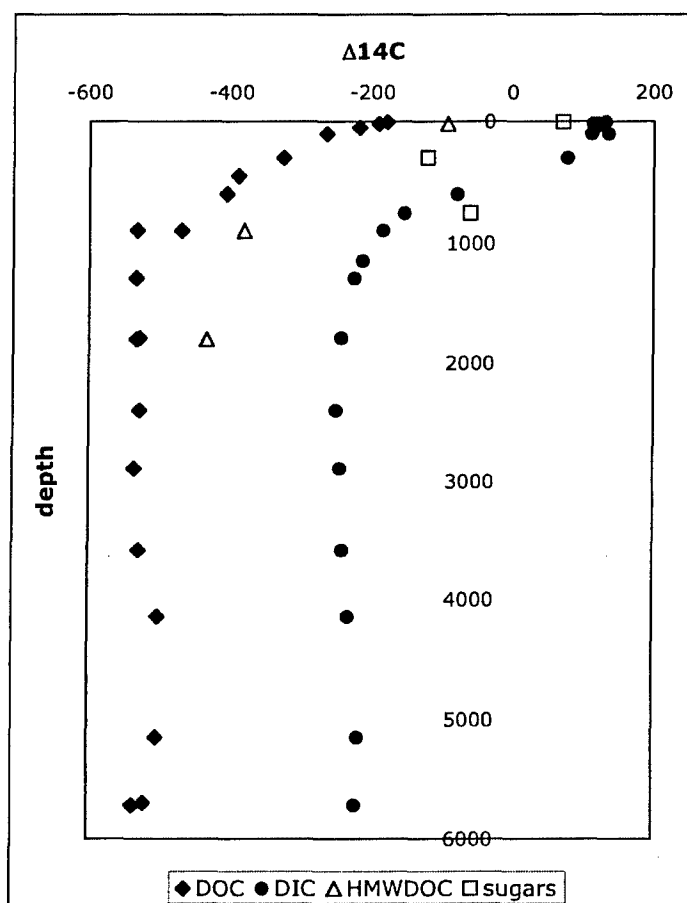
In spite of all the advances in the characterization of the chemical components of HMWDOM, there are still many questions still to be answered. Only 20% of the total organic carbon in surface HMWDOM and less than 10% of the deep organic HMW carbon has been identified at the molecular level. The concentration of carbohydrate measured on a molecular level does not match the amount of carbohydrate-type carbon as determined by spectroscopic methods. Chapter 2 of this thesis examines the discrepancy between the amount of carbohydrate as calculated from the proton and carbon NMR spectra of HMWDOM and the concentration of monosaccharides measured by acid hydrolysis. The goal of this chapter is to characterize the unidentified carbohydrate fraction of HMWDOM using periodate over-oxidation.

1.3 HMWDOM Cycling Via Compound Specific Radiocarbon Measurements

Incorporation of bomb radiocarbon into the different organic matter pools can be used as a means to provide information about the cycling of carbon between DOC, POC and DIC fractions (Druffel et al., 1992; Raymond and Bauer, 2001). Radiocarbon concentrations are reported as $\Delta^{14}\text{C}$ values, which represents the measured ^{14}C content normalized to 1950 atmospheric values in units of permil (‰). The inorganic carbon fraction shows incorporation of bomb radiocarbon down to a depth of 850 m in the Sargasso Sea, and 900 m in the central North Pacific (Figure 1.3) (Williams and Druffel, 1987; Druffel et al., 1992). The POC fraction has radiocarbon ages very similar to those of DIC in the surface waters, and retains a modern signature at all depths. On the other

hand, the DOC radiocarbon values are depleted in ^{14}C by 300-350‰ compared to the DIC at all depths, implying that little bomb radiocarbon has been incorporated into this carbon

Figure 1.3: $\Delta^{14}\text{C}$ values for DIC (solid circles), DOC (solid diamonds), HMWDOC (open triangles) and neutral sugars isolated from HMWDOC (open squares). All samples were obtained from Central North Pacific except for the neutral sugars, which were collected from the Mid-Atlantic Bight. DOC and DIC data reported by Druffel et al., 1992; HMWDOC data by Loh et al., 2004, and neutral sugars by Aluwihare et al., 2002.



pool. This translates into an average radiocarbon age for the DOC pool of approximately 3000-3500 ^{14}C years older than the DIC in the surface and greater than 5000 ^{14}C years older than the DIC at depth (Druffel et al., 1992). The radiocarbon content of the deep DOC pool indicates that the average residence time of the DOC is longer than the ocean circulation, and that a significant amount of the oldest DOC is not remineralized in

transit. This implies that DOC takes longer to cycle than DIC and POC, and thus contains older carbon than the other two pools (Druffel et al., 1992). As a result, the DOC pool must contain a fraction with a very old radiocarbon age that is continually cycled through the ocean in order to balance the new, modern production by organisms.

In addition to the DOC, POC, and DIC measurements, compound class radiocarbon measurements provide information about the cycling of different types of carbon within each pool of organic matter. Analyses of sub-fractions within different carbon pools provide information about which compounds are rapidly produced and removed and which are older, more refractory compounds. With this information, separate sources, production patterns, and decomposition pathways for individual portions of the carbon pool can be identified, depending on the specificity of the compounds isolated. Only a few studies have measured the radiocarbon data for HMWDOC and POC compound classes. Radiocarbon concentration has been measured for four separate compound class fractions isolated from sinking POC in the northeast Pacific Ocean: total amino acids, total carbohydrates, lipids, and acid insoluble compounds (Wang et al., 1996; Hwang and Druffel, 2003). These studies revealed that the $\Delta^{14}\text{C}$ of bulk POC was approximately 0‰. The ^{14}C content of the total amino acid fraction and the carbohydrate fraction were both enriched relative to the bulk POC, while the lipid and acid insoluble fraction were both slightly depleted compared to bulk POC (Wang et al., 1996; Hwang and Druffel, 2003). These results indicate that the amino acid and carbohydrate fractions are younger than the bulk POC carbon, and the lipid and acid insoluble fractions are much older.

Similar radiocarbon values have been measured for the lipid, protein, carbohydrate, and acid insoluble fractions of surface HMWDOC from the Atlantic and Pacific Oceans, with the lipid and acid insoluble fractions in the surface ocean older than the bulk carbon, and the amino acid and carbohydrate fractions containing modern carbon (Loh et al., 2004). This general trend ($\Delta^{14}\text{C}$ lipid < $\Delta^{14}\text{C}$ acid insoluble < $\Delta^{14}\text{C}$ amino acid and carbohydrate fractions) persists in deeper water HMWDOC samples, though the ages of all the fractions grow progressively older with depth. In addition, the HMWDOC fraction is younger than both the total DOC and the low molecular (LMW) weight DOC fraction (Loh et al., 2004). As yet, the only HMWDOM compounds measured for radiocarbon are individual monosaccharides released by hydrolysis (Aluwihare et al., 2002). These monosaccharides contain modern radiocarbon concentrations similar to DIC radiocarbon values, and are rapidly cycled. The monosaccharides also carry their modern radiocarbon signature down to at least 600m. The presence of modern radiocarbon signal at depth indicates that monosaccharides are preferentially vertically transported relative to the DIC.

With compound specific radiocarbon measurements for only one compound class of HMWDOM, it is impossible to fully describe the dynamics of different fractions within the HMWDOM pool. Compound specific measurements are necessary to obtain the most detailed characterization of sources, turnover times, and lability of different parts of the bulk carbon. In particular, amino acids are ideal compounds for radiocarbon analysis, in that they can potentially be used as nitrogen sources, as well as released in the form of various cell proteins. In chapter 3, I present the first radiocarbon measurements

of individual amino acids isolated from HMWDOM, in addition to a new method for the isolation and purification of these compounds.

1.4 Dynamics of Nitrogen in a Biologically Complex System

Release of DOC and DON by photoautotrophic organisms has been thought to occur by two processes: direct release from the cell by means of exudation or lysis, and release mediated by zooplankton grazing and fecal pellet dissolution. The direct release of dissolved organic matter (DOM) from plankton assemblages in culture has been studied extensively (Baines and Pace, 1991; Aluwihare et al., 1997; Hama and Yanagi, 2001). The average DOC release by phytoplankton in culture is approximately 10% of the primary production, but the range was very large (Baines and Pace, 1991; Hama and Yanagi, 2001). For DON, the typical measured rates of release range from 23-41% of the gross nitrogen uptake, with some studies reporting a maximum of 90% gross nitrogen uptake as released DON (Bronk and Ward, 1999; Bronk and Ward, 2000). The correlation between DOC and DON release seems to indicate more carbon released relative to nitrogen (Karl et al., 1997; Karl et al., 1998), but the ratio of DOC to DON released seems to vary with the seasons (Bronk and Ward, 1999). The reasons for the wide variations in the reported values for DOC and DON release are as yet unknown, as is the molecular basis for the preferential release of DOC as opposed to DON.

The molecular composition of the released DON remains largely undetermined. Nitrogen containing compounds, such as amino sugars, proteins, urea and nucleic acids have been measured in seawater, but constitute only a small fraction of DON (Karl and Bailiff, 1989; Cowie and Hedges, 1992; McCarthy et al., 1997; Aluwihare et al., 2002).

Hydrolyzable amino acids and N-acetyl aminosugars constitute the bulk of the dissolved organic nitrogen from cultures (Aluwihare and Repeta, 1999). The majority of the organic compounds released by phytoplankton are low molecular weight (LMW) compounds, nominally defined as those less than 1000 daltons in size, and as yet uncharacterized (Bronk and Glibert, 1991; Glibert and Bronk, 1994; Aluwihare and Repeta, 1999). The high molecular weight fraction of phytoplankton culture exudates has been better characterized by spectroscopic methods as well as molecular level analyses of the hydrolysis products. ^{15}N NMR spectroscopy of the high molecular weight fraction of oceanic DON indicates that the majority of the nitrogen is in amide form, with only 6-26% as non-amide compounds (McCarthy et al., 1997; Aluwihare, 1999).

While the characterization of organic matter from autotrophic phytoplankton in culture is challenging, the addition of zooplankton grazers, bacteria or viruses - while more representative of the surface ocean - causes the system to become even more complex. These organisms can mediate release of dissolved organic compounds from phytoplankton. Sloppy feeding, or the breakage of phytoplankton cells during ingestion, has been shown to result in the release of labile organic nitrogen and carbon compounds (Urban-Rich, 1999; Hasegawa et al., 2000). Zooplankton can also release organic compounds themselves, either by excretion, or via passive dissolution from fecal pellets (Urban-Rich, 1999; Steinberg et al., 2000). Bacteria can also release organic compounds to the DOM pool. Hydrolyzable amino acids bearing the enantiomeric signatures of bacterial peptidoglycan have been measured in natural surface HMWDOM (McCarthy et al., 1998). Proteins similar in sequence to porin P and outer membrane bacterial proteins have been measured in a variety of seawater samples (Tanoue, 1995; Yamada et al.,

2000; Yamada and Tanoue, 2003). In addition, assemblages of marine bacteria converted simple organic compounds into a refractory fraction of DOM that shared certain characteristics with natural DOM (Ogawa et al., 2001). Viruses also seem to play a role in the input and alteration of DOM by facilitating cell lysis or by controlling algal bloom conditions, but quantitative investigations are limited (Bratbak et al., 1994; Tarutani et al., 2000).

One of the major challenges in understanding the role of DON in the larger oceanic nitrogen cycles is the complexity of the system, and the interactions between nutrients, phytoplankton, grazers, and viruses. Though it is certain that these factors produce and alter the composition of the dissolved organic matter, too many factors are present in natural samples to allow for identification of processes and quantification of release and loss rates. By using incubations, the behavior of each culture to different treatments can be measured and compared. Chapter 4 describes measurements of dissolved organic nitrogen compounds (DNA, RNA, and hydrolyzed amino acids) from a set of culture experiments. These experiments were specifically designed to provide data for DON release and uptake by measuring samples from a set of phytoplankton cultures from Chesapeake Bay. Four different incubations were initiated: a control consisting of the natural assemblage of phytoplankton, bacteria and viruses, one with all viruses and bacteria removed, a third containing 10 times the virus concentration, and the last with the addition of copepod grazers. By conducting these cultures in parallel, the production, removal, and alterations of DON in each of the treatments can be compared and quantified.

1.5 The Goals of the Thesis

In spite of the large size of the DOC reservoir and its ubiquity in the ocean, very little detailed information regarding composition, turnover times, and input mechanisms is available. Until now, less than 30% of the total DOC has been molecularly characterized, and the overall structure is still unknown. Radiocarbon analyses have only been performed on bulk and compound class DOC samples, providing only incomplete information about the temporal differences between input and remineralization of important components. The sources and dynamics of the production of DOC are still largely undetermined. The main goal of this thesis is to use a combination of novel and conventional techniques to derive new information about the molecular composition, turnover time, and variations in production of the DOC pool and fractions within.

1.6 References

- Aluwihare, L. I. (1999). High molecular weight (HMW) dissolved organic matter (DOM) in seawater: chemical structure, sources and cycling, PhD, Massachusetts Institute of Technology/Woods Hole Oceanographic Institution: 224.
- Aluwihare, L. I. and D. J. Repeta (1999). A comparison of the chemical characteristics of oceanic DOM and extracellular DOM produced by marine algae. Marine Ecology Progress Series **186**: 105-117.
- Aluwihare, L. I., D. J. Repeta and R. F. Chen (1997). A major biopolymeric component to dissolved organic carbon in surface seawater. Nature **387**: 166-169.
- Aluwihare, L. I., D. J. Repeta and R. F. Chen (2002). Chemical composition and cycling of dissolved organic matter in the Mid-Atlantic Bight. Deep-Sea Research II **49**: 4421-4437.
- Baines, S. B. and M. L. Pace (1991). The production of dissolved organic matter by phytoplankton and its importance to bacteria: Patterns across marine and freshwater systems. Limnology and Oceanography **36**(6): 1078-1090.
- Bates, N. R. and D. A. Hansell (1999). A high resolution study of surface layer hydrographic and biogeochemical properties between Chesapeake Bay and Bermuda. Marine Chemistry **67**: 1-16.
- Benner, R. and K. Kaiser (2003). Abundance of amino sugars and peptidoglycan in marine particulate and dissolved organic matter. Limnology and Oceanography **48**(1): 118-128.
- Biersmith, A. and R. Benner (1998). Carbohydrates in phytoplankton and freshly produced dissolved organic matter. Marine Chemistry **63**: 131-144.
- Borch, N. H. and D. L. Kirchman (1997). Concentration and composition of dissolved neutral sugars (polysaccharides) in seawater determined by HPLC-PAD. Marine Chemistry **57**: 85-95.
- Bratbak, G., F. Thingstad and M. Heldal (1994). Viruses and the microbial loop. Microbial Ecology **28**: 209-221.
- Bronk, D. A. and P. M. Glibert (1991). A ^{15}N tracer method for the measurement of dissolved organic nitrogen release by phytoplankton. Marine Ecology Progress Series **77**: 171-182.

- Bronk, D. A. and B. B. Ward (1999). Gross and net nitrogen uptake and DON release in the euphotic zone of Monterey Bay, California. Limnology and Oceanography **44**: 573-585.
- Bronk, D. A. and B. B. Ward (2000). Magnitude of dissolved organic nitrogen release relative to gross nitrogen uptake in marine systems. Limnology and Oceanography **45**(8): 1879-1883.
- Carlson, C. A., H. W. Ducklow and A. F. Michaels (1994). Annual flux of dissolved organic carbon from the euphotic zone in the northwestern Sargasso Sea. Nature **371**: 405-408.
- Carlson, C. A., D. A. Hansell, E. T. Peltzer and W. O. Smith Jr. (2000). Stocks and dynamics of dissolved and particulate organic matter in the southern Ross Sea, Antarctica. Deep-Sea Research II **47**: 3201-2335.
- Cowie, G. L. and J. I. Hedges (1992). Sources and reactivities of amino acids in a coastal marine environment. Limnology and Oceanography **37**(4): 703-724.
- Daly, K. L., W. O. Smith Jr., G. C. Johnson, G. R. DiTullio, D. R. Jones, C. W. Mordy, R. A. Feely, D. A. Hansell and J.-Z. Zhang (2001). Hydrography, nutrients, and carbon pools in the Pacific sector of the Southern Ocean: Implications for carbon flux. Journal of Geophysical Research **106**(C4): 7101-7124.
- Dittmar, T., H.-P. Fitznar and G. Katiner (2001). Origin and biochemical cycling of organic nitrogen in the eastern Atlantic Ocean as evident from D- and L-amino acids. Geochimica et Cosmochimica Acta **65**(22): 4103-4114.
- Druffel, E. R. M., P. W. Williams, J. E. Bauer and J. R. Ertel (1992). Cycling of dissolved and particulate organic matter in the open ocean. Journal of Geophysical Research **97**(C10): 15,639-15,659.
- Glibert, P. M. and D. A. Bronk (1994). Release of dissolved organic nitrogen by marine diazotrophic cyanobacteria, *Trichodesmium* spp. Applied and Environmental Microbiology **60**(11): 3996-4000.
- Guo, L., C. H. Coleman Jr. and P. H. Santschi (1993). The distribution of colloidal and dissolved organic carbon in the Gulf of Mexico. Marine Chemistry **44**: 1-15.
- Guo, L. and P. H. Santschi (1997). Composition and cycling of colloids in marine environments. Reviews of Geophysics **35**(1): 17-40.
- Guo, L., P. H. Santschi and K. W. Warnken (1995). Dynamics of dissolved organic carbon (DOC) in oceanic environments. Limnology and Oceanography **40**(8): 1392-1403.

- Hama, T. and K. Yanagi (2001). Production and neutral aldose composition of dissolved carbohydrates excreted by natural marine phytoplankton populations. Limnology and Oceanography **46**(8): 1945-1955.
- Hansell, D. A. and C. A. Carlson (1998). Deep-ocean gradients in the concentration of dissolved organic carbon. Nature **395**: 263-266.
- Hasegawa, T., I. Koike and H. Mukai (2000). Dissolved organic nitrogen dynamics in coastal waters and the effect of copepods. Journal of Experimental Marine Biology and Ecology **244**: 219-238.
- Hedges, J. I. (1992). Global biogeochemical cycles: progress and problems. Marine Chemistry **39**: 67-93.
- Hwang, J. and E. R. M. Druffel (2003). Lipid-like material as the source of the uncharacterized organic carbon in the ocean. Science **299**: 881-884.
- Karl, D., R. Letelier, L. Tupas, J. Dore, J. Christian and D. Hebel (1997). The role of nitrogen fixation in biogeochemical cycling in the subtropical North Pacific Ocean. Nature **388**: 533-538.
- Karl, D. M. and M. D. Bailiff (1989). The measurement and distribution of dissolved nucleic acids in aquatic environments. Limnology and Oceanography **34**(3): 543-558.
- Karl, D. M., D. V. Hebel, K. Björkman and R. M. Letelier (1998). The role of dissolved organic matter release in the productivity of the oligotrophic North Pacific Ocean. Limnology and Oceanography **43**(6): 1270-1286.
- Loh, A. N. and J. E. Bauer (2000). Distribution, partitioning and fluxes of dissolved and particulate C, N and P in the eastern North Pacific and Southern Ocean. Deep-Sea Research I **47**: 2287-2316.
- Loh, A. N., J. E. Bauer and E. R. M. Druffel (2004). Variable ageing and storage of dissolved organic components in the open ocean. Nature **430**: 877-881.
- Mannino, A. and H. R. Harvey (1999). Lipid composition in particulate and dissolved organic matter in the Delaware Estuary: Sources and diagenetic patterns. Geochimica et Cosmochimica Acta **63**(15): 2219-2235.
- McCarthy, M., J. Hedges and R. Benner (1996). Major biochemical composition of dissolved high molecular weight organic matter in seawater. Marine Chemistry **55**: 281-297.
- McCarthy, M., T. Pratum, J. Hedges and R. Benner (1997). Chemical composition of dissolved organic nitrogen in the ocean. Nature **390**: 150-154.

- McCarthy, M. D., J. I. Hedges and R. Benner (1998). Major bacterial contribution to marine dissolved organic nitrogen. Science **281**: 231-234.
- Ogawa, H., Y. Amagai, I. Koike, K. Kaiser and R. Benner (2001). Production of refractory dissolved organic matter by bacteria. Science **292**: 917-920.
- Peltzer, E. T. and N. A. Hayward (1996). Spatial and temporal variability of total organic carbon along 140°W in the equatorial Pacific Ocean in 1992. Deep-Sea Research II **43**(4-6): 1155-1180.
- Perez, M. T., C. Pausz and G. J. Herndl (2003). Major shift in bacterioplankton utilization of enantiomeric amino acids between surface waters and the ocean's interior. Limnol. Oceanogr. **48**(2): 755-763.
- Raymond, P. A. and J. E. Bauer (2001). Use of ^{14}C and ^{13}C natural abundances for evaluating riverine, estuarine, and coastal DOC and POC sources and cycling: a review and synthesis. Organic Geochemistry **32**: 469-485.
- Sakugawa, H. and N. Handa (1985). Isolation and chemical characterization of dissolved and particulate polysaccharides in Mikawa Bay. Geochimica et Cosmochimica Acta **49**(5): 1185-1193.
- Steinberg, D. K., C. A. Carlson, N. R. Bates, S. A. Goldthwait, L. P. Madin and Michale (2000). Zooplankton vertical migration and the active transport of dissolved organic and inorganic carbon in the Sargasso Sea. Deep-Sea Research I **47**: 137-158.
- Tanoue, E. (1995). Detection of dissolved protein molecules in oceanic waters. Marine Chemistry **51**: 239-252.
- Tarutani, K., K. Nagasaki and M. Yamaguchi (2000). Viral impacts on total abundance and clonal composition of the harmful bloom-forming phytoplankton *Heterosigma akashiwo*. Applied and Environmental Microbiology **66**(11): 4916-4920.
- Urban-Rich, J. (1999). Release of dissolved organic carbon from copepod fecal pellets in the Greenland Sea. Journal of Experimental Marine Biology and Ecology **232**: 107-124.
- Wakeham, S. G., T. K. Pease and R. Benner (2003). Hydroxy fatty acids in marine dissolved organic matter as indicators of bacterial membrane material. Organic Geochemistry **34**: 857-868.
- Wang, X.-C., E. R. M. Druffel and C. Lee (1996). Radiocarbon in organic compound classes in particulate organic matter and sediment in the deep northwest Pacific Ocean. Geophysical Research Letters **23**(24): 3583-3586.
- Williams, P. M. and E. R. M. Druffel (1987). Radiocarbon in dissolved organic matter in the central North Pacific Ocean. Nature **330**: 246-248.

Yamada, N., S. Suzuki and E. Tanoue (2000). Detection of *Vibrio (Listonella) anguillarum* porin homologue proteins and their source bacteria from coastal seawater. Journal of Oceanography **56**: 583-590.

Yamada, N. and E. Tanoue (2003). Detection and partial characterization of dissolved glycoproteins in oceanic waters. Limnology and Oceanography **48**(3): 1037-1048.

2. Characterization of High Molecular Weight Dissolved Organic Matter Using Periodate Over-Oxidation

2.1 Introduction

2.2.1 Background

One of the major challenges in the study of oceanic dissolved organic matter (DOM) is characterization on a molecular level. The majority of structural analyses have been performed on high molecular weight dissolved organic matter (HMWDOM), operationally defined as the size fraction that passes through a 0.2 μm filter cartridge, but is retained by a 1000 Da ultrafiltration membrane. Proton nuclear magnetic resonance (^1H NMR) spectra of HMWDOM show the presence of large amounts of “carbohydrate”, “acetate” and “lipids” with a characteristic ratio of $80\pm4:10\pm2:9\pm4$ (Aluwihare et al., 1997; Aluwihare and Repeta, 1999). The ^{13}C NMR spectra also show strong carbohydrate, aliphatic and carboxylic carbon (McCarthy et al., 1996; Aluwihare, 1999). These molecular components of HMWDOM are consistent from sample to sample, between oceans, and with water column depth. Monosaccharides have also been isolated from HMWDOM after acid hydrolysis. Aluwihare et al. (1997) show that seven neutral monosaccharides (arabinose, fucose, xylose, rhamnose, galactose, mannose, and glucose) are present in approximately equimolar concentrations with highest absolute concentrations in surface waters. These sugars, along with acetate, are ubiquitous throughout the oceans, and appear to be part of a common biopolymer. Minor amounts of other compounds have also been identified, including aminosugars, hexosamines, and lipids (McCarthy et al., 1997; Aluwihare, 1999; Mannino and Harvey, 1999; Benner and Kaiser, 2003).

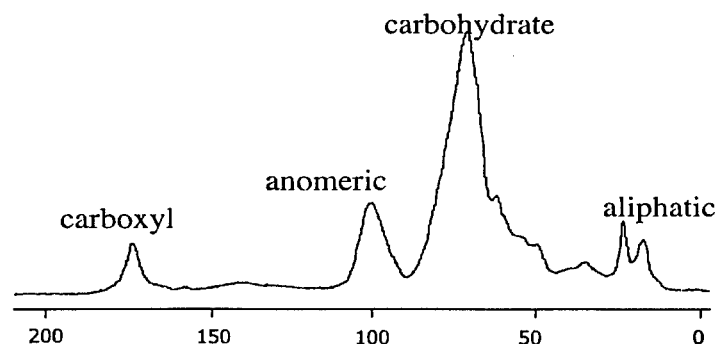
One of the most intriguing problems in the structural determination of HMWDOM is the inability of molecular analysis to account for the quantity and types of functional groups seen in NMR spectra. Less than 30% of the carbohydrate identified by NMR spectroscopy can be accounted for as individual monosaccharides following conventional acid hydrolysis, and the complete composition of the polysaccharide is yet to be determined (McCarthy et al., 1996; Aluwihare, 1999; Benner and Kaiser, 2003). In addition, the fraction of identifiable biomolecules decreases with depth (McCarthy et al., 1997; Aluwihare, 1999). Both ^1H and ^{13}C NMR spectra show distinct aliphatic peaks that are not accounted for by molecular level analysis. Previous studies have attempted to isolate a lipid fraction using solvent extraction and saponification techniques, but these have not been successful at yielding the amount of carbon seen in NMR spectra (Aluwihare, 1999; Mannino and Harvey, 1999; Wakeham et al., 2003). The inability to isolate sufficient carbon to account for the complete lipid NMR signal implies that the lipids are either physically protected, or not accessible using normal saponification methods.

2.2.2 Characterization of the Unknown Fraction of HMWDOM Using NMR Spectroscopy

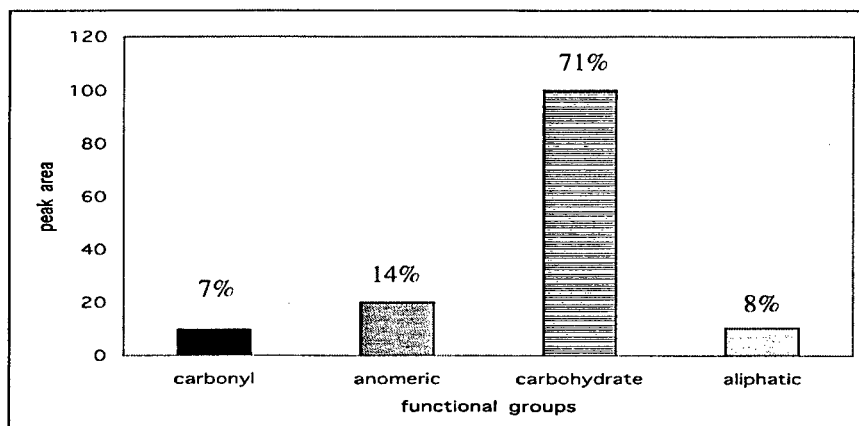
The known components of HMWDOM such as monosaccharides, amino acids and hexosamines, constitute approximately 30% of the total organic carbon. The remainder of the carbon has yet to be conclusively identified; however, the functional groups present in the uncharacterized fraction of HMWDOM can be determined from

Figure 2.1 Mathematical analysis of the unknown fraction of HMWDOM, starting with the total solid state ^{13}C NMR spectra of surface seawater HMWDOM(A). The peak areas were translated to a normalized histogram (B), and the previously isolated molecular components were sequentially subtracted. The histograms represent the carbon remaining after subtraction of neutral sugars (C), acetate (D), hexoseamines (E), and amino acids (F). The remaining peak areas in part F represent the as yet unidentified fraction.

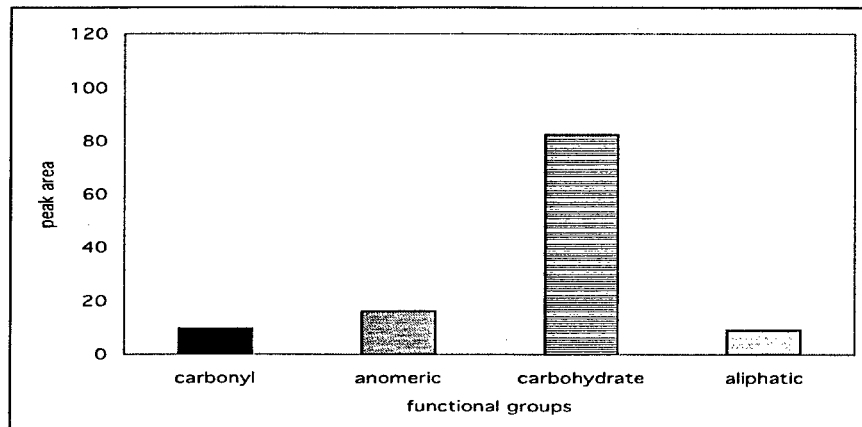
A: ^{13}C NMR spectrum



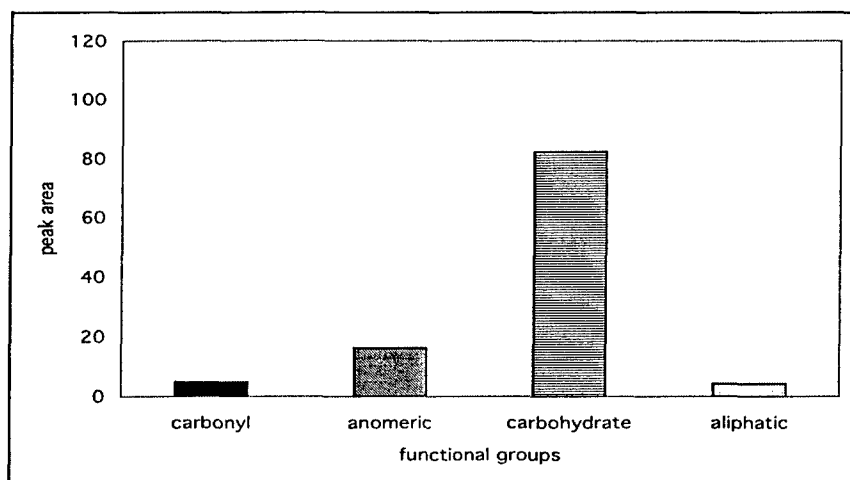
B: Total carbon histogram; values shown above bars are percent of total mass for each functional group



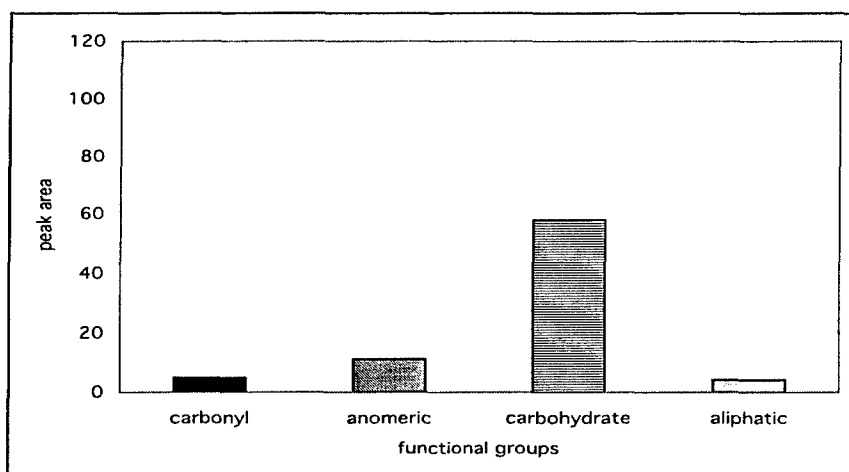
C: Histogram after subtraction of neutral sugars



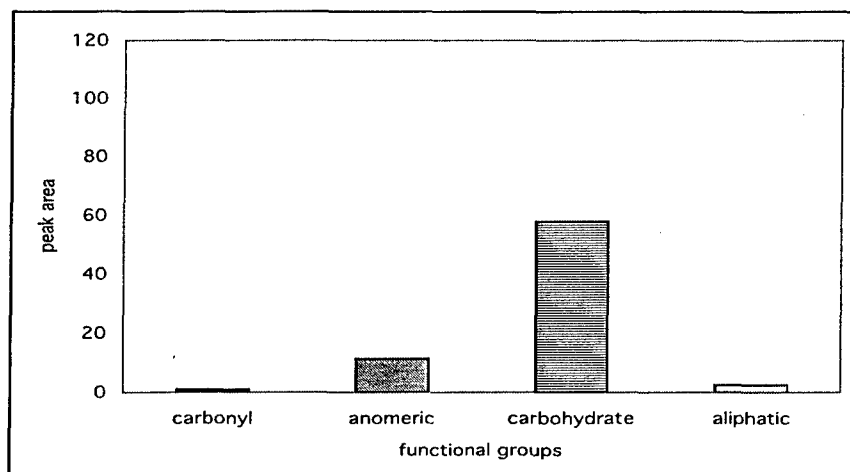
D. Histogram after subtraction of neutral sugars and acetate



E. Histogram after subtraction of neutral sugars, acetate and hexosamines



F. The unknown fraction of HMWDOM (neutral sugars, acetate, hexosamines and amino acids removed)



^{13}C NMR spectra by subtracting the spectral contributions from known constituents from the total spectra. This process is shown graphically in Figure 2.1. The ^{13}C NMR spectra of North Pacific surface seawater. HMWDOM shows four major types of carbon functionalities in HMWDOM: carboxyl (COO, 160-180 ppm), anomeric (OCO, 85-115 ppm), carbohydrate (COH, 60-85 ppm), and aliphatic (CH_x , 20-50 ppm) (Figure 2.1a). In NMR spectra, the peak area is proportional to the relative amount of each type of carbon present in the sample. Since an individual NMR spectrum represents all the carbon in the sample, the peak area can be quantified, normalized, and translated into histogram form (Figure 2.1b). The spectral contributions from the known HMWDOM compounds can then be subtracted, with the remaining peak area representing the unknown fraction.

The COO:OCO:COH: CH_x ratio normalized to the COH peak area for this sample is 10:20:100:10. The carbon present in the high molecular weight compounds identified at the molecular level, such as monosaccharides, amino acids, amino sugars and acetate, can be categorized into carbonyl, anomeric, carbohydrate and aliphatic type functional groups. Neutral sugars in HMWDOM contain three types of carbon, OCO, COH, and CH_x , that can be subtracted from the total carbon histogram to yield a COO:OCO:COH: CH_x ratio of 10:16:82:9 for the remaining HMWDOM (Figure 2.1c). Acetate contains both a COO and a CH_x carbon, and is approximately 7% of the organic carbon (Aluwihare, 1999). Subtraction of this component from the remaining ^{13}C NMR spectrum leaves a COO:OCO:COH: CH_x ratio of 5:16:82:4 (Figure 2.1d). This acetate is bound to amino sugars, which contain OCO and COH carbon. Removal of the amino sugar fraction leaves a COO:OCO:COH: CH_x ratio for HMWDOM of 5:11:58:4 from the ^{13}C NMR spectrum (Figure 2.1e). Amino acids constitute 4% of the organic carbon in

this sample, and the associated COO and CH_x carbon can be subtracted from the histogram of the ¹³C NMR. The remaining carbon from the ¹³C NMR spectrum represents the functional groups present in the fraction of the carbon within HMWDOM that have not been characterized at the molecular level. This unknown fraction contains a COO:OCO:COH:CH_x ratio of 1:11:58:3 (Figure 2.1f). The ratio of the anomeric (OCO) to COH type carbon is approximately 1:5, consistent with the majority of this unknown carbon being carbohydrate-like in composition, with some minor carbonyl (COOH) and aliphatic (CH_x) contributions. The presence of the additional carbohydrate in this unknown fraction agrees well with previous data from molecular and NMR spectroscopic analyses indicating the majority of the carbohydrate observed in NMR spectra is not released by acid hydrolysis.

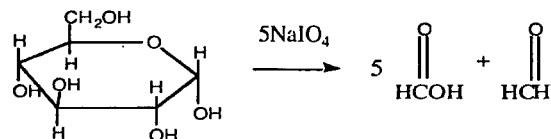
While this mathematical analysis suggests that the remaining unknown fraction of HMWDOM consists of carbohydrates, further studies are needed to characterize this fraction. The technique of periodate over-oxidation can be used to identify this portion of the unknown fraction and reconcile the difference between the amount of COH observed by NMR spectroscopy and the quantity determined by molecular analysis.

2.2.3 Introduction to Periodate Over-Oxidation

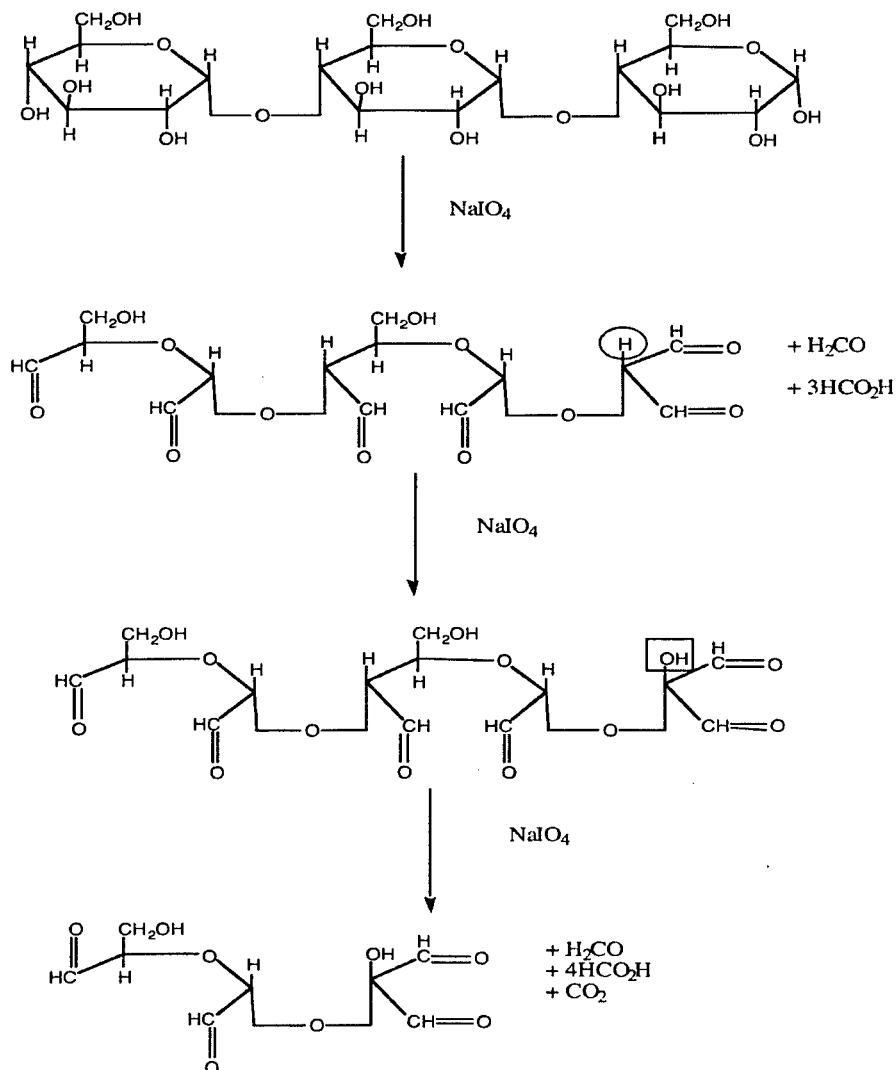
Periodate oxidation is a technique often used in carbohydrate chemistry. This reaction provides a controlled method of cleavage by breaking the carbon-carbon bond between vicinal glycols, and oxidizing alcohol and amino groups. In addition to the specificity of reaction, periodate oxidation uses one periodate ion for every carbon-carbon bond broken, and this stoichiometry can aid in structural identification (Sklarz, 1967; House, 1972). The over-oxidation technique used in this study converts the

Figure 2.2 The reaction mechanism for periodate oxidation of a glucose monomer (A) and for the over-oxidation of a polysaccharide (B). The activated hydrogen circled in part B, step 2 is converted by periodate to the -OH functional group marked by a square.

Part a:



Part b:



individual carbohydrates in a polysaccharide chain into carboxylic acids, ketones and carbon dioxide, breaking apart the glycosidic linkages (Figure 2.2a). Reaction of periodate with simple monosaccharides yields formaldehyde (HCOH), formic acid (HCOOH), ammonia (NH₃), and acetic acid (CH₃COOH). Complex polysaccharides can yield a variety of other aldehyde and carboxylic acid products in addition to these, depending on the structure of the polysaccharide.

Due to the specificity of reaction, periodate oxidation methods have often been used to determine the structure of monosaccharides, the monosaccharide content and conformation of polysaccharides, and the identity of terminal monosaccharides (Parrish and Whelan, 1959; Whelan, 1964; Veelart et al., 1997; Kim et al., 2000). For example, periodate oxidation has been used to identify the 1:3 linkages connecting the β -D-glucopyranose residues in the structure of laminarin (Peat et al., 1958). Currently, periodate oxidation is one technique used to provide structural information for more complex biomolecules such as lipopolysaccharides (Perry and MacLean, 1999). Periodate oxidation of polysaccharides using conventional methods usually oxidizes the available glycols within the carbohydrate chain but cannot completely break the ether linkages between units. The periodate over-oxidation protocol used in this paper uses heat to aid in the complete destruction of the polymer to non-oxidizable ketones, aldehydes and carbon dioxide (Figure 2.2b). Periodate oxidation has also been used for analysis of proteins, such as determining amounts of threonine and serine in samples (Shinn and Nicolet, 1941; Shinn and Nicolet, 1941).

Periodate does not oxidize aliphatic carbon, but will slowly oxidize unsaturated and aromatic compounds (House, 1972). This specificity makes it ideal for

characterizing HMWDOM constituents. Since the relative amount of COH is much higher than the amount of aliphatic carbon in the unknown HMWDOM fraction, there must be regions within the macromolecular structure that are easily oxidized by periodate. In addition, since the ^{13}C and ^1H NMR spectra of HMWDOM do not indicate the presence of significant amounts of unsaturated or aromatic moieties, the aliphatic portion should be lipid-like, and therefore remain unchanged and easily extracted from aqueous solution after oxidation.

In this chapter, periodate over-oxidation is used to identify the composition of the unknown fraction in surface and deep water HMWDOM samples that cannot be accessed by conventional hydrolysis techniques. This chapter also details the development of a method for the periodate over-oxidation of HMWDOM, along with experimental UV-Vis and NMR data. The result of this experiment is the identification of the presence of 6-deoxysugars, a new set of carbohydrates found in HMWDOM.

2.2 Materials and Methods

2.2.1 Sample Location and Collection

HMWDOM samples from both surface and deep water were used in this experiment. Surface seawater was drawn from the 15 m seawater intake at the Natural Energy Laboratory in Kona, Hawaii in January 2001 (H0100C) and February 2002 (H0200D and H0200C). The water samples were filtered to remove bacteria and small particles using a cleaned Suporflow dual stage (0.8 μm and 0.2 μm) Gelman polyether sulfone cartridge filter (Chisolm Corp., Lincoln, RI) fitted to an Advanta stainless steel housing. This filter was cleaned with 10% HCl, then flushed with low carbon deionized

Milli-Q water. High molecular weight DOM samples were collected using a large volume cross flow ultrafiltration system consisting of a stainless steel centripetal pump and membrane housings and a fluorinated high density polyethylene reservoir. The system was plumbed with teflon tubing and fitted with PVDF valves. The ultrafiltration membrane (Separation Engineering, Escondido, CA) nominally retains organic matter with a molecular weight of greater than 1000 Da, calibrated by greater than 99% retention of vitamin B12 (1.36 kDa). Membranes were cleaned using isopropanol, detergent (0.01% Micro), 0.01 M HCl and 0.01 M NaOH, stored in 0.55 mM sodium azide, and rinsed with water immediately before use. Between 30,000 and 60,000 L of seawater were concentrated to approximately 20 L, frozen in Teflon carboys and returned to Woods Hole for further processing. The HMWDOM samples were desalted by diafiltration with water, reduced to 2 L, and lyophilized to yield a fluffy white powder. The H0200D and H0200C samples were different subsamples taken from the same HMWDOM sample.

A deep water sample from 5200 m (H995200), was taken from the North Central Pacific (31°00' N, 159°00' W) in June 1999. This sample (1000 L) was collected using rosette mounted Niskin bottles, filtered (0.2 µm Criticap polycarbonate filter cartridges), then processed using a spiral wound 1000 Da nominal molecular weight cutoff filter (Amicon Corp.) mounted on an Amicon DC-10 pump (Aluwihare et al., 2002).

2.2.2 Analyses

Low carbon deionized (Milli-Q) water was used in all procedures. Glassware and sodium sulfate were combusted for a minimum of 8 h at 450°C, and pipette tips, syringes and teflon-lined vial lids were rinsed with 10% HCl and water before use. Only amber

colored or foil covered vials were used for all periodate reactions due to the sensitivity of periodate to light. Proton and ^{13}C NMR spectra were acquired on a Bruker 400MHz spectrometer using a water suppression program (zgpr). All ^1H NMR spectra were run using D_2O as a solvent, and chemical shifts were referenced to water at 4.8 ppm, and the ^{13}C NMR spectra were taken using solid state techniques. Elemental analyses (CHN) were performed on a CE Instruments (Flash EA 1112) elemental analyzer with a thermal conductivity detector.

2.2.3 Periodate Over-Oxidation

A number of different techniques exist in the literature for periodate oxidation of various mono- and polysaccharide compounds. These methods differ in the concentration of periodate added, the temperature of reaction, and the duration of the experiment. The more conventional methods for the quantification of the extent of periodate oxidation are detection of products such as formaldehyde and formic acid using colorimetric assays or paper chromatography. For the most part, these techniques of periodate oxidation required significant alteration in regards to temperature and analytical procedure to be used with HMWDOM.

Periodate can be used to oxidize the easily available glycols in a polysaccharide chain, leaving the glycosidic linkages intact, or it can be used to over-oxidize the polysaccharide, breaking down the chain completely into low molecular weight aldehydes and ketones along with carbon dioxide. In theory, leaving these glycosidic linkages intact retains the backbone of the polysaccharide. In this chapter, references to periodate oxidation or over-oxidation will always refer to the over-oxidation technique.

2.2.3.1 Standards and Samples

Commercially available sugars (glucose, laminarin, amylose starch, maltooligosaccharide) and a protein (bovine serum albumin) were used to test the periodate oxidation procedure and to determine the stoichiometry of periodate oxidation. Calculations of molarity and molecular ratios for polysaccharides (laminarin, starch, and maltooligosaccharide) were based on the molecular weight of 162 Da ("dehydrated" glucose). Albumin concentrations were based on the average molecular weight of individual amino acids present (110 Da) rather than the molecular weight of the albumin protein (66,000 Da). Octyl- β -glucopyranoside (OGP), a glucose monomer with a C₈ lipid chain attached via an ether bond to the 1-carbon of the glucose molecule, was used a standard compound for a carbohydrate-lipid sample.

Three different HMWDOM samples were over-oxidized by periodate. H0200D and H0100C were surface samples, while H995200 was a deep water sample. High molecular weight DOM samples were treated as glucose polysaccharides with calculated molarity and periodate: 'glucose' stoichiometric ratios based on an assumed molecular weight of 162 Da.

2.2.3.2 Periodate Over-Oxidation Method

Periodate over-oxidation experiments were based on the procedure of Dixon and Lipkin, 1954. A 12-14 fold excess of 0.015 M aqueous solution of sodium (meta) periodate (Fisher Chemical Corp.) was combined with a 0.015 M aqueous solution of glucose, polysaccharide, bovine serum albumin, or HMWDOM (based on estimated carbohydrate) and oxidized in triplicate. Using glucose as a model monosaccharide, it was found that the reaction was completed within 24 h at an incubation temperature of

40°C, but more complex polysaccharides such as laminarin, maltooligosaccharide, and amylose starch required a higher incubation temperature of 80°C for the oxidation to go to completion within a reasonable amount of time (1-2 weeks). For all samples, the experiment proceeded until periodate consumption, as measured by UV-Vis spectroscopy, ceased. Only small amounts of sample H995200 were available for this study. This sample was oxidized with the same ratio of sugar to periodate, but as a more dilute solution (0.004 M glucose equivalents).

The initial OGP experiments were run at concentrations similar to the other glucose and polysaccharide standards, but due to the low solubility of the octanol product, the concentrations of OGP in subsequent over-oxidation experiments were decreased to 0.1 mM OGP and mixed with an appropriate amount of periodate.

The majority of periodate oxidation methods reported in the literature evaluated the extent of reaction based on the measurements of products such as formic acid and formaldehyde via colorimetric analysis (Halsall et al., 1947; Hay et al., 1965; Painter, 1994). Since the periodate oxidation requires the presence of vicinal glycols, for relatively pure monosaccharide and small oligosaccharides, the oxidation products can be traced backwards to give structural information about the original compound and the oxidative yield. The ratios of the products relative to each other and their structure can be used to deduce what the structure of the original molecule could have been based on the action of the periodate. Evaluation of products to determine the composition of HMWDOM is not practical due to the heterogeneity of the HMWDOM samples. For this reason, the extent of reaction was determined by measuring the loss of the periodate ion.

The loss of periodate ion during the course of the oxidation reaction was measured using the spectrophotometric analysis procedure of Hay et al. (1965). Changes in the concentration of periodate were determined by UV-Vis spectroscopy using a HP8452 diode array spectrophotometer. Absorbance spectra between 190 and 820 nm were measured daily, and the reaction was considered complete when the calculated percent oxidation was greater than 97%, or the change in absorbance values was less than 5% from the previous day. The fraction periodate consumed by the reaction at time t (F_t) was calculated as the ratio of blank corrected absorbance at 230 nm (B_t) to the initial periodate blank (P_0) where $F_t = B_t/P_0$ (Dixon and Lipkin, 1954). The maximum absorbance for periodate occurs at 223 nm, but a slight drift (± 2 nm) in the periodate maximum during reaction was detected. In addition, the periodate reduction product (iodate) has a maximum at 190 nm. To avoid the influence from the shoulder of the iodate peak, the amount of glucose oxidized was calculated using the off-maximum absorbance values at 230 nm. Variations of absorbance values for the periodate and glucose blanks were $< 5\%$ throughout the course of the reaction. The stoichiometry of oxidation was calculated assuming complete oxidation of each substance.

To monitor compositional changes in HMWDOM as a result of the periodate over-oxidation reaction, proton NMR spectra of some samples were taken during the course of the oxidation reaction. Samples analyzed using both NMR and UV/Vis spectroscopy were prepared as described above, but with 99.9% D_2O (Aldrich) as the solvent. Measurements were made daily for the first 3 days, then every second day until the reaction was considered complete. Subsamples of the reaction solution (600-700 μL) for NMR analyses were spiked with 10-50 μL of a 0.022 M benzoic acid as a reference

standard. Benzoic acid was chosen as a standard because the ^1H NMR signals appear between 7-8 ppm, outside the range of the usual HMWDOM peaks, and because it is resistant to oxidation by periodate on 1-2 day time scales. Some degradation did occur when the benzoic acid was reacted with periodate for longer time periods, so it was necessary to add the standard to the individual NMR subsamples rather than the bulk sample.

2.2.4 Molecular Analyses

2.2.4.1 Monosaccharide Analysis

Monosaccharides were analyzed by gas chromatography (GC) as their alditol acetates. Approximately 2 mg samples of HMWDOM (0.8 mg HMWDOC) were treated with 0.5 mL of 2 M trifluoroacetic acid (TFA) aqueous solution which contained myo-inositol (20 μg) as an internal standard. The sample was flushed with nitrogen, sealed and heated to 121°C. After 2 hr, the samples were cooled to room temperature and the TFA was removed under a stream of nitrogen. To remove residual TFA, isopropanol (250 μL) was added and the sample was taken to dryness under nitrogen (2x). Sugars were reduced to alditols by treatment with 10 mg/mL sodium borohydride in 0.25 mL of 1M ammonium hydroxide solution and allowed to react for 1 hr. The reduction was quenched by the dropwise addition of glacial acetic acid. After the effervescence stopped, borates were removed by repeated evaporation of 9:1 v/v methanol:acetic acid (0.5 mL; 4x), followed by three evaporations with methanol. Alditols were acylated using 0.1 mL acetic anhydride and 0.02 mL of 1-methyl imidazole and allowed to react for 15 min at room temperature. Water (0.5 mL) was added to each vial, and after 10

min, the alditol acetates extracted with 0.5 mL dichloromethane. Trace amounts of water were removed from the organic extract with anhydrous sodium sulfate, the samples were evaporated to dryness with nitrogen, redissolved in methanol and analyzed by GC. The samples and blanks were run on a HP 5960 gas chromatograph equipped with a Supelco SP-2330 (30 m, 0.25 mm ID, 0.2 μ m film) column and an FID detector (250°C). The temperature program was 55/20/150/4/240(15) (initial T°C/ramp(°C/min)/T°C/ramp/final T°C(hold time)).

2.2.4.2 Lipid Analysis

Lipids released during periodate oxidation of H0200D were analyzed by NMR spectroscopy and GC. After oxidation was complete, the pH of the sample was adjusted to a pH of 3 and the lipids extracted with 1.5 mL perdeuterated dichloromethane. NMR spectra were taken of the aqueous and the organic phases. The organic extract was transferred into a GC vial, evaporated under nitrogen, and silylated by reaction with N,O-bis(trimethylsilyl)trifluoroacetamide (BSTFA) for 15 min at 70°C. The sample was then analyzed on a HP 6890 GC/5973 mass spectrometer (MS) using a DB-XLB column (J&W Scientific, 60 m/0.25 mm ID/0.25 μ m film). Injection was splitless and the temperature ramping was 50(1)/10/320(37) (initial T°C(hold time)/ramp(°C/min)/final T°C(hold time)).

2.3 Results

2.3.1 Ancillary Data

Nuclear magnetic resonance spectroscopy and molecular level monosaccharide analysis of the HMWDOM samples showed the samples are similar to those previously

measured for surface and deep sea HMWDOM (Aluwihare et al., 1997; Aluwihare et al., 2002). All proton NMR spectra show important contributions from carbohydrate (5.5-5.0 ppm, anomeric H (4.5-3 ppm, **H**-COH), acetate (2 ppm, OOCCH₃), and aliphatic proton (1.7-0.9 ppm, CH₂) functional groups. Acetate is most likely bound to the polysaccharide, and aliphatic protons have been attributed to bound lipids (Aluwihare et al., 1997). The surface HMWDOM samples contained 35-38% organic carbon, while the sample from 5200 m contained 21% organic carbon. The C/N ratios for all three samples ranged from 10-12.5. Molecular level analyses of neutral sugars measured using acid hydrolysis yielded approximately equimolar amounts of rhamnose, fucose, arabinose, xylose, mannose, galactose and glucose (Table 2.1). The molar distribution of these seven sugars was similar to those reported in the other marine samples (Aluwihare et al., 1997). Neutral sugars contributed between 12-16% of the total organic carbon in both surface samples, and 3% of the total organic carbon in the deep sea (H995200) sample. Surface samples also contained small amounts of N-acetyl-glucosamine and N-acetyl-galactosamine (Table 2.1).

Table 2.1 Elemental data and monosaccharide distribution for the HMWDOM samples. For monosaccharides, R=rhamnose, F=fucose, A=arabinose, X=xylose, M=mannose, Gal=galactose, Glu=glucose, GluA= glucosamine, GalA= galactosamine, N.D.= not measured.

sample	% C	C/N	monosaccharide data- mole percent									% C as sugars
			R	F	A	X	M	Gal	Glu	GluA	GalA	
H0200D	38	10.6	11	20	9.8	11.1	13.1	17.6	11.5	3.5	2.2	12.4
H0100C	35	12.5	10.7	18.6	10.1	13	13.4	18.3	11.5	2.4	1.9	16.3
H995200	21	10	14.7	26	8.1	8.6	19.1	11.5	12.1	N.D.	N.D.	2.9

2.3.2 Periodate Over-Oxidation Data

2.3.2.1 Carbohydrate and Amino Acid Standards

Carbohydrates and a protein of known composition were used to experimentally determine the reaction stoichiometry for periodate oxidation (Table 2.2). The stoichiometric ratios for periodate and glucose were calculated by assuming that all of the standard was completely oxidized, and that all of the periodate removed was used by the over-oxidation process during the reaction. Periodate oxidation of glucose yielded a reaction stoichiometry of 5:1 (moles of periodate: moles of glucose), in agreement with previous reports (Sklarz, 1967). Laminarin, amylose, and maltooligoaccharide, all linear homopolysaccharides of glucose, yielded periodate:glucose ratios ranging from 5.8 to 6.7 with an average for the three polysaccharides of 6.2 ± 0.5 . Excess periodate is needed to depolymerize the polysaccharide compared to the monosaccharide, resulting in an apparent over-oxidation (Figure 2.2b, adapted from Whelan, 1964). When the periodate utilization was evaluated on a per carbon basis (6 carbon per glucose), the periodate demand for the polysaccharide standards is correspondingly greater than for glucose. NMR spectra of the final reaction solution compared to the initial compound confirmed complete over-oxidation as carbohydrate peaks in the 3-4 ppm range were completely removed.

Table 2.2 The periodate:glucose and periodate:amino acid stoichiometric ratios calculated for the glucose, polysaccharide and albumin standards, along with the periodate demand per glucose or amino acid carbon.

sample	Stoichiometry* (replicates)	Periodate per carbon**
glucose	5 (n=1)	0.8
Amylose	6.7±0.4 (n=3)	1.1
Maltooligosaccharide	6.2±0.5 (n=6)	1.0
Laminarin	5.8±0.9 (n=3)	1.0
Polysaccharide average	6.2±0.5	1.0
Albumin	0.6±0.1 (n=3)	0.1

* Periodate to glucose stoichiometry calculated by dividing moles of periodate lost by the moles of glucose calculated using an assumed molecular weight of 162 D. For the albumin sample, an average amino acid molecular weight of 100 D was used. Complete oxidation of the standards by periodate was assumed.

** Periodate use per carbon is the periodate demand per carbon per glucose unit. For the polysaccharides, there are 6 carbons per glucose unit. For albumin, an average of 4.8 carbon per amino acid was used.

Bovine serum albumin had a reaction stoichiometry of 0.6:1 periodate to amino acid, significantly less than that of carbohydrates. This value was well below the expected yield for complete oxidation based on the amino acid structure indicating that proteins were not extensively oxidized by periodate under our experimental conditions, consistent with previous reports (Clamp and Hough, 1965; Pascual and Herraez, 1985; Pascual et al., 1989). The periodate demand on a per carbon basis, calculated by assuming 4.8 carbons per amino acid, was also extremely low. Proteins are not a major sink for periodate in our HMWDOM samples due to the low consumption of periodate by

protein, and the relatively small amount of proteins in HMWDOM (McCarthy et al., 1997). Since the major use of periodate occurs during carbohydrate oxidation and unknown material, all subsequent calculations ignore the contributions of amino acids to periodate removal.

2.3.2.2 HMWDOM Data

To calculate the stoichiometry of periodate oxidation of HMWDOM carbohydrates in surface samples, the amount of carbohydrate in each sample was determined using ^{13}C NMR spectroscopy as the ratio of anomeric (110 ppm) and COH carbon (70 ppm) to the total area of the spectra (200-0 ppm) (Figure 2.3). Surface water samples H0100C, H0200D and H0200C were between 70-75% carbohydrate. There was insufficient sample to collect a ^{13}C NMR spectrum of H995200, the 5200 m sample, and it was assumed a percent carbohydrate carbon value of 45% based on the ^{13}C NMR spectrum of a companion sample collected at 1800 m. This is the same value as obtained by integration of the HCOH peak (4.5-3 ppm) from the ^1H NMR spectrum for H995200. Both the 1800m and 5200 m deep water samples had comparable ^1H NMR spectra, monosaccharide distributions and yields, as well as C/N ratios.

For all three HMWDOM samples used in this study (H0100C, H0200D and H995200), the periodate: 'glucose' stoichiometric ratio of oxidation (Table 2.3) was larger than the ratio determined for glucose and glucose homopolysaccharide standards (Table 2.2). Again, it was assumed that the entire carbohydrate fraction as calculated from ^{13}C NMR spectroscopy was over-oxidized to completion by periodate, and all periodate lost was due to the reaction with the carbohydrates. Surface seawater samples had a lower

stoichiometric ratio (7.2-9.9) than H995200 (18:1). When the periodate utilization for each sample was calculated by dividing the periodate consumed by the total amount of

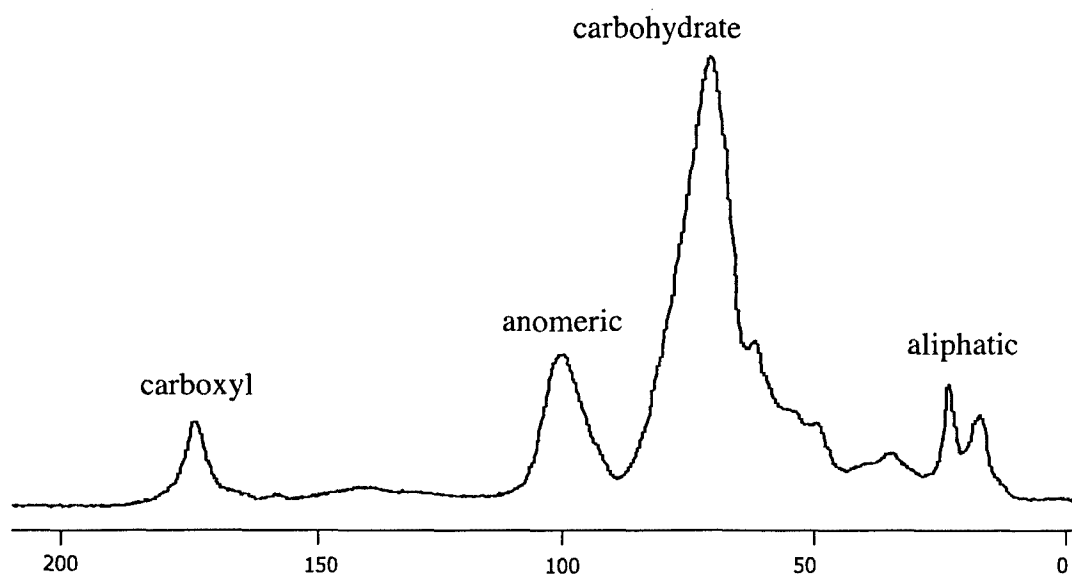
Table 2.3 Data from the periodate over-oxidation of H0100C, H0200D and H995200 HMWDOM samples. The calculations for μmol glucose in sample are based on the percent carbohydrate of the total carbon from ^{13}C NMR analysis: 70% for H0100C, 75% for H0200D and 45% for H995200.

HMWDOM samples	mg sample	mmol periodate	%C in sample	μmol 'glucose' in sample	μmol periodate used	Stoichiometric periodate:glucose ratio	Periodate: total carbon ratio
H0100C	1.08	0.09	35	4.41	31.75	7.2:1	1:1
H0100C	1.2	0.09	35	4.90	27.54	5.6:1	0.8:1
H0100C	14.9	0.66	35	60.8	599.47	9.9:1	1.4:1
H0100C	15.0	0.66	35	61.2	558.51	9.1:1	1.3:1
H0100C	15.0	0.66	35	61.2	531.47	8.7:1	1.2:1
H0100C	14.8	0.66	35	60.4	553.43	9.2:1	1.3:1
average						9.1:1	1.2:1
H0200D	54.8	2588.25	38	260.08	2216	8.5:1	1.3:1
H0200D	55.3	2588.25	38	262.46	2236	8.5:1	1.3:1
H0200C	14.9	0.66	38	70.7	609.68	8.6:1	1.3:1
H0200C	14.9	0.65	38	70.7	600.36	8.4:1	1.3:1
H0200C	15.0	0.66	38	71.2	607.98	8.5:1	1.3:1
H0200C	14.6	0.66	38	69.3	611.41	8.8:1	1.3:1
average						8.6:1	1.3:1
H995200	7.33	1285.71	21	21.38	172	18:1	1.3:1

organic carbon in the sample, the periodate demand on a per carbon basis for the surface and deep water HMWDOM samples was approximately equal, with the exception of the two small H0100C sample reactions (1.08 g and 1.2 g), which had lower periodate:total carbon ratios. This was probably due to the inaccuracy of weighing such small HMWDOM samples rather than differences in the periodate reaction. If these small sample ratios were not included in the H0100C average, the periodate demand per carbon for H0100C rises slightly to 1.3:1, the same as for the other surface water HMWDOM

sample. The fact that the periodate:glucose ratio for deep sea HMWDOM is higher than the surface ratios while the periodate utilization on a per carbon basis is the same for both

Figure 2.3: Solid state ^{13}C NMR for surface water H0200 HMWDOM sample. The functional group assignments for each peak are also marked.



samples may be an artifact of the low amount of carbon that can be assigned to carbohydrate in the deep HMWDOM sample. The amount of carbohydrate in the deep sample was calculated based on the COH peak area in the ^1H NMR spectrum. This deep water ^1H NMR spectrum has a relatively higher baseline of carbon than cannot be assigned to any particular peak than the surface HMWDOM ^1H NMR spectrum. As a result, integration of the COH peak may underestimate the total amount of carbohydrate carbon present.

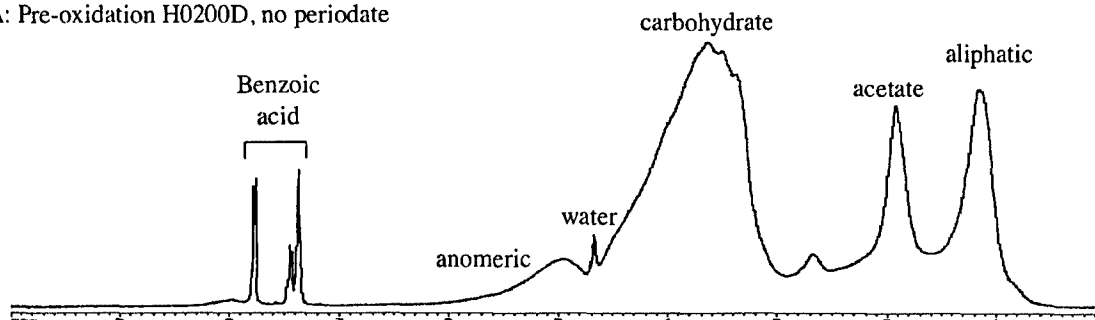
Proton NMR spectroscopy was used to monitor changes in functional groups abundances within HMWDOM during oxidation of sample H0200D (Figure 2.4). Figure 2.4a shows the baseline NMR spectrum of H0200D before addition of periodate. This

spectrum is characteristic for marine HMWDOM, with the presence of peaks representing anomeric (5.5-5.0 ppm), HCOH (4.5-3.0 ppm), acetate (2.0 ppm) and aliphatic (1.7-0.9 ppm) hydrogen atoms (Aluwihare et al., 1997). In comparison, the NMR spectrum taken an hour after periodate addition (Figure 2.4b), showed a decrease in anomeric (5.5-5 ppm), HCOH, (4.5-3 ppm) and aliphatic (1.7-0.9 ppm) functional groups. Formic acid, acetic acid and acetate, important over-oxidation products of the HMWDOM and periodate reaction, appeared as sharp singlets at 8.2 ppm, 2.0 ppm and 1.9 ppm respectively. The acetic acid and acetate form two separate peaks due to the pH of the reaction solution, which was approximately pH 4.5. After 2 days, the amounts of anomeric, HCOH and aliphatic hydrogen had decreased further (Figure 2.4c), and after 10 days (Figure 2.4d) the reaction was complete and only small carbohydrate and aliphatic peaks remained, with the bulk of the HMWDOM oxidized completely. A peak at 3.2 ppm also appeared in the ^1H spectra after 2 days, indicating the presence of methanol liberated from methyl sugars by the periodate over-oxidation reaction. In addition, there was also a decrease in the broad baseline of the spectra, though this was not completely eliminated. This experiment was repeated with the H0100C and H995200 sample with similar results. The decrease in the baseline between the initial and the final ^1H NMR spectra was even more evident in the H995200 sample (Figure 2.5a and 2.5b).

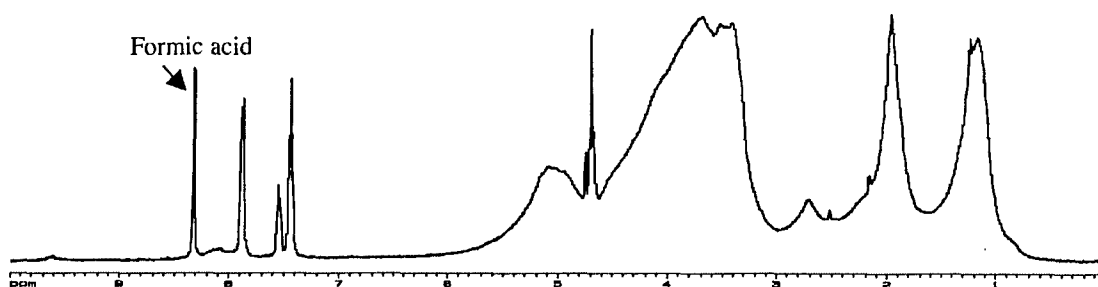
By integrating the ^1H NMR spectrum, the changes in hydrogen functional group abundance during the course of HMWDOM oxidation by periodate can be quantitatively measured (Figure 2.6a). All peak areas were normalized to benzoic acid (8 ppm and 7.6-7.4 ppm), which was added as an internal reference immediately prior to spectral

Figure 2.4 Series of ^1H NMR spectra of the periodate over-oxidation of H0200D surface HMWDOM. The initial spectrum (A) was taken before the addition of periodate. The other spectra were taken from subsamples of the oxidation reaction after 1 hour (B), 2 days (C), and after 10 days (D).

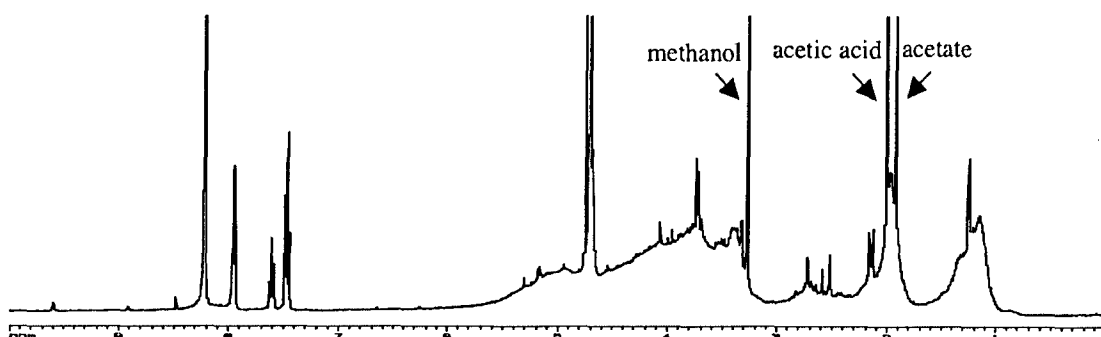
A: Pre-oxidation H0200D, no periodate



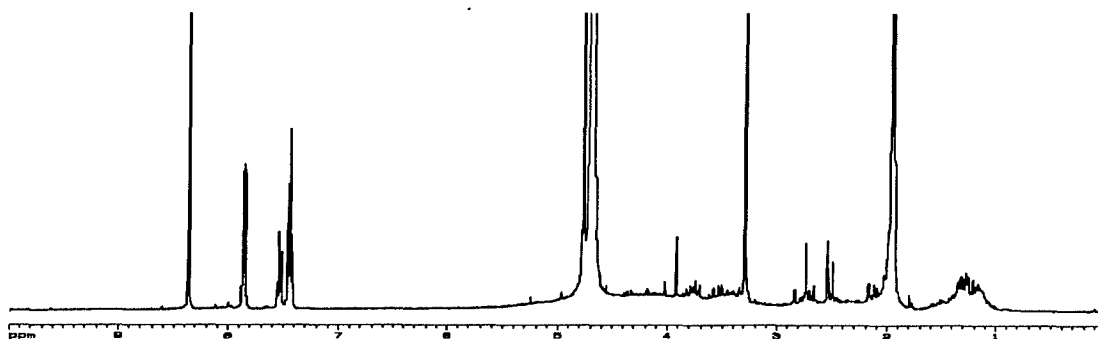
B: Oxidation after 1 hour



C: Oxidation after 2 days



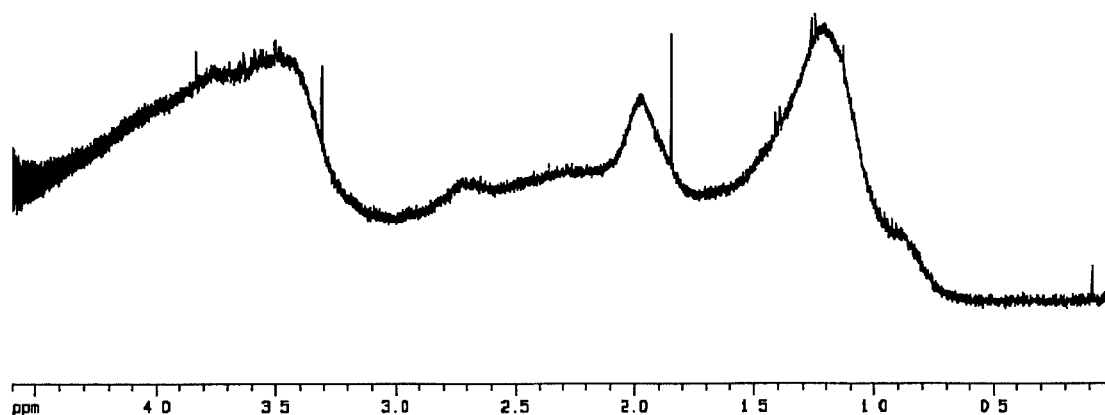
D: Oxidation after 10 days



acquisition. Figure 2.6a shows a histogram of the peak areas from each time point for each of the main functional groups of HMWDOM: anomeric (5.5-4.5 ppm), HCOH (4.5-3.0 ppm), acetate (2.0 ppm) and aliphatic (1.7-0.9 ppm). Over the course of a 10 day reaction of periodate with H0200D HMWDOM, the anomeric, HCOH, and aliphatic

Figure 2.5 Excerpts from the ^1H NMR spectra of the periodate over-oxidation of H995200 deep water HMWDOM. The initial spectrum (A) was taken before the addition of periodate. Spectrum B was taken after 9 days of oxidation.

A: Pre-oxidation H995200, no periodate



B: Oxidation after 9 days

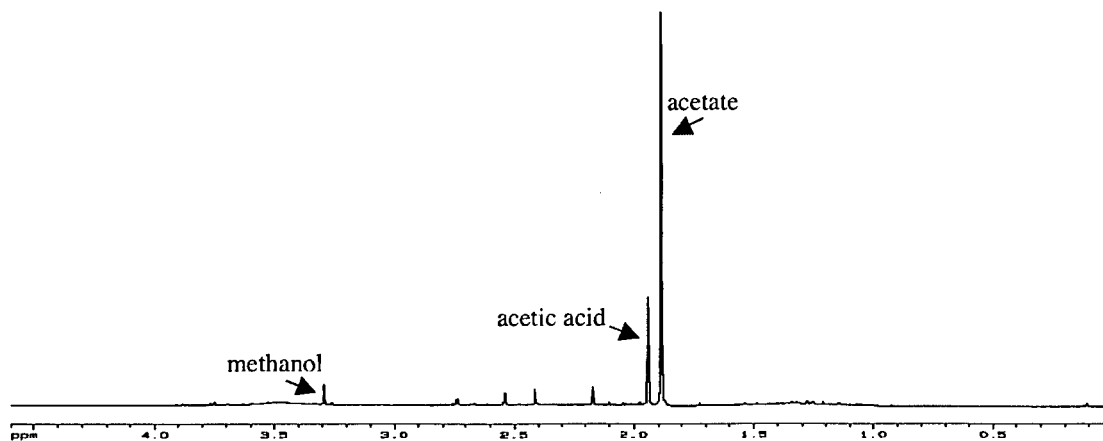
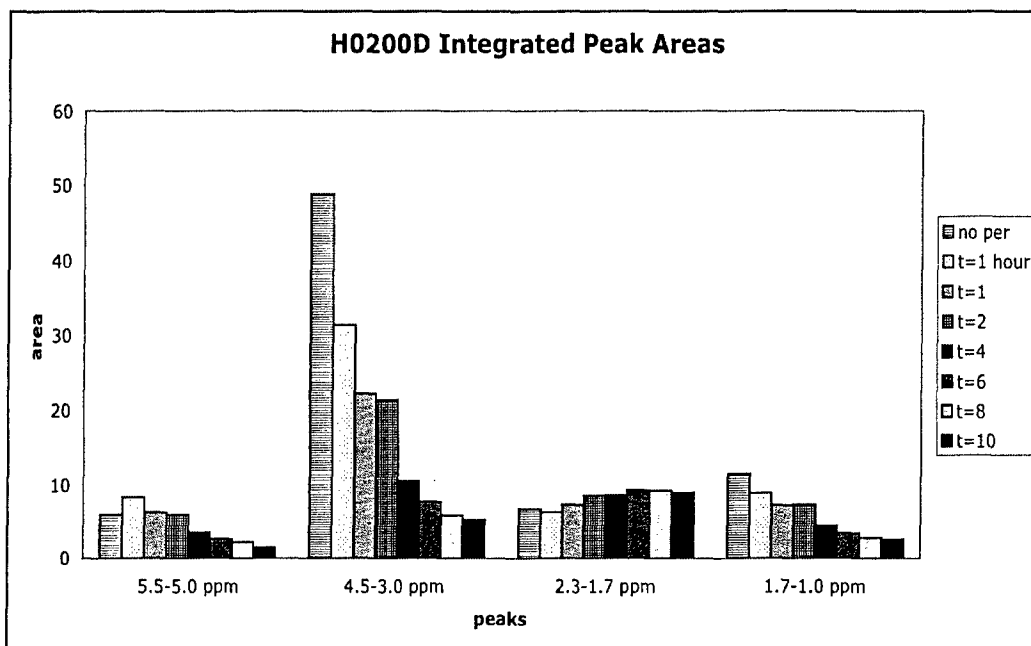


Figure 2.6 Histograms of the change in ^1H functional group peak areas over the course of the H0200D oxidation (A), and the H995200 oxidation (B).

A: H0200D periodate oxidation



B: H995200 periodate oxidation

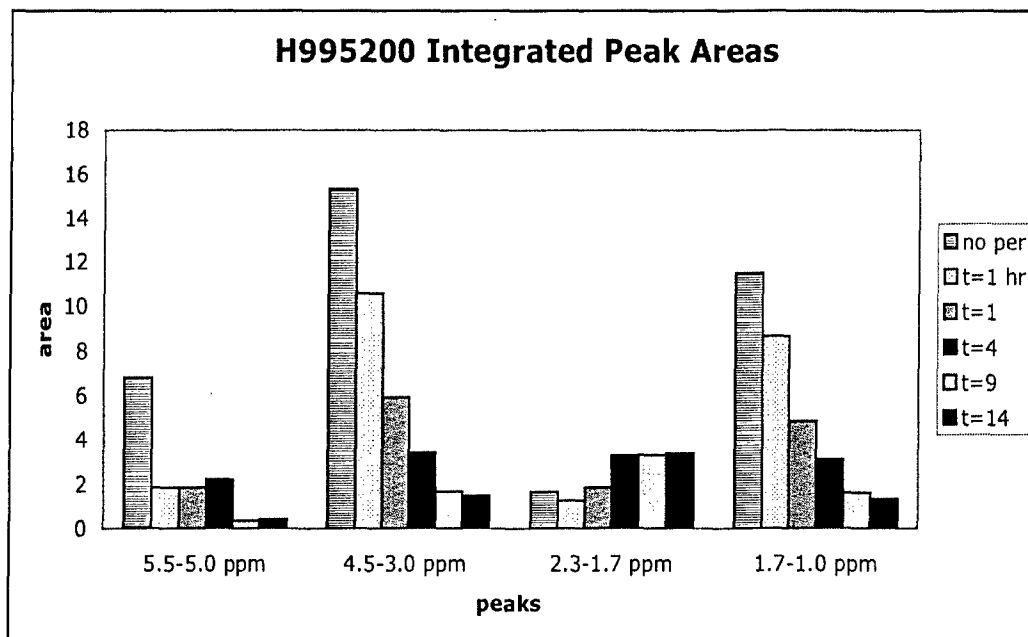
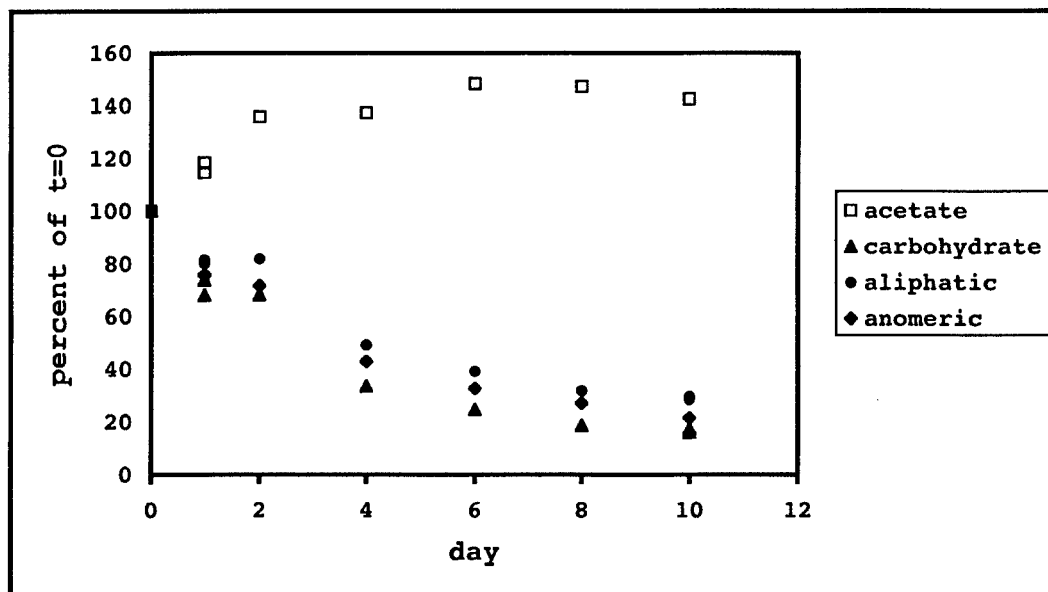
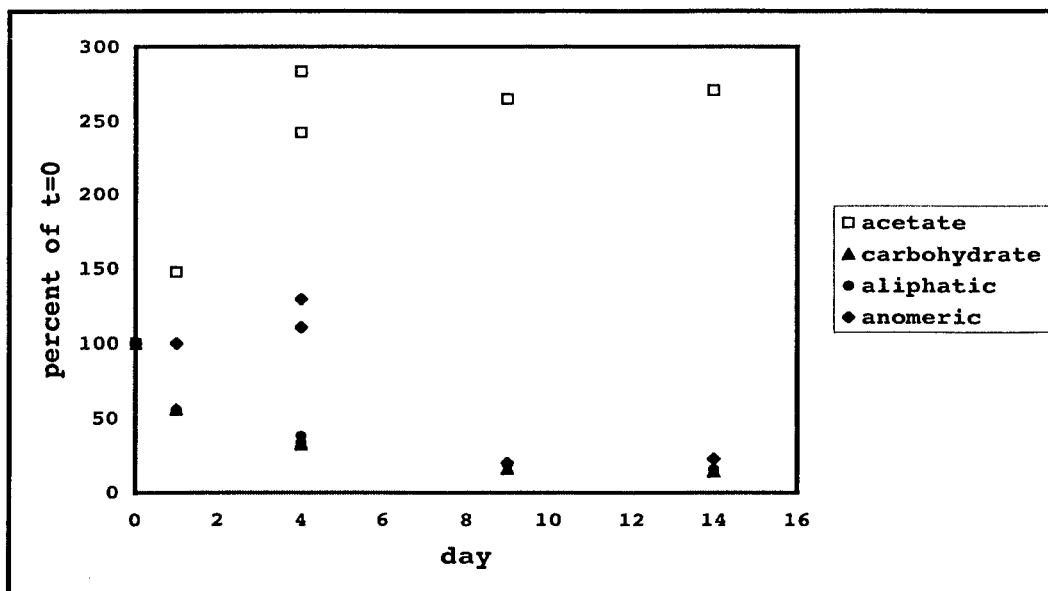


Figure 2.7 Percent change relative to the initial values for the functional groups present in H0200D (A) and H995200 (B) during the course of periodate oxidation.

A: H0200D over-oxidation



B: H995200 over-oxidation



functional groups decreased sharply, while the formic acid and acetic acid plus acetate peaks increased in area. Compared to the pre-reaction H0200D spectra, periodate

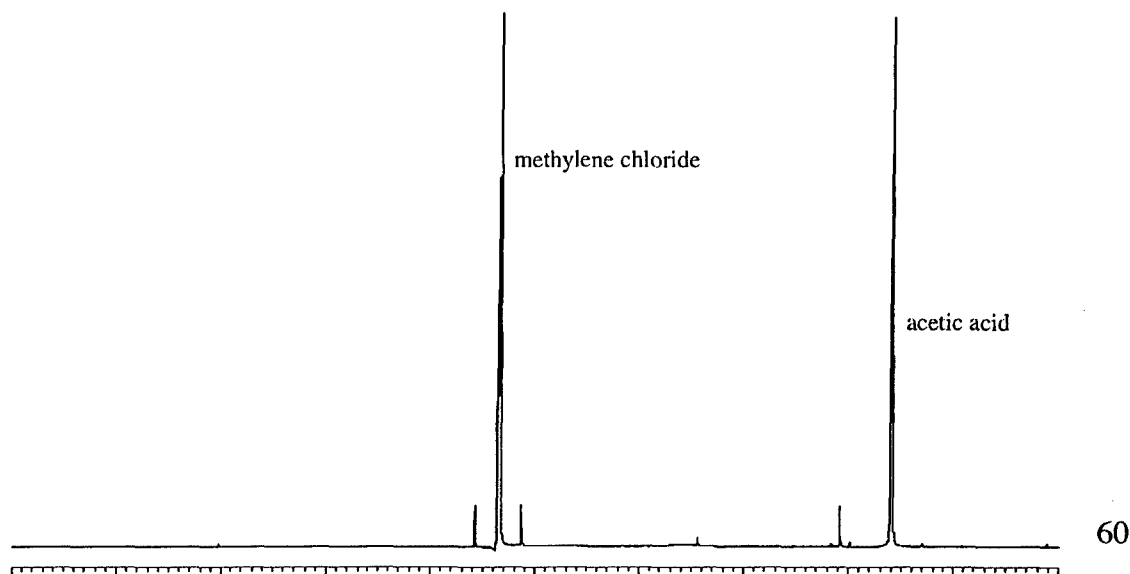
oxidation had removed approximately 85% of the anomeric, carbohydrate and aliphatic peaks, while the acetate peak had increased by 40% (Figure 2.7a). The similarity of the percent change between each type of functional group indicates a common process of alteration.

Similar results were obtained for the deep ocean sample, H995200. Figure 2.6b shows the decrease in peak area for anomeric, HCOH , and aliphatic functional groups with periodate oxidation, and nearly two fold increase in the amount of acetic acid and acetate for the deep HMWDOM sample. Analysis of the change in functional groups over the course of the reaction showed that the anomeric, carbohydrate and aliphatic peaks decreased by 80%, while the area of the acetate peak tripled (Figure 2.7b).

2.3.2.3 Lipid Analysis

Lipid analysis was also performed on one H0200D sample after periodate over-oxidation. After the 10 day over-oxidation procedure, the sample was acidified and lipids

Figure 2.8 The ^1H NMR of the methylene chloride extracted fraction of the H0200D sample reaction solution after the completion of the over-oxidation reaction.



extracted into d_2 -methylene chloride. The NMR spectrum of the organic layer showed the presence of acetate (1.6 ppm), but no aliphatic compounds such as fatty acids (Figure 2.8). Further analyses of the persilylated extracts by gas chromatography showed no GC-identifiable lipids were liberated by oxidation.

2.3.2.4 Octyl- β -glucopyranoside Oxidation

Periodate should not oxidize any molecule that does not contain vicinal glycols or other immediately adjacent oxidizable functional groups. In order to determine whether longer duration periodate oxidation experiments conducted at relatively high temperatures had any effect on any lipid components within HMWDOM, octyl- β -glucopyranoside (OGP) was reacted with periodate. Theoretically, periodate oxidation would oxidize the glucose part of the molecule, releasing octanol. Experiments performed with concentrations of OGP equal to that of the other standards but resulted in the formation of a separate, immiscible organic phase. As a result of this phase separation, the NMR spectra were not quantifiable since the amount of octanol in the aliquots of reaction solution varied during the course of the experiment. Further experiments with lower concentrations of OGP showed the complete removal of all functional groups after oxidation, including the aliphatic peaks assigned to the C_8 alkyl chain.

2.4 Discussion

Periodate oxidation of neutral sugars such as glucose is a simple reaction with a fixed stoichiometry, requiring one periodate molecule to break one carbon-carbon bond (Figure 2.2a). The reaction of periodate with polysaccharides is more complicated, as

illustrated for maltotriose in Figure 2.2b (Whelan, 1964). In the over-oxidation of simple polysaccharides, the reaction proceeds as expected until all readily oxidized vicinal alcohols are oxidized (Figure 2.2b, Step 2). Simple oxidation would stop at this point, and yield a polyaldehyde as the product. However, the carbon bonded to an activated hydrogen (Figure 2.2b, Step 3, marked by a circle) is oxidized by periodate and converted to an alcohol, allowing the oxidation to continue. This results in the oxidative removal of one glucose monomer unit from the polysaccharide (Figure 2.2b, Step 4). Repetition of steps 2 and 3 gradually oxidizes the entire polysaccharide to formic acid, formaldehyde, and carbon dioxide. This process of over-oxidation is the main reaction that occurs during the reaction of HMWDOM with periodate.

The periodate oxidation reaction was monitored using two methods. UV-Vis spectroscopy was used to measure the loss of periodate and the production of its reduced form, iodate. Measurements of the periodate content in the oxidation solution during the course of the reaction provided information about the extent of reaction at any particular time, and the periodate to 'glucose' stoichiometric ratio.

While UV-vis spectroscopy provides a quick way to track the progress of the oxidation reaction, this spectroscopic technique cannot offer any information regarding the products of the reaction. Additional monitoring of the reaction using proton NMR spectroscopy serves two purposes. Since HMWDOM has a very characteristic NMR spectrum with little variation between samples, integration of the peaks in the NMR spectra during the reaction can be used to quantitatively determine the changes in the functional groups present due to oxidation. NMR can also be used to identify possible products, especially the ubiquitous ones such as acetic acid, methanol and formic acid

(Hirano et al., 1974). Both NMR and UV-Vis spectroscopy are ideal for monitoring the over-oxidation reaction as they can be used while the oxidation is in progress without quenching the periodate oxidation, and these spectroscopy techniques do not require additional chemical processing.

While NMR spectra of HMWDOM indicate the presence of large amounts of COH-type functional groups, conventional methods of acid hydrolysis have been unable to liberate the equivalent concentrations of monosaccharides from the larger macromolecule. The unidentified fraction of HMWDOM, as determined by NMR spectroscopy (Section 2.1.2) shows an anomeric to carbohydrate carbon ratio of 1 to 5, characteristic of carbohydrates. The periodate over-oxidation technique used in this chapter supported the hypothesis that the unknown fraction was predominately carbohydrate through complete removal of the carbohydrate signal (5.5-5.0 ppm, 4.5-3.0 ppm) seen in the ^1H NMR spectrum. At the same time, the increase in peaks corresponding to the formyl (8.2 ppm) and methyl (2.0 ppm and 1.9 ppm) hydrogens indicated the presence of formic acid, acetic acid, and acetate products produced by the oxidation (Figure 2.4). Coincident with the changes seen in the NMR spectrum, UV-Vis spectroscopy showed that the amount of periodate in the sample solutions also decreased, indicating that the loss of carbohydrate seen in the NMR spectrum and the drop in periodate were related. Duplicate samples for NMR spectroscopy were taken at certain timepoints during the experiment; these had an error of approximately 8% in the integrated peak area.

Additional characteristics of this periodate oxidizable carbohydrate fraction of HMWDOM can be inferred by comparing the periodate:glucose ratios from the

HMWDOM samples and known mono- and polysaccharides. The periodate:glucose ratio for HMWDOM samples was consistently higher than the average periodate: glucose stoichiometric ratio of 6.2:1 determined using polysaccharide standards. The deep water H995200 yielded a sample ratio of 18:1, approximately twice that of the surface water samples (7.2-9.9:1). On a per carbon basis, HMWDOM samples required more periodate per carbon (1.3 periodate per carbon) than the average polysaccharide standard (1.0 periodate per carbon). Since so little of the actual structure of HMWDOM is known, it is impossible to assign conclusively one specific reason for the difference in periodate demand between standards and samples. The most likely explanation lies in the complexity of the HMWDOM polysaccharide structure. This can be illustrated by comparing the periodate demand for complete monosaccharide oxidation versus that for linear polysaccharide standards. The periodate:glucose ratio for glucose is 5:1, while the average periodate demand for laminarin, maltoligosaccharide, and amylose starch is 6.2 periodate for every glucose unit (Table 2.2). Since the only difference lies in the connectivity of the glucose, the extra periodate must be needed to convert a hydrogen atom on an activated carbon to a hydroxyl group, allowing the over-oxidation to continue to break apart the polysaccharide chain (Figure 2.2b). If each additional degree of structural complexity requires more periodate per glucose unit for complete over-oxidation, it can be concluded that HMWDOM structure is more highly branched and crosslinked than a straight chain polysaccharide. All of the polysaccharide standards used in this study were too simple in structure and composition to accurately represent HMWDOM. Laminarin, maltoligosaccharide and amylose starch are all linear glucose homopolymers. The periodate demand per carbon for these linear monosaccharides with

each monomer attached to two others was 1:1, higher than that of the glucose monomer alone (0.8:1). Based on the HMWDOM average periodate:carbon ratio of 1.3:1, each monosaccharide within the HMWDOM macromolecule could be crosslinked, with branching at all possible carbons, . HMWDOM, on the other hand, is thought to be extremely heteropolymeric, containing hexosamines, uronic acids, and at least seven different neutral monosaccharides with extensive cross linking (Aluwihare et al., 1997; Aluwihare, 1999). For example, a methyl sugar monomer theoretically utilizes an additional periodate relative to glucose for complete oxidation. As a result, it seems likely that more periodate per glucose unit was required to over-oxidize HMWDOM due to its complex structure. It is also possible that other types of as yet unknown compounds are present in HMWDOM that require a greater amount of periodate to be over-oxidized. The highly complex and heterogeneous state of HMWDOM may be a factor in the inability of usual hydrolysis techniques to account for all of the carbohydrate seen in NMR spectra.

The presence of amino acids in HMWDOM does not have a significant affect on the periodate stoichiometry of the oxidation reaction. Some amino acids such as proline, threonine and serine consume two moles of periodate per mole of amino acid oxidized (Pascual and Herraiez, 1985; Pascual et al., 1989), while other amino acids, such as glutamic acid are less easily oxidized (Clamp and Hough, 1965). The extremely low ratio of periodate to amino acid, along with the relatively small amount of amino acids in HMWDOM suggested that periodate consumption by amino acids was insignificant. As shown using a bovine albumin standard, proteins and amino acids present in the HMWDOM sample would also be oxidized by periodate, but the effect of these

compounds on the calculated amount of HMWDOM oxidized was minimal. Based on measurements of amino acids released by acid hydrolysis methods, amino acids make up less than 20% of the total organic nitrogen and less than 5% of the total organic carbon in samples H0200D, H0100C and H995200 (Aluwihare, 1999). In addition, the stoichiometry for amino acid oxidation is less than 0.6:1 periodate: amino acid, based on experiments with bovine serum albumin measured by the same method as the polysaccharide standards reported in this chapter. The combination of these two factors indicates that the majority of the periodate consumed during reaction was not used to oxidize amino acids. It is therefore unlikely that the unknown fraction contains significant amounts of amino acids.

One of the more interesting results from the periodate over-oxidation of HMWDOM samples was the decrease in the aliphatic hydrogen peak (1.7-1.0 ppm) in the proton NMR spectrum. This was seen both in the surface and deep samples. It has long been assumed that this peak represents the "lipid" fraction of HMWDOM (Aluwihare et al., 1997; Aluwihare and Repeta, 1999; Hedges et al., 2001). Some fatty acids and other lipid types have been identified, but these constitute less than 1% of the total carbon (Mannino and Harvey, 1999; Wakeham et al., 2003). In his ^{13}C NMR-based model of the composition of particulate organic carbon, Hedges et al. (2001) assigns the 'lipid' component the structure of stearic acid. While there are significant compositional differences between particulate and dissolved organic matter, the ^{13}C NMR spectra for both contain very similar peaks in the aliphatic carbon region. Other studies assign the aliphatic peak to low-molecular weight non-acetate lipids or the muramic acid component of peptidoglycan (Aluwihare et al., 1997; Benner and Kaiser, 2003) based on proton

NMR spectra and chemical analysis. While it has become generally accepted that these aliphatic peaks are assigned to lipids, the concentration of isolated lipid compounds are insufficient to account for the relative size of the peaks in the NMR spectra.

Since periodate cannot theoretically oxidize molecules that lack vicinal diols or similar substituents, the drastic decrease of this aliphatic peak indicates that the majority of the signal must come from periodate oxidizable molecules. Periodate oxidation will not oxidize fatty acids and other lipid compounds; unsaturated lipids would be slowly oxidized but are not seen in the NMR spectra of HMWDOM. To test the behavior of periodate on lipid compounds, octyl- β -glucopyranoside (OGP), a glucose molecule with an ether-linked eight carbon lipid chain attached at the C1 position was over-oxidized using the same procedure as the HMWDOM samples. The anomeric and COH peaks in the proton NMR spectra decreased during the course of the experiment as expected due to the oxidation of the glucose molecule. While the aliphatic peak also decreased, the percent decrease was significantly smaller. In addition, a second non-miscible phase appeared in the D₂O solution during reaction and increased as the oxidation of OGP progressed. Therefore, the decrease of the aliphatic peak is probably due to phase separation of the aliphatic portion of OGP from the polar reaction solution, and not due to the oxidative breakdown of the alkyl chain by periodate. In order to prevent the released octanol from forming a separate phase, the periodate oxidation was repeated with OGP and periodate concentrations 100 times lower than that of those used for the glucose and polysaccharide standards. The results for this lower concentration experiment were more ambiguous in that the proton NMR spectra at the end of 14 days showed a complete removal of all OGP functional group signals, including those in the aliphatic region. This

inability to obtain the predicted results for the reaction of OGP with periodate requires further investigation. The disappearance of the octanol product during periodate oxidation was unexpected, especially as periodate oxidations can be performed in alcohol/water mixtures (House, 1972). The concentration of octanol produced was within the solubility range for octanol in water, and should have been seen in the NMR spectrum. The most likely explanations are that the octanol was volatilized during the reaction or remained on the walls of the reaction vials and was not included in the aliquot removed for NMR spectroscopy. This contradiction of the expected result of periodate oxidation could possibly be resolved by oxidizing octanol or other lipid compounds with periodate, adding a little methanol to the reaction solution to increase the solubility of the organic products, or using methylene chloride to extract the octanol from the aqueous solution. However, reaction solutions for HMWDOM oxidation showed no evidence of a second phase, and the rate of decrease in the aliphatic peak seen in the NMR spectra during the reaction was similar to those of the anomeric and carbohydrate peaks.

In addition, solvent extraction of oxidized samples did not show any appreciable amounts of lipids. This confirms previous studies indicating that lipids make up only a minute portion of HMWDOM carbon. Aluwihare (1999) used diethyl ether to extract previously hydrolyzed HMWDOM samples but could not detect the presence of any fatty acids using either gas chromatography or proton NMR spectroscopy. Ether cleavage of HMWDOM using BBr_3 also failed to yield any lipids. Two studies measuring lipids in dissolved organic matter using coastal ocean samples were able to detect the presence of several types of lipids in the fraction of DOM from 0.2 μm to 1000 Da, including various saturated and unsaturated fatty acids, methyl esters, and sterols (Mannino and Harvey,

1999; Wakeham et al., 2003). However, the total lipid concentration, excluding hydrocarbons, was less than 2% of the total organic carbon present in the samples, and the samples had not been pre-extracted to remove associated, but unbound, lipids. Isolation of the bulk lipids from HMWDOM using solvent extraction with a mixture of methylene chloride and methanol yielded a fraction that ranged from 0.1-0.3% of the HMW dissolved organic carbon at various depths (Loh et al., 2004). These low concentrations of lipids seem unlikely to be the sole source of the intense aliphatic signal found in proton NMR spectra of HMWDOM. It is also unknown whether these lipids are chemically bound into the macromolecular HMWDOM structure or merely physically associated with this fraction.

While the nature of the periodate reaction means that the molecular level structural composition of HMWDOM cannot be conclusively determined, the data from the periodate over-oxidation experiments provides a set of criteria that proposed compounds must meet. Evaluation of UV-Vis and NMR spectroscopy data shows that the majority of the carbon consists of periodate oxidizable compounds, confirming the presence of a significant amount of unidentified carbohydrates as seen in HMWDOM NMR spectra. Comparison of periodate:glucose ratios from standards and from HMWDOM surface and deep samples indicates that HMWDOM is highly branched in structure. In addition, the components that resonate in the aliphatic region of the proton NMR spectra are also periodate over-oxidizable, and therefore cannot be due to large concentrations of lipids and fatty acids as previously assumed. Therefore, candidate molecules must have a sugar-like ratio of anomeric to carbohydrate carbons, must be

periodate oxidizable, and must contain an aliphatic functional group that is converted to another type of carbon, probably a carboxylic acid group, after oxidation.

Based on the above constraints, it is proposed that the most probable contributor to the uncharacterized fraction of HMWDOM are 6-deoxysugars. These compounds contain an aliphatic functional group on carbon number 6 but are also oxidizable by periodate. Two such sugars, fucose and rhamnose, have already been measured in acid hydrolyzed HMWDOM, and deoxysugars have been detected by direct temperature-resolved mass spectrometry (DT-MS) of HMWDOM and DOM fractions separated by high performance size-exclusion chromatography (HPSEC) (McCarthy et al., 1996; Aluwihare et al., 1997; Boon et al., 1998; Aluwihare et al., 2002; Minor et al., 2002). Deoxysugars, like all other saccharides, contain vicinal glycol groups, a necessary condition for periodate oxidation. The products of deoxysugar oxidation are formic acid and acetic acid plus acetate, which increase in the proton NMR spectra over the duration of the experiment. Of particular interest are deoxysugars where the alcohol group has been removed from the C-6 carbon, similar to fucose and rhamnose. The hydrogens of the methyl group have a chemical shift in the aliphatic region (1.3 ppm). After oxidation, the C-5 carbon and its attached methyl group is converted by periodate to acetic acid. The distribution between acetic acid and acetate is dictated by the pH of the sample. This has the effect of removing the signal attributed to these hydrogens from the aliphatic peak in the proton NMR spectra and shifting it into the acetate region, matching the trends shown in the NMR data for HMWDOM oxidation. Deoxysugars with the alcohol group removed from positions other than C-6 do not fulfill all of the criteria determined by periodate over-oxidation, as the carbons from which the -OH group was removed

continue to resonate in the aliphatic region in the form of propanedioic (malonic) acid.

Methyl sugars cannot not sufficiently explain the patterns seen in the NMR spectra as the initial hydrogen signal of the $-OCH_3$ group does not fall into the aliphatic regions (Table 2.4). However, methyl sugars may also be a significant component of HMWDOM as the main source of the methanol (3.2 ppm) that results from the periodate over-oxidation reaction.

Table 2.4 Evaluation of three different possible source structures for the aliphatic carbon present in the HMWDOM sample based on the criteria from the results of periodate over-oxidation experiments.

structure	Periodate oxidizable?	Sugar-like anomeric:COH ratio?	Removal of aliphatic peak?	Products	Other data
Fatty acid	No	No	No	N/A	Total lipid conc <2% (Mannino and Harvey, 1999)
Methylsugar	Yes	Yes	No	Formaldehyde Formic acid methanol	Some methanol released during oxidation
Deoxysugar	Yes	Yes	Yes	Formic acid Acetic acid	Some evidence from hydrolysis; 2D NMR?

A rough estimate of the percentage of 6-deoxysugars present in the surface samples can be calculated using the HMWDOM proton NMR spectra. The ratio of carbohydrate:acetate:aliphatic carbon for surface seawater is 8:1:1. Carbohydrates (HCOH) are approximately 70% of the total organic carbon, and correspondingly 70% of

the total hydrogen. The remaining acetate and aliphatic peaks in the hydrogen NMR spectra constitute 15% of the total hydrogen each. An upper limit can be determined by assuming that the aliphatic peak is assigned to the CH_3 group in the C-6 position of deoxysugars; this peak then represents 5% of the total organic carbon. Since each deoxysugar contains 5 carbon atoms in addition to the methyl group, the total deoxysugar fraction would comprise up to 30% of the total organic carbon. This number corresponds well with measurements of neutral monosaccharides (20%), estimates of amino sugars (30%), and leaves a remaining 10% of the total organic carbon for amino acids, lipids, and other as yet unidentified compounds. This concentration of 6-deoxysugars should be considered a maximum value, since the generation of methanol during oxidation indicates the presence of methyl sugars in these HMWDOM samples. Based on the ^1H NMR peak area ratio for methanol to acetic acid plus acetate, there would be one methyl sugar per every 5 6-deoxysugars. If the concentration of 6-deoxysugars is 30% of the total carbon, the percentage of methyl sugars is approximately 6% of the total carbon.

The ^1H NMR spectra taken during the periodate oxidation of the deep water H995200 HMWDOM sample also shows the presence of 6-deoxysugars and methyl sugars. Compared to the surface sample, the amount of acetic acid plus acetate generated during periodate oxidation is much greater compared to the surface sample (Figure 2.7 B), suggesting a higher relative concentration of 6-deoxysugars. This is supported by the carbohydrate:aliphatic peak ratio for the sample of 1.3:1, calculated from the ^1H NMR spectra. This 1.3:1 carbohydrate:aliphatic ratio is the same as that for deoxysugars, which have 4 carbohydrate hydrogen atoms for every three aliphatic hydrogen atoms. Based on the ratio of methanol to acetic acid/acetate in the final ^1H NMR spectra taken

during the periodate oxidation, the deep water HMWDOM has a methyl sugar to 6-deoxysugar ratio of 1:41.7, nearly 8 times more deoxysugar per methyl sugar than in the surface HMWDOM. While the comparison between surface and deep HMWDOM sample is limited due to slightly different NMR instrument settings, the higher concentration of 6-deoxysugars in the H995200 sample is logical, since the amount of unidentified material is larger in the deep HMWDOM samples compared to surface HMWDOM. For example, neutral sugars released by acid hydrolysis constitute less than 3% of the total organic carbon for the H995200 sample. Considering that the $\Delta^{14}\text{C}$ values for HMWDOM decrease as the amount of 6-deoxysugars increases from the surface to the deep sample, 6-deoxysugars would be good candidates for the old, $\Delta^{14}\text{C}$ depleted fraction of HMWDOM that persists throughout the water column. Measurement and identification of the products of the periodate oxidation reaction using alternate methods, or direct quantification of 6-deoxysugars seems to be the next step for analysis.

One way to determine more about the macromolecular structure of HMWDOM is to analyze the intermediates produced during the periodate reaction. The reaction pathway shown in Figure 2.2 part B taken from Whelan (1964) indicates that the more easily oxidized glycol groups are removed first, followed by the more difficult task of breaking down the polysaccharide backbone. If this were the case in HMWDOM, the NMR spectra taken during the middle of the experiment would show the broad HMWDOM peaks gradually replaced by sharper, more refined peaks indicating the removal of the easily oxidized carbon and the production of the intermediate polysaccharide. This polysaccharide intermediate would be observed by the presence of sharp resonances between 3.0 and 3.6 ppm, indicating the presence of diketones. Instead,

the NMR spectra showed that the broad HMWDOM peaks just decreased in size, without producing more defined peaks other than those for methanol, acetic acid and formic acid. This would indicate that the complete HMWDOM structure is oxidized at the same time, as each carbon becomes available for oxidation, rather than in two different steps. Quenching the reaction before completion and analyzing both the low molecular weight products (methanol, acetic acid, formic acid and any other ketones and carboxylic acids present) as well as the higher molecular weight residue may provide additional information about the kinetics of periodate oxidation and the structure of HMWDOM.

Analysis of intermediates may also provide information about why large amounts of carbohydrate can be identified using periodate analysis that could not be released from HMWDOM using acid hydrolysis. There are peaks that have not yet been identified present in the GC chromatogram of the monosaccharides present in HMWDOM, but they are of insufficient size to represent the amount of deoxysugars and methyl sugars present according to periodate oxidation. One hypothesis is that the three dimensional macromolecular structure of HMWDOM inhibits the action of acid hydrolysis by preventing access to the glycosidic linkages. The periodate oxidation reaction is more destructive in that it degrades the HMWDOM in pieces, rather than as whole monosaccharides. As a result, there is always a reactive part of the HMWDOM macromolecular structure available for oxidation. However, this explanation is limited by both the extremely small size of the H^+ ion and the fact that the macromolecular structure of HMWDOM does not seem to be that complex. Periodate oxidation of the unhydrolyzable HMWDOM may provide more information about the composition and cross-linking of this fraction. Similarly, acid hydrolysis of a partially periodate oxidized

fraction of HMWDOM would help determine whether the process of oxidation permits additional monosaccharides to be released by acid. Another factor that may explain the incomplete acid hydrolysis compared to the periodate oxidation is the length of the reaction time. Conventional acid hydrolysis protocols hydrolyze HMWDOM at over 100°C for a few hours, while the periodate oxidation method calls for a slightly lower temperature but for a much longer period of time. While half the periodate oxidation of HMWDOM takes place within the first 24 hours, the remaining half requires approximately 10 additional days to completely oxidize. This hypothesis can be easily tested by performing acid hydrolysis at the temperature and time usually used for periodate oxidation.

2.5 Conclusion

Periodate over-oxidation of HMWDOM samples indicated that the majority of total organic carbon exists within periodate oxidizable structures, such as carbohydrates and other vicinal glycols. In both surface and deep water samples, the majority of the organic carbon was over-oxidized, as can be seen via NMR and UV-Vis spectroscopy. The periodate required for HMWDOM over-oxidation was greater than for linear glucopolysaccharide standards, indicating that the structure of HMWDOM contains a greater degree of branching and heterogeneity. In addition, the removal of over 70% of the aliphatic ^1H NMR peak during the experiment indicated that there are no significant concentrations of lipid-type structures present in HMWDOM, a major shift in paradigm. Based on the generation of acetic acid and methanol seen in the ^1H NMR spectra taken during the course of the oxidation, it is concluded that the majority of the unknown carbon in both surface and deep HMWDOM samples consists of 6-deoxusugars and

methyl sugars. The matching patterns of oxidation for both samples indicated a structural consistency in HMWDOM throughout the water column; however the greater amount of acetic acid produced in the oxidation of the deep sea sample suggests a much higher relative concentration of 6-deoxysugars compared to surface HMWDOM.

2.6 References

- Aluwihare, L. I. (1999). High molecular weight (HMW) dissolved organic matter (DOM) in seawater: chemical structure, sources and cycling, PhD, Massachusetts Institute of Technology/Woods Hole Oceanographic Institution: 224.
- Aluwihare, L. I. and D. J. Repeta (1999). A comparison of the chemical characteristics of oceanic DOM and extracellular DOM produced by marine algae. Marine Ecology Progress Series **186**: 105-117.
- Aluwihare, L. I., D. J. Repeta and R. F. Chen (1997). A major biopolymeric component to dissolved organic carbon in surface seawater. Nature **387**: 166-169.
- Aluwihare, L. I., D. J. Repeta and R. F. Chen (2002). Chemical composition and cycling of dissolved organic matter in the Mid-Atlantic Bight. Deep-Sea Research II **49**: 4421-4437.
- Benner, R. and K. Kaiser (2003). Abundance of amino sugars and peptidoglycan in marine particulate and dissolved organic matter. Limnology and Oceanography **48**(1): 118-128.
- Boon, J. J., V. A. Klap and T. I. Eglinton (1998). Molecular characterization of microgram amounts of oceanic colloidal organic matter by direct temperature-resolved ammonia chemical ionization mass spectrometry. Organic Geochemistry **29**(5-7): 1051-1061.
- Clamp, J. R. and L. Hough (1965). The periodate oxidation of amino acids with reference to studies on glycoproteins. Biochemistry Journal **94**: 17-24.
- Dixon, J. S. and D. Lipkin (1954). Spectrophotometric determination of vicinal glycols: Application to the determination of ribofuranosides. Analytical Chemistry **26**(6): 1092-1093.
- Halsall, T. G., E. L. Hirst and J. K. N. Jones (1947). Oxidation of carbohydrates by the periodate ion. Journal of the American Chemical Society: 1427-1432.
- Hay, G. W., B. A. Lewis and F. Smith (1965). Periodate oxidation of polysaccharides: general procedures. Methods in Carbohydrate Chemistry. Whistler, BeMiller and Wolfram. **5 General polysaccharides**: 357-392.
- Hedges, J. I., J. A. Baldock, Y. G  linas, C. Lee, M. Peterson and S. G. Wakeham (2001). Evidence for non-selective preservation in sinking marine particles. Nature **409**: 801-804.

- Hirano, S., T. Fukuda and M. Sato (1974). Periodate oxidation of some carbohydrates as examined by NMR spectroscopy. Agricultural Biological Chemistry **38**(12): 2539-2543.
- House, H. O. (1972). Modern Synthetic Reactions. Menlo Park, CA, W. A. Benjamin, Inc.
- Kim, U.-J., S. Kuga, M. Wada, T. Okano and T. Kondo (2000). Periodate oxidation of crystalline cellulose. Biomacromolecules **1**: 488-492.
- Loh, A. N., J. E. Bauer and E. R. M. Druffel (2004). Variable ageing and storage of dissolved organic components in the open ocean. Nature **430**: 877-881.
- Mannino, A. and H. R. Harvey (1999). Lipid composition in particulate and dissolved organic matter in the Delaware Estuary: Sources and diagenetic patterns. Geochimica et Cosmochimica Acta **63**(15): 2219-2235.
- McCarthy, M., J. Hedges and R. Benner (1996). Major biochemical composition of dissolved high molecular weight organic matter in seawater. Marine Chemistry **55**: 281-297.
- McCarthy, M., T. Pratum, J. Hedges and R. Benner (1997). Chemical composition of dissolved organic nitrogen in the ocean. Nature **390**: 150-154.
- Minor, E. C., J.-P. Simjouw, J. J. Boon, A. E. Kerkhoff and J. van der Horst (2002). Estuarine/marine UDOM as characterized by size-exclusion chromatography and organic mass spectroscopy. Marine Chemistry **78**: 75-102.
- Painter, T. (1994). Periodate oxidation: a source of error in the assay of formaldehyde with chromotropic acid. Carbohydrate Polymers **23**: 137-138.
- Parrish, F. W. and W. J. Whelan (1959). Determination of molecular weights of polysaccharides by over-oxidation with periodate. Nature **183**: 991-992.
- Pascual, R. and M. A. Herraez (1985). The mechanism of the oxidative deamination and decarboxylation of serine and threonine by periodate in acid medium. Canadian Journal of Chemistry **63**(2349-2353).
- Pascual, R., M. A. Herraez and E. Calle (1989). Kinetics and mechanism of the oxidation of proline by periodate. Canadian Journal of Chemistry **67**: 634-638.
- Peat, S., W. J. Whelan and H. G. Lawley (1958). The structure of laminarin. Part I. The main polymeric linkage. Journal of the Chemical Society: 724-728.
- Perry, M. B. and L. L. MacLean (1999). Structural characterization of the antigenic O-chain of the lipopolysaccharide of *Escherichia coli* serotype O65. Carbohydrate Research **322**: 57-66.

- Shinn, L. A. and B. H. Nicolet (1941). The determination of serine by the use of periodate. Journal of Biological Chemistry **139**: 687-692.
- Shinn, L. A. and B. H. Nicolet (1941). The determination of threonine by the use of periodate. Journal of Biological Chemistry **138**: 91-96.
- Sklarz, B. (1967). Organic chemistry of periodates. Quarterly Reviews, Chemical Society **21**(1): 3-28.
- Veelart, S., D. de Wit, K. F. Gotleib and R. Verhe (1997). Chemical and physical transitions of periodate oxidized potato starch in water. Carbohydrate Polymers **33**: 153-162.
- Wakeham, S. G., T. K. Pease and R. Benner (2003). Hydroxy fatty acids in marine dissolved organic matter as indicators of bacterial membrane material. Organic Geochemistry **34**: 857-868.
- Whelan, W. J. (1964). Determination of reducing end-groups. Methods in Carbohydrate Chemistry. R. L. Whistler. **4**: 72-78.

3. Radiocarbon analysis of individual amino acids isolated from marine high molecular weight dissolved organic matter

3.1 Introduction

Dissolved organic carbon (DOC) is the major oceanic reservoir of organic carbon, equal in mass to the atmospheric and terrestrial biosphere reservoirs (Hedges, 1992). As a result, changes in the behavior and distribution of compounds within this organic carbon pool can have large effects on the carbon cycle as a whole. The DOC reservoir contains a wide variety of compound types, with various input sources and different removal rates. Characterizing the compounds and turnover times of DOC is crucial to understanding the role that DOC plays in the larger carbon cycle. Just as only a small percent of the DOC carbon has been molecularly characterized, ^{14}C ages of an even smaller percent of the compounds have been obtained to constrain their residence times in the ocean. The problem lies in several areas: identifying the molecular structures within DOC, isolating compounds of interest and determining their $\Delta^{14}\text{C}$ values. This chapter will focus on the use of compound specific radiocarbon analyses to determine turnover time of the amino acid fraction of HMWDOC.

Approximately 30% of DOC can be isolated as high molecular weight dissolved organic matter (HMWDOM), which is operationally defined as the fraction that passes through a 0.2 μm filter cartridge but is retained by a 1000 Da ultrafiltration membrane. The composition and cycling of this fraction has been studied in more detail than the remainder of the DOC pool. Using a variety of chemical, chromatographic, and spectroscopic methods, several classes of molecules have been identified in the HMWDOM pool, including monosaccharides, amino acids, amino sugars, and lipids

(McCarthy et al., 1996; Aluwihare et al., 1997; McCarthy et al., 1997; McCarthy et al., 1998; Aluwihare, 1999; Benner and Kaiser, 2003; Hwang and Druffel, 2003; Wakeham et al., 2003). The chemical characteristics and distributions of monosaccharides and amino acids in HMWDOM have been shown to be remarkably consistent throughout the ocean (McCarthy et al., 1996; Aluwihare et al., 1997; Aluwihare, 1999). The specific sources, sinks and cycling patterns of individual components of HMWDOM remain undetermined. One of the ways to identify possible sources, as well as to constrain the age and cycling of a particular component of HMWDOM is to use compound specific radiocarbon (^{14}C) measurement.

Radiocarbon has been frequently used as a tracer for organic matter at both the bulk and molecular level. Radiocarbon is produced in the atmosphere naturally by cosmogenic reactions and was also released to the atmosphere in higher concentrations during above-ground nuclear weapons tests in the 1950s and 1960s. This “bomb ^{14}C ” is introduced into the oceans through CO_2 exchange with the atmosphere, incorporated into the inorganic carbon pool, which is then fixed by aquatic organisms into organic carbon. In this way, the ^{14}C signal has been incorporated into the carbon cycle of the oceans and is useful as a tracer of modern biological production. Both the delineation between prebomb and postbomb $\Delta^{14}\text{C}$ values and the amount of radiocarbon in a sample can be used to provide constraints on when the compound was made. Radiocarbon content can also be used to differentiate between various pools of organic carbon in terms of sources and turnover times. As chemical isolation techniques for various types of oceanic carbon have become more sophisticated, radiocarbon has become an important tracer for determining the relative age, carbon source, and cycling down to the compound class and

individual compound level for a variety of organic molecules (Wang et al., 1996; Eglinton et al., 1997; Wang et al., 1998; Pearson et al., 2001; Reddy et al., 2004).

Radiocarbon data on DOC have been limited, in terms of amount of measurements, spatial and temporal resolution, and compounds analyzed. Studies of particulate organic carbon (POC), DOC and dissolved inorganic carbon (DIC) have indicated that the total DOC pool is older than the DIC at corresponding depths, with the POC fraction the youngest of the three (Druffel et al., 1992). Radiocarbon measurements of bulk DOC show an average radiocarbon age of 2000 years in the surface and 5000 years below 800 m (Druffel et al., 1992). The $\Delta^{14}\text{C}$ of the HMWDOM fraction has been found to range from -5‰ to -434‰ (Aluwihare et al., 2002; Loh et al., 2004). These radiocarbon data provide general information regarding the utilization of each carbon pool and the cycling of carbon between pools but are limited due to the chemical heterogeneity of each fraction. The production, exchange, and labilities of specific compounds cannot be determined from bulk radiocarbon content. $\Delta^{14}\text{C}$ signatures of certain compound classes such as total carbohydrate, total amino acid, and total lipid have obtained from POC and DOC (Wang et al., 1996; Wang et al., 1998; Hwang and Druffel, 2003; Loh et al., 2004).

Within the HMWDOM pool, very few compound specific radiocarbon measurements have been made due to low concentration and the difficulty of isolation. Analysis of seven neutral sugars showed the presence of bomb ^{14}C down to 750m depth, indicating that these compounds were modern in origin, and enriched relative to the total HMWDOM and total DOM (Aluwihare et al., 2002). This information allows the monosaccharides to be used as a tracer of both modern HMWDOM production, and

carbon exchange between DOC and POC pools. The goal of this chapter is to develop and utilize a method to determine the compound-specific radiocarbon content for another fraction of HMWDOM, amino acids.

Macromolecules composed of amino acids are a very important fraction of HMWDOM. While fairly low in concentration and percentage of the total carbon, they form the majority of the high molecular weight dissolved organic nitrogen (HMWDON) compounds identified so far, making them attractive as a potential nitrogen source for bacteria and phytoplankton. In addition, amino acids may supply a clue to identify the sources of HMWDOM. Hydrolyzable amino acids (HAA) are generally less than 20% of the total HMWDON and approximately 4-5% of the total HMWDOC (McCarthy et al., 1996; McCarthy et al., 1997; Aluwihare, 1999). The HAA fraction also seems to be more variable in individual amino acid composition and concentration than monosaccharides, which may be the result of differing hydrolysis conditions or loss of certain amino acids to vial walls (Cowie and Hedges, 1992; Aluwihare, 1999). Amino acids have attracted attention lately as potential indicators of bacterial protein contribution to the HMWDOM pool (McCarthy et al., 1998; Yamada et al., 2000). McCarthy et al., (1998) measured the enantiomeric D/L ratios of individual amino acids and concluded that the D/L ratios of aspartic acid (asp), glutamic acid (glu), serine (ser) and alanine (ala) were abnormally high relative to the other amino acids, indicating a bacterial source of D-enantiomers, perhaps from the protein peptidoglycan. These D-enantiomers have been detected at a variety of depths and oceanic environments, providing the potential for using D-amino acids as tracers for microbial production (Dittmar et al., 2001). However, it remains unclear whether these compounds mark new

production or differences in labilities between enantiomers (Pérez et al., 2003). Gel electrophoresis and amino acid sequencing indicates that bacterial porin proteins may be another potential source of amino acids (Tanoue, 1995; Yamada et al., 2000; Yamada and Tanoue, 2003).

In addition to being potential sources of carbon and nitrogen to HMWDOM, amino acids have also been used to investigate carbon and nitrogen removal. Variations in the concentrations of individual HAA have been used as indicators of microbial degradation, and these variations are also linked to the reactivity of the bulk organic matter pool (Dauwe and Middelburg, 1998; Dauwe et al., 1999). Culture experiments with HMWDOM indicate that some types of phytoplankton and bacteria are able to utilize organically bound nitrogen (Jørgensen et al., 1993; Jørgensen et al., 1994; Berg et al., 1997; Kahler et al., 1997). Since HAA are one of the few nitrogen compound classes in HMWDOM to be identified and measured, they are useful tracers for investigations of organic nitrogen uptake.

This chapter provides a new method for isolating underivatized HAA using high-pressure liquid chromatography (HPLC). The first set of individual amino acid radiocarbon measurements for HMWDOM are also reported. These radiocarbon measurements provide additional data for both carbon cycling between organic carbon pools, and more importantly, help constrain nitrogen cycling as well. Knowing the radiocarbon content of the HAA fraction, we can compare the radiocarbon values of this portion to the bulk HMWDOM sample and other compound classes. By measuring the radiocarbon contents of individual HAA, we can identify any anomalous amino acids, which can provide more information on which amino acids are either preferentially

preserved or preferentially consumed. Radiocarbon values can also be combined with values from other HMWDOM components, along with ^{14}C data from POC and bulk DOC to determine how carbon and nitrogen cycle between organic carbon pools.

3.2 Materials and Methods

3.2.1 Sample Location and Collection

A surface water HMWDOM sample (H0200) from the North Central Pacific was used in this experiment. Surface seawater was drawn from the 15 m seawater intake at the Natural Energy Laboratory in Kona, Hawaii in February 2002. The water samples were filtered to remove bacteria and small particles using a cleaned Suporflow dual stage (0.8 μm and 0.2 μm) Gelman polyether sulfone cartridge filter (Chisolm Corp., Lincoln, RI) fitted to an Advanta stainless steel housing. This filter was cleaned with 10% HCl, then flushed with low carbon deionized Milli-Q water. High molecular weight DOM samples were collected using a large volume cross flow ultrafiltration system consisting of a stainless steel centripetal pump and membrane housings and a fluorinated high density polyethylene reservoir. The system was plumbed with teflon tubing and fitted with PVDF valves. The ultrafiltration membrane (Separation Engineering, Escondido, CA) nominally retains organic matter with a molecular weight of greater than 1000 Da, calibrated by the retention of $\geq 99\%$ vitamin B12. Membranes were cleaned using isopropanol, detergent (0.01% micro), HCl and NaOH, stored in 0.55 mM sodium azide, and rinsed with water immediately before use. Between 30,000 and 60,000 L of seawater were concentrated to approximately 20 L, frozen and returned to Woods Hole for further

processing. The HMWDOM samples were desalted by diafiltration with water, reduced to 2 L, and lyophilized to a fluffy white powder.

3.2.2 Analytical Protocols

Low-carbon deionized (Milli-Q) water was used in all procedures. All glassware was combusted for a minimum of 8 h at 450°C. Syringes and teflon-lined vial lids were rinsed with 10% HCl and water before use. Two different HPLC instruments were used for the isolation procedure: an Agilent 1100 series binary pump with a Rheodyne manual injector was used for the albumin standard, and an Agilent 1100 series quaternary pump with a degassing unit and an autoinjector was used for the HMWDOM sample. For both instruments, detection of amino acids using absorbance was performed using an Agilent diode array detector set to measure absorbance at wavelengths of 195, 210 and 230 nm. All HPLC buffers and eluants were filtered through a GF/F filter and degassed by sonication under vacuum when a degasser was not present. NMR tubes were cleaned using aqua regia (1:3 HNO₃:HCl) overnight, then rinsed with water and dried in a drying oven. Proton NMR spectra were acquired on a Bruker 400MHz spectrometer using a water suppression program (zgpr). Chemical shifts were referenced to water at 4.8 ppm. All spectra were run using D₂O as a solvent. Elemental analysis (CHN) was measured by combustion using a CE Instruments (Flash EA 1112) elemental analyzer with a thermal conductivity detector. All attempts were made to prevent any contamination, including that by potential sources of radiocarbon.

3.2.1 Standards

Fifteen individual amino acid standards (ICN Biomedicals) were used to determine HPLC retention times and create reference NMR spectra. Bovine serum

albumin (Sigma) was used as a procedural standard for both HPLC and radiocarbon measurements. The o-phthalaldehyde (OPA) analysis results were calibrated using Pierce Amino Acid Standard H.

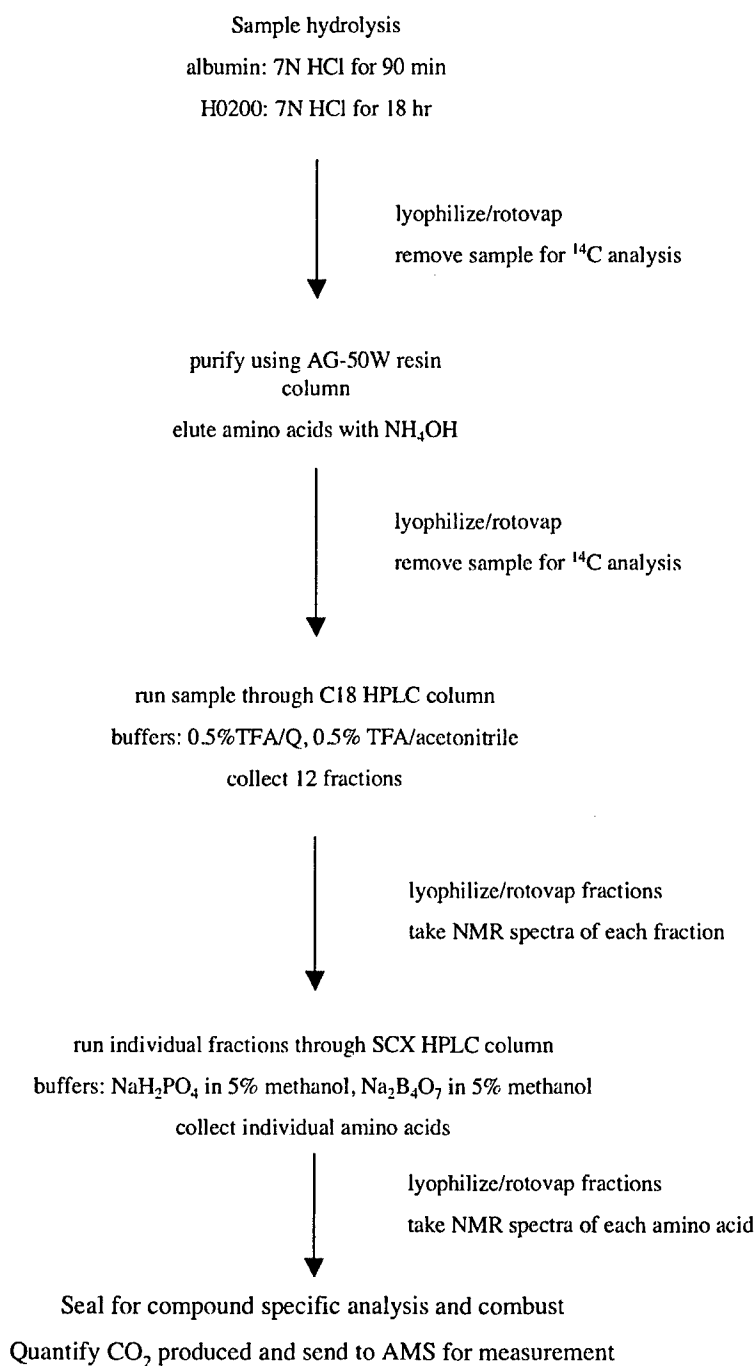
3.2.2 Amino Acid Isolation and Purification

The focus of this chapter is the development of a new method to isolate individual amino acids released after hydrolysis of HMWDOM, without derivatization, using resin and HPLC chromatography. NMR was used to monitor the isolation and purification procedures. A summary of this method is shown in Figure 3.1. This method was developed specifically for collection of samples for radiocarbon analysis. While many techniques exist for the measurement of amino acids in seawater and HMWDOM samples, these methods require derivatization of the amino acids for low level fluorometric detection. While corrections to the $\Delta^{14}\text{C}$ measurements can be made to take into account the radiocarbon signal due to the extra carbons present in the derivatizing agent, it is analytically simpler to avoid derivatization of samples in the first place. This new method takes advantage of the absorbance of amino acids at low wavelength UV, as well as the differences in the chemical behavior of individual amino acids on a reverse phase C18 HPLC column versus a strong cation exchange column.

3.2.2.1 Hydrolysis and Column Chromatography

Albumin (800mg) was hydrolyzed with 400 mL of 7 M HCl for 90 minutes at 150°C in a sand bath. The hydrolysis solution was flushed with nitrogen before heating. The HMWDOM sample, H0200 (1.7 g), was also hydrolyzed using 1 L 7M HCl, but at a slightly higher temperature (165°C) for 18 hours in an attempt to improve amino acid yields. Due to the larger sample size, the H0200 sample was hydrolyzed in two separate

Figure 3.1: Schematic representation of the purification protocol used to isolate amino acids for radiocarbon analysis.



half batches. After hydrolysis, the samples were lyophilized or evaporated to dryness, and an aliquot removed for NMR and radiocarbon measurement.

The dried HAA fraction was concentrated using Bio-Rad AG 50W-X8 resin (Bio-Rad Laboratories, 50-100 mesh, hydrogen form). Approximately 5 g (6.5 mL) of resin were packed into a 15 cm tall by 1 cm diameter column plugged with combusted glass wool with a teflon stopcock. The resin was pre-cleaned using 25 mL of 6 N HCl (trace metal grade, Fisher Scientific), rinsed with water until pH neutral, then 25 mL of 6 N NH_4OH (trace metal grade, Fisher Scientific) were added, again rinsing with water until neutral. The resin was then conditioned with 25 mL of 1.5 N HCl and flushed with water until neutral. The sample was neutralized using approximately 6 mmols KOH, then applied to the resin. Non-amino acid components were removed by flushing with 50 mL of water (referred to in this chapter as the 'neutral fraction'). The amino acid fraction was then eluted from the column using 50 mL of 1.5 N NH_4OH ('amino acid fraction'). The amino acid fraction was collected when the warm zone and dark brown band that signaled the start of the NH_4OH eluant front reached the end of the column. This HAA fraction was then lyophilized to dryness, with an aliquot removed for NMR and radiocarbon analysis. A new resin column was used for the albumin standard and each half of the HMWDOM sample.

3.2.2.2 OPA Analysis

Amino acid content in the original sample was measured using the standard o-phthalaldialdehyde (OPA) derivitization method (Ingalls et al., 2003). Briefly, the samples were neutralized with 6N KOH before derivitization with OPA. The derivatized amino acids were separated using an Alltech Alltima C18 column (5 μm , 250x4.6mm) with a gradient of sodium acetate (0.05M, pH 5.7, 5% tetrahydrofuran) and methanol. Amino acids were detected using a Hitachi 1000 fluorometer (ex: 330, em: 418). Flow rates

were 0.95 ml/min. Concentrations of amino acids were determined using the response factors (nmoles/area) for each peak in the standard mixture (Pierce Standard H). A smaller H0200 sample (1.5 mg) was hydrolyzed with 0.5 mL 7M HCl for 90 minutes at 150°C and purified using the AG-50W resin column procedure as described above. Amino acid concentrations were measured in the hydrolyzed material, and the amino acid and neutral eluted fractions from the resin purification step.

3.2.2.3 C18 HPLC Separation

The amino acid fraction isolated from the AG-50W resin column was separated into twelve fractions by reverse phase HPLC using a trifluoroacetic acid (TFA)/water/acetonitrile gradient. The presence of TFA in the eluant is to serve as a volatile ion-pairing agent to the amino acid compounds. The eluants were 0.5%(v/v) TFA in acetonitrile (Fisher Scientific, HPLC grade) (A) and 0.5%(v/v) TFA (Fisher Scientific) in water (B) with a gradient of 0% to 50% A in 30 min, followed by a 15 minute post-run flush with 100% TFA/water eluant. The dried samples were dissolved in approximately 1 mL TFA/water eluant per gram sample and centrifuged if necessary to remove any insoluble material. The albumin standard was processed using a standard analytical Alltech Alltima C18 column (5 µm, 250x4.6 mm), with a flow rate of 1 ml/min and an injection volume of 100 µL. The chromatogram was monitored at 195, 210 and 230nm. The HMWDOM sample (H0200) was separated using an Alltech Alltima prep-C18 column (5 µm, 250x10 mm) with an Alltech Alltima C18 guard column (5 µm, 70x7 mm) at a flow rate of 2.5 ml/min and an injection volume of 80 µL. A total of 12 amino acid fractions were collected using this method, with 6 amino acids co-eluting in pairs. The twelve fractions were collected based on a 15 amino acid standard solution whose

concentration was approximately 10 mM each amino acid for the prep column and 2 mM for the standard column. While there were slight variations in the chromatograms, the general retention times for the collected fractions were as follows: $F_1=5.0-6.5$ min, $F_2=6.5-7.2$ min, $F_3=7.2-7.9$ min, $F_4=7.9-9.0$ min, $F_5=9.0-10.6$ min, $F_6=13.1-14.4$ min, $F_7=16.7-17.2$ min, $F_8=17.2-17.8$ min, $F_9=17.8-18.3$ min, $F_{10}=18.3-18.9$ min, $F_{11}=18.4-19.4$ min, and $F_{12}=19.4-20.1$ min. The waste between fractions was collected from 4 min to 30 min. Collected fractions were lyophilized or evaporated to dryness, and aliquots removed for NMR and radiocarbon analysis.

3.2.2.4 Strong Cation Exchange HPLC Separation

A second HPLC method was used to further purify the fractions collected from the C18 separation and to separate the co-eluting amino acids. NMR spectra showed that the fractions collected off the C18 column were not pure amino acids, and thus needed an additional purification step. A strong cation exchange (SCX) column was chosen for the second HPLC step to take advantage of the cationic character of the amino acids. The cationic character of the amino group allows for retention on the column, while the other HMWDOM components, such as monosaccharides are not retained. This SCX procedure has the additional advantage of being a completely different separation process than the C18 column, which allows the amino acid pairs that co-eluted in the previous step to be fully resolved.

The procedure was modified from Konishi et al., 1989. An Alltech Adsorbosphere strong cation exchange (SCX) column (5 μm , 250x4.6 mm) was used with a system of phosphate and borate buffers. For the albumin sample, buffer A was a

0.2 M solution of sodium phosphate dibasic (NaH_2PO_4) in 5% methanol/95% water. The NaH_2PO_4 was dissolved in water, adjusted to pH 3.0 using concentrated phosphoric acid, and the methanol (Fisher Scientific, HPLC grade) was added. Buffer B contained 0.11 M sodium borate ($\text{Na}_2\text{B}_4\text{O}_7$; combusted at 450°C for 4 hours) dissolved in 30% methanol/70% water. The $\text{Na}_2\text{B}_4\text{O}_7$ was added to water and adjusted to pH 10 with 1M NaOH, then methanol was added (Konishi et al., 1989). For the HMWDOM sample, the NaH_2PO_4 and $\text{Na}_2\text{B}_7\text{O}_{14}$ concentrations were reduced to 0.05 M for both buffers A and B in order to avoid large amounts of salt interfering with the radiocarbon measurements. All solutions were filtered prior to use. The elution gradient started with 5 min of 100% buffer A, followed by a 15 min linear gradient to 35.7%B, and ending with a 10 minute gradient to 100% B. A 10 minute post-run flush was done with 100% buffer A. The flow rate was 0.5 ml/min. Prior to injection, the dried fractions collected from the C18 procedure were dissolved in buffer A. Individual amino acid peaks were collected by time based on a set of individual amino acid standards. These fractions were also dried by lyophilization or rotary evaporation, and NMR analyses were used to check the purity of each amino acid.

3.2.2.5 Radiocarbon Sample Preparation

To prepare organic carbon samples for radiocarbon, the samples need to be first combusted to carbon dioxide (CO_2). The resulting CO_2 is then purified, quantified, and transferred into smaller tubes, and submitted to the accelerator mass spectrometry lab for analysis. Since the presence of borate and phosphate salts in the final amino acid samples was a concern, a test solution was made with approximately 1 mg leucine combined with 100 mg each sodium phosphate and sodium borate salts, a concentration similar to the

actual samples. Amino acids are not soluble in organic solvents, so it was necessary to transfer them to the tubes as an aqueous solution. Since the behavior of the SCX buffer salts present in the samples under combustion temperatures was not known, the leucine test solutions were placed in short quartz inserts (5 cm long x 6 mm diameter, Finkenbiener, Inc) inserted into a larger quartz tube (20.3 cm long x 9 mm diameter), then dried in a heating block set to 40°C under a nitrogen stream. When the nitrogen drying proved too slow and inefficient, the aqueous samples were lyophilized instead. Approximately 1 cm of precombusted copper oxide wires (300-500 mg, Elemental Microanalysis, Ltd, and 5 mm silver powder (crystalline, -10+20 mesh, 99.99%, Alfa Aesar) and a drop of 100% phosphoric acid were then added to the tubes. The purpose of the silver and the phosphoric acid was to bind any halogen atoms present and to prevent the formation of sodium carbonate salts derived from the sodium salts in the SCX buffers. The tubes were then evacuated on the dedicated ^{14}C sample vacuum line, sealed using an oxy-propane torch, and combusted at 850°C for 5 h. The oven temperature was ramped to 700° C at 6.0°C/min, held at 700°C for 30 min, then heated at 4.0°C/min to 850°C. The CO_2 liberated from the organic sample is then measured in terms of its partial pressure (P) within a known volume (V) and temperature (T). The moles of CO_2 generated by the sample can then be calculated using the ideal gas law ($n=PV/RT$). The measured CO_2 gas is then transferred to smaller pyrex tubes, sealed, and submitted for analysis.

Unfortunately, the majority of the tubes that were sealed containing the leucine test solution experienced tube failure during the high temperature combustion. Several other variations on this procedure were tried, including larger 12 mm diameter quartz

tubes containing both 6 mm and 9 mm diameter nested inserts, letting the tubes sit at 500°C for 2 h in the oven after the 5 h combustion at 850°C, and isolation of the sample within the tube with a layer of combusted quartz chips placed between the sample and the catalysts. Sample tubes were also lyophilized directly on the vacuum line both as liquid and after freezing, utilizing a second cold trap and a needle valve to control the vacuum intensity in an attempt to ensure that the samples were completely dry before they were sealed. In all cases, the majority of the tubes still failed. While the actual cause of this repeated tube failure for high temperature combustion is unknown, it is suspected that either the presence of the buffer salts from the SCX chromatography interacted with the quartz tubes, or that the samples were not completely dry due to the retention of water within the salt matrix, leading to excessive high pressure buildup during combustion.

One option to solve this problem is to remove the sodium phosphate and borate salts by passing the samples through sequential cation exchange and anion exchange resin columns. Since amino acids have both cationic and anionic character, they can be retained on both types of resin, letting the anionic phosphate and borate ions elute through the cation exchange column, and the sodium pass through the anion exchange column. The remaining solution should only contain the amino acid sample, with minimal amount of salt.

To test this approach, the anion exchange resin used was AG 50W-X8, hydrogen form (Bio-Rad Laboratories), and the cation exchange resin used was AG 1X8, hydroxide form (Bio-Rad Laboratories). A test leucine sample consisting of 2 mg leucine plus 146 mg sodium phosphate and 90 mg sodium borate was first passed through 10 mL of anion exchange resin packed into a 15 cm long by 20 mm diameter column plugged with

combusted glass wool to remove the sodium ions. The size of the resin column was calculated based on the concentration and charge of the leucine, phosphate and borate ions in the sample, so that the resin column was no larger than 10 times the required size in order to minimize non-specific binding. The anion resin was conditioned with 30 mL of 10 mM NH_4OH , and the leucine test sample (pH 11-12) was added to the column. The column was washed with 50 mL of 10 mM NH_4OH , then the leucine, phosphate and borate ions were eluted from the column with 20 mL of 0.1 M HCl. The eluant was then adjusted to pH 2 in preparation for the next resin column.

The size of the cation exchange column caused some difficulty. Based on the concentration needed to exchange the leucine, the column would be extremely small in size, approximately 0.07 mg, even with the additional 10 fold excess. Such a column is completely impractical due to its extremely small size, which means that the sample may not have enough time to interact with the resin, and may be washed out with the contaminants. In order to prevent this, 100 μL (80 mg) of resin were used, even though this size was 1000 fold greater than that required by leucine concentration in the sample. The resin was packed into a 5.75 inch glass Pasteur pipet plugged with combusted glass wool in order to provide enough surface area for exchange to occur. The cation resin was conditioned with 2 mL of 10mM HCl before the sample was added. The column was then washed with 6 mL of 10mM HCl to remove the sodium ions, and the leucine was eluted with 2 mL of 1M NH_4OH . The purified leucine was then lyophilized and checked for purity and concentration using the C18 HPLC method.

Two test samples were run through this tandem column procedure. The first sample was the leucine test standard containing buffer salts in similar concentrations to

the actual samples collected from the SCX HPLC step mentioned above. The HPLC C18 chromatogram of the amino acid after the removal of the salts showed no peak at the retention time associated with leucine. Repeating the two column procedure with a leucine-only (5 mg) test sample using 100 μ L columns for both cation and anion resins yielded a recovery of only 34% of the initial mass. The loss of leucine in both test solutions was probably due to non-specific exchange with the resin columns, especially the anion exchange column. Since the size of the actual amino acid samples is already expected to be small, it was decided not to use this procedure.

The second option to avoid the tube failure at high temperatures was to use pyrex tubes instead of quartz and combust at 550°C rather than 850°C. Combustion at the lower temperature should still provide complete conversion of the amino acids to carbon dioxide since amino acids are relatively small compounds. Using pyrex would eliminate any interactions between the sodium phosphate and sodium borate salts and the quartz tubes. The dissolved samples were added to 5 cm long by 6 mm diameter pyrex inserts inside larger 9 mm diameter pyrex tubes (20 cm long) and lyophilized directly on the dedicated ^{14}C sample vacuum line using a second cold trap and a needle valve to control the vacuum. Tubes were also heated gently using a heat gun while under vacuum to drive off any water trapped within the salt matrices. Once dry, a layer of combusted pyrex chips (1 cm high) was then added on top of the sample to separate the salts from the pre-combusted copper oxide catalyst (1 cm). A 0.5 cm layer of silver granules and a drop of 100% phosphoric acid were also added to each tube on top of the copper oxide to bind halogens and prevent the formation of sodium carbonate salts. Sample tubes were then sealed under vacuum using a handheld butane torch and combusted at 550°C for 5

hours. The oven was heated at 6.0°C/min to 500°C, held at that temperature for 30 min, then heated again at 4.0°C/min to 550°C. The carbon dioxide released by combustion was then purified, quantified, and transferred to smaller pyrex tubes for radiocarbon measurements at the National Ocean Science Accelerated Mass Spectrometry (NOSAMS) facility. A 10% subsample of the CO₂ from each sample was removed for $\delta^{13}\text{C}$ measurement.

This procedure was tested using the leucine-salt test mix (1 mg leucine plus 100 mg each sodium phosphate and sodium borate) with over 90% recovery of carbon dioxide after combustion. This procedure was then used for the albumin and HMWDOM samples. For the albumin and H0200 samples, each amino acid fraction was split into two or more pyrex tubes depending on concentration to prevent tube failure due to high pressure, and to allow for accidental contamination or loss of one sample tube. This also provides the chance to submit replicates for measurement. An additional tube containing a procedural blank was also processed but not submitted for measurement. This blank was collected during the SCX HPLC step from a H0200 sample fraction, and did not show any peaks in the ¹H NMR spectrum.

3.2.2.6 Accelerator Mass Spectrometry (AMS)

All samples were measured using AMS at the National Ocean Sciences AMS (NOSAMS) facility. All of the CO₂ samples from both the H0200 and albumin samples contained less than 300 µg carbon, requiring the use of microscale AMS techniques (Pearson et al., 1998). Briefly, the CO₂ samples were reduced to graphite over a cobalt catalyst, pressed onto aluminum AMS targets, and analyzed. The primary standards

measured were NBS Oxalic Acid I (NIST-SRM-4990) and Oxalic Acid II (NIST-SRM 4990C), in addition to a process blank composed of pure graphite powder.

The fraction modern (F_m) of a sample is computed from the $^{14}\text{C}/^{12}\text{C}$ ratios of the blank ($(^{14}\text{C}/^{12}\text{C})_B$), sample ($(^{14}\text{C}/^{12}\text{C})_S$), and the modern reference ($(^{14}\text{C}/^{12}\text{C})_M$), according to the equation $F_m = [(^{14}\text{C}/^{12}\text{C})_S - (^{14}\text{C}/^{12}\text{C})_B] / [(^{14}\text{C}/^{12}\text{C})_M - (^{14}\text{C}/^{12}\text{C})_B]$, and represents the deviation of the measured sample from the modern standard. This value is corrected for fractionation using the $\delta^{13}\text{C}$ of the sample using the equation $F_m^* = F_m [(1 - 25/1000) / (1 + \delta^{13}\text{C}/1000)]^2$. Radiocarbon concentrations are also reported as $\Delta^{14}\text{C}$ values, and calculated using the equation $\Delta^{14}\text{C} = [F_m^* e^{(Y_c - 1950)\lambda} - 1] * 1000$, where $\lambda = 1/8267 \text{ yr}^{-1}$, F_m = fraction modern, and Y_c is the year the sample was collected (Stuiver and Polach, 1977). For the H0200 samples, Y_c is 2002. Using $\Delta^{14}\text{C}$ allows comparison between samples collected on different dates.

3.3 Results

3.3.1 Ancillary Data

In Table 3.1, the HAA distribution for the H0200 surface water HMWDOM sample is compared to two other reports of HMWDOM HAA. The H0200 sample contains 34.3% organic carbon and has a C/N ratio of 13.6. Based on the OPA measurements, amino acids make up an average of 12.1% of the total organic nitrogen in the sample. The average amino acid distribution for this sample is also shown in Table 3.1, in mole percent individual amino acid of the total amino acid fraction. Due to the conversion of asparagine and glutamine to aspartic acid (asp) and glutamic acid (glu), respectively, during hydrolysis, the mol percent values for asp and glu are the sum of

both the acid and neutral forms. This convention applies to all asp and glu fractions for albumin and H0200 in this chapter, since both samples were hydrolyzed prior to amino acid measurement and isolation.

Table 3.1: Hydrolyzable amino acid distribution (mole percent of total) for HMWDOM sample H0200 compared to two literature sources of HAA distribution for HMWDOM. The Aluwihare 1999 values are an average of replicates from a coastal HMWDOM sample from Woods Hole, MA. The McCarthy et al., 1996 values are an average of surface water HMWDOM values from the N. Pacific, Sargasso Sea, and Gulf of Mexico.

Amino acid	H0200 mol%aa-N	Aluwihare 1999 mol%aa-N	McCarthy et al., 1996 mol%aa-N
asp	2.6±0.2	19±5	11.3±1
glu	2.4±1	7.8±0.7	16.3±1
ser	0.4±0.4	11±2	10.0±1
his	12.3±0.9		0.5±0.7
thr	6.4±3		7.5±1
arg	30±7	8.8±1	4.3±1
gly	11.4±0.9	14±3	16.0±1
ala	24±3	15.2±1	14.8±2
tyr	2.9±2	1.7±0.6	2.0±0.4
met	0.2±0.1	0.9±0.7	0.8±0.8
val	1.4±0.8	3.7±0.8	3.9±1
phe	0.7±0.3	2.6±0.4	2.2±0.3
ile	0.6±0.4	11±2	3.2±1
leu	4.0±2	2.5±1	4.0±1
lys	0.92±0.08	1.1±0.6	2.1±0.4
% N as aa	12±4	17±3	23±9

Literature data of hydrolyzed amino acids from surface HMWDOM samples from four different locations (coastal N. Atlantic, N. Pacific, Sargasso Sea, and Gulf of Mexico) are also shown in Table 3.1 (McCarthy et al., 1996; McCarthy et al., 1997; Aluwihare, 1999). Comparison of the literature data with the H0200 sample in this study shows a significantly lower relative concentration of asp, glu, isoleucine (ile), and phenylalanine (phe), but higher levels of arginine (arg), alanine (ala) and histidine (his). The relative concentrations of amino acids can vary greatly depending on hydrolysis

technique, which, along with natural variability between samples, may be a factor in explaining the differences in distribution between the H0200 sample and the literature data (Aluwihare, 1999). The yield of the total amino acid fraction as a percent of the total organic carbon for the H0200 sample is consistent with other published data.

3.3.2 Hydrolysis and Resin Column Results

The elemental and recovery data for albumin and H0200 is summarized in Table 3.2. Five percent aliquots of each sample were dried and weighed after every step, and the total mass calculated from that measurement. In the case of albumin, very little mass was lost during the hydrolysis and resin cleaning steps, as was expected for a sample containing only protein. During the same steps the H0200 sample lost over 95% of the original mass, indicating that some type of purification took place. The loss of 20% of the H0200 mass after hydrolysis is likely due to the formation of volatile organic compounds or an insoluble residue that remained on the inside of the hydrolysis flask during that step. While as much of this residue as possible was scraped off with the rest of the sample, it was too insoluble to be passed through the resin column easily, and was separated from the dissolved sample by centrifugation. This residue was not analyzed using elemental analysis or NMR spectroscopy, but it was assumed that no amino acids were present in the insoluble residue.

Table 3.2: Basic elemental and recovery data for albumin and H0200 samples.

sample	%C	C/N	initial mass (mg)	after hydrolysis (mg)	% yield	after resin (mg)	%yield
albumin	n/d	n/d	174.8	213.9	122.4	161.1	92.1
H0200	34.3	13.6	1703.3	1392.5	81.8	81.5	4.8

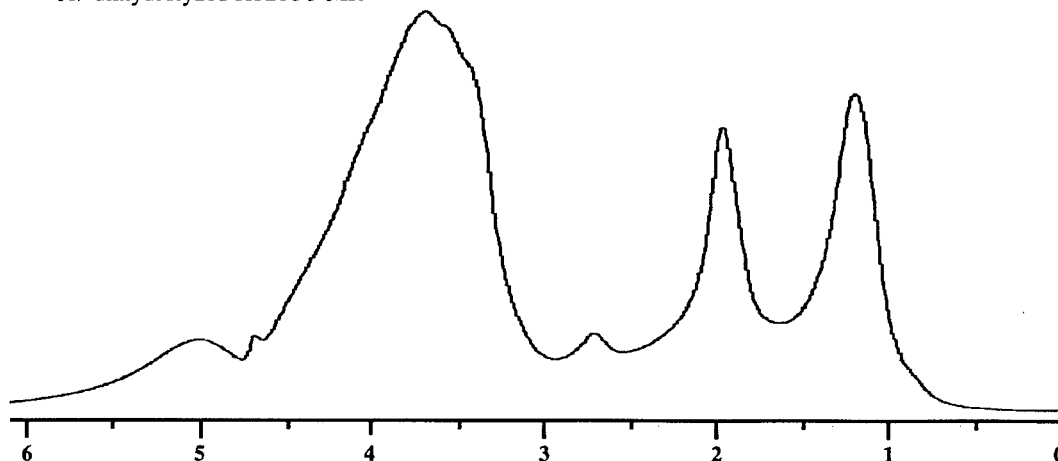
The H0200 yield after purification via the resin column seemed to match well with the expected 4-5% of the organic carbon that is present as amino acids, thus

suggesting that the "amino acid fraction" eluted from the column is composed mostly of amino acids. NMR spectra taken before and after the resin column step showed that, while a large amount of the carbohydrate and other components present in HMWDOM were removed, a significant amount still remained in the amino acid fraction (Figure 3.2).

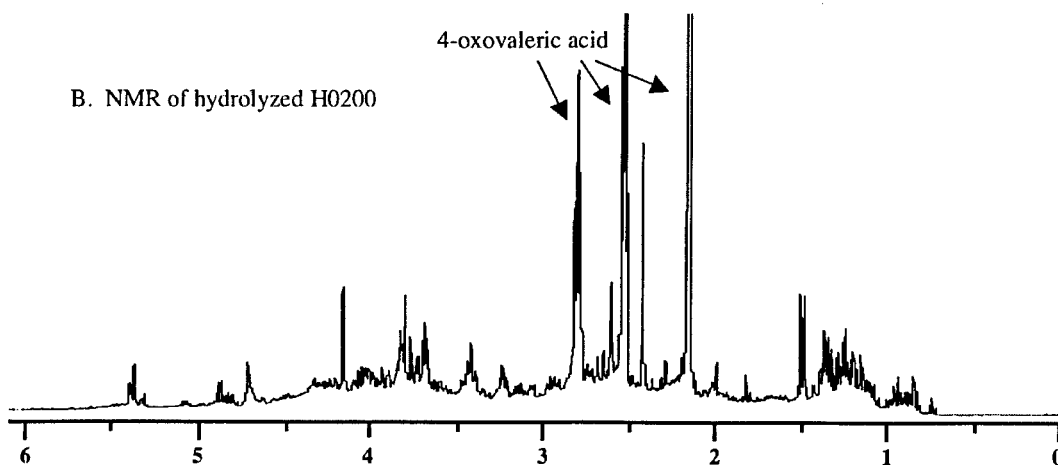
Figure 3.2A shows the ^1H NMR spectrum of the H0200 HMWDOM before hydrolysis. Resonances were assigned as: anomeric H (5.5-5.0 ppm), carbohydrates (4.5-3 ppm, H-COH), acetate (2 ppm, OOCCH_3), and aliphatic protons (1.7-0.9 ppm, CH_2). The acetate peak was removed during lyophilization, and all of the other functional group peaks became less broad and were represented by sharper peaks within the ranges above, indicating that some glycosidic and peptide bonds were hydrolyzed (Figure 3.2B). The trio of large peaks at 2.8 ppm, 2.6 ppm, and 2.2 ppm are attributed to be from 4-oxovaleric acid, a compound that sometimes forms from carbohydrates heated in acid. After purification using the AG-50W resin column, the amount of carbohydrate and other components of the HMWDOM decreased relative to the amount of amino acids present in the sample (Figure 3.2C). This can be seen by the removal of significant amounts of unresolved components, in addition to the removal of the 4-oxovaleric acid peaks between 2-3 ppm. The carbohydrate peak (4.5-3 ppm) and aliphatic peaks between 1.5-1.0 ppm have also decreased in area, with the exception of the range between 4-3.5 ppm, where the methyne hydrogen ($\text{R-CHNH}_2\text{COOH}$) resonates in amino acids. A fairly large amount of non-amino acid compounds still remained in the amino acid fraction.

Figure 3.2 Proton NMR spectra for the unhydrolyzed H0200 sample (A), the hydrolyzed sample (B), and the hydrolyzed amino acid fraction collected from the AG-50W cation exchange resin (C). In all spectra, the water peak is at 4.8 ppm.

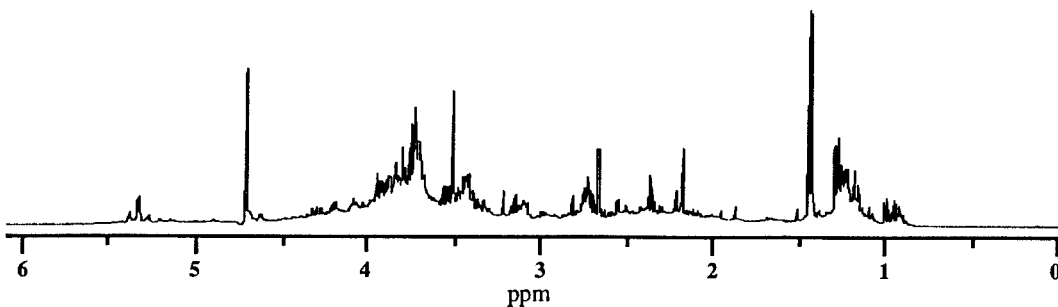
A. unhydrolyzed H0200 NMR



B. NMR of hydrolyzed H0200



C. NMR of amino acid eluted
H0200 fraction



3.3.3 C18 HPLC results

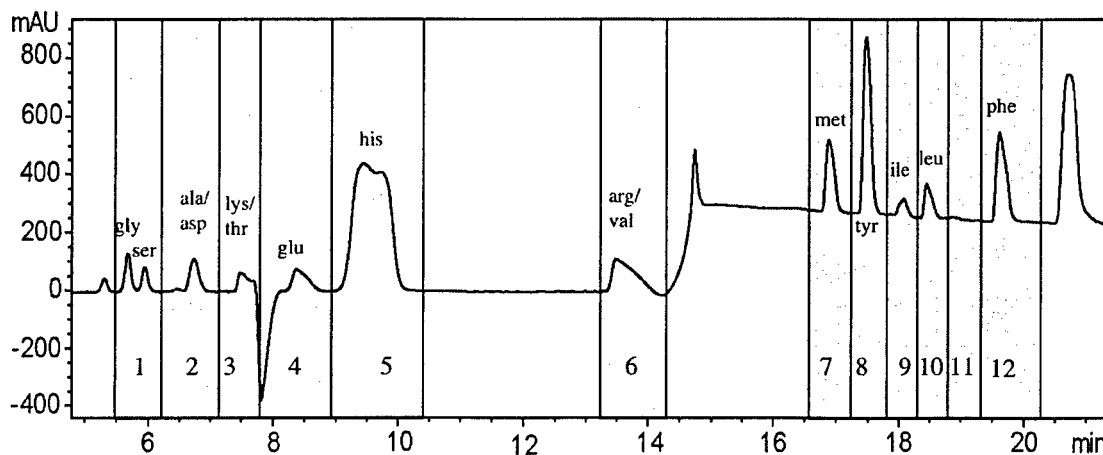
Figure 3.3 shows C18 HPLC absorbance chromatograms (210 nm) of the amino acid separation of the 15 amino acid standard (Figure 3.3 A) and that of the H0200 base fraction sample (Figure 3.3 B). All of the amino acids in the standard can be separated cleanly with the exception of three pairs: alanine/aspartic acid (ala/asp), lysine/threonine (lys/thr), and arginine/valine (arg/val). The dip in the baseline after the lys/thr peak, and the baseline jump after the arg/val peak also occur in non-injection blank runs and therefore must be related to the solvent system used. The peak before glycine and the peak after phenylalanine also occur in TFA/Q solvent-only injections, and therefore are not amino acids. The amino acid peaks in the chromatogram of H0200 are less distinct than those of the standard due to the elevated baseline and to interference from non-amino acid compounds that also absorb at 210 nm, which were especially pronounced for components eluting after 15 minutes. The 12 fractions collected off the C18 HPLC column are marked on both the 15 amino acid standard and the H0200 chromatogram (Figure 3.3). The timing of collections were based on the peaks from the 15 amino acid standard, but adjusted to account for slight differences in the H0200 chromatogram peaks from run to run.

The concentrations of each amino acid in the H0200 and albumin sample were calculated based on response factors determined from the 15 amino acid standard. For the peaks where two amino acids co-elute, the response factor was calculated based on the area of the total peak and the total concentration of both amino acids. Using these response factors, the concentration of amino acids in the total albumin and H0200 sample were calculated (Table 3.3). Based on the amino acid concentrations calculated using the

peak areas from the C18 chromatography, the total hydrolyzed amino acid yield for albumin was 80% of the amino acid fraction obtained from the AG-50W resin column. The mass yield for the H0200 sample was approximately 40% of the sample mass eluted from the resin column.

Figure 3.3: Chromatograms from the C18 HPLC procedure for A: 15 amino acid standard, B: H0200 amino acid fraction. The amino acids are labeled in A. The 12 collected fractions are marked on both chromatograms.

A: 15 amino acid standard



B: H0200 amino acid fraction sample

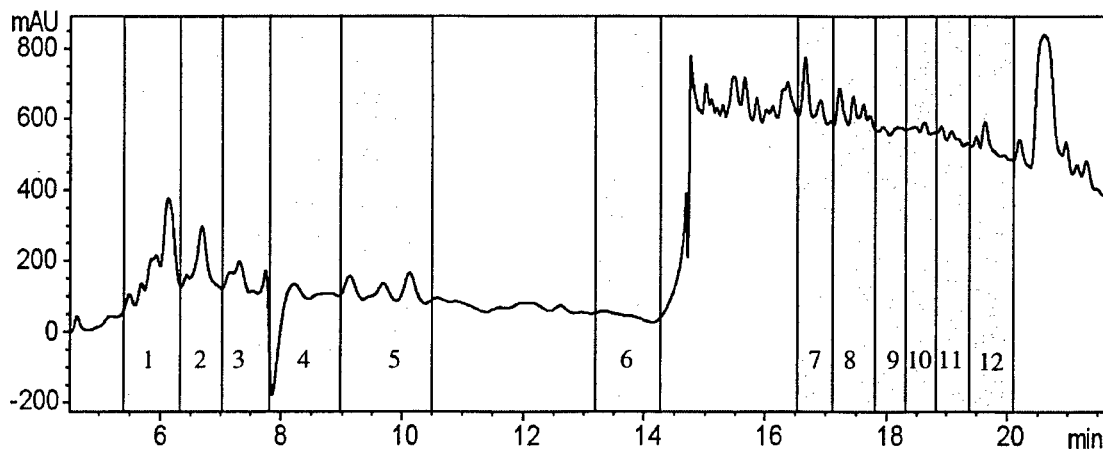


Table 3.3 Average mass of each amino acid as calculated from the C18 chromatograms for albumin and H0200 samples, along with the percent standard deviation. The vial number each amino acid peak was collected in is also noted. Percent standard deviation is determined from the mass calculated from all of the individual injections.

amino acid	gly+ser	ala+asp	lys+thr	glu	his	arg+val	met	tyr	ile	leu	phe	total mg	
albumin													
C18 mg ave	2.3	3.0	6.3	39.0	22.4	0.8	26.9	1.8	6.1	6.6	8.1	5.5	128.9
% stdn dev	21	13	16	15	56	118	43	26	40	48	45	20	28
C18 fraction	1	2	3	4	5	6	7	8	9	10	12		
H0200													
C18 mg ave	1.5	1.3	6.9	9.2	4.6	0.5	3.1	0.8	0.7	1.3	1.8	0.9	32.6
% stdn dev	27	30	39	40	26	32	58	32	26	79	62	58	19
C18 fraction	1	2	3	4	5	6	7	8	9	10	12		

Proton NMR spectra were taken of each collected fraction of both albumin and H0200 samples to check for purity. In general, the amino acids present in each vial matched those assigned to the peaks collected, though there was some contamination from amino acids in adjacent fractions. For the albumin samples, there was little contamination from compounds other than amino acids. The H0200 samples often contained some amount of carbohydrate and/or aliphatic contamination, especially those fractions collected early in the chromatogram. Figure 3.4 shows the ¹H NMR spectrum of vial 12 (part A) compared to a pure phenylalanine (phe) standard spectrum (part B). Compared to the phenylalanine standard NMR spectrum, the H0200 vial 12 spectrum had a higher baseline, and indications of the presence of carbohydrates and aliphatic contaminants. The peak at 2.0 ppm in the C18 vial 12 spectrum was from acetonitrile, one of the eluants used in the chromatography. The peaks were slightly shifted due to the fact that the vial 12 sample was not pH neutralized before NMR analysis in order to avoid the addition of salts. However, the isolation of phenylalanine in the vial 12 from the H0200 sample indicates the level of purification achieved by the C18 HPLC method.

Figure 3.4 Proton NMR spectrum of C18 HPLC collected vial 12 from H0200 sample (A) and a standard phenylalanine spectrum (B). The peak at 4.8 ppm in both spectra is assigned to water, and the peak at 2.0 ppm in part A is acetonitrile. Small shifts in H0200 peaks relative to the standard are due to the fact the H0200 sample was not neutralized prior to NMR acquisition.

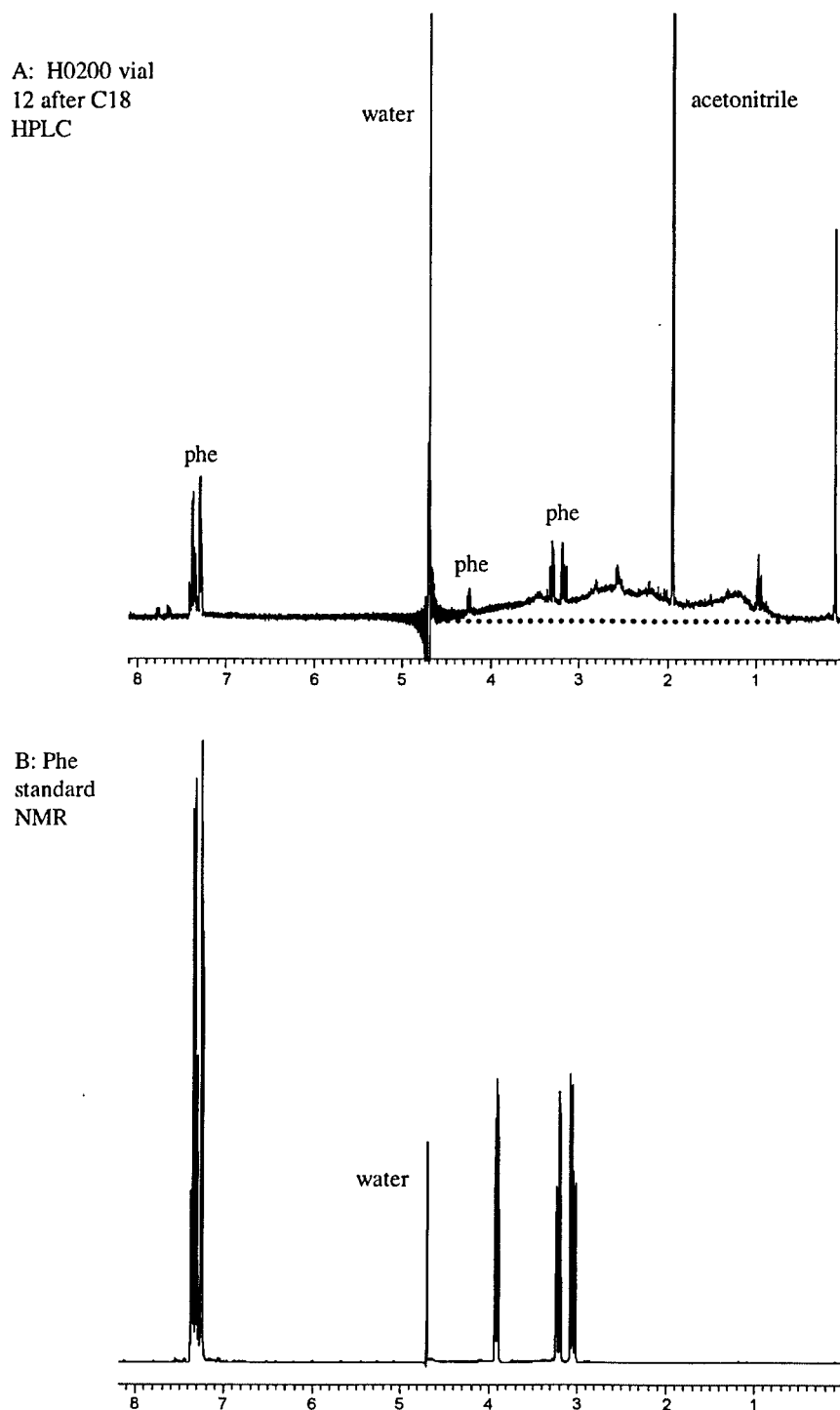
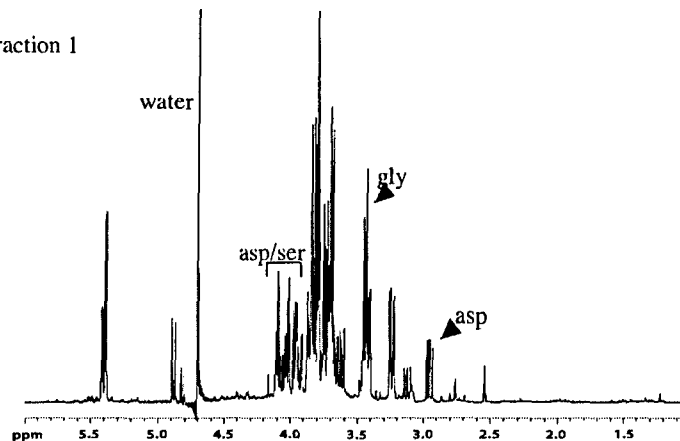
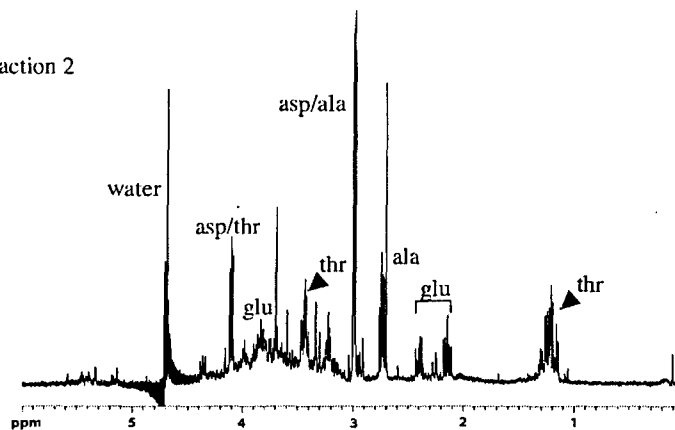


Figure 3.5: ^1H NMR spectra of the amino acid fractions collected during the C18 purification of H0200 HMWDOM. With the exception of fraction 4, none of the subsamples were neutralized to pH 7 prior to NMR spectroscopy, which results in the shifting of some peaks relative to standard spectra. Peak at 4.8 ppm in all spectra is assigned to water.

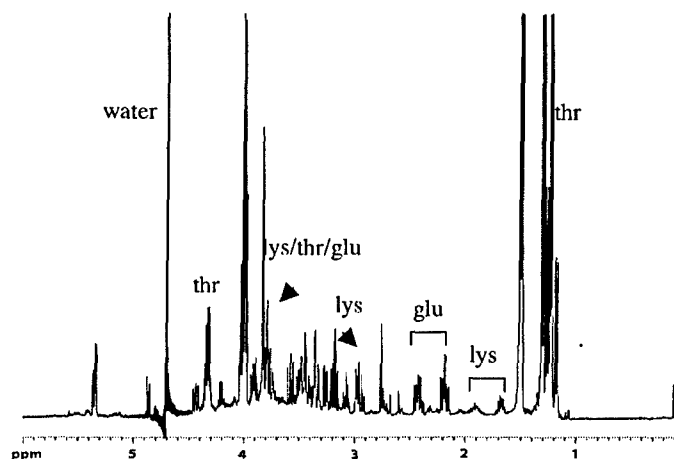
A: H0200 C18 fraction 1



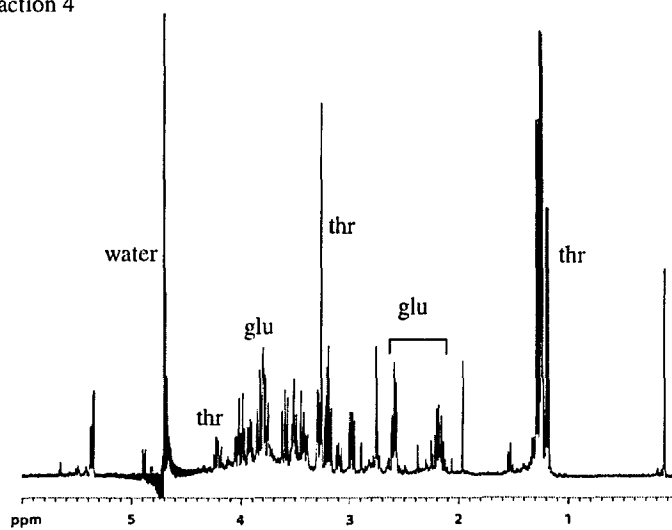
B: H0200 C18 fraction 2



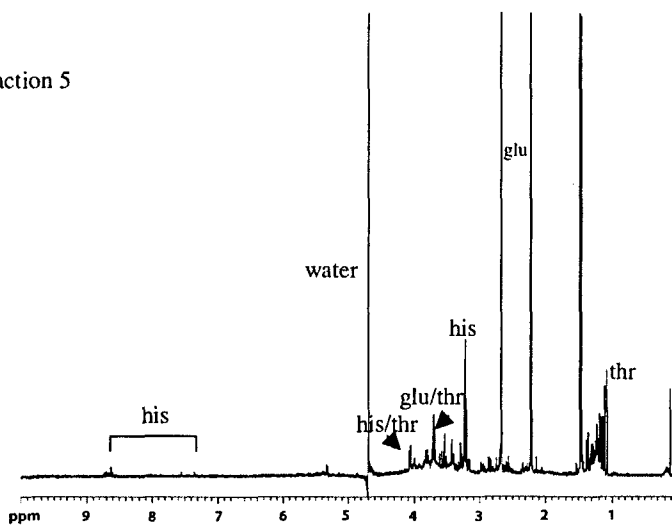
C: H0200 C18 fraction 3



D: H0200 C18 fraction 4



E: H0200 C18 fraction 5



F: H0200 C18 fraction 6

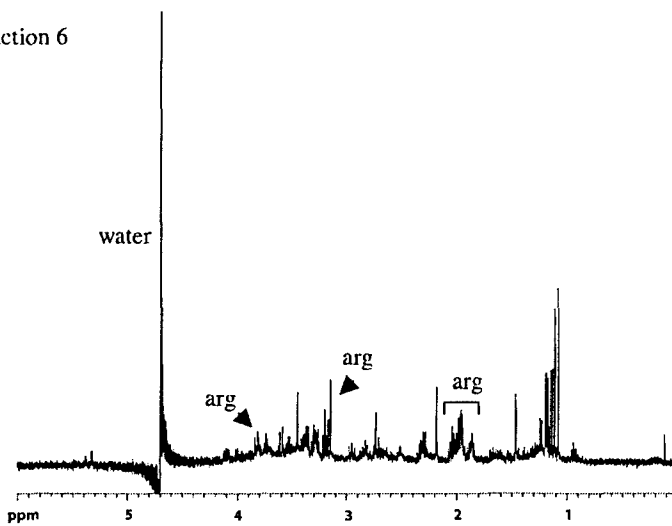
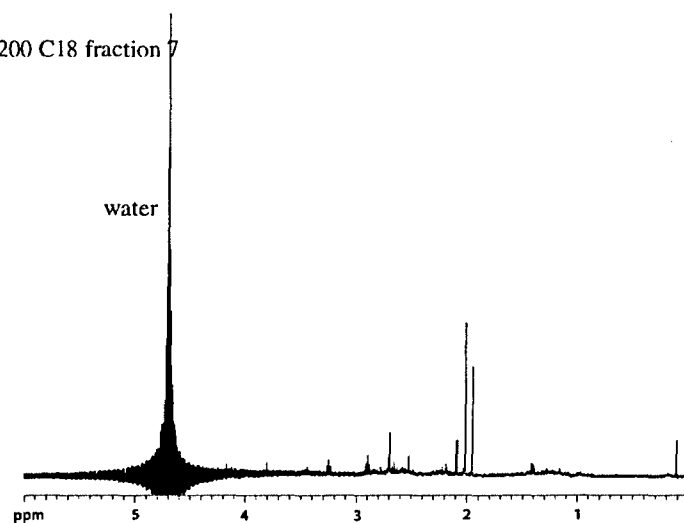
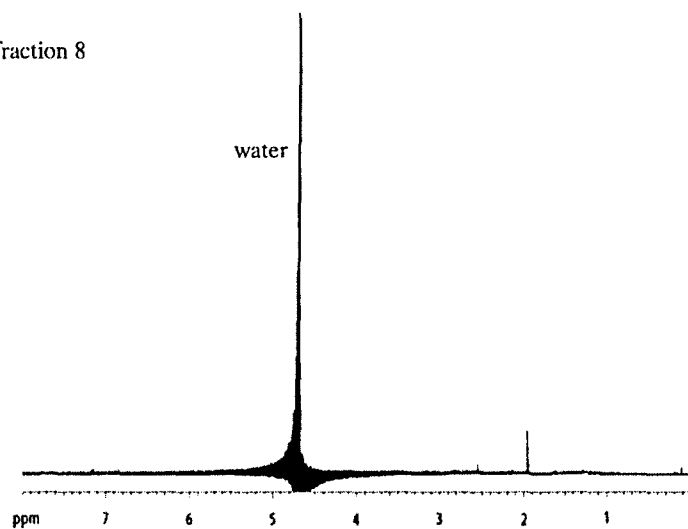


Figure 3.5G: H0200 C18 fraction 7



H: H0200 C18 fraction 8



I: H0200 C18 fraction 9

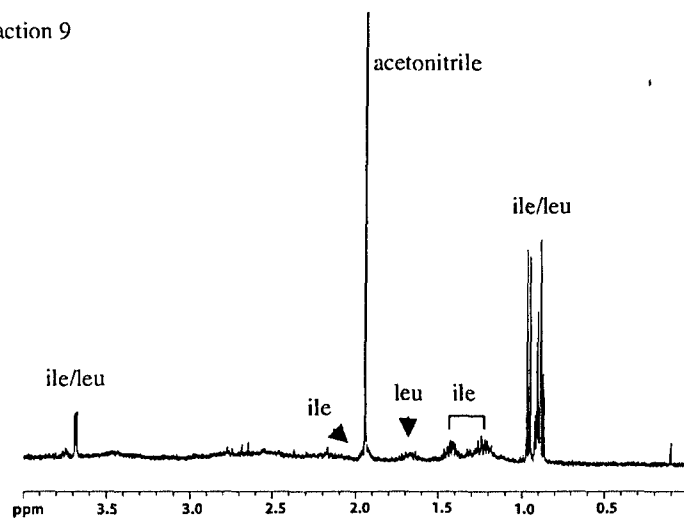
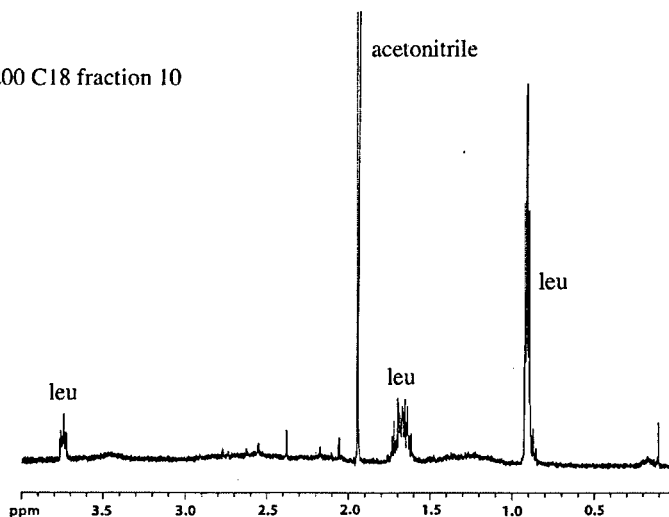
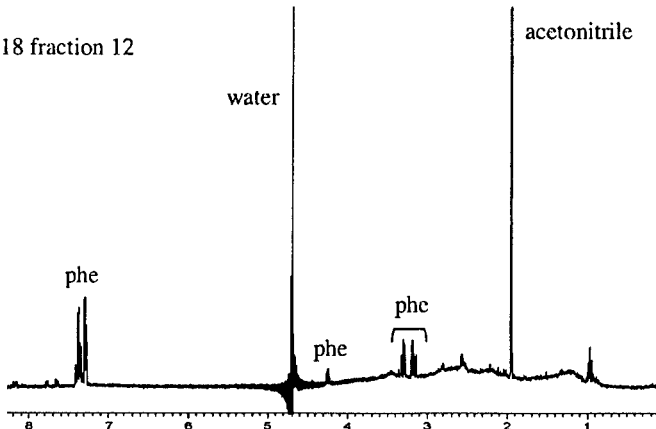


Figure 3.5J: H0200 C18 fraction 10



3.5K: H0200 C18 fraction 12



^1H NMR spectra for each of the 12 collected fractions from the C18 HPLC column are shown in Figure 3.5. The amino acids contained in each fraction were identified based on NMR spectra of individual amino acid standards. The fractions that had early elution times had generally higher concentrations of monosaccharide impurities. Fractions 7 and 8 did not have a high enough concentration of amino acids in the fraction to give a significant NMR signal, and were not processed through the cation exchange column.

3.3.4 SCX HPLC Results

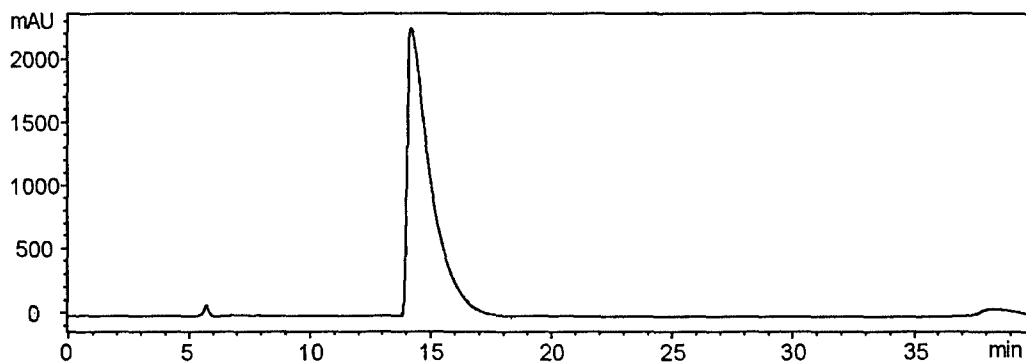
Due to the fact that the ^1H NMR spectra of the fractions collected from the C18 HPLC procedure contained a mixture of amino acids and often, in the case of the H0200

sample, showed contamination by carbohydrate and aliphatic moieties, a second chromatographic step was needed to further purify the individual amino acids for radiocarbon measurement. Strong cation exchange, or SCX, HPLC was chosen because it provided a different separation mechanism from the previous C18 method, taking advantage of the cationic character of the amino acid functional groups, rather than relying on the ion-pairing reverse phase separation. As a result, the elution order on the SCX column is different from that of the C18 column, allowing the separation of the co-eluting amino acids from the previous step. A glucose standard eluted with the solvent peak, and therefore was not retained on the column. All amino acids were separable using the SCX column with the exception of valine, which eluted with the solvent peak, and the co-eluting leucine/isoleucine pair.

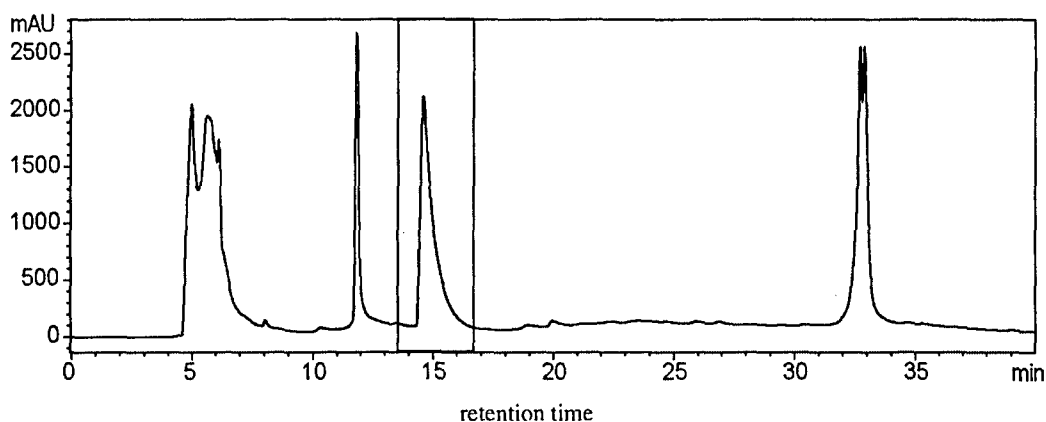
Only the collected H0200 and albumin fractions that contained a significant amount of amino acids according to NMR spectroscopy were run through the SCX column. Fraction 4 collected from the C18 column was the only one neutralized prior to rotary evaporation, and was not analyzed due to the precipitation of salts during evaporation that could not be redissolved in the SCX phosphate buffer. Due to the less consistent nature of the SCX column as compared to the C18 column, and the slight peak shifting that resulted between different batches of buffer eluants, individual amino acid standards were run every day for the amino acids present in the C18 fraction being processed. A blank injection was run between the amino acid standards and the actual samples to avoid standard carry-over. Figure 3.6A shows the chromatogram of a phenylalanine standard, with the phenylalanine peak eluting at 15 min.

Figure 3.6 SCX HPLC chromatograms for a phenylalanine standard (A) and the H0200 C18 vial 12 (B). Previous NMR spectra of fraction 12 showed the presence of phenylalanine (shaded area) along with some contamination. The peaks at 5 min and 12 min in the fraction 12 chromatogram are solvent peaks.

A: Phe standard



B: H0200 vial 12 from C18



In general, the chromatograms of amino acid standards on the SCX column yielded poorer peak shapes with significant tailing, and less stable baselines than the C18 chromatograms, especially for weakly absorbing amino acids that eluted near the solvent peak at 6 min. As a result, all major peaks eluted from the C18 fractions were collected off the SCX column, whether or not they corresponded to amino acid standard peaks.

Figure 3.6B shows the SCX chromatogram taken from the H0200 C18 vial 12. As shown

in Figure 3.4 A, the NMR spectrum of this vial collected from the C18 column showed a strong phenylalanine signal, along with the presence of some carbohydrate and aliphatic-type contamination. All of the SCX chromatograms of the H0200 C18 collected fractions showed two separate solvent peaks similar to those shown in Figure 3.6 B; the expected one at 5 min and one unexpected at 12 min. Analysis of these peaks using ^1H NMR spectroscopy of the peak at 12 min showed no NMR signals present except for those corresponding to methanol and water. In addition, the amino acid peaks from some C18 fractions were shifted to longer retention times on the SCX column compared to the respective standards. Many amino acid peaks that eluted in the 7-10 minute range as standards eluted after the 12 min solvent peak from the C18 collected fractions, with no change in relative elution order. Whether this difference in elution behavior was due to the presence of some other compounds in the H0200 C18 samples or just due to slightly degraded column performance remains unknown.

As with the fractions collected from the C18 HPLC column, the amino acid peaks from the SCX procedure were analyzed for purity using ^1H NMR. This was also helpful in identifying the contents of peaks that did not correspond to the standards. The phenylalanine peak seen in the SCX chromatogram from Figure 3.6 was collected and analyzed vial NMR (Figure 3.7A). With the exception of the peaks assigned to methanol (3.2 ppm) and acetonitrile (1.9 ppm), the spectrum of the phenylalanine collected off the SCX column matches that of the phenylalanine standard. This comparison demonstrates that the sample from the SCX column was indeed phenylalanine, and that with the exception of some volatile solvents, the phenylalanine collected was pure (>95%). The ^1H NMR spectra of other collected peaks from the SCX column showed they still

Figure 3.7 Proton NMR spectrum of the phenylalanine peak collected from the SCX HPLC column, (A) and the phenylalanine standard spectrum (B). The peak at 4.8 ppm corresponds to water, while the peaks at 3.2 ppm and 1.9 ppm in A correspond to methanol and acetonitrile, respectively.

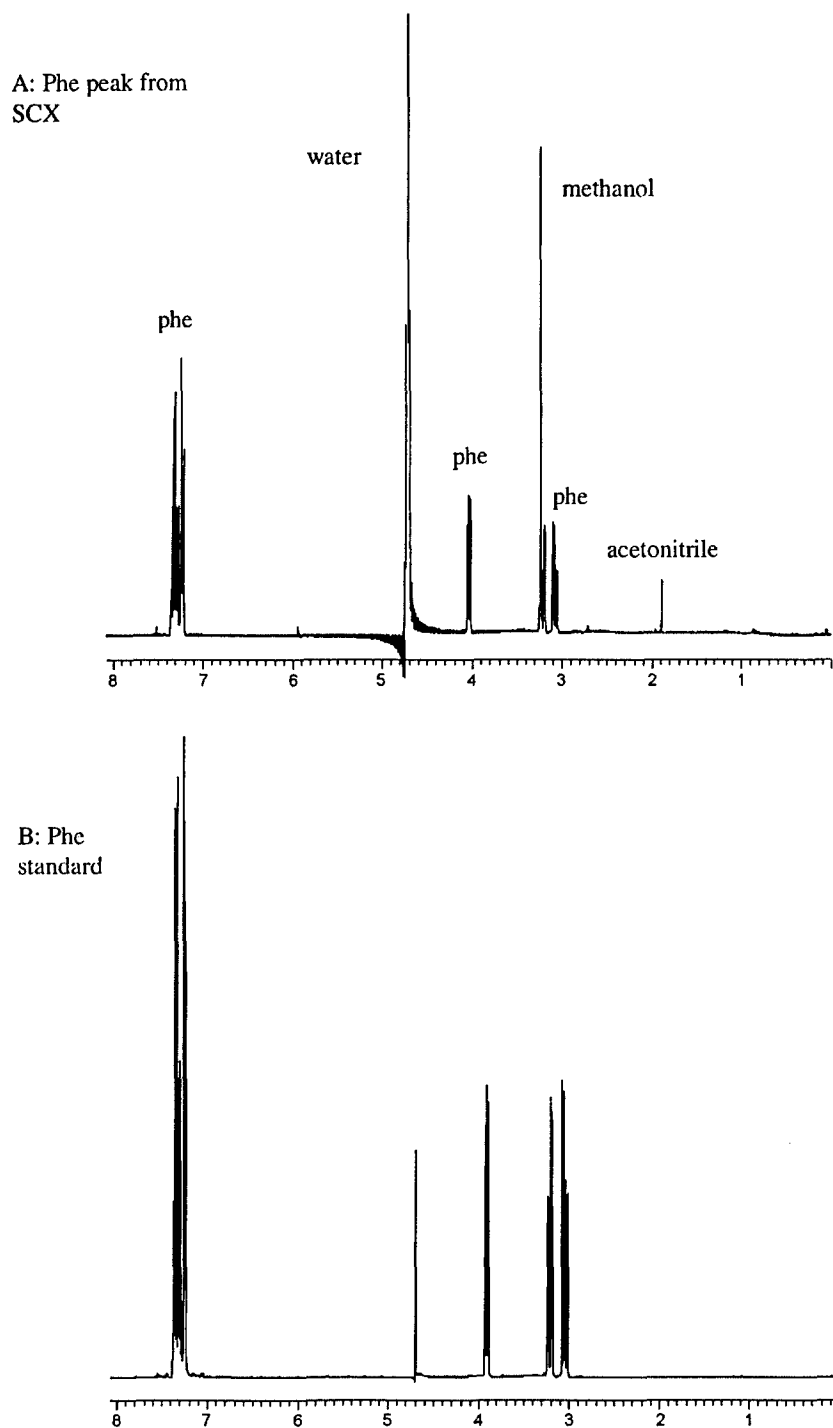


Table 3.4: List of ¹H NMR spectra from SCX collected fractions with the amino acid content of each fraction. This table lists the collection time for each fraction, along with an estimate of the amino acid purity based on the NMR spectra. The identifiable contaminants or functional groups are also listed.

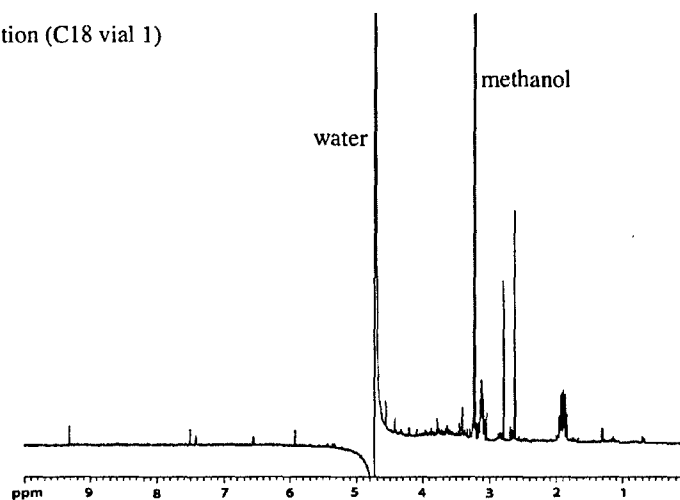
peak	collection time (min)	Fig. 3.8 NMR spectra	amino acids present	estimated % amino acid purity*	identifiable contaminants present
vial 1					
ser	6.0-10.5	A	none	N/A	methanol, amine cmpds?
gly	10.5-12.6	B	ser+gly	80%	methanol, monosaccharides
13.5 min	12.6-14.2	C	gly	80%	methanol, monosaccharides
15 min	14.2-15.9	D	none	N/A	methanol, monosaccharides
20-22 min	19.0-23.1	E	none	N/A	methanol, monosaccharides
vial 2					
thr	8.5-10.2		none	N/A	methanol only
13 min	12.3-13.5	F	asp	40%	methanol, amine cmpds?
14 min	13.5-14.7	G	asp+ala	50%	methanol, monosaccharides
16 min	15.0-17.2	H	none	N/A	methanol, monosaccharides
ala	23.0-25.8	I	ala	60%	methanol, deoxysugars
vial 3					
thr	7.2-8.7		none	N/A	methanol only
glu	8.7-10.2		none	N/A	methanol only
12-14 min	12.1-14.0	J	glu	30%	methanol, deoxysugars
17 min	16.1-17.8	K	thr	95%	methanol, alkyl cmpds
18.5-19.5 min	18.5-19.5	L	none	N/A	methanol, deoxysugars
lys	27.0-31.2	M	none	N/A	methanol, deoxysugars
vial 5					
glu	6.7-9.3	N	thr	40%	methanol, monosaccharides
thr	6.8-11.6	O	thr	50%	methanol, acetonitrile
17-19.5 min	17.0-19.5	P	none	N/A	methanol, deoxysugars
his	35.0-37.1	Q	his	20%	methanol, amine and alkyl cmpds?
vial 6					
7 min	6.5-8.7		none	N/A	methanol, acetonitrile only
13-15 min	13.1-14.9	R	glu	50%	methanol, alcohol cmpds
arg	16.0-17.6		none	N/A	methanol, acetonitrile only
vial 9					
ile/leu	12.2-18.7	S	ile	90%	methanol, amine cmpds?
vial 10					
11 min	9.8-12.7		none	N/A	methanol, acetonitrile only
leu/ile	13.5-20.2	T	leu	95%	methanol
vial 12					
phe	13.6-19	U	phe	95%	methanol, acetonitrile

* Presence of known volatile compounds (methanol and acetonitrile) are not included in estimates of amino acid purity

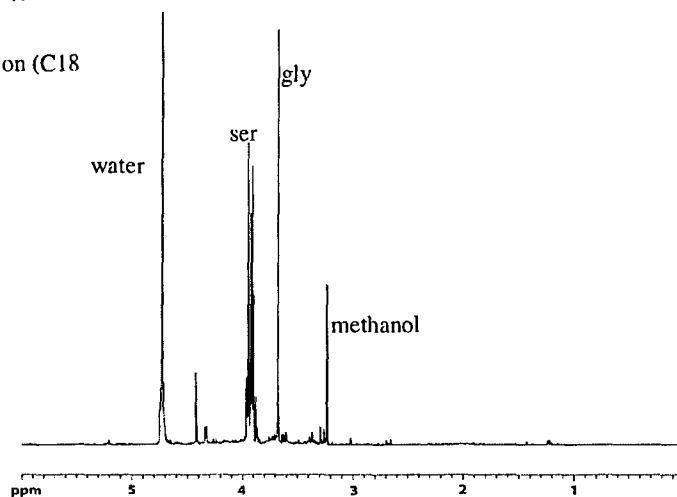
contained some amount of contamination, mainly in the form of monosaccharides and unidentifiable amine, hydroxy and alkyl compounds for the H0200 sample (Figure 3.8). Peaks eluting after 17 min in the SCX chromatograms of H0200 C18 fractions often

Figure 3.8: ^1H NMR spectra for the collected peaks from the SCX HPLC procedure. Collected fractions that did not contain any functional groups other than water and methanol are not included in this figure. Small shifts in peaks relative to amino acid standards may be seen due to the presence of SCX buffer salts in the samples. In all spectra, the water peak is at 4.8 ppm, and methanol is present at 3.2 ppm. A list of the NMR spectra shown can be found in Table 3.4.

A: H0200 ser fraction (C18 vial 1)



B: H0200 gly fraction (C18 vial 1)



C: H0200 13.5 min peak (C18 vial)

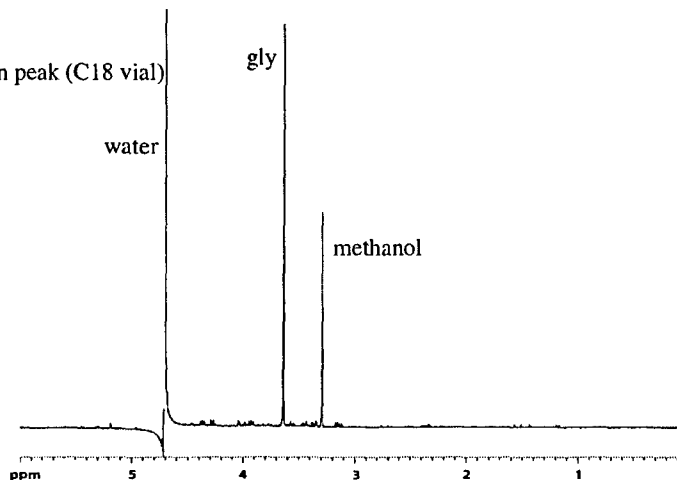
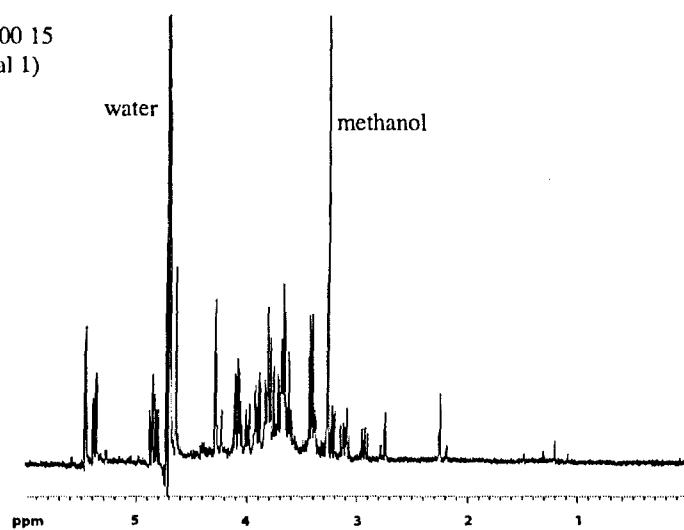
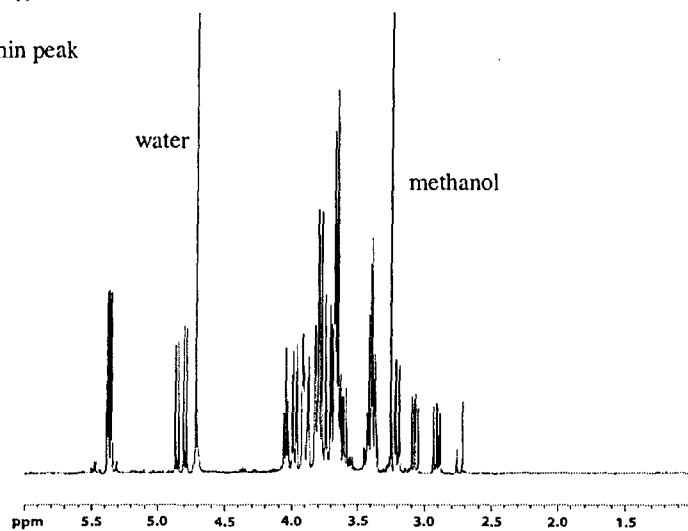


Figure 3.8D: H0200 15 min peak (C18 vial 1)



E: H0200 20-22 min peak (C18 vial 1)



F: H0200 13 min peak (C18 vial 2)

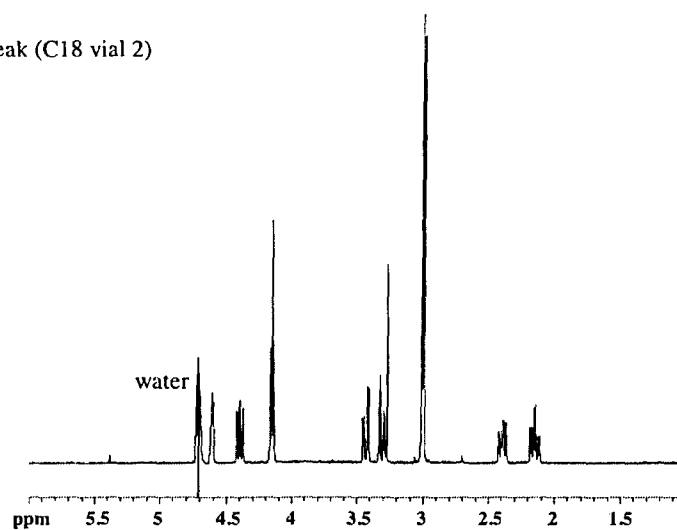
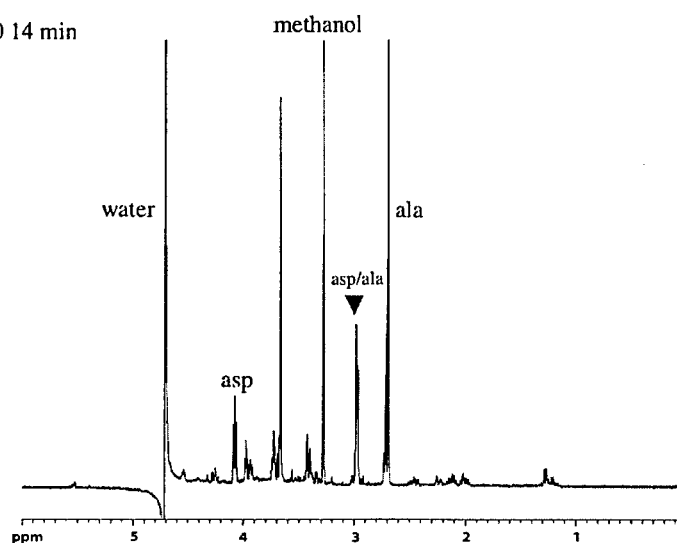
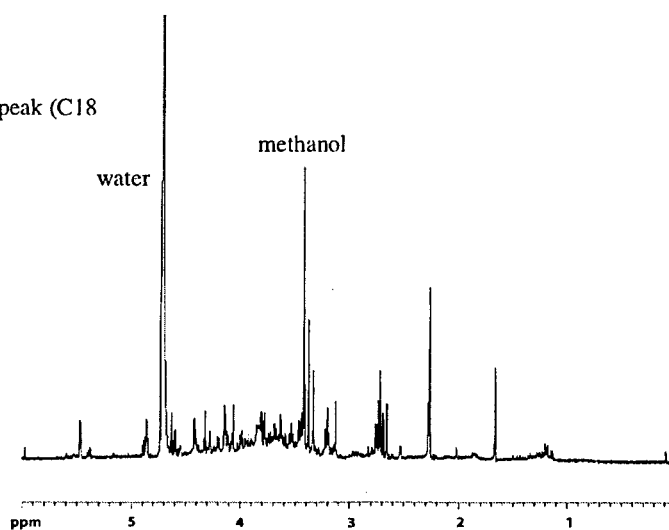


Figure 3.8G: H0200 14 min
peak (C18 vial 2)



H: H0200 16 min peak (C18
vial 2)



I: H0200 ala fraction (C18 vial 2)

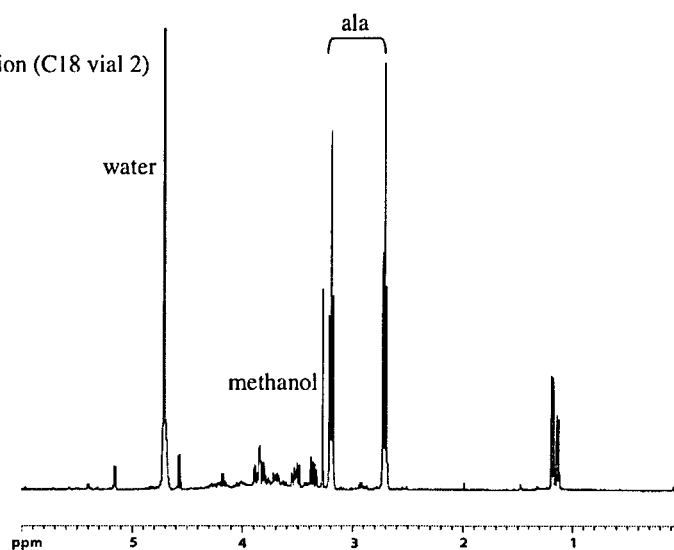
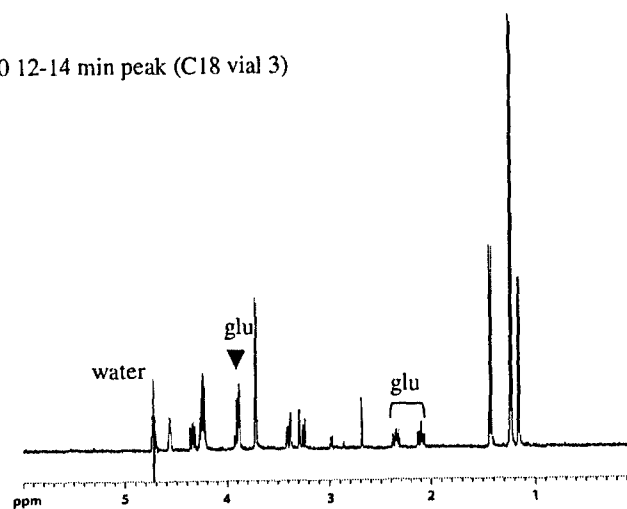
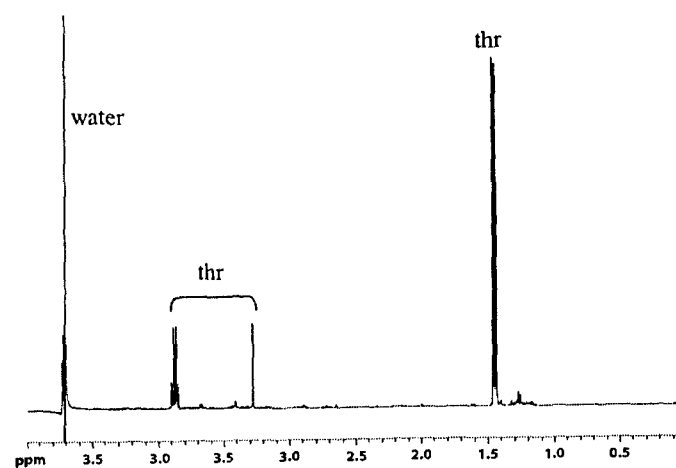


Figure 3.8J: H0200 12-14 min peak (C18 vial 3)



K: H0200 17 min peak (C18 vial 3)



L: H0200 18.5-19.5 min peak (C18 vial 3)

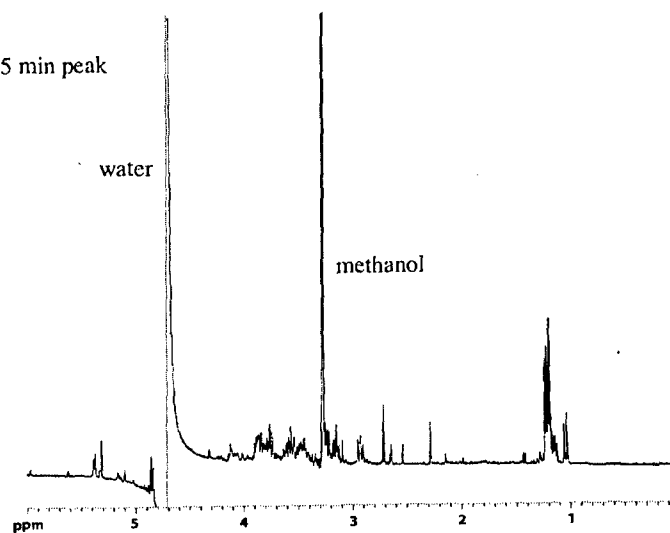
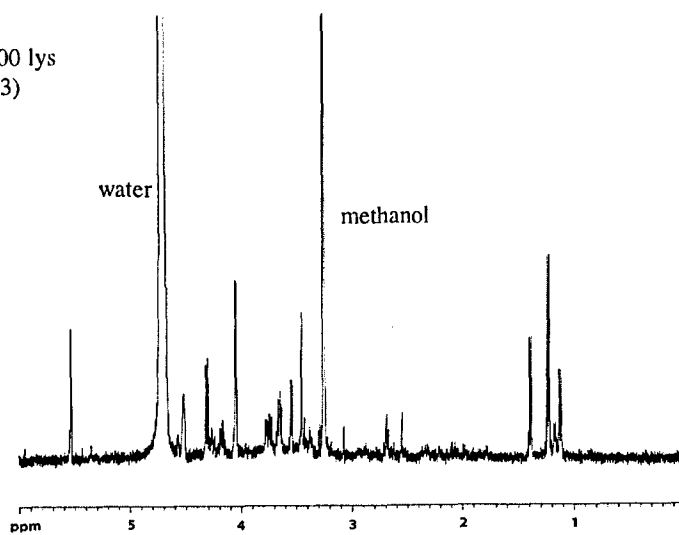
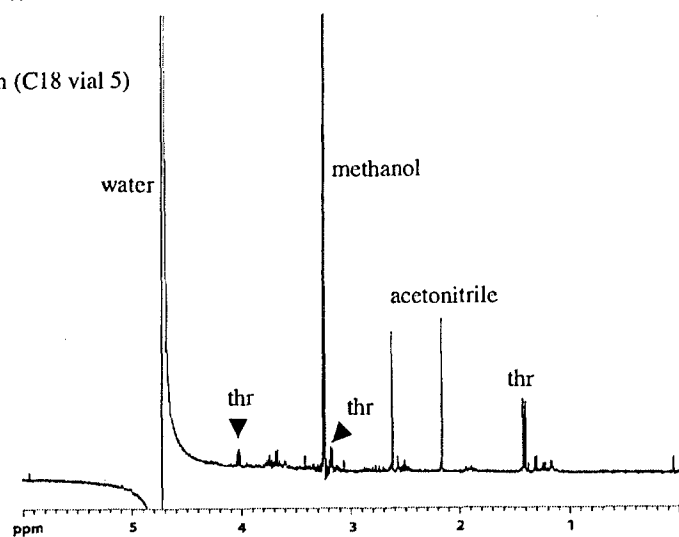


Figure 3.8M: H0200 lys
fraction (C18 vial 3)



N: H0200 glu fraction (C18 vial 5)



O: H0200 thr fraction
(C18 vial 5)

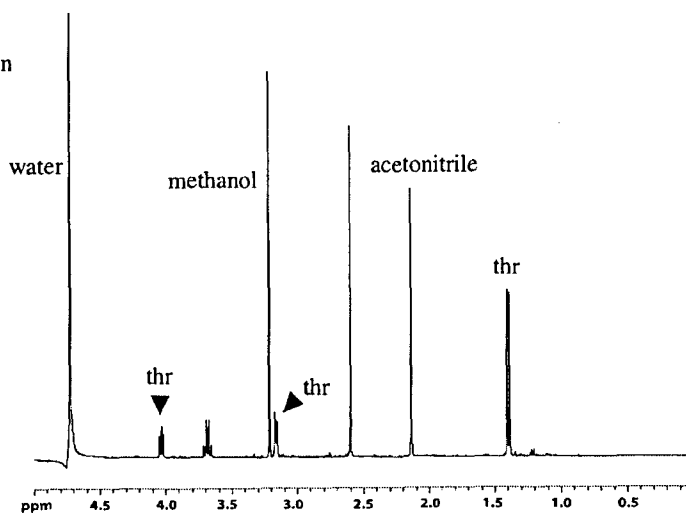
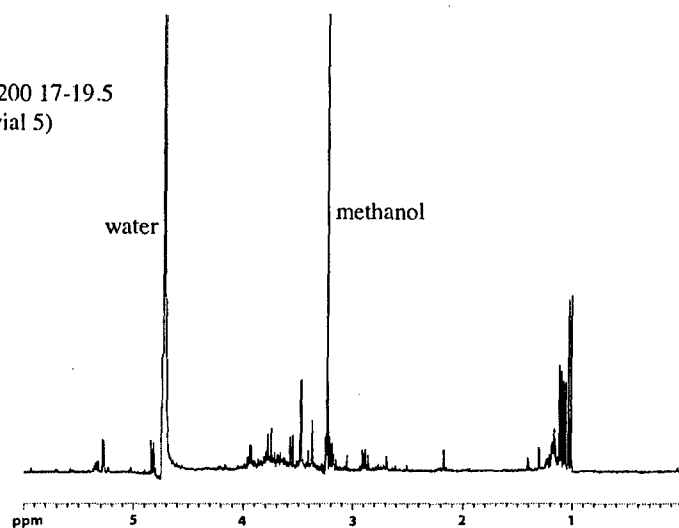
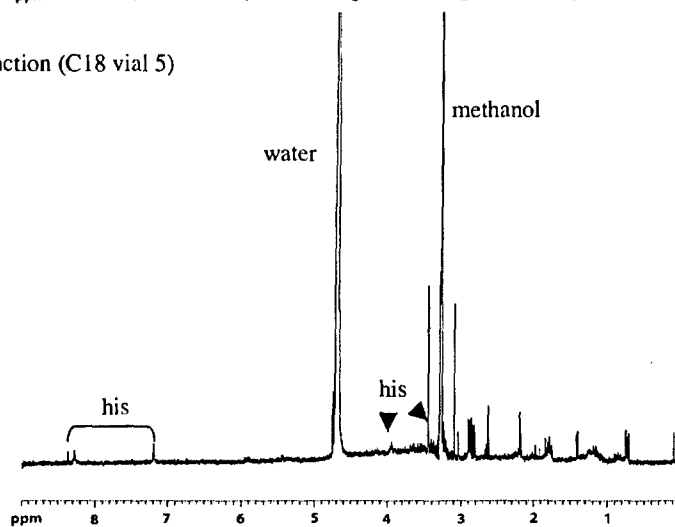


Figure 3.8P: H0200 17-19.5
min peak (C18 vial 5)



Q: H0200 his fraction (C18 vial 5)



R: H0200 13-15
min peak (C18 vial
6)

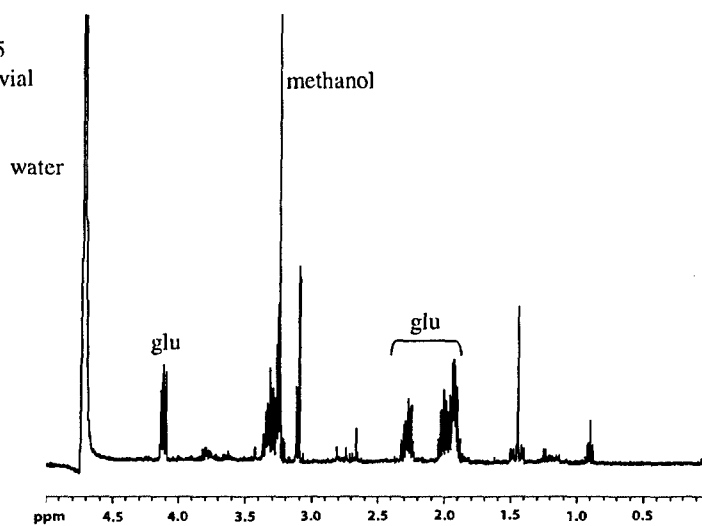
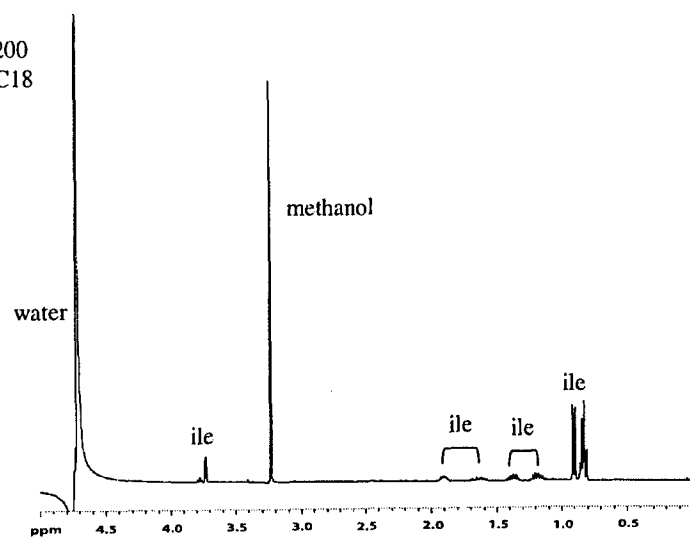
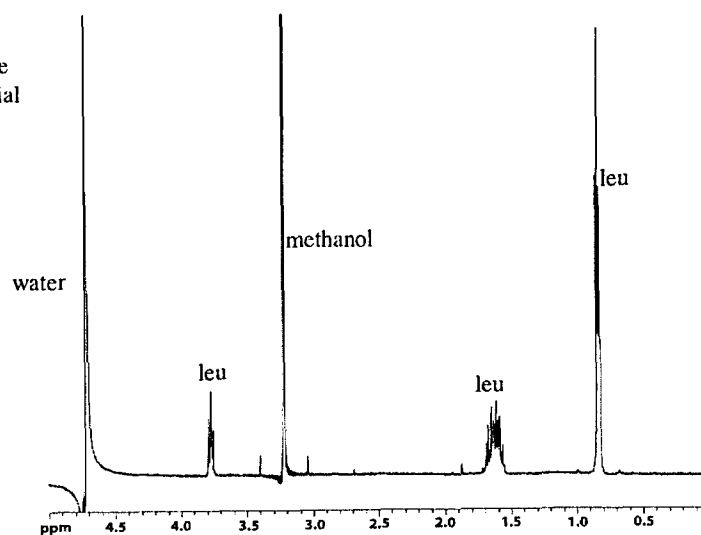


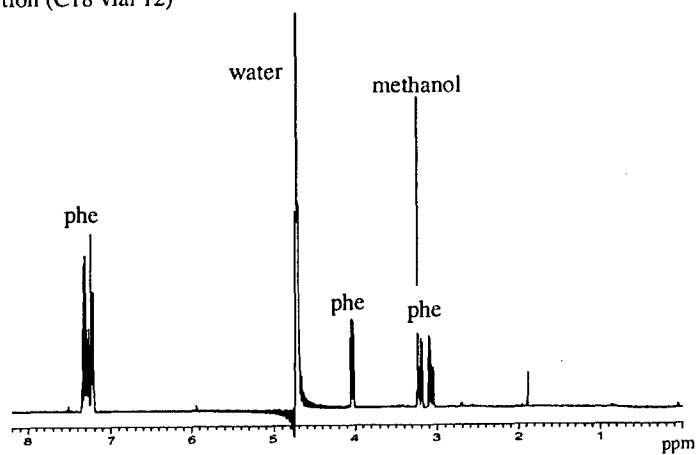
Figure 3.8S: H0200
ile/leu fraction (C18
vial 9)



T: H0200 leu/ile
fraction (C18 vial
10)



U: H0200 phe fraction (C18 vial 12)



contained deoxysugars. NMR spectra of SCX fractions that contained only methanol and acetonitrile are not included in Figure 3.8. The estimated purity of the amino acids and the identifiable contaminants of the ^1H NMR spectra of the collected peaks from the SCX chromatography are listed in Table 3.4. Collected amino acid fractions that were judged to be sufficiently pure ($> 80\%$ purity) and in high enough concentration were processed for radiocarbon measurement.

3.3.5 Radiocarbon Analyses

Four amino acids from albumin and five amino acids from H0200 HMWDOM were sealed in pyrex tubes as described in Section 3.2.4.4 and processed for radiocarbon analysis. Subsamples for both albumin and H0200 were taken after acid hydrolysis and of the amino acid fractions after resin column chromatography were also sealed and processed (Table 3.5). The individual albumin amino acid samples included two acidic amino acids, aspartic acid (asp) and glutamic acid (glu), a neutral amino acid, leucine (leu), and a basic amino acid, lysine (lys). The amino acids isolated and measured from the H0200 sample were the neutral amino acids glycine (gly), threonine (thr), isoleucine (ile), leucine (leu), phenylalanine (phe), and a serine/glycine (ser/gly) combined sample.

Using the low temperature (550°C) combustion method in pyrex tubes, all samples were sealed and combusted, then the resulting CO_2 gas was quantified and submitted to NOSAMS for analysis. Each amino acid from the albumin sample was split into three tubes, while the H0200 samples were divided into two separate tubes, with the exception of the serine/glycine pair which was divided in thirds. Except for the leucine replicates from both samples, only one tube from each amino acid was submitted for radiocarbon analysis. The ^1H NMR spectrum for the serine/glycine sample from H0200

showed the presence of some minor contaminant peaks, possibly monosaccharides. It was uncertain whether additional purification would be beneficial, so the sample was split. Half was sealed into pyrex tubes, combusted, and submitted for analysis. The results of this fraction are listed in Table 3.4 as the 'H0200 ser/gly' sample. The

Table 3.5 The results for the albumin and H0200 samples submitted for $\delta^{13}\text{C}$ and $\Delta^{14}\text{C}$ analysis. The H0200 ser/gly C18 sample was re-cleaned using the C18 column after the SCX procedure.

sample	$\mu\text{g C}$	$\delta^{13}\text{C}$	$\Delta^{14}\text{C}$	Fm	Fm error	purification steps*
albumin	959.5	-11.5	117	1.1245	0.004	untreated
alb. hydrolysis	406.3	-11.2	122	1.129	0.005	1
alb. amino acid fr.	296	-11.57	125	1.132	0.004	1, 2
alb. asp	182.5	-10.35	121	1.13	0.01	1, 2, 3, 4
alb. lys	203	-10.74	130	1.14	0.01	1, 2, 3, 4
alb. glu	201.8	-9.52	93.7	1.10	0.01	1, 2, 3, 4
alb. leu	306.7	-21.93	72.7	1.0798	0.0034	1, 2, 3, 4
alb. leu	298.4	-22.26	79.4	1.0865	0.0035	1, 2, 3, 4
H0200 HMWDOM		-21.9	11.3	1.017	0.004	untreated
H0200 hydrolysis	232.4	-21.64	-17.3	0.9892	0.006	1
H0200 amino acid fr.	531	-20.33	43.1	1.050	0.004	1, 2
H0200 ser/gly	134.6	-20.09	60.5	1.07	0.01	1, 2, 3, 4
H0200 gly	71	16.97	98.6	1.11	0.01	1, 2, 3, 4
H0200 thr	111.1	-25	-246	0.759	0.009	1, 2, 3, 4
H0200 ile	90.2	-22.11	121	1.13	0.01	1, 2, 3, 4
H0200 leu	58.4	-25.97	290	1.30	0.01	1, 2, 3, 4
H0200 leu	58.6	-25.81	283	1.29	0.01	1, 2, 3, 4
H0200 phe	181.6	-30.21	-454	0.549	0.004	1, 2, 3, 4
H0200 ser/gly C18	363.1	-34.62	-786	0.216	0.003	1, 2, 3, 4, 5

Purifications steps:

1. hydrolyzed
2. AG 50W cation exchange resin
3. C18 HPLC
4. SCX HPLC
5. recleaned using C18 HPLC

remaining half was re-processed through the C18 column in order to determine whether additional purification could eliminate the minor contamination, then processed for

radiocarbon measurement. This re-purified fraction is listed as 'H0200 ser/gly C18'. A water blank and a blank consisting only of buffer salts collected from the SCX procedure were also combusted but not submitted for AMS analysis since these blanks produced only 9 μg and 12 μg of carbon respectively. There was no correlation between sample size and $\Delta^{14}\text{C}$ values. For all samples, some uncondensable gases were generated during combustion. It was assumed that these gases were nitrogen compounds and would not affect the CO_2 yield.

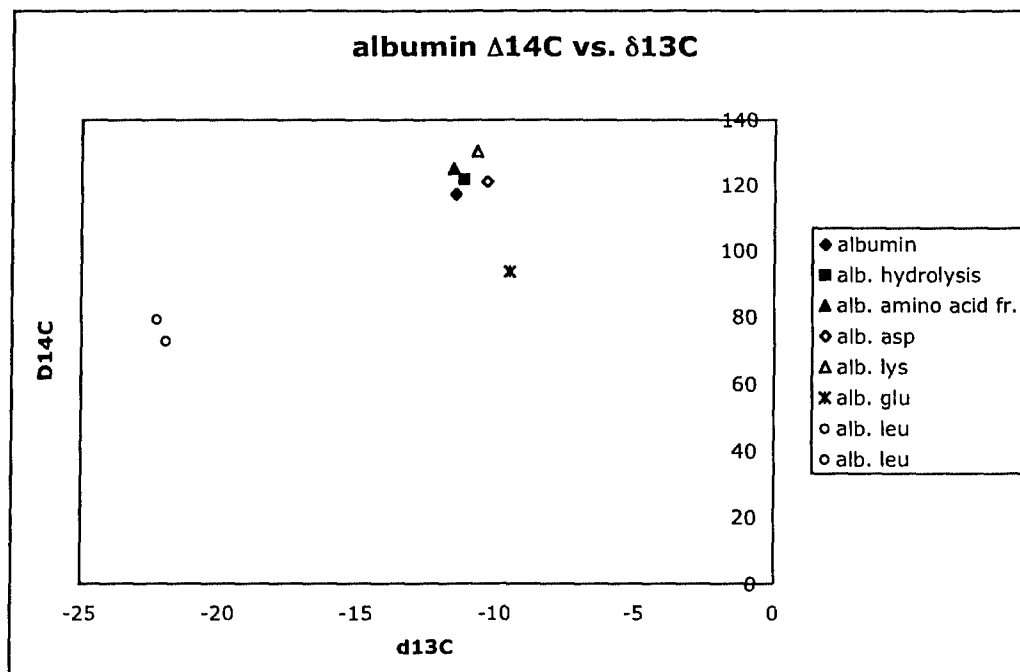
The $\delta^{13}\text{C}$ and $\Delta^{14}\text{C}$ values for the isolated amino acids can also be seen in graphical form in Figure 3.9 for albumin data and Figure 3.10 for the H0200 sample. The leucine (leu) samples from both H0200 and albumin samples were split and combusted in replicate tubes in order to provide an estimate of precision. Total (non-hydrolyzed) albumin and H0200 samples were combusted using the conventional high temperature combustion (quartz tubes combusted at 850°C) rather than the low temperature pyrex method used for the hydrolyzed, base fraction, and amino acid samples. The different combustion method may affect the $\Delta^{14}\text{C}$ results and limit comparison with samples combusted at low temperature.

The samples of albumin before and after hydrolysis, and the amino acid fraction from the AG-50W resin column are marked in Figure 3.9 in the filled symbols. Radiocarbon measurements indicated that the albumin sample has a fraction modern greater than 1, indicating that the protein incorporated bomb radiocarbon and was synthesized after 1950. The $\delta^{13}\text{C}$ measurements were consistent with the source of the bovine serum albumin protein, cows presumably fed on C_4 plants such as corn. The post-hydrolysis and base-eluted albumin fractions showed similar $\Delta^{14}\text{C}$ and $\delta^{13}\text{C}$ values to

the original bulk sample, indicating that no fractionation occurred during hydrolysis and resin column purification steps.

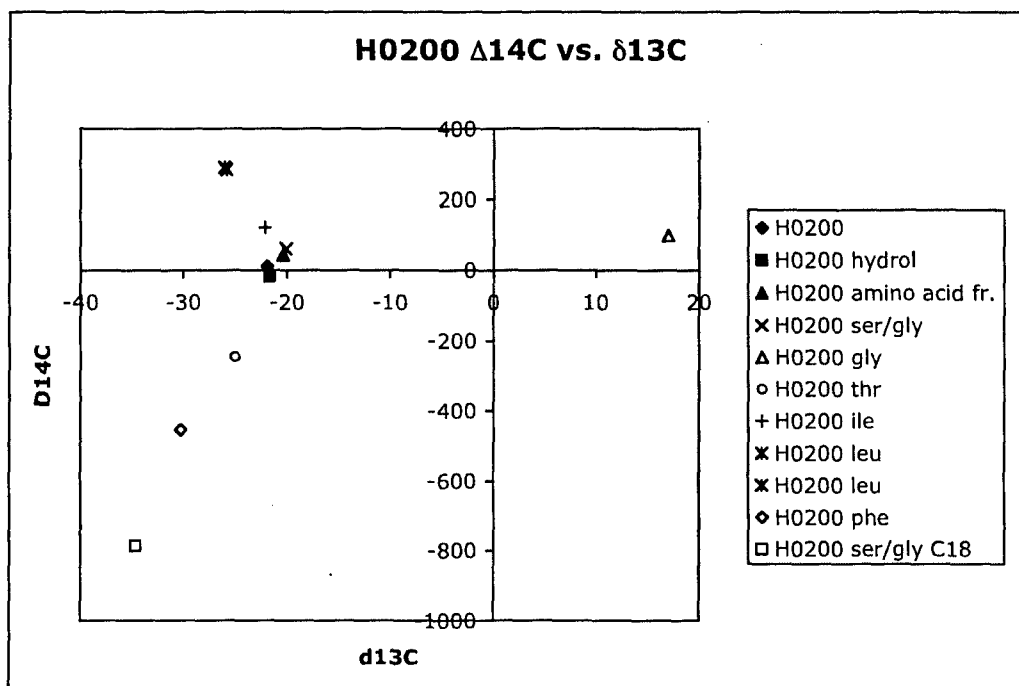
The open symbols represent the compound specific radiocarbon measurements for the individual amino acids for albumin. Two of the individual amino acids, aspartic acid and lysine, had $\Delta^{14}\text{C}$ and $\delta^{13}\text{C}$ values similar to the total albumin protein. The glutamic acid sample was slightly depleted compared to total albumin, but still had a $\delta^{13}\text{C}$ value reflecting the source material. The two replicate measurements of the leucine sample showed good consistency with each other, but had very different $\Delta^{14}\text{C}$ and $\delta^{13}\text{C}$ values relative to the total albumin and the other amino acids. While the rest of the total albumin and amino acid samples had a $\Delta^{14}\text{C}$ of greater than 90‰, the leucine replicates were more depleted, with an average value of 76.1‰. Given that the precision for replicates of standards using small sample ^{14}C measurements is approximately 20‰, this difference was considered relatively small (Pearson, 1999; Hwang and Druffel, in press). Instead of a $\delta^{13}\text{C}$ value of around -11‰, the leucine samples were much more ^{13}C depleted (average value of -22.1‰). Since each of the leucine samples were sealed in separate tubes and individually combusted and analyzed, it was unlikely that any contamination occurred after the sample was processed for radiocarbon analysis. The contamination must have occurred prior to sealing the samples.

Figure 3.9 $\Delta^{14}\text{C}$ versus $\delta^{13}\text{C}$ for the albumin bulk and amino acid samples. Leucine samples are replicate CO_2 submissions of a sample split before combustion.



The radiocarbon measurements for the H0200 sample were more varied in nature (Figure 3.10). The unhydrolyzed H0200 sample had a $\delta^{13}\text{C}$ value typical of marine biomass at -21.9‰ , with a $\Delta^{14}\text{C}$ value of 11.3‰ . The hydrolyzed H0200 sample had a similar $\delta^{13}\text{C}$ value but a $\Delta^{14}\text{C}$ of -17.3 , implying this fraction is older than the non-hydrolyzed sample. This difference may be due to the use of the high temperature combustion method for the non-hydrolyzed sample compared to the low temperature combustion procedure used for the hydrolyzed sample. The hydrolyzed amino acid eluted fraction off the AG-50W resin column still had a $\delta^{13}\text{C}$ value of -20‰ , but the $\Delta^{14}\text{C}$ was 43‰ , more enriched in radiocarbon than both the hydrolyzed and unhydrolyzed H0200 samples. This fractionation may be due to the removal of a large amount of older carbon by the resin column procedure.

Figure 3.10: $\Delta^{14}\text{C}$ versus $\delta^{13}\text{C}$ for the H0200 bulk and amino acid samples. Leucine samples are replicate CO_2 submissions of a sample split before combustion.



The measured values for individual amino acid samples isolated from H0200 are much more variable than those from albumin. The $\delta^{13}\text{C}$ and $\Delta^{14}\text{C}$ values for the serine/glycine pair (-20.09‰ and 60.5‰ respectively) and the isoleucine (-22.11‰ and 121‰) sample had modern (post 1950) $\Delta^{14}\text{C}$ values, though the isoleucine sample was more enriched in radiocarbon. The glycine only sample had a modern $\Delta^{14}\text{C}$ value of 98.6‰ , but was very highly enriched in ^{13}C , with a $\delta^{13}\text{C}$ of $+16.97\text{‰}$. In contrast, the leucine replicates, while in close agreement with each other, had $\delta^{13}\text{C}$ values of -25.9‰ but extremely high $\Delta^{14}\text{C}$ values of over 280‰ . On the opposite end of the $\Delta^{14}\text{C}$ scale, the amino acids phenylalanine and threonine were much more depleted than both the bulk H0200 and the other amino acid samples, with $\Delta^{14}\text{C}$ values of -454‰ and -246‰ , respectively. Phenylalanine also had a more depleted $\delta^{13}\text{C}$ (-31.21‰) signal than the

other amino acids (+16.97‰ to -25.9‰), while the $\delta^{13}\text{C}$ for threonine was not directly measured and assumed to be -25‰. The fraction of the serine/glycine mixed sample that was re-purified through the C18 HPLC column had the lowest $\delta^{13}\text{C}$ and $\Delta^{14}\text{C}$ values of all the samples, at -34.6‰ and -786‰ respectively.

3.4 Discussion

The main goal of the research described in this chapter was to develop a method to separate and purify amino acids without derivitization. The final method for amino acid purification was a combination of three chromatographic steps that took advantage of the different aspects of the chemical properties of amino acids. The sample was hydrolyzed to liberate the amino acid residues and then passed through an AG-50W cation exchange resin column designed to separate the positively charged amino acids from other compounds in the sample. In other studies, this "amino acid fraction" had been assumed to contain only amino acids, based on the recovery of non-protein amino acid internal standards or the yield of a standard set of amino acids (Henrichs, 1980; Wang et al., 1996; Wang et al., 1998; Hwang and Druffel, 2003; Loh et al., 2004). However, analysis of this amino acid fraction for H0200 by ^1H NMR spectroscopy indicated that this fraction was not pure amino acid in content (Figure 3.2 C). While the amount of non-amino acid contaminants was certainly reduced, the NMR spectrum shows a significant amount of carbohydrate and aliphatic protons that did not belong to any amino acids. As a result, any radiocarbon measurements of this sample would actually reflect a combination of amino acids and non-amino acid compounds that may or may not have had similar $\Delta^{14}\text{C}$ values. In the future, if the total amino acid fraction

isolated by cation exchange column chromatography is to be used for radiocarbon analysis, it is recommended that the resulting sample should be analyzed using NMR spectroscopy in order to confirm the purity of the amino acid fraction. Using a technique that measures at the total content of the amino acid fraction is necessary, as this contamination may not be discovered if only amino acid specific derivitization reactions are used to assess the contents of the sample.

The amounts of albumin and H0200 hydrolyzed were calculated to provide a yield of approximately 1 mg of carbon for every amino acid. The amount CO₂ measured after the combustion of the amino acids actually submitted for radiocarbon analysis was at most 808 µg C for albumin leucine sample and 304 µg C for the H0200 phenylalanine sample. Over 20% of the albumin sample and 70% of the H0200 sample was lost during sample purification. The loss of amino acids, especially for the H0200, is a cause for concern. The average yield of amino acids from the H0200 column after C18 HPLC purification seems to match well with the 1 mg per amino acid estimate, assuming that the area of the peaks are due to amino acids only. If this is correct, the loss of the amino acids must be due to the SCX column, or the during rotary evaporation and transfer of each sample after collection. However, ¹H NMR spectra from the fractions collected from the C18 column showed that these fractions are not pure amino acids, so the yield of amino acids calculated is only a maximum estimate, and amino acids may be lost during this step as well.

The purity of the amino acids submitted for isotopic analysis was excellent (>90%) with the exception of the H0200 serine/glycine pair (>80% estimated purity). In addition to the two co-eluting amino acids, this sample also contained about 20% of an

unidentified contaminant, and was subsequently split and half re-cleaned via C18 HPLC. This re-cleaned serine/glycine sample had a slightly improved purity, but was also contaminated with C18 column bleed. The remaining albumin samples consisted of amino acids without other known carbon compounds, but these amino acid samples were not submitted due to low concentration or co-eluting amino acid pairs. For the H0200 samples, most of the samples not submitted for analysis contained some amount of contamination (Figure 3.8). For most samples, the contamination was in the form of monosaccharides or deoxysugars, but in some cases, the type of contaminating compound could not be identified. Based on previous studies, the precision of replicates of standards using small sample ^{14}C measurements was assumed to be approximately 20‰ (Pearson, 1999; Hwang and Druffel, in press). An error of $\pm 20\%$ would allow for differentiation of turnover time on a 10-20 year timescale, but not on a year to year basis.

The H0200 HMWDOM sample has a $\Delta^{14}\text{C}$ value of 11.3‰, indicating the majority of this sample was modern (< 50 yrs old). This is significantly younger than the total DOC as measured in both the Mid-Atlantic Bight, which ranged from -32‰ to -414‰, and in the North Central Pacific, with an average value of -179‰ (Druffel et al., 1992; Aluwihare et al., 2002). The H0200 $\Delta^{14}\text{C}$ value was also more enriched than a similar HMWDOM fraction from the Central North Pacific at 20 m depth, which was determined to be -92‰ (Loh et al., 2004). The relatively enriched $\Delta^{14}\text{C}$ for the H0200 sample may be a function of the different ultrafiltration membranes than used by Loh et al., 2004 resulting in retention of a slightly different set of HMWDOM compounds, the effect of different carbon blanks, or the different sample collection locations and times. The $\delta^{13}\text{C}$ measurement for the bulk H0200 sample confirms the marine source of the

HMWDOM fraction. The $\delta^{13}\text{C}$ and $\Delta^{14}\text{C}$ values for the hydrolyzed H0200 sample correspond well with the bulk H0200 sample, indicating that no significant fractionation took place in the sample during hydrolysis. The shift in $\Delta^{14}\text{C}$ from 11.3‰ for the total H0200 sample to a more enriched value (43.1‰) for the amino acid fraction comes as a result of the removal of older, ^{14}C depleted compounds by the cation exchange column.

It was anticipated that the isotopic measurements of amino acids from the H0200 surface HMWDOM sample would result in modern radiocarbon ages and similar $\delta^{13}\text{C}$ values. Amino acids have been shown to be released as products from bacteria and phytoplankton cultures, and various types of proteins have been isolated directly from the HMWDOM (Tanoue, 1995; Yamada et al., 2000; Yamada and Tanoue, 2003). In turn, these amino acids can be utilized as nitrogen sources by bacteria and phytoplankton (Flynn and Butler, 1986; Palenik and Morel, 1990; Jørgensen et al., 1994). This combination of rapid production and remineralization would result in an amino acid fraction that turns over quickly. The radiocarbon results for the H0200 sample do not support this hypothesis. The $\delta^{13}\text{C}$ values for the amino acid sample ranged from almost +17‰ to -35‰, with $\Delta^{14}\text{C}$ values from +290‰ to -790‰. Considering that the bulk H0200 sample had a $\delta^{13}\text{C}$ of -22‰ and a $\Delta^{14}\text{C}$ of 11.3‰, and that the maximum level of radiocarbon in the oceanic DIC was never as high as +290‰ (Bauer, 2002), the wide-ranging amino acid measurements are a cause for concern. Of particular interest are the enriched $\delta^{13}\text{C}$ value of glycine, the extremely enriched $\Delta^{14}\text{C}$ value of leucine, and the relative depletion of both isotopes for threonine and phenylalanine. If the isotopic measurements of these samples are correct, the average age of phenylalanine in the sample is approximately 5000 years old and the threonine sample age is 3000 years old,

compared to the modern ages for the serine/glycine, glycine and isoleucine samples. It can be concluded that the high $\Delta^{14}\text{C}$ levels for leucine must be due to contamination, and the extremely enriched $\delta^{13}\text{C}$ may be a result of either contamination or a very intensive fractionation process.

Contamination of the isolated amino acids can occur by other compounds present in HMWDOM that were not cleanly removed from the amino acid samples, or by other contaminants introduced during the purification method. While the ^1H NMR spectra of the samples submitted for radiocarbon analysis were estimated to be over 90% pure amino acid, there were still some non-amino acid peaks present. These contaminants were mostly sugars, which given the composition of HMWDOM was not unexpected. Some unidentified alkyl and amine type protons also appear in the NMR spectra. Since only proton NMR spectroscopy was performed, there may be other carbon compounds present that do not have resonant hydrogen atoms, but this seems unlikely. If the source of the contaminating compounds were sugars, the $\Delta^{14}\text{C}$ values should not change significantly, given that compound specific monosaccharide $\Delta^{14}\text{C}$ values also range from 49-92‰ (Aluwihare et al., 2002).

Contamination can also include compounds introduced either during the purification method, or accidentally introduced into the sample from other outside sources. The sample of serine/glycine that was re-cleaned using the C18 HPLC method again in an attempt to remove the slight contamination seen in the NMR spectrum shows evidence of column bleed. Compared to the sample that was not passed through the C18 column again, the $\delta^{13}\text{C}$ and $\Delta^{14}\text{C}$ values are very depleted. This is most likely the result of bleed from the octyldecyl carbon chains that make up the separation phase of the C18

column. This carbon chain was most likely generated from petroleum products, and had a very depleted $\Delta^{14}\text{C}$ value, explaining the 850‰ decrease of the C18 recleaned serine/glycine sample (-786‰) compared to the original amino acid pair (60.5‰) (Reddy, personal communication). While this also may have occurred to the other samples, the extra carbon was then removed during the SCX purification. The H0200 leucine samples were also certainly contaminated by an outside source, this time causing an enrichment in the ^{14}C , resulting in extremely high $\Delta^{14}\text{C}$ values (289.5‰). It is highly unlikely that this level of enrichment could be the result of natural fractionation processes in the HMWDOM sample. The source of the contamination in the H0200 leucine samples is not known, but it was probably an isolated incident, since none of the other amino acid samples have extremely enriched $\Delta^{14}\text{C}$ values. The contamination occurred before the sample was sealed for radiocarbon analysis, since the $\Delta^{14}\text{C}$ values are very similar for both leucine replicates.

The depleted $\Delta^{14}\text{C}$ values for phenylalanine and threonine isolated from H0200 HMWDOM are very interesting. Given the purity of the phenylalanine and threonine samples based on the ^1H NMR spectra, it seems unlikely that the depleted $\Delta^{14}\text{C}$ values were caused by contamination. Compared to the DIC, surface DOC has a $\Delta^{14}\text{C}$ depletion of approximately 300‰, indicating that some fraction of the DOC is much older than the DIC. HMWDOM is also depleted in ^{14}C compared to the DIC, indicating that the HMWDOM fraction also contains some amount of older carbon compounds. This older fraction of HMWDOM has not been conclusively identified, though compound class radiocarbon measurements have indicated that the lipid and acid insoluble fractions of HMWDOM have lower $\Delta^{14}\text{C}$ values than the carbohydrate and amino acid fractions (Loh

et al., 2004). The $\Delta^{14}\text{C}$ values for phenylalanine (-454‰) and threonine (-246‰) isolated from H0200 surface HMWDOM indicates that these amino acids have a longer turnover time than any of the other samples measured. This long turnover time may be due to all of the amino acids in the samples having one, consistent $\Delta^{14}\text{C}$ value, or there may be two or more fractions within each sample, each having a different $\Delta^{14}\text{C}$ value. If it is assumed that the second scenario is correct, a mass balance equation can be used to calculate the relative percentages of the modern amino acids and the older phenylalanine and threonine fractions. The average of the $\Delta^{14}\text{C}$ values from the H0200 isoleucine, glycine, and serine/glycine amino acids (93.4‰) was used for the modern $\Delta^{14}\text{C}$ value, and the $\Delta^{14}\text{C}$ value for the deep Pacific DOC (-550‰) was used for the older fraction. Using these values, phenylalanine sample was calculated to contain 85% older carbon ($\Delta^{14}\text{C}=-550‰$) phenylalanine, and the threonine sample had 53% old threonine.

Of the six amino acids that were isolated from the surface HMWDOM sample, phenylalanine and threonine were the only ones to show a possible mix of both old and modern carbon. This is slightly unexpected, as it has long been assumed that the proteins that contain amino acids are produced by phytoplankton and bacteria from the ambient DIC and retain the modern $\Delta^{14}\text{C}$ values. These proteins were either rapidly utilized by other organisms, since amino acids are good sources for both nitrogen and carbon, or preferentially transported to deeper waters, similar to monosaccharides. Instead, the compound specific radiocarbon measurements indicate that while some amino acids may have modern (post-1950) $\Delta^{14}\text{C}$ values similar to the DIC, at least two amino acids (phenylalanine and threonine) also contain some fraction of older material. This older fraction may be due to the preferential preservation of phenylalanine- and threonine-rich

proteins with long turnover times that are mixed back into the surface water. When hydrolyzed, these proteins release $\Delta^{14}\text{C}$ depleted phenylalanine and threonine, which is then combined with the newly produced amino acids during isolation. This then results in a turnover time of approximately 5000 years for phenylalanine and 3000 years for threonine. It is also possible that the phenylalanine and threonine pools do not contain any modern carbon, perhaps due to rapid utilization in the surface waters by organisms. Instead, all of the phenylalanine and threonine measured may come from older, preferentially preserved proteins cycling through the ocean. Unfortunately, analysis of HMWDOM samples from other locations and depths is necessary to confirm the phenylalanine and threonine $\Delta^{14}\text{C}$ values as well as the explanation behind these values.

Whenever fractionation of ^{13}C versus ^{12}C occurs in a sample, ^{14}C fractionation also occurs, scaled to twice that of the $^{13}\text{C}/^{12}\text{C}$ pair due to the difference in molecular weight. The $\Delta^{14}\text{C}$ values are adjusted using the measured $\delta^{13}\text{C}$ signal and corrected to a $\delta^{13}\text{C}$ of -25‰ in order to remove any fractionation affecting the samples. As a result, the $\Delta^{14}\text{C}$ values can be considered independent of each other, and the possible explanations for the anomalous values for $\delta^{13}\text{C}$ and $\Delta^{14}\text{C}$ can be addressed separately. There are a few possible explanations for the $\delta^{13}\text{C}$ values measured for H0200 glycine, phenylalanine, and to a lesser extent, leucine, samples. One is alteration of ^{13}C signals due to incomplete hydrolysis. The second explanation is that natural variations in the initial formation or later microbial alteration of the amino acids may change the relative values of $\delta^{13}\text{C}$ between amino acids. Lastly, inadvertent fractionation may occur because of HPLC columns and peak collection procedures. In contrast, because of the $\delta^{13}\text{C}$ correction to

the $\Delta^{14}\text{C}$ measurement, the only process that could alter the $\Delta^{14}\text{C}$ but not the $\delta^{13}\text{C}$ would be inadequate HPLC peak collection biasing the isotopic composition.

One explanation for the relatively light $\delta^{13}\text{C}$ phenylalanine may be the effects of incomplete hydrolysis (Silfer et al., 1992; Silfer et al., 1994). Tracking the $\delta^{13}\text{C}$ for the reactants, products, and total system during the hydrolysis of a glycine based protein (glycylglycine) shows that as the percent hydrolysis increases, the free glycine released becomes increasingly depleted in ^{13}C , and remains depleted even after the substrate is consumed, which is unexpected in a closed system (Silfer et al., 1992). The initial glycine protein had a $\delta^{13}\text{C}$ value of -39‰ and was hydrolyzed at 160°C . At the beginning of the hydrolysis (13.1% hydrolyzed), the released glycine had a $\delta^{13}\text{C}$ value of -40‰ . After 92% hydrolysis, this value had shifted to -43.6‰ , a depletion of 4.6‰ compared to the initial protein. If a similarly sized depletion had occurred during H0200 hydrolysis, the initial $\delta^{13}\text{C}$ value for phenylalanine would be approximately 25.7‰ . Due to its hydrophobic nature, phenylalanine is often enriched in cell wall proteins. Incomplete hydrolysis of these proteins may result in an artificially depleted $\delta^{13}\text{C}$ signal for phenylalanine. However, it is unlikely that fractionation caused by incomplete hydrolysis is the cause of the ^{13}C depletion in H0200 phenylalanine. The degree of depletion is not large enough to account for the measured difference between $\delta^{13}\text{C}$ values for phenylalanine (-30.21‰) and the total amino acid fraction (-20.33‰). In addition, if fractionation due to partial hydrolysis did occur, the $\delta^{13}\text{C}$ values for more of the isolated amino acids should have been affected. Instead, only phenylalanine has a depleted $\delta^{13}\text{C}$ values.

There are slight natural variations in the $\delta^{13}\text{C}$ between amino acids within a common source organism due to the different biosynthetic pathways for amino acid formation. In particular, glutamic acid, aspartic acid, and glycine tend to be enriched in ^{13}C relative to other amino acids and the bulk carbon values in both mollusk shells and corn proteins (Qian et al., 1995; Fogel and Tuross, 1999). Analysis of the amino acids isolated from proteins in corn plants showed that the $\delta^{13}\text{C}$ values were not all the same. The $\delta^{13}\text{C}$ value for serine was -28.1‰ , valine was -22.2 , and leucine had a $\delta^{13}\text{C}$ value of -20.6 , while phenylalanine, proline, and glutamic acid have $\delta^{13}\text{C}$ values of -13.5‰ , -12.4‰ , and -12.8‰ , respectively. Aspartic acid and glycine were more enriched in ^{13}C , with $\delta^{13}\text{C}$ values of -6.3‰ and -5.1‰ (Fogel and Tuross, 1999). The hydrolyzed amino acids isolated from mollusk shells have $\delta^{13}\text{C}$ were also equally variant. For this sample, leucine (-33.2‰), proline (-27.8‰), valine (-27.4‰) and alanine (-23.3‰) are much more depleted than aspartic acid (-16.2‰), glycine (-16.0‰), and glutamic acid (-9.4‰) (Qian et al., 1995). These variations may be as a result of the larger ratio of carboxyl carbon to non-carboxyl carbon in those particular amino acids, since the carboxyl carbon has been shown to be isotopically heavier than the total amino acid by $17\text{--}24\text{‰}$ (Abelson and Hoering, 1961; Macko et al., 1987). This effect can be seen in the slightly heavier $\delta^{13}\text{C}$ values for the albumin glutamic acid sample in this study (-9.52‰), as well as the much heavier H0200 glycine value (16.97‰); however the large degree of the enrichment in ^{13}C H0200 glycine is not explainable by this effect.

In contrast, leucine, isoleucine, and lysine are more depleted in ^{13}C by approximately -10‰ to -5‰ due to fractionation within the enzymatic formation pathway (DeNiro and Epstein, 1977; Macko et al., 1987). Measurements of $\delta^{13}\text{C}$ for

hydrolyzed amino acids in DOM in freshwater confirms the relative depletion of $\delta^{13}\text{C}$ for leucine (-34.7‰ to -30.9‰) and isoleucine (-31.1‰ to -25.8‰) compared to the bulk organic carbon (-28.1‰ to -22.6‰), at various sampling locations (Ziegler and Fogel, 2003). While the lighter $\delta^{13}\text{C}$ values are seen for leucine in both albumin (-22‰) and H0200 (-25.9‰), the H0200 isoleucine (-22.11‰) and albumin lysine (-10.74‰) are not drastically different from the total amino acid fraction (-11.57‰ for albumin, -20.33‰ for H0200). These natural variations in $\delta^{13}\text{C}$ values due to different metabolic pathways can also explain the relative depletion in $\delta^{13}\text{C}$ values for phenylalanine. Analysis of the individual amino acids isolated from three oceanic photoautotrophic species also shows relative enrichment of alanine, aspartic acid, and glycine relative to the average amino acid $\delta^{13}\text{C}$ values, and depleted $\delta^{13}\text{C}$ values for valine, leucine, and phenylalanine (McCarthy et al., 2004).

The other potential natural cause of fractionation may be as a result of isotopic alterations after the initial creation of the amino acid. Degradation of a specific protein from corn samples showed alteration in the individual amino acid $\delta^{13}\text{C}$ values when compared to the original, non-degraded sample (Fogel and Tuross, 1999). For example, the $\delta^{13}\text{C}$ value for serine began from 0.23‰ before degradation, decreased to -9.4‰ after 3 months, then increased to -6.3‰ after 7 months, while leucine showed an opposing trend increasing from -20.0‰ initially to -14.7‰ after 7 months. $\delta^{13}\text{C}$ measurements on hydrolyzed amino acids isolated from sediments showed ^{13}C enrichment of glycine relative to the other amino acids, indicating that microbial reworking of glycine to form other amino acids results in ^{13}C enrichment in the unused fraction (Keil and Fogel, 2001; Ziegler and Fogel, 2003). As part of an analysis of amino acids in marine sediments

along the Washington coast, Kiel and Fogel, 2001 report a $\delta^{13}\text{C}$ value of 5.8‰ for glycine, compared to the bulk organic carbon $\delta^{13}\text{C}$ of -22.1‰ in locations with the largest relative amount of marine organic matter, hypothesizing that the glycine signals reflect microbial alteration of planktonic amino acids. This study site also measured $\delta^{13}\text{C}$ values for phenylalanine (-26.7‰), leucine (-25.0‰) and isoleucine (-22.3‰) that are very similar to those from H0200 HMWDOM (-30.21‰ for phenylalanine, -25.9‰ for leucine, and -22.11‰ for isoleucine). It is their theory that much of the variation between the amino acid $\delta^{13}\text{C}$ values can be explained by the work of microbial reworking. The $\delta^{13}\text{C}$ of 5.8‰ for glycine is the closest to the H0200 glycine $\delta^{13}\text{C}$ value of 16.97, indicating that fractionation due to microbial reworking may be the main cause of this enrichment in ^{13}C . Analysis of the $\delta^{13}\text{C}$ values of glycine obtained from cultured oceanic heterotrophs measured glycine $\delta^{13}\text{C}$ values that were enriched in ^{13}C relative to the average amino acid $\delta^{13}\text{C}$ values by 12-20‰ (McCarthy et al., 2004). Microbial fractionation may also be the cause of the smaller variations seen in the H0200 $\Delta^{14}\text{C}$ amino acid values relative to the total amino acid fraction (43.1‰), such as the isoleucine $\Delta^{14}\text{C}$ value of 121‰ (McCarthy et al., 2004); however, the lack of any other compound specific amino acid radiocarbon measurements make this conclusion hard to prove.

There is also a mechanistic explanation for the unusual $\delta^{13}\text{C}$ and $\Delta^{14}\text{C}$ values found in the H0200 samples. During chromatography, the carbon isotopes tend to separate from each other. In any particular peak, the ^{12}C , ^{13}C , and ^{14}C enriched molecules elute at slightly different points during the peak (Barrie et al., 1984; Quinn Baumann et al., 1992). Therefore, failing to collect the entire peak will bias the isotopic measurements of the compound. For a HPLC separation of leucine, the ^{13}C and ^{14}C

labeled molecules preferentially eluted in the back half of the peak compared to the ^{12}C molecules (Quinn Baumann et al., 1992). This could explain the extremely depleted values of $\Delta^{14}\text{C}$ for the H0200 phenylalanine and threonine samples. Peak fractions were collected by hand based on the elution timing for amino acid standard solutions. While collection times were adjusted based on the sample so that the entire peaks were collected, it is not impossible, given the close proximity of the peaks and the speed of the solvent flow that the peak collection was incomplete, or preferentially biased towards the front half of the peak. However, this chromatographic fractionation is probably not the main cause of the low $\Delta^{14}\text{C}$ values for phenylalanine and threonine due to the very large magnitude of the depletion, which was about -500‰ for phenylalanine and -300‰ for threonine, compared to the total amino acid fraction. It seems unlikely that the so little of the amino acid peaks could be collected to yield the depleted $\Delta^{14}\text{C}$ values but still have enough amino acid carbon for radiocarbon analysis.

3.5 Conclusion

In this chapter a novel method using three different modes of chromatography was developed for the isolation and purification of underivatized hydrolyzed amino acids from surface HMWDOM for isotopic analysis. The conventional use of column chromatography using a cation exchange resin in order to separate amino acids from HMWDOM was found not to result in a pure amino acid fraction. Since this amino acid fraction also contained a significant amount of monosaccharide and other compounds, use of this fraction to represent the total amino acids within HMWDOM is not recommended. In order to further separate and purify the amino acids, two HPLC

separations were performed, first using a reverse-phase C18 column, then a strong cation exchange (SCX) column. Using this method, six amino acid samples were obtained and analyzed for radiocarbon, though the remaining amino acids isolated from HMWDOM were either too low in concentration or not pure enough for radiocarbon analysis.

The six samples were the first individual amino acids to be isolated from HMWDOM and measured for radiocarbon analysis. Most of the amino acids measured were modern in age, but there were some anomalous values. Glycine was enriched in ^{13}C (17‰), phenylalanine and threonine were depleted in ^{14}C (-454‰ and -246‰), and leucine had a very high $\Delta^{14}\text{C}$ value (>283‰). It is most likely that outside point source contamination was the cause of the extremely high $\Delta^{14}\text{C}$ value for leucine. The $\Delta^{14}\text{C}$ values for phenylalanine and threonine indicate that these amino acids have a longer turnover time than the others, which may indicate differences in preservation for some amino acids. The enriched $\delta^{13}\text{C}$ value for glycine and the smaller variations in $\delta^{13}\text{C}$ and $\Delta^{14}\text{C}$ H2000 values are likely the result of isotopic fractionation due to microbial reworking. Further conclusions about the variations of $\delta^{13}\text{C}$ and $\Delta^{14}\text{C}$ values measured for the individual amino acids, and their implications for compound cycling will require additional samples and method modifications.

Based on NMR spectra of the collected amino acid samples, the method developed in this chapter for amino acid purification produced adequate results but could use some additional refinement. Some of the HMWDOM fractions still retained some contamination, even after three different purification steps. Most of the contamination consisted of monosaccharides and deoxysugars. The SCX HPLC process did not seem to perform as well for the HMWDOM sample as it did for albumin, both in terms of elution

times, peak quality, and separation from other compounds. Whether this was due to a slight change in the concentration of the buffer salts or to the degradation of the column is unknown. Also undetermined are the sources of the contamination seen in the $\Delta^{14}\text{C}$ values for H0200 leucine, phenylalanine, and threonine. While it is hoped that this contamination is not a result of any steps within purification procedure, these measurements cannot be used.

Obviously, radiocarbon measurement in amino acids requires future work in two areas: additional sample measurements from a variety of locations and depths, and an improvement in the separation methods used. There are currently no other measurements from other depths or locations to compare to the amino acids isolated from H0200 surface HMWDOM. Analysis of amino acids from other surface water samples may confirm or refute the variations in $\delta^{13}\text{C}$ and $\Delta^{14}\text{C}$ samples seen in this chapter, and allow for stronger conclusions regarding the cause of these variations, whether natural or due to contamination. Measurement of the $\delta^{13}\text{C}$ and $\Delta^{14}\text{C}$ values from amino acids at other depths would allow comparison to the $\delta^{13}\text{C}$ and $\Delta^{14}\text{C}$ values for DIC at the same depth. This information could then be used to determine whether amino acids at depth are transported there from the surface or whether they are made in situ by bacteria.

Obviously, if these other measurements are to be performed, the amino acid isolation method also needs to be improved. Ideally, this procedure should produce clean separations of each amino acid, with a nearly 100% yield. In particular, the SCX HPLC step could be improved. The behavior of the SCX column with the H0200 sample was very different than for amino acid standards and albumin, both in terms of peak shape and elution times. It is unknown whether this was caused by other compounds present in the

HMWDOM sample, or due to column degradation. In addition, this step also introduces phosphate and borate salts into the amino acid samples that complicate sample combustion. Replacement of the SCX step with another that is better at purification and does not need buffer salts would be ideal.

3.6 References

- Abelson, P. H. and T. C. Hoering (1961). Carbon isotope fractionation in the formation of amino acids by photosynthetic organisms. Proceedings of the National Academy of Sciences **47**(5): 623-632.
- Aluwihare, L. I. (1999). High molecular weight (HMW) dissolved organic matter (DOM) in seawater: chemical structure, sources and cycling, PhD, Massachusetts Institute of Technology/Woods Hole Oceanographic Institution: 224.
- Aluwihare, L. I., D. J. Repeta and R. F. Chen (1997). A major biopolymeric component to dissolved organic carbon in surface seawater. Nature **387**: 166-169.
- Aluwihare, L. I., D. J. Repeta and R. F. Chen (2002). Chemical composition and cycling of dissolved organic matter in the Mid-Atlantic Bight. Deep-Sea Research II **49**: 4421-4437.
- Barrie, A., J. Bricout and J. Koziat (1984). Gas chromatography-stable isotope ratio analysis at natural abundance levels. Biomedical Mass Spectrometry **11**(11): 583-588.
- Bauer, J. E. (2002). Carbon isotopic composition of DOM. Biogeochemistry of Marine Dissolved Organic Matter. D. A. Hansell and C. A. Carlson. San Diego, CA, Academic Press: 405-453.
- Benner, R. and K. Kaiser (2003). Abundance of amino sugars and peptidoglycan in marine particulate and dissolved organic matter. Limnology and Oceanography **48**(1): 118-128.
- Berg, G. M., P. M. Glibert, M. W. Lomas and M. A. Burford (1997). Organic nitrogen uptake and growth by the chrysophyte *Aureococcus anophagefferens* during a brown tide event. Marine Biology **129**: 377-387.
- Cowie, G. L. and J. I. Hedges (1992). Improved amino acid quantification in environmental samples: charge-matched recovery standards and reduced analysis time. Marine Chemistry **37**: 223-238.
- DeNiro, M. J. and S. Epstein (1977). Mechanism of carbon isotope fractionation associated with the lipid synthesis. Science **197**: 261-363.
- Dittmar, T., H.-P. Fitznar and G. Katiner (2001). Origin and biochemical cycling of organic nitrogen in the eastern Atlantic Ocean as evident from D- and L-amino acids. Geochimica et Cosmochimica Acta **65**(22): 4103-4114.

- Druffel, E. R. M., P. W. Williams, J. E. Bauer and J. R. Ertel (1992). Cycling of dissolved and particulate organic matter in the open ocean. Journal of Geophysical Research **97**(C10): 15,639-15,659.
- Eglinton, T. I., B. C. Benitez-Nelson, A. Pearson, A. P. McNichol, J. E. Bauer and E. R. M. Druffel (1997). Variability in radiocarbon ages of individual organic compounds from marine sediments. Science **277**: 796-799.
- Flynn, K. J. and I. Butler (1986). Nitrogen sources for the growth of marine microalgae: role of dissolved free amino acids. Marine Ecology Progress Series **34**: 281-304.
- Fogel, M. L. and N. Tuross (1999). Transformation of plant biochemicals to geological macromolecules during early diagenesis. Oecologia **120**: 336-346.
- Hedges, J. I. (1992). Global biogeochemical cycles: progress and problems. Marine Chemistry **39**: 67-93.
- Henrichs, S. M. (1980). Biogeochemistry of dissolved free amino acids in marine sediments, MIT/WHOI.
- Hwang, J. and E. R. M. Druffel (2003). Lipid-like material as the source of the uncharacterized organic carbon in the ocean. Science **299**: 881-884.
- Hwang, J. and E. R. M. Druffel (in press). Blank correction for $\Delta^{14}\text{C}$ measurements in organic compound classes of oceanic particulate matter. Radiocarbon.
- Ingalls, A. E., C. Lee, S. G. Wakeham and J. I. Hedges (2003). The role of biominerals in the sinking flux and preservation of amino acids in the Southern Ocean along 170°W. Deep-Sea Research II **50**(3-4): 713-738.
- Jørgensen, N. O. G., N. Kroer and R. B. Coffin (1994). Utilization of dissolved organic nitrogen by heterotrophic bacterioplankton: Effect of substrate C/N ratio. Applied and Environmental Microbiology **60**(11): 4124-4133.
- Jørgensen, N. O. G., N. Kroer, R. B. Coffin, X.-H. Yang and C. Lee (1993). Dissolved free amino acids, combined amino acids, and DNA as sources of carbon and nitrogen to marine bacteria. Marine Ecology Progress Series **98**: 135-148.
- Kahler, P., P. K. Bjørnsen, K. Lochte and A. Antia (1997). Dissolved organic matter and its utilization by bacteria during the spring in the Southern Ocean. Deep-Sea Research II **44**(1-2): 341-353.
- Keil, R. G. and M. L. Fogel (2001). Reworking of amino acid in marine sediments: Stable carbon isotopic composition of amino acids in sediments along the Washington coast. Limnology and Oceanography **46**(1): 14-23.

- Konishi, T., M. Kamada and H. Nakamura (1989). High performance liquid chromatography of amino acids and peptides on strong cation-exchange polymer gel. Analytical Sciences **5**.
- Loh, A. N., J. E. Bauer and E. R. M. Druffel (2004). Variable ageing and storage of dissolved organic components in the open ocean. Nature **430**: 877-881.
- Macko, S. A., M. L. Fogel, P. E. Hare and T. C. Hoering (1987). Isotopic fractionation of nitrogen and carbon in the synthesis of amino acids by microorganisms. Chemical Geology **65**: 79-92.
- McCarthy, M., J. Hedges and R. Benner (1996). Major biochemical composition of dissolved high molecular weight organic matter in seawater. Marine Chemistry **55**: 281-297.
- McCarthy, M., T. Pratum, J. Hedges and R. Benner (1997). Chemical composition of dissolved organic nitrogen in the ocean. Nature **390**: 150-154.
- McCarthy, M. D., R. Benner, C. Lee, J. I. Hedges and M. L. Fogel (2004). Amino acid carbon isotopic fractionation patterns in oceanic dissolved organic matter: an unaltered photoautotrophic source for dissolved organic nitrogen in the ocean? Marine Chemistry **92**: 123-134.
- McCarthy, M. D., J. I. Hedges and R. Benner (1998). Major bacterial contribution to marine dissolved organic nitrogen. Science **281**: 231-234.
- Palenik, B. and F. M. M. Morel (1990). Amino acid utilization by marine phytoplankton: a novel mechanism. Limnology and Oceanography **35**(2): 260-269.
- Pearson, A. (1999). Biogeochemical applications of compound specific radiocarbon analysis, PhD, Massachusetts Institute of Technology/Woods Hole Oceanographic Institution: 348.
- Pearson, A., A. P. McNichol, B. C. Benitez-Nelson, J. M. Hayes and T. I. Eglinton (2001). Origins of lipid biomarkers in Santa Monica Basin surface sediment: A case study using compound-specific $\Delta^{14}\text{C}$ analysis. Geochimica et Cosmochimica Acta **65**(18): 3123-3137.
- Pearson, A., A. P. McNichol, R. J. Schneider, K. F. Von Reden and Y. Zheng (1998). Microscale AMS ^{14}C measurement at NOSAMS. Radiocarbon **40**(1): 61-75.
- Pérez, M. T., C. Pausz and G. J. Herndl (2003). Major shift in bacterioplankton utilization of enantiomeric amino acids between surface waters and the ocean's interior. Limnology and Oceanography **48**(2): 755-763.

Qian, Y., M. H. Engel, G. A. Goodfriend and S. A. Macko (1995). Abundance and stable carbon isotope composition of amino acids in molecular weight fractions of fossil and artificially aged mollusk shells. Geochimica et Cosmochimica Acta **59**(6): 1113-1124.

Quinn Baumann, P., D. B. Ebenstein, B. D. O'Rourke and K. S. Nair (1992). High-performance liquid chromatographic technique for non-derivatized leucine purification: evidence for carbon isotope fractionation. Journal of Chromatography **573**: 11-16.

Reddy, C. M., L. Xu, G. W. O'Neil, R. K. Nelson, T. I. Eglinton, D. J. Faulkner, R. Norstrom, P. S. Ross and S. A. Tittlemier (2004). Radiocarbon evidence for naturally produced, bioaccumulating halogenated organic compound. Environmental Science and Technology **38**: 1992-1997.

Silfer, J. A., M. H. Engel and S. A. Macko (1992). Kinetic fractionation of stable carbon and nitrogen isotopes during peptide bond hydrolysis: Experimental evidence and geochemical implications. Chemical Geology **101**: 211-221.

Silfer, J. A., Y. Qian, S. A. Macko and M. H. Engel (1994). Stable carbon isotope compositions of individual amino acid enantiomers in mollusc shell by GC/C/IRMS. Organic Geochemistry **21**(67): 603-609.

Stuiver, M. and H. A. Polach (1977). Discussion: Reporting of ^{14}C data. Radiocarbon **19**: 355-363.

Tanoue, E. (1995). Detection of dissolved protein molecules in oceanic waters. Marine Chemistry **51**: 239-252.

Wakeham, S. G., T. K. Pease and R. Benner (2003). Hydroxy fatty acids in marine dissolved organic matter as indicators of bacterial membrane material. Organic Geochemistry **34**: 857-868.

Wang, X.-C., E. R. M. Druffel, S. Griffin, C. Lee and M. Kashgarian (1998). Radiocarbon studies of organic compound classes in plankton and sediment of the northeastern Pacific Ocean. Geochimica et Cosmochimica Acta **62**(8): 1365-1378.

Wang, X.-C., E. R. M. Druffel and C. Lee (1996). Radiocarbon in organic compound classes in particulate organic matter and sediment in the deep northwest Pacific Ocean. Geophysical Research Letters **23**(24): 3583-3586.

Yamada, N., S. Suzuki and E. Tanoue (2000). Detection of *Vibrio* (*Listonella*) *anguillarum* porin homologue proteins and their source bacteria from coastal seawater. Journal of Oceanography **56**: 583-590.

Yamada, N. and E. Tanoue (2003). Detection and partial characterization of dissolved glycoproteins in oceanic waters. Limnology and Oceanography **48**(3): 1037-1048.

Ziegler, S. E. and M. L. Fogel (2003). Seasonal and diel relationships between the isotopic compositions of dissolved and particulate organic matter in freshwater ecosystems. Biogeochemistry **64**: 25-52.

4. The Influence of Viruses and Grazers on Amino Acid and Nucleic Acid Release

4.1 Introduction

Dissolved organic matter (DOM) is the primary oceanic reservoir of bioavailable organic carbon and nitrogen and is therefore of particular interest in terms of nutrient cycling research. This pool of dissolved organic carbon (DOC) is just under 700 Gt C, and the dissolved organic nitrogen (DON) pool is the largest reservoir of fixed nitrogen (Abell et al., 2000; Bronk, 2002; Hansell et al., 2002). The average concentration of DON in the surface water is $5.8 \pm 2.0 \mu\text{M}$, while the deep water average concentration is $3.9 \pm 1.8 \mu\text{M}$ (Bronk, 2002). Concentrations of DON are lowest at the equator, even though the majority of marine production occurs in tropical waters and is then transferred to higher latitudes (Hansell and Waterhouse, 1997). DON is also higher along the coasts, as DON levels in estuaries and rivers are elevated relative to oceanic values. Production of DON in analyses of the carbon and nutrient cycles has been assumed to be from both heterotrophic and autotrophic organisms, but the composition, mechanism and rates of release have not been well quantified, and the effects of other organisms such as bacteria, viruses and grazers on the composition and release rates of DON have not yet been determined (Björnson, 1988; Baines and Pace, 1991; Glibert and Bronk, 1994; Biddanda and Benner, 1997; McCarthy et al., 1998).

Production of DON and DOC in culture has been observed from a wide variety of phytoplankton and bacterioplankton species, and from a range of different types of environments. However, this production has been hard to quantify. Stable isotopes such

as ^{13}C and ^{15}N have been used to estimate the amount of nutrient uptake, and by correlation, organic matter release (Bronk and Glibert, 1991; Norrman et al., 1995; Bronk, 1999; Ward and Bronk, 2001; Varela et al., 2003). Estimates of DOC release as a percentage of new production ranges from 10% to 30%, with an apparent dependence on growth rate, as well as the presence or absence of bacteria (Baines and Pace, 1991; Norrman et al., 1995). The rates of DON release ranges from 3% to 86% of the gross nitrogen uptake, with an average of approximately 30% (Bronk and Ward, 2000). These values cover a wide range of nitrogen substrates, measurement methods, and environments. DON release in natural assemblages has been determined to be correlated to ammonium uptake, but was higher with NO_3^- as a substrate (Ward and Bronk, 2001; Varela et al., 2003). While the release of DON by phytoplankton seems to be ubiquitous, many questions remain concerning the mechanisms of DON release and the type of nitrogen compounds that are produced.

Several different modes of DON release have been identified in phytoplankton cultures. Loss of low molecular weight (LMW) compounds through the cell membrane is a passive form of DON release that occurs even in healthy cells (Bjørnson, 1988). Analysis of cyanobacteria *Trichodesmium* species and natural assemblages from Chesapeake Bay show that the low molecular weight (LMW) fraction (defined in these papers as less than 10,000 D) comprised 60 to 80% of the DON released by *Trichodesmium* only cultures, while the Chesapeake Bay incubation LMW fraction was initially 78% of the total DON but dropped to 21% within 6 hours (Bronk and Glibert, 1991; Glibert and Bronk, 1994). The relative drop in LMW fraction compared to the

total DON pool indicates that other release mechanisms of a higher molecular weight fraction increased in importance during the course of the incubation.

Another form of DON release is that mediated by zooplankton and protozoan grazing, as a result of sloppy feeding or release from compromised cells. This can be illustrated by the correlation of DON release and ammonium regeneration, as the breakage of cells releases ammonium back into the culture (Ward and Bronk, 2001; Varela et al., 2003). Grazers themselves can release DON in the form of fecal pellets and excretion (Urban-Rich, 1999; Xu and Wang, 2003). Similarly, cell lysis caused by viruses is another way the contents of a phytoplankton cell can be released in bulk (Furhman, 1999). Bacteria are also a source of DON, especially in the form of proteins and amino acids (McCarthy et al., 1998; Yamada et al., 2000; Yamada and Tanoue, 2003). It is unknown how this DON release is controlled, or the environmental factors that may favor one type of release over another.

There also seems to be a connection between the characteristics of the phytoplankton community in terms of species, community structure, and trophic levels and the release of DON. Copepod grazing upon phytoplankton under high chlorophyll *a* conditions often adds to the DON release, but under lower chlorophyll *a* conditions, the presence of copepods has a negative effect on the DON concentration as the copepods shift food sources to microzooplankton, which also release DON (Hasegawa et al., 2000). This interplay between different food sources may affect DON release during bloom and post-bloom conditions. Maximum release of DON is seen when small phytoplankton dominate in terms of total biomass, due to their comparatively higher surface to volume ratio (Varela et al., 2003). DON excretion by zooplankton migrating through the water

column contributes an average of 30% of the total dissolved nitrogen to deeper waters below 150 m (Steinberg et al., 2000; Steinberg et al., 2002).

There is little data regarding the types of compounds released, and how the composition of DOC and DON change both as a function of changing community composition and available nutrients. Isolated nitrogenous compounds include amino acids and amino sugars, but a large fraction of DON remains unidentified (McCarthy et al., 1997; Aluwihare et al., 2002). ^{15}N NMR spectroscopy of the high molecular weight fraction of oceanic DON indicates that the majority of the nitrogen is in amide form, with only 6-26% as non-amide compounds (McCarthy et al., 1997; Aluwihare, 1999).

Structural protein homologues from bacteria have been isolated from coastal and oceanic seawater (Tanoue, 1995; Yamada et al., 2000) but it is unknown what other protein types are present. Dissolved nucleic acids also have been identified in coastal and open ocean waters, with DNA concentrations ranging from 0.1-80 $\mu\text{g/L}$ and RNA concentrations from 4-190 $\mu\text{g/L}$, with generally higher concentrations for coastal waters (Karl and Bailiff, 1989).

Other phytoplankton can use these DON compounds as sources of both carbon and nitrogen, even in the presence of inorganic nitrogen sources. In addition to being a source of dissolved organic nitrogen, phytoplankton can also use compounds such as amino acids to fulfill their own nitrogen needs, even developing specific oxidases to oxidize amines to H_2O_2 , α -keto acids, and NH_4^+ , the latter of which can then be used as a nitrogen source (Flynn and Butler, 1986; Palenik and Morel, 1990; Palenik and Morel, 1990; Palenik and Morel, 1991; Palenik and Henson, 1997). Phytoplankton in culture have also been shown to use other nitrogen compounds such as acetamide, purines, and

urea, as well as the DON extract isolated from algal incubations (Berg et al., 1997; Palenik and Henson, 1997). Organic nitrogen useage results in lower growth rates, and may only occur when inorganic forms of nitrogen are depleted (Wheeler et al., 1974; Flynn and Butler, 1986). The ability to use DON to satisfy nitrogen requirements may provide an advantage to some phytoplankton species such as *Aureococcus anophagefferens* to grow at low nutrient levels, resulting in the formation of large algal blooms (Keller and Rice, 1989; Nixon et al., 1994; Berg et al., 1997).

Bacteria have also been shown to utilize organic nitrogen compounds (Wheeler and Kirchman, 1986; Jørgensen et al., 1993; Capone et al., 1994; Jørgensen et al., 1994; Berg et al., 1997; Kahler et al., 1997; Pérez et al., 2003). Amino acid uptake is approximately 40-80% of the total nitrogen usage by bacteria in incubations, and bacteria can utilize both L and D enantiomers (Wheeler and Kirchman, 1986; Pérez et al., 2003). Utilization of the nitrogen obtained from the uptake of dissolved free amino acids, dissolved combined amino acids, and dissolved DNA can sustain a wide range of net bacterial nitrogen production, from 14-180%, with bacterial production using free amino acids as the dominant nitrogen source having similar values to ammonium (Jørgensen et al., 1993; Jørgensen et al., 1994).

DON release is affected by a wide variety of mechanisms and controlling factors, including the amount of inorganic nutrients present, the types of organisms present, and the balance between release and uptake of organic nitrogen compounds. In order to both identify individual factors and analyze the interactions as a whole, this chapter looks at the hydrolyzable amino acid fraction, dissolved DNA and dissolved RNA resulting from a set of incubation experiments. Four incubations are used in this experiment. The

control incubation consists of a natural assemblage of phytoplankton, zooplankton, bacteria, and viruses, with the ambient concentrations. A second incubation has the bacteria and virus population removed from the natural water sample by filtration, providing phytoplankton-only baseline values, without alteration by viruses or bacteria. To quantify the effects of viruses, a third incubation has ten times the concentration of viruses added to the natural assemblage. The exaggerated amounts of viruses should provide a clear signal that can be attributed to the effects of viral lysis. The last incubation contains added copepod grazers to the water sample in order to examine the effects of grazer-related DON release mechanisms such as sloppy feeding and fecal pellet dissolution. Comparison of differences in the total hydrolyzable amino acid fraction, dissolved DNA and dissolved RNA between the four different incubations at different time points should allow the contributions of the different types of DON release mechanisms to be identified and quantified.

4.2 Methods

Low carbon deionized (Milli-Q) water was used in all procedures. All glassware was combusted for a minimum of 8 hours at 450°C. Syringes and teflon-lined vial lids were rinsed with 10% HCl and water before use. Plastic tubes, centrifuge filters, and pipette tips were not autoclaved before use.

4.2.1 Sample Collection and Incubation

The sample incubations for this biocomplexity experiment were performed by Dr. Deborah Bronk and collaborators in July 2004 during a cruise to Chesapeake Bay. Four different culture treatments were set up as shipboard incubations, each using 50 L

Chesapeake Bay water collected from a depth of 2 m, filtered through a 150 μm Nitex pre-filter, to remove large particles without releasing DOC or DON via cell damage, and placed in triple rinsed carboys. A control incubation (C) consisted of the natural level of phytoplankton, zooplankton, bacteria, and viruses present in the water. The second incubation (10V) had approximately 10 times the natural virus levels added to the water sample. The virus concentrate for this sample was made by pre-filtering water through a 30 μm Spectra Mesh screen, then passed through a 0.22 μm Pellicon cartridge filter (Millipore) powered by a ProFlux M-12 peristaltic pump (Millipore) which traps the bacteria and allows the viruses and water to pass through. This filtrate was then filtered through a 30 kDa Helicon S10 spiral wound cartridge filter (Millipore) powered by the ProFlux M-12 peristaltic pump, which concentrates the viruses. Using this process, 725 L of water was concentrated to 2.6 L, with a final concentration of 290 times the ambient level. Based on this data, 687 mL of the viral concentrate was added to the 10 V incubation to achieve 10 times the original virus concentration. The zero virus sample (0V) had all of the viruses and bacteria removed via ultrafiltration, using a 2 μm Nitex mesh filter to concentrate the phytoplankton and zooplankton from 50 L of Chesapeake Bay water, then diluting with virus free water obtained from the 30 kDa filtrate. The last culture (G) had picked copepod grazers collected by plankton tows added to the natural water samples. Two replicates of each treatment were made and incubated at the light and temperature on deck. The cultures were incubated for 5 days, with subsamples removed for analysis of 7 timepoints: at the start of the incubations (T0), after 12 hours (T1), after 24 hours (T2), and every 24 hours subsequently (T3, T4, T5, and T6). The experiment ended after 120 hours. Approximately 40 mL were removed for amino acid

analysis, and 100 mL aliquots for nucleic acid measurements. Subsamples were frozen and were only thawed immediately prior to analysis.

4.2.2 Amino Acid Analysis

The samples were analyzed for total hydrolyzable amino acids (THAA) content using acid hydrolysis. Approximately 2 mL sample was combined with 3 mL concentrated HCl to make a 7 M HCl solution, with the exception of the T3 timepoint samples, which contained twice the sample and acid volumes. Two charge-matched standards, 2-DL-aminoadipic acid (aaaa, Aldrich Chemicals) and 5-hydroxy-DL-lysine HCl (hlys, Aldrich Chemicals) were used following the amino acid protocol of Cowie and Hedges, 1992. All hydrolysis samples except for the T2 and T3 timepoints for all 8 cultures contained 2.5 μ L of a 12.5 μ M solution of both standards dissolved in 0.2 M H_3BO_4 (pH 8.5) added to each vial before hydrolysis and used as an internal standard. The T2 timepoint samples contained 2.5 μ L of 1.25 mM aaaa and hlys standard solution, while the T3 timepoint hydrolyses contained 5 μ L of the 12.5 μ M solution to match the doubling of the total volume. The original protocol also called for a third charge-matched standard, L-leucine methyl ester (mleu; Aldrich Chemicals), but this standard co-eluted with the leucine amino acid peak upon test analysis and was not used. Each vial was flushed with nitrogen for 5 min, capped and heated in a sand bath at 110°C for 24 h. Samples were then transferred to conical vials, rotovaped to dryness, and neutralized by repeated additions of 0.2 M H_3BO_4 (adjusted to pH 10 with KOH) followed by drying until the sample had a pH between 8.5 and 9. The samples were then dissolved in 500 μ L water, transferred to small 4 mL vials, and frozen for amino acid analysis.

Amino acids were analyzed using high-pressure liquid chromatography (HPLC) using fluorescent derivitization by o-phthaldialdehyde (OPA, Sigma) according to the method of Cowie and Hedges, (1992). The OPA reagent consisted of 50 mg OPA dissolved in 0.5 mL methanol. To this solution was added 4 mL of 1 N potassium borate pH 10.4, 50 μ L Brij 35 solution (Pierce), and 25 μ L mercaptoethanol (Sigma). The OPA reagent was flushed with nitrogen and kept in the freezer prior to use. A 10 mM solution of charge-matched standards aaaa and hllys was made using 0.2 M pH 8.5 H_3BO_4 , and diluted to 1.25 mM with the same solvent for a working solution. This solution was diluted again with the 0.2 M borate buffer to 12.5 μ M for addition to the sample prior to hydrolysis. An amino acid standard mix was created by combining 1 mL Pierce standard H (2.5 mM each amino acid) with 1.25 mL of the 1.25 mM charge matched standard solution and diluting to 10 mL with 0.2 M pH 8.5 H_3BO_4 buffer. This was then diluted to 20 μ M for a working injection standard, which was used to calculate the amino acid concentrations for the hydrolyzed unknown samples.

HPLC separation was performed using an Agilent 1100 series binary pump, with an autoinjector and a fluorescence detector. The column was an Alltech Alltima C18 column (4.6 x 25 mm, 5 μ m). Buffer A consisted of a 50 mM solution of sodium acetate (anhydrous), adjusted to pH 6.40 with acetic acid. Buffer B was HPLC grade methanol. Both solvents were filtered though a GF/F filter prior to use. The solvent gradient is shown in Table 4.1, and the flow rate was constant at 1.5 mL/min. The amino acid-OPA derivatives are detected fluorometrically with an excitation of 330 nm and an emission wavelength of 450 nm.

Table 4.1: HPLC buffer gradient for amino acid analysis via OPA derivatives

Time (min)	% solvent B
0	10
3	12
10	27
20	33
25	50
30	55
32	57
34	60
36	60
38	70
40	70
46	10
56	10

Table 4.2: Agilent autoinjector injection program for the OPA-amino acid derivitization reaction

step	action	speed
1	Draw 30 μ L from vial 1	200 μ L/min
2	Eject 30 μ L into sample	200 μ L/min
3	Draw 100 μ L from sample	200 μ L/min
4	Eject 100 μ L into sample	200 μ L/min
5	Draw 100 μ L from sample	200 μ L/min
6	Eject 100 μ L into sample	200 μ L/min
7	Wait 0.5 min	
8	Draw 100 μ L from sample	200 μ L/min
9	Inject	

Each amino acid hydrolysis sample was split in half and transferred to HPLC autoinjector vials. Enough water was added to each vial to make the total volume 475 μ L. The hydrolyzed samples were usually run in sets of 8, with 3 injections of Pierce standard H solution interspersed within the sample sequence. The standard vials contained 475 μ L of the 20 μ M standard H plus aaaa and hlys injection solution for timepoints T0 through T2. For the remaining samples, 200 μ L of the 20 μ M standard solution were diluted with 250 μ L 0.2 M borate buffer, pH 8.5 in order to match peak heights more closely to the unknown samples. Each sample was mixed with 30 μ L of the

OPA reagent using the autoinjector with the injection program shown in Table 4.2. All injections were 100 μ L.

Amino acid peaks for the hydrolyzed samples were integrated and the concentration of each amino acid was calculated using the average response factors (concentration/peak area) determined from the three standard H solution chromatograms. For all samples, the concentration of the charge-matched standards was set to the initial amount added prior to hydrolysis and used as internal standards. The remainder of the amino acids are then scaled to the standards depending on their type: acid amino acids such as aspartic acid and glutamic acid are adjusted using aaaa, and the neutral and basic amino acids are scaled using hlys (Cowie and Hedges, 1992). In this way, any loss of amino acids during any of the procedures can be taken into account.

4.2.3 Nucleic Acid Analysis

The basic procedure for the analysis of nucleic acids was adapted from the method of Matsui et al., (2004). The nucleic acids were precipitated with ethanol, isolated and concentrated in centrifugal filter devices, then measured by fluorescent probes. Quantification of DNA and RNA in the unknown samples was calculated using a standard addition method. Individual 2 μ g/mL standards of each nucleic acid were made by dissolving DNA (sodium salt, type XIV from herring testes; Sigma) or RNA (type III from baker's yeast *S. cerevisiae*; Sigma) in Tris-EDTA (TE) buffer (Sigma), which were then split into 60 individual 1 mL aliquots and frozen until use. The concentration of DNA or RNA in the standards was determined by UV-Vis spectroscopy using an HP 8452A diode array spectrophotometer with a 1 cm pathlength. A concentration of 2

$\mu\text{g/mL}$ DNA corresponds to an absorbance at 260 nm of 0.04, while an absorbance at 260 nm of 0.05 correlates to an RNA concentration of 2 $\mu\text{g/mL}$.

In order to determine the concentration of nucleic acid in an unknown sample, each sample was split into four disposable centrifuge tubes. Each tube contained an equal amount of the sample, approximately 10-13 mL. The first tube did not contain any additional nucleic acids, while the second, third and fourth tubes had 10 μL , 100 μL , and 500 μL of the 2 $\mu\text{g/mL}$ nucleic acid standard added, respectively. Since the samples were obtained from Chesapeake Bay, none of the additional salt solutions used by Matsui et al., (2004) needed to be added in order for the precipitation to occur (DeFlaun et al., 1986). Thirty-three mL of absolute (200 Proof) ethanol was added to each tube, and tubes were kept at -20°C for 12 to 36 hours. Previous analyses did not notice a difference in nucleic acid concentration due to the different precipitation times (Matsui et al., 2004). The tubes were then centrifuged using an Eppendorf 5810R centrifuge in a fixed angle rotor for 40 min at 7000 x g at 4°C . Tubes were carefully balanced using TE buffer before all centrifugation steps. The supernatant was removed and the precipitate was dried under nitrogen for 5 min, then dissolved in 5 mL TE buffer.

The dissolved nucleic acid solution was then transferred to individual Centriplus centrifugal filter tubes (Amicon Biosciences) with a 30,000 D cutoff. These filter devices consist of a sample reservoir with a filter on the bottom, through which the water and any salts are pushed through during centrifugation into a filtrate vial attached below. The tubes were centrifuged in a swinging bucket rotor at 2500 x g for 30 min at 4°C , or until the amount of liquid remaining in the sample reservoir above the filter is less than 500 μL . Since any extra salt remaining interferes with the fluorescent probes, the concentrate

was washed twice with an additional 5 mL TE buffer added to the sample reservoir and then flushed through via centrifugation. The top filter section of the centrifugal device was removed, inverted over a retentate vial and centrifuged at $2000 \times g$ at 4°C for 4 min to transfer the final nucleic acid concentrate off the filter. The solution was then transferred to tared microcentrifuge tubes and weighed to determine the final volume.

The concentration of nucleic acids in the samples was measured using fluorescent nucleic acid probes. Duplicate 100 μL aliquots from each of the four tubes for the sample were pipetted into a 96-well plate. The fluorescent probes used were PicoGreen (Molecular Probes) for DNA measurement and RiboGreen (Molecular Probes) for RNA quantification. Both probes were diluted 200 fold according to the directions with TE buffer, and 100 μL added to each sample well. The dilutions were made directly before the samples were measured, and kept in the dark as much as possible. The well plate was then placed in an Eppendorf Thermomixer R and mixed at room temperature for 5 min at 1000 rpm. The plate was then transferred to the Cytofluor Series 400 multiwell plate reader fluorometer (PerSeptive Biosystems) to be read. The instrument was set to a gain of 40, with 10 reads per well, 1 scan per cycle. The excitation was 530 nm with a bandwidth of 25 nm, and the emission wavelength was set to 485 nm with a bandwidth of 20 nm.

To calculate the concentration of nucleic acid in the unknown sample, the fluorometric signal for each well was divided by the final volume for each tube in order to normalize for any variation in signal intensity due to the difference in volumes between the four tubes of each sample. The normalized signal intensities were plotted versus the mass of nucleic acid added, and a linear regression line fit to the data.

Assuming that there is no signal attributable to nucleic acids when none are present, the amount of nucleic acids in the unknown sample is equal to the intercept divided by the slope of the regression line. This calculated nucleic acid concentration is then divided by the volume of the original sample in each of the tubes for conversion to a whole sample concentration in $\mu\text{g/L}$.

While it was planned to add both DNA and RNA standards to the same tubes, the fluorescence signals from a test seawater sample from Vineyard Sound with both standards produced poor linear regression lines, and the calculated DNA and RNA concentrations did not match the concentrations determined with only one standard added. In addition, the RNA probe was an indiscriminate total nucleic acid probe that also responded to the presence of DNA; however calculated total nucleic acid levels were lower than the DNA concentration alone. The company literature for the PicoGreen DNA probe indicates that the presence of RNA greater than 10 times the DNA concentration may interfere with the fluorescent signal, but the reason for the inability of the RNA probe to account for all of the known nucleic acids in the test sample is unknown. To avoid the problems caused by using the DNA and RNA standards together, the DNA and RNA samples were set up in different sets of tubes. Each unknown sample was split in half. The DNA standard was added to one set of 4 tubes as described above to measure the DNA concentration, and the second half is reserved for the RNA determination. To eliminate the seeming conflict with the DNA, the RNA samples were treated with DNase I (Ambion) to remove all the DNA in the samples. Since the DNase I removes $2\text{ }\mu\text{g}$ DNA per $1\text{ }\mu\text{L}$ DNase, the appropriate amount of DNase was added to the second half of each sample, then incubated at 37°C for 2 hours. The DNA-free sample is

then split into 4 tubes, and the standard addition of RNA to each tube is performed as above.

4.3 Results and Discussion

4.3.1 Ancillary Data

The nutrient, dissolved organic carbon (DOC), total nitrogen (TDN), productivity, chlorophyll a, and bacterial count measurements were performed by other investigators as part of the larger DOMINOS biocomplexity investigation. NH_4^+ and urea concentrations are shown in Table 4.3, and are the average of both A and B duplicate cultures for each timepoint (Deborah Bronk, VIMS). All measurements are in $\mu\text{M N}$. Unfortunately, the nitrate and nitrite measurements were not available in time for this thesis. The ammonium concentrations for the control, grazer, and 10 times virus (10V) incubations were similar at the initial T0 timepoint, with values between 2.5 ± 0.2 - $3.8 \pm 0.5 \mu\text{M N}$. For these cultures, the NH_4 concentration dropped to less than $1 \mu\text{M N}$ rapidly within the first 12-24 hours. NH_4 concentrations for all three incubations rose slightly at time points T3 and T4, then decreases to a constant 0.14 - $0.17 \mu\text{M N}$ for all cultures. Urea concentrations for the control, grazer added, and 10 times virus incubations were also very similar in magnitude, falling between 0.29 ± 0.05 - $0.38 \pm 0.05 \mu\text{M N}$ and remaining constant throughout the duration of the experiment. The zero virus incubation (0V) had higher NH_4 concentrations for the initial T0 timepoint ($5.9 \pm 0.1 \mu\text{M N}$), and remained higher for the first 24 hours. By the T3 (48 hr) timepoint the 0V incubation had a NH_4 level had decreased to $0.7 \pm 0.4 \mu\text{M N}$, which was similar to the other three incubations at this timepoint. After the T3 timepoint, the NH_4 levels were very similar in magnitude to

Table 4.3: NH_4 and urea concentrations for the control, 0 virus (0V), grazer added, and 10 times virus (10V) incubations at 7 timepoints. Each value is the average of both A and B duplicate incubations. Measurements were performed by Deborah Bronk, VIMS.

control incubation		
timepoints	NH_4 ($\mu\text{M N}$)	urea ($\mu\text{M N}$)
T0	2.5 ± 0.2	0.29 ± 0.05
T1	1.5 ± 1	0.310 ± 0.008
T2	0.6 ± 0.5	0.34 ± 0.02
T3	0.28 ± 0.08	0.30 ± 0.02
T4	0.6 ± 0.6	0.35 ± 0.01
T5	0.17 ± 0.03	0.36 ± 0.02
T6	0.143 ± 0.002	0.36 ± 0.02
0V incubation		
timepoints	NH_4 ($\mu\text{M N}$)	urea ($\mu\text{M N}$)
T0	5.9 ± 0.1	0.505 ± 0.003
T1	5.7 ± 0.5	0.50 ± 0.03
T2	4.7 ± 0.7	0.56 ± 0.02
T3	0.7 ± 0.4	0.46 ± 0.01
T4	0.17 ± 0.01	0.33 ± 0.02
T5	0.148 ± 0.009	0.38 ± 0.05
T6	0.20 ± 0.04	0.32 ± 0.06
grazer incubation		
timepoints	NH_4 ($\mu\text{M N}$)	urea ($\mu\text{M N}$)
T0	3.10 ± 0.05	0.33 ± 0.04
T1	0.6 ± 0.1	0.353 ± 0.006
T2	0.28 ± 0.05	0.3666 ± 0.0004
T3	0.6 ± 0.4	0.29 ± 0.01
T4	0.6 ± 0.6	0.367 ± 0.003
T5	0.13 ± 0.03	0.38 ± 0.02
T6	0.171 ± 0.003	0.34 ± 0.01
10V incubation		
timepoints	NH_4 ($\mu\text{M N}$)	urea ($\mu\text{M N}$)
T0	3.8 ± 0.5	0.318 ± 0.001
T1	2.2 ± 0.8	0.317 ± 0.004
T2	0.17 ± 0.01	0.364 ± 0.002
T3	0.7 ± 0.6	0.32 ± 0.05
T4	0.27 ± 0.05	0.350 ± 0.001
T5	0.17 ± 0.09	0.320 ± 0.003
T6	0.14 ± 0.03	0.34 ± 0.01

those of the previous three incubations, declining to a constant level of approximately 0.2 $\mu\text{M N}$. Urea levels for the zero virus incubations started much higher than the control,

grazer, and 10V incubations, with a concentration of $0.505 \pm 0.003 \mu\text{M N}$. This concentration gradually dropped to $0.33 \pm 0.02 \mu\text{M N}$ after 72 hr (timepoint T4), and remained constant to the end of the experiment. The urea concentrations after the T4 timepoint were exactly the same as the other three incubations.

DOC and total dissolved nitrogen (TDN) concentrations for all four incubations are listed in Table 4.4 (Aubrey Cano/Craig Carlson, UCSB). All DOC and TDN values were blank corrected and considered preliminary values only, due to slightly greater than desired blank values. DON concentrations were to be calculated by subtracting the dissolved inorganic nitrogen (DIN) species (NO_2^- , NO_3^- , and NH_4^+) from the TDN values; unfortunately NO_2^- and NO_3^- measurements were not available in time for this thesis. All

Table 4.4: Dissolved organic carbon (DOC) and total nitrogen (TDN) concentrations for the control, 0 virus (0V), grazer added, and 10 times virus (10V) incubations. All concentrations are in $\mu\text{M C}$ for DOC and $\mu\text{M N}$ for the TDN measurements, and are averages of the A and B duplicate carboys for each incubation. Measurements performed by Aubrey Cano/Craig Carlson, UCSB.

	control incubation		10V incubation	
timepoints	DOC ($\mu\text{M C}$)	TDN ($\mu\text{M N}$)	DOC ($\mu\text{M C}$)	TDN ($\mu\text{M N}$)
T0	188 ± 1	18.8 ± 0.1	223 ± 2	21.9 ± 0.4
T1	188 ± 5	16.94 ± 0.04	222 ± 1	20 ± 1
T2	190 ± 10	14.7 ± 0.3	208 ± 4	16.2 ± 0.2
T3	180 ± 26	12 ± 1	250 ± 60	18 ± 3
T4	189 ± 2	13.2 ± 0.3	209 ± 8	14.7 ± 0.3
T5	194 ± 4	13.5 ± 0.8	216.1 ± 0.3	14.90 ± 0.02
T6	190 ± 5	13.6 ± 0.4	220 ± 3	15.2 ± 0.3
	0V incubation		grazer incubation	
timepoints	DOC ($\mu\text{M C}$)	TDN ($\mu\text{M N}$)	DOC ($\mu\text{M C}$)	TDN ($\mu\text{M N}$)
T0	177 ± 1	19.80 ± 0.03	188 ± 2	18.7 ± 0.3
T1	174 ± 4	20.3 ± 0.1	185 ± 5	16.9 ± 0.4
T2	176 ± 2	20.0 ± 0.3	188.7 ± 0.3	14.5 ± 0.3
T3	169 ± 9	18 ± 2	190 ± 3	13.4 ± 0.8
T4	169 ± 5	16.3 ± 0.7	190 ± 2	13.45 ± 0.09
T5	165.9 ± 0.4	13.7 ± 0.5	191 ± 5	13.2 ± 0.2
T6	169 ± 4	12.6 ± 0.4	192.5 ± 0.7	13.7 ± 0.3

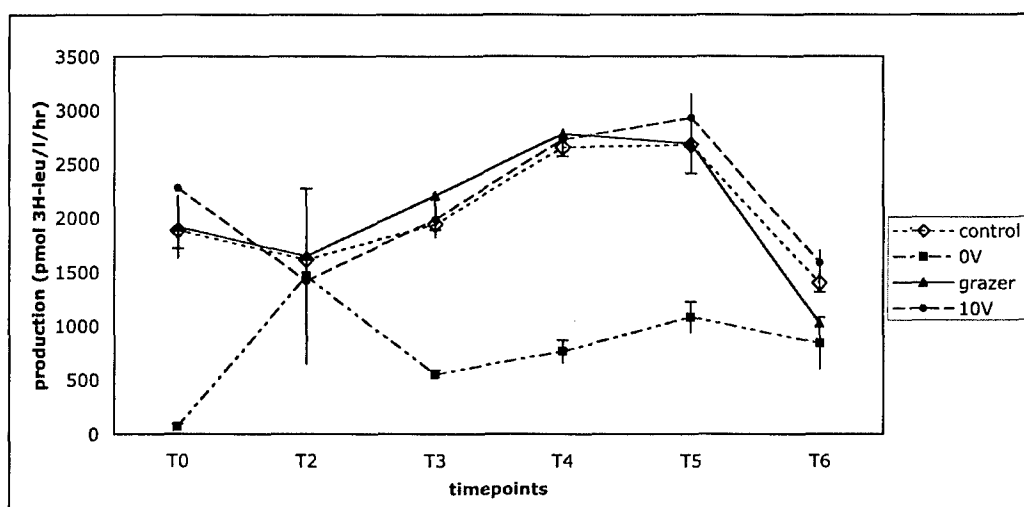
concentrations were averaged from the values from both the two replicate carboys of each incubation treatment. The DOC concentrations for the control and grazer incubations were very similar, starting at $188 \mu\text{M C}$, and increasing gradually to a final concentration of 190 ± 5 - $192.5 \pm 0.7 \mu\text{M C}$. The zero virus culture started at a slightly lower DOC concentration of $177 \pm 1 \mu\text{M C}$, and had a small and gradual decrease over the course of the incubation to a final concentration of $169 \pm 4 \mu\text{M C}$. The 10 times virus incubation contained a higher initial concentration of DOC, $223 \pm 2 \mu\text{M C}$. The DOC level dropped to a concentration of $208 \pm 4 \mu\text{M C}$ after 24 hr (timepoint T2), rose to $250 \pm 60 \mu\text{M C}$ within the next 24 hours (timepoint T3), decreased again to $209 \pm 8 \mu\text{M C}$ by the T4 timepoint, then increased to $216.1 \pm 0.3 \mu\text{M C}$ and remained constant until the end of the experiment.

TDN concentrations were more consistent between the four incubation treatments. The initial TDN concentrations were approximately 18.7 - $19.8 \mu\text{M N}$, with the 10V incubation slightly higher at $21.9 \mu\text{M N}$. TDN values decreased in all cultures over the course of the 120 hr experiment, to a final concentration of 12.6 - $13.7 \mu\text{M N}$ for the control, 0V, and grazer incubations. Again, the final concentration at T6 for the 10V incubation was slightly higher ($15.2 \pm 0.3 \mu\text{M N}$).

Bacterial productivity within each carboy was determined by measuring the incorporation of ^3H labeled leucine (Aubrey Cano/Craig Carlson, UCSB). Samples were measured by counting decays per minute, then converting this rate to $\text{pmol } ^3\text{H leu/L/hr}$. All rates were the average of both A and B carboys for each incubation treatment, and are shown in Figure 4.1. Control, grazer added, and 10 times virus (10V) incubations showed similar trends and similar values. All three of these cultures had an initial

production rate of approximately 1900 pmol ^3H leu/L/hr, with the grazer incubation slightly larger. The production rate for the control, grazer and 10V treatments rose to maximum values (2700 pmol ^3H leu/L/hr) at timepoints T4 and T5, then dropped

Figure 4.1: Production measurements (pmol ^3H leu/L/hr) for the control (open diamonds), 0 virus (0V; solid squares), grazers added (solid triangles), and 10 times virus (10V; solid circles). Values were the average of the A and B duplicate carboys for each treatment. Measurements made by Aubrey Cano/Craig Carlson, UCSB.

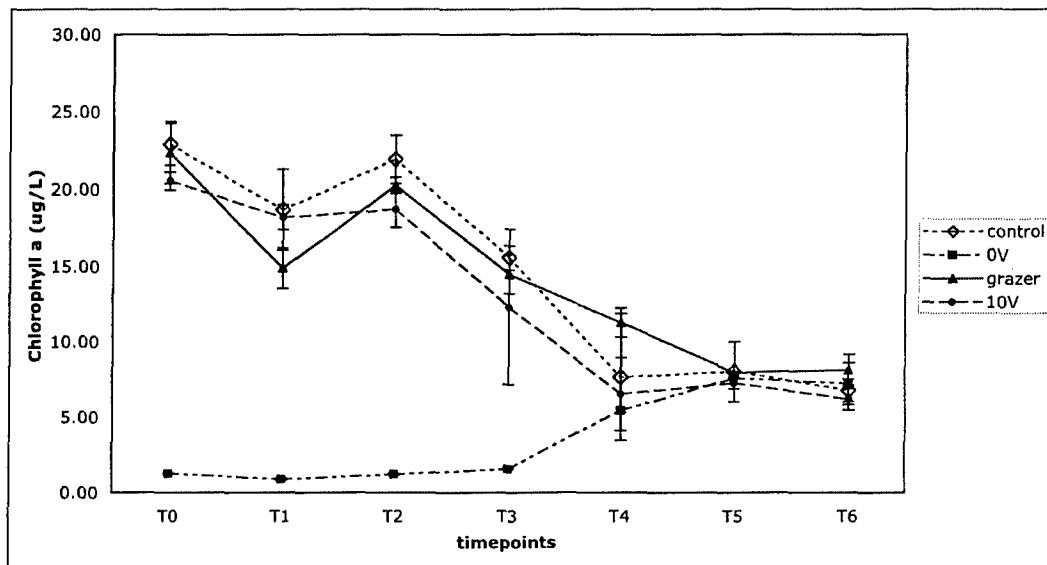


drastically at 120 hr (timepoint T6). The 0 virus (0V) treatment had a very different production rate trend. The production rate for the 0V incubation started at 71 pmol ^3H leu/L/hr, then increased to 1461 pmol ^3H leu/L/hr after 24 hours, the maximum rate for this experiment. This production rate at the T2 timepoint was the same as for the other three incubations, even though the production rates for the incubations were at a minimum. The production rate then decreased to 551 pmol ^3H leu/L/hr at timepoint T3, followed by a smaller maxima at T5. The final production rate was 840 pmol ^3H leu/L/hr at the T6 timepoint, only slightly less than the other three treatments.

Chlorophyll a (chl a) concentrations from the four culture treatments are shown in Figure 4.2 (Grace Henderson/Deborah Steinberg, VIMS). Each value was the average of

both the A and B carboys for each timepoint. The chl *a* concentrations for the control, 0 virus, and 10 times virus incubations were very similar in concentration and general behavior during the duration of the experiment. Chl *a* concentrations were the highest at

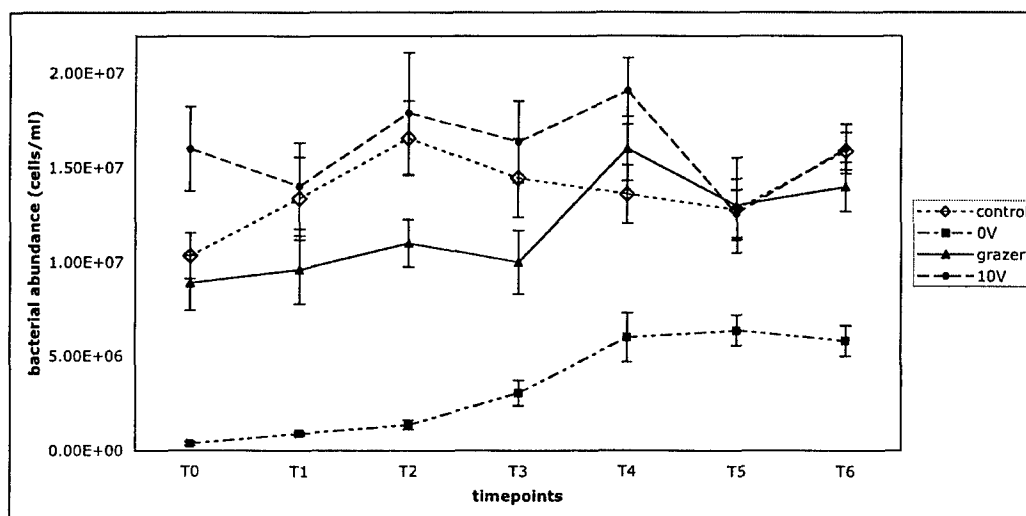
Figure 4.2: Chlorophyll *a* concentrations in $\mu\text{g/L}$ for the control (open diamond), 0 virus (0V; solid squares), grazer added (solid triangles), and 10 times virus (10V; solid circles) culture treatments. Data measured by Grace Henderson/Deborah Steinberg, VIMS.



the beginning of the incubation, measuring between 20-22 $\mu\text{g/L}$. The concentration gradually decreased over the course of 96 hours to a constant concentration of approximately 7 $\mu\text{g/L}$ chl *a* for the last two timepoints (T5 and T6). The chl *a* concentration for the 0 virus incubation during the experiment showed the opposite trends seen in the other three cultures. The chl *a* levels for the 0 virus incubation started at 1.27 $\mu\text{g/L}$, and remained constant for the first 48 hours (timepoints T0-T3). The concentration then gradually rose to 7.60 $\mu\text{g/L}$ by timepoint T5, and remained at that concentration until the end of the experiment. This final chl *a* concentration was the same as the end concentrations for the other three incubations.

Bacterial cell counts were also performed to determine the abundance of bacteria in each of the cultures (Figure 4.3; Aubrey Cano/Craig Carlson, UCSB). Again, the cell counts were the averages for both replicate carboys for each treatment type. The control, 10 times virus, and grazer incubations all had bacterial counts ranging between 9.6×10^6 -

Figure 4.3: Bacterial abundance counts (cells/mL) for the control (open diamonds), 0 virus (0V; solid squares), grazers added (solid triangles) and 10 times virus (10V; solid circles) incubation treatments. All measurements were averages of A and B duplicate carboys for each treatment. Data measured by Aubrey Cano/Craig Carlson, UCSB.

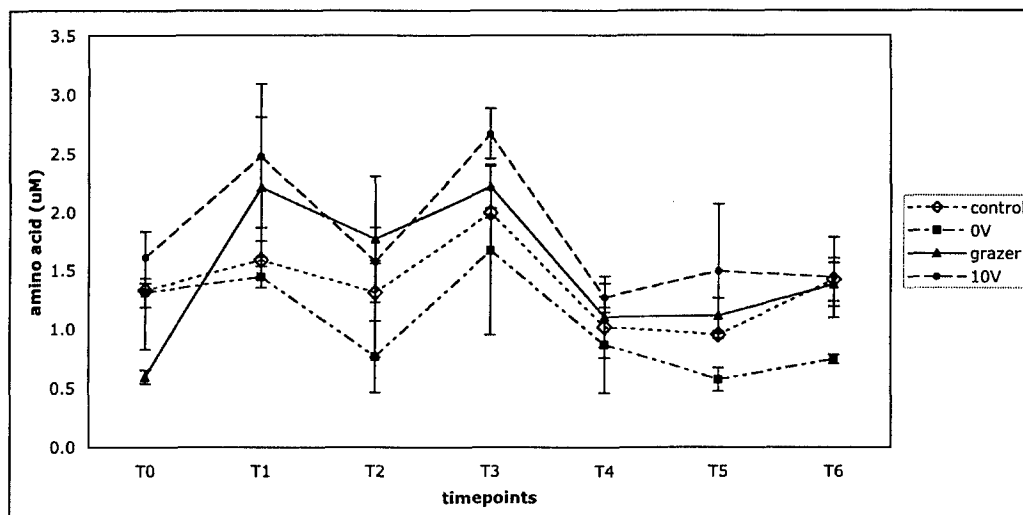


1.9×10^7 cells/mL, without any definitive pattern. The control culture had a maximum 24 hours after the beginning of the incubation (timepoint T2), while the maximum cell count for the grazer carboys occurred at timepoint T4, 72 hours after the experiment began. The 10V culture bacterial cell counts were generally higher than the other two incubations. The 0 virus culture consistently had the lowest bacterial count, starting with 3.7×10^5 cells/mL and increasing gradually to a final count of 5.8×10^6 cells/mL.

4.3.2 Amino Acid Results

The object of this chapter was to compare the dissolved organic nitrogen content of four different cultures, specifically for amino acid and nucleic acid content and distribution. Hydrolyzable amino acids were measured using the charge-matched protocol of Cowie and Hedges, 1992. Fourteen amino acids were chromatographically separated, with glycine and threonine co-eluting. The concentrations for the neutral amino acids (histidine, serine, glycine, threonine, alanine, tyrosine, methionine, valine, phenylalanine, isoleucine and leucine) were calculated using the basic internal standard, hlys. Since the recoveries for the neutral amino acids were generally less varied than the acidic and basic amino acids, using only 2 internal standards was analytically solid (Cowie and Hedges, 1992). The correct pH of both the sodium acetate buffer and the samples themselves was very important, as variations in either caused peaks to shift, though the elution order was not changed. The best results were obtained when the samples had a final pH between 8 and 8.5 after rotory evaporation and neutralization using a pH 9.5 borate buffer. A higher pH resulted in peak shifts to earlier retention times, but did not seem to have an affect on peak areas. It was preferable to samples with a pH higher than 8.5 than a pH lower than 8. Each culture treatment was performed on two carboys (A and B). Duplicate amino acid measurements were made for each carboy, then all the values for both carboys were averaged. Differences in the amino acid concentration between the A and B carboys resulted in relatively high standard deviations for some timepoints, as the deviation between duplicate measurements from the same carboy were generally small.

Figure 4.4: Total hydrolyzable amino acid concentration for control (open diamonds), 0 virus (0V; solid squares), grazer added (solid triangles), and 10 times virus (10V; solid circles). Values were averages of duplicate measurements for both A and B replicate carboy treatments.



The amino acid concentrations were calculated as μM of each amino acid, then converted to $\mu\text{M C}$ and $\mu\text{M N}$, based on the amount of carbon and nitrogen present in each amino acid. Table 4.5 lists the hydrolyzed amino acid concentrations for the control incubation (Table 4.5A), the 0 virus treatment (Table 4.5B), the grazers added culture (Table 4.5C) and the 10 times virus added carboys (Table 4.5D). Figure 4.4 shows the total hydrolyzable amino acid concentration for all cultures over the course of the experiment.

The total hydrolyzable amino acids (THAA) for all of the incubations ranged by a factor of four, from $0.60 \pm 0.06 \mu\text{M}$ to $2.7 \pm 0.2 \mu\text{M}$. The THAA concentration for all samples also followed the same basic trends: two concentration maxima at T1 and T3, returning to approximately the initial concentration in between. After the second maxima, the concentrations decrease back to the initial values and remain constant for the rest of the experiment. In general, the 10 times virus incubation released more THAA

than the other cultures. The grazer incubation had the widest range of hydrolyzed amino acids, with the lowest initial values increasing to the second highest concentrations for the rest of the experiment. With the exception of the initial concentration, the 0 virus treatment had the lowest overall hydrolyzable amino acid levels.

For the control incubation, the THAA concentration remained fairly consistent, ranging from $0.95 \pm 0.03 \mu\text{M}$ to $1.99 \pm 0.04 \mu\text{M}$, with the maximum concentration occurring 48 hours (T3) after the start of the experiment. In terms of carbon, the values ranged from $4.1 \pm 0.1 \mu\text{M C}$ to $8.5 \pm 0.2 \mu\text{M C}$, which constituted 2.1 to 4.7% of the DOC (Table 4.6A), with the highest percentage coinciding with the amino acid maxima at the T3 timepoint. Total hydrolyzable amino acids also made up 7.6-17.7% of the total dissolved nitrogen, with nitrogen concentrations ranging from $1.03 \pm 0.04 \mu\text{M N}$. Again, the highest concentration of amino acid nitrogen and the highest percentage of total nitrogen as amino acid occurred 48 hours after the start of the incubations, at the T3 timepoint.

In general, the THAA concentrations for the 0 virus treatment were lower than the other three incubations, ranging from $0.75 \pm 0.04 \mu\text{M}$ to $1.7 \pm 0.7 \mu\text{M}$, with the highest concentration at the T3 timepoint. The amino acid carbon concentration was 3.3 ± 0.2 - $7 \pm 4 \mu\text{M C}$, representing 1.5-4.1% of the total DOC (Table 4.6B). This amino acid fraction was 5-10% of the total dissolved nitrogen, with concentrations from 0.82 ± 0.05 - $1.8 \pm 0.9 \mu\text{M N}$. The percent carbon as amino acids for this experiment was very similar to the percentage for the control experiment, but the percent nitrogen was slightly smaller.

Table 4.5: Hydrolyzable amino acid concentrations for the control (part A), 0 virus (part B), grazer added (part C), and 10 times virus (part D) incubations. The concentrations for each timepoint were averaged from duplicate measurements of both A and B replicate incubation treatments.

Part A: Control incubation

amino acid	T0			T1			T2			T3		
	μM amino acid	μM C	μM N	μM amino acid	μM C	μM N	μM amino acid	μM C	μM N	μM amino acid	μM C	μM N
asp	0.14 \pm 0.05	0.6 \pm 0.2	0.14 \pm 0.05	0.12 \pm 0.01	0.47 \pm 0.04	0.12 \pm 0.01	0.11 \pm 0.04	0.5 \pm 0.1	0.11 \pm 0.04	0.17 \pm 0.01	0.67 \pm 0.05	0.17 \pm 0.01
glu	0.13 \pm 0.03	0.7 \pm 0.2	0.13 \pm 0.03	0.11 \pm 0.01	0.57 \pm 0.03	0.11 \pm 0.01	0.11 \pm 0.02	0.55 \pm 0.09	0.11 \pm 0.02	0.14 \pm 0.01	0.69 \pm 0.07	0.14 \pm 0.01
ser	0.1 \pm 0.1	0.9 \pm 0.6	0.2 \pm 0.1	0.19 \pm 0.02	1.2 \pm 0.1	0.19 \pm 0.02	0.14 \pm 0.07	0.8 \pm 0.4	0.14 \pm 0.07	0.23 \pm 0.02	1.4 \pm 0.1	0.23 \pm 0.02
his	0.05 \pm 0.03	0.2 \pm 0.1	0.05 \pm 0.03	0.11 \pm 0.03	0.3 \pm 0.01	0.11 \pm 0.03	0.06 \pm 0.02	0.17 \pm 0.07	0.06 \pm 0.02	0.24 \pm 0.02	0.71 \pm 0.05	0.24 \pm 0.02
gly/thr	0.5 \pm 0.2	1.6 \pm 0.7	0.5 \pm 0.2	0.49 \pm 0.07	1.7 \pm 0.2	0.49 \pm 0.07	0.4 \pm 0.2	1.4 \pm 0.6	0.4 \pm 0.2	0.53 \pm 0.03	1.9 \pm 0.1	0.53 \pm 0.03
arg	0.08 \pm 0.07	0.2 \pm 0.2	0.3 \pm 0.3	0.04 \pm 0.03	0.1 \pm 0.1	0.2 \pm 0.1	0.013 \pm 0.005	0.04 \pm 0.01	0.05 \pm 0.02	0.028 \pm 0.001	0.084 \pm 0.003	0.112 \pm 0.004
ala	0.087 \pm 0.005	0.26 \pm 0.01	0.087 \pm 0.005	0.19 \pm 0.04	0.6 \pm 0.1	0.19 \pm 0.04	0.2 \pm 0.1	0.5 \pm 0.3	0.2 \pm 0.1	0.067 \pm 0.001	0.269 \pm 0.005	0.067 \pm 0.001
tyr	0.02 \pm 0.01	0.09 \pm 0.04	0.02 \pm 0.01	0.03 \pm 0.01	0.12 \pm 0.04	0.03 \pm 0.01	0.02 \pm 0.01	0.07 \pm 0.03	0.02 \pm 0.01	0.0021 \pm 0.0004	0.010 \pm 0.002	0.0021 \pm 0.0004
met	0.02 \pm 0.03	0.1 \pm 0.1	0.02 \pm 0.03	0.004 \pm 0.001	0.02 \pm 0.01	0.004 \pm 0.001	0.01 \pm 0.01	0.05 \pm 0.04	0.01 \pm 0.01	0.097 \pm 0.004	0.48 \pm 0.02	0.097 \pm 0.004
val	0.03 \pm 0.02	0.1 \pm 0.1	0.03 \pm 0.02	0.08 \pm 0.02	0.40 \pm 0.08	0.08 \pm 0.02	0.08 \pm 0.01	0.39 \pm 0.07	0.08 \pm 0.01	0.05 \pm 0.01	0.42 \pm 0.07	0.05 \pm 0.01
phe	0.03 \pm 0.02	0.3 \pm 0.2	0.03 \pm 0.02	0.05 \pm 0.01	0.42 \pm 0.06	0.05 \pm 0.01	0.05 \pm 0.03	0.4 \pm 0.3	0.05 \pm 0.03	0.041 \pm 0.003	0.24 \pm 0.02	0.041 \pm 0.003
ile	0.05 \pm 0.04	0.3 \pm 0.3	0.05 \pm 0.04	0.05 \pm 0.01	0.28 \pm 0.04	0.05 \pm 0.01	0.04 \pm 0.03	0.3 \pm 0.2	0.04 \pm 0.03	0.041 \pm 0.003	0.24 \pm 0.02	0.041 \pm 0.003
leu	0.03 \pm 0.02	0.15 \pm 0.06	0.03 \pm 0.01	0.09 \pm 0.01	0.52 \pm 0.07	0.09 \pm 0.01	0.08 \pm 0.04	0.5 \pm 0.3	0.08 \pm 0.04	0.98 \pm 0.001	0.59 \pm 0.01	0.098 \pm 0.001
lys	0.06 \pm 0.02	0.4 \pm 0.1	0.12 \pm 0.04	0.05 \pm 0.01	0.32 \pm 0.03	0.11 \pm 0.01	0.05 \pm 0.02	0.3 \pm 0.1	0.10 \pm 0.04	0.0453 \pm 0.0004	0.272 \pm 0.003	0.091 \pm 0.001
total	1.3 \pm 0.5	6 \pm 2	1.6 \pm 0.7	1.6 \pm 0.02	7.0 \pm 0.8	1.8 \pm 0.2	1.3 \pm 0.6	6 \pm 3	1.4 \pm 0.7	1.99 \pm 0.04	8.5 \pm 0.2	2.12 \pm 0.05

amino acid	T4			T5			T6		
	μM amino acid	μM C	μM N	μM amino acid	μM C	μM N	μM amino acid	μM C	μM N
asp	0.07 \pm 0.01	0.29 \pm 0.04	0.07 \pm 0.01	0.072 \pm 0.001	0.29 \pm 0.01	0.072 \pm 0.001	0.105 \pm 0.006	0.42 \pm 0.02	0.11 \pm 0.01
glu	0.06 \pm 0.01	0.31 \pm 0.07	0.06 \pm 0.01	0.064 \pm 0.008	0.32 \pm 0.04	0.06 \pm 0.01	0.084 \pm 0.003	0.42 \pm 0.01	0.084 \pm 0.003
ser	0.12 \pm 0.02	0.7 \pm 0.1	0.12 \pm 0.02	0.11 \pm 0.01	0.29 \pm 0.09	0.11 \pm 0.01	0.17 \pm 0.03	1.1 \pm 0.2	0.17 \pm 0.03
his	0.16 \pm 0.06	0.5 \pm 0.2	0.16 \pm 0.06	0.17 \pm 0.02	0.51 \pm 0.06	0.17 \pm 0.02	0.13 \pm 0.02	0.39 \pm 0.06	0.13 \pm 0.02
gly/thr	0.25 \pm 0.06	0.9 \pm 0.2	0.25 \pm 0.06	0.20 \pm 0.03	0.7 \pm 0.1	0.20 \pm 0.03	0.39 \pm 0.07	1.4 \pm 0.3	0.39 \pm 0.07
arg	0.018 \pm 0.003	0.05 \pm 0.01	0.07 \pm 0.01	0.019 \pm 0.001	0.058 \pm 0.002	0.078 \pm 0.002	0.020 \pm 0.004	0.06 \pm 0.01	0.08 \pm 0.01
ala	0.12 \pm 0.02	0.37 \pm 0.07	0.12 \pm 0.02	0.11 \pm 0.01	0.32 \pm 0.03	0.11 \pm 0.01	0.18 \pm 0.002	0.53 \pm 0.05	0.18 \pm 0.02
tyr	0.02 \pm 0.01	0.07 \pm 0.03	0.02 \pm 0.01	0.019 \pm 0.001	0.074 \pm 0.003	0.019 \pm 0.001	0.04 \pm 0.01	0.16 \pm 0.05	0.04 \pm 0.01
met	0.01 \pm 0.02	0.05 \pm 0.08	0.01 \pm 0.02	0.03 \pm 0.04	0.2 \pm 0.2	0.03 \pm 0.04	0.004 \pm 0.004	0.02 \pm 0.02	0.004 \pm 0.004
val	0.05 \pm 0.01	0.24 \pm 0.05	0.05 \pm 0.01	0.039 \pm 0.005	0.19 \pm 0.03	0.04 \pm 0.01	0.081 \pm 0.008	0.41 \pm 0.04	0.08 \pm 0.01
phe	0.029 \pm 0.004	0.26 \pm 0.03	0.029 \pm 0.004	0.028 \pm 0.002	0.25 \pm 0.01	0.028 \pm 0.002	0.041 \pm 0.007	0.37 \pm 0.06	0.04 \pm 0.01
ile	0.03 \pm 0.01	0.18 \pm 0.06	0.03 \pm 0.01	0.023 \pm 0.003	0.14 \pm 0.02	0.023 \pm 0.003	0.046 \pm 0.006	0.27 \pm 0.03	0.05 \pm 0.01
leu	0.05 \pm 0.01	0.32 \pm 0.07	0.05 \pm 0.01	0.051 \pm 0.006	0.31 \pm 0.04	0.05 \pm 0.01	0.09 \pm 0.02	0.6 \pm 0.1	0.09 \pm 0.02
lys	0.02 \pm 0.01	0.03 \pm 0.04	0.04 \pm 0.01	0.019 \pm 0.001	0.11 \pm 0.01	0.038 \pm 0.003	0.04 \pm 0.01	0.22 \pm 0.07	0.07 \pm 0.02
total	1.0 \pm 0.2	4.4 \pm 0.8	1.1 \pm 0.2	0.95 \pm 0.03	4.1 \pm 0.1	1.03 \pm 0.04	1.4 \pm 0.02	6.2 \pm 0.9	1.5 \pm 0.2

Table 4.5B: 0 virus incubation

amino acid	uM amino acid	T0 uM C	uM N	uM amino acid	T1 uM C	uM N	uM amino acid	T2 uM C	uM N	uM amino acid	T3 uM C	uM N
asp	0.092±0.006	0.37±0.02	0.09±0.01	0.09±0.02	0.37±0.06	0.09±0.02	0.06±0.03	0.34±0.1	0.06±0.03	0.09±0.02	0.35±0.07	0.09±0.02
glu	0.11±0.01	0.53±0.06	0.11±0.01	0.10±0.02	0.5±0.01	0.10±0.02	0.08±0.02	0.44±0.1	0.08±0.02	0.09±0.03	0.4-0.1	0.09±0.03
ser	0.18±0.03	1.1±0.2	0.18±0.03	0.18±0.02	1.1±0.1	0.18±0.02	0.057±0.002	0.34±0.03	0.057±0.002	0.2±0.1	1.2±0.7	0.2±0.1
his	0.06±0.02	0.17±0.07	0.06±0.02	0.04±0.04	0.1±0.1	0.04±0.04	0.04±0.01	0.12±0.03	0.04±0.01	0.11±0.05	0.3±0.1	0.11±0.05
gly/thr	0.44±0.04	1.6±0.2	0.44±0.04	0.50±0.04	1.8±0.2	0.51±0.04	0.214±0.001	0.750±0.002	0.214±0.001	0.6±0.2	1.9±0.8	0.5±0.2
arg	0.02±0.01	0.05±0.04	0.07±0.05	0.01±0.01	0.03±0.03	0.05±0.04	0.03±0.05	0.24±0.2	0.03±0.05	0.04±0.03	0.11±0.08	0.1±0.1
ala	0.12±0.02	0.35±0.07	0.12±0.02	0.18±0.05	0.5±0.1	0.18±0.05	0.03±0.03	0.09±0.1	0.03±0.03	0.3±0.1	0.8±0.4	0.3±0.1
tyr	0.4±0.03	0.2±0.1	0.04±0.03	0.04±0.02	0.17±0.07	0.04±0.02	0.01±0.01	0.6±0.6	0.01±0.02	0.04±0.04	0.2±0.2	0.04±0.04
met	0.010±0.007	0.05±0.03	0.01±0.01	0.01±0.01	0.07±0.06	0.01±0.01	0.031±0.009	0.16±0.05	0.03±0.01	0.06±0.02	0.3±0.1	0.06±0.02
val	0.06±0.04	0.3±0.2	0.06±0.04	0.052±0.001	0.261±0.005	0.052±0.001	0.013±0.003	0.12±0.02	0.013±0.003	0.03±0.02	0.3±0.2	0.03±0.02
phe	0.036±0.007	0.32±0.06	0.04±0.01	0.042±0.005	0.38±0.04	0.042±0.005	0.02±0.02	0.1±0.1	0.02±0.02	0.052±0.003	0.31±0.02	0.052±0.003
ile	0.029±0.007	0.18±0.04	0.03±0.01	0.04±0.01	0.26±0.04	0.04±0.01	0.021±0.003	0.12±0.2	0.021±0.003	0.06±0.04	0.4±0.2	0.06±0.04
leu	0.07±0.01	0.41±0.06	0.07±0.01	0.08±0.01	0.47±0.03	0.08±0.01	0.021±0.003	0.15±0.08	0.021±0.003	0.05±0.02	0.3±0.1	0.11±0.03
lys	0.05±0.02	0.3±0.1	0.10±0.04	0.05±0.01	0.30±0.08	0.10±0.03	0.02±0.01	3±1	1.0±0.4	1.7±0.7	7±4	1.8±0.9
total	1.3±0.1	5.9±0.6	1.4±0.2	1.45±0.09	6.4±0.4	1.5±0.1	0.8±0.3					

amino acid	uM amino acid	T4 uM C	uM N	uM amino acid	T5 uM C	uM N	uM amino acid	T6 uM C	uM N
asp	0.1±0.05	0.4±0.2	0.10±0.05	0.046±0.004	0.18±0.01	0.046±0.004	0.055±0.001	0.219±0.004	0.055±0.001
glu	0.09±0.05	0.4±0.3	0.09±0.05	0.05±0.01	0.24±0.06	0.05±0.01	0.052±0.003	0.26±0.01	0.052±0.003
ser	0.10±0.04	0.6±0.3	0.10±0.04	0.07±0.02	0.4±0.1	0.07±0.02	0.09±0.01	0.57±0.07	0.09±0.01
his	0.06±0.04	0.2±0.1	0.06±0.04	0.04±0.01	0.13±0.02	0.04±0.01	0.046±0.006	0.14±0.02	0.05±0.01
gly/thr	0.24±0.9	0.8±0.3	0.24±0.09	0.17±0.04	0.6±0.02	0.17±0.04	0.24±0.02	0.85±0.08	0.24±0.02
arg	0.02±0.01	0.06±0.04	0.08±0.05	0.015±0.002	0.05±0.01	0.06±0.01	0.015±0.002	0.05±0.01	0.06±0.01
ala	0.10±0.04	0.3±0.1	0.10±0.04	0.06±0.02	0.19±0.07	0.06±0.02	0.079±0.005	0.24±0.01	0.079±0.005
tyr	0.014±0.003	0.06±0.01	0.014±0.003	0.011±0.003	0.05±0.01	0.011±0.003	0.024±0.003	0.10±0.01	0.024±0.003
met	0.003±0.001	0.017±0.005	0.003±0.001	0.01±0.01	0.06±0.05	0.01±0.01	0.0035±0.0002	0.018±0.001	0.0035±0.0002
val	0.05±0.04	0.3±0.2	0.05±0.04	0.02±0.01	0.12±0.04	0.02±0.01	0.032±0.004	0.16±0.02	0.032±0.004
phe	0.02±0.01	0.14±0.05	0.02±0.01	0.015±0.001	0.13±0.01	0.015±0.001	0.015±0.002	0.14±0.02	0.015±0.002
ile	0.02±0.01	0.11±0.04	0.02±0.01	0.01±0.01	0.08±0.03	0.01±0.01	0.024±0.002	0.14±0.01	0.024±0.002
leu	0.04±0.02	0.3±0.1	0.04±0.02	0.028±0.002	0.17±0.01	0.028±0.002	0.04±0.003	0.24±0.02	0.040±0.003
lys	0.02±0.01	0.12±0.04	0.04±0.01	0.014±0.003	0.08±0.02	0.03±0.01	0.02±0.01	0.15±0.06	0.05±0.02
total	0.9±0.4	4±2	1.0±0.5	0.6±0.1	2.5±0.05	0.6±0.1	0.75±0.04	3.3±0.2	0.82±0.05

Table 4.5C: Grazer added incubation

amino acid	uM amino acid	T0 uM C	uM N	uM amino acid	T1 uM C	uM N	uM amino acid	T2 uM C	uM N	uM amino acid	T3 uM C	uM N
asp	0.09±0.06	0.4±0.02	0.09±0.06	0.14±0.03	0.6±0.1	0.14±0.03	0.13±0.01	0.52±0.05	0.13±0.01	0.162±0.006	0.65±0.01	0.162±0.006
glu	0.10±0.03	0.5±0.1	0.10±0.03	0.15±0.04	0.8±0.2	0.15±0.04	0.16±0.03	0.8±0.1	0.16±0.03	0.15±0.02	0.8±0.1	0.15±0.02
ser	0.07±0.04	0.4±0.2	0.07±0.04	0.28±0.09	1.7±0.6	0.28±0.09	0.18±0.07	1.1±0.4	0.18±0.07	0.23±0.03	1.4±0.2	0.23±0.03
his	0.007±0.003	0.02±0.01	0.007±0.003	0.12±0.04	0.4±0.1	0.12±0.04	0.09±0.03	0.3±0.1	0.09±0.03	0.23±0.04	0.7±0.1	0.23±0.04
gly/thr	0.17±0.06	0.6±0.2	0.17±0.06	0.7±0.2	2.4±0.7	0.7±0.2	0.37±0.05	1.3±0.2	0.37±0.05	0.55±0.08	1.9±0.3	0.55±0.08
arg	0.032±0.004	0.10±0.01	0.13±0.01	0.03±0.02	0.09±0.06	0.12±0.08	0.05±0.05	0.2±0.2	0.12±0.08	0.07±0.01	0.22±0.03	0.29±0.04
ala	0.02±0.02	0.06±0.06	0.02±0.02	0.24±0.05	0.7±0.2	0.24±0.05	0.12±0.09	0.4±0.3	0.12±0.09	0.29±0.05	0.9±0.1	0.29±0.05
tyr	0.015±0.005	0.06±0.02	0.015±0.005	0.4±0.02	0.16±0.06	0.04±0.02	0.02±0.01	0.09±0.03	0.02±0.01	0.053±0.002	0.21±0.01	0.053±0.002
met	0.01±0.01	0.06±0.03	0.01±0.01	0.05±0.05	0.3±0.3	0.05±0.05	0.03±0.02	0.14±0.08	0.03±0.02	0.03±0.02	0.1±0.1	0.03±0.02
val	0.007±0.004	0.04±0.02	0.007±0.004	0.10±0.03	0.5±0.1	0.10±0.03	0.3±0.3	2±1	0.4±0.3	0.13±0.03	0.6±0.2	0.13±0.03
phe	0.017±0.002	0.15±0.02	0.017±0.002	0.06±0.02	0.6±0.2	0.06±0.02	0.05±0.02	0.5±0.2	0.05±0.02	0.05±0.01	0.49±0.05	0.05±0.01
ile	0.03±0.01	0.16±0.08	0.03±0.01	0.08±0.04	0.5±0.2	0.08±0.04	0.05±0.01	0.31±0.03	0.05±0.01	0.08±0.02	0.5±0.1	0.08±0.02
leu	0.004±0.001	0.025±0.004	0.004±0.001	0.14±0.06	0.9±0.4	0.14±0.06	0.08±0.03	0.5±0.2	0.08±0.03	0.13±0.02	0.78±0.09	0.13±0.02
lys	0.02±0.01	0.12±0.09	0.04±0.03	0.08±0.03	0.5±0.2	0.15±0.05	0.09±0.02	0.5±0.1	0.17±0.05	0.071±0.003	0.42±0.02	0.14±0.01
total	0.60±0.06	2.7±0.3	0.71±0.07	2.2±0.6	10±3	2.4±0.8	1.8±0.5	8±3	2.0±0.7	2.2±0.2	9.6±0.9	2.5±0.2

amino acid	uM amino acid	T4 uM C	uM N	uM amino acid	T5 uM C	uM N	uM amino acid	T6 uM C	uM N
asp	0.067±0.004	0.27±0.02	0.067±0.004	0.09±0.03	0.4±0.1	0.09±0.03	0.10±0.02	0.40±0.08	0.10±0.02
glu	0.064±0.004	0.32±0.02	0.064±0.004	0.10±0.03	0.5±0.1	0.10±0.03	0.08±0.03	0.4±0.1	0.08±0.03
ser	0.13±0.05	0.8—0.3	0.13±0.05	0.14±0.02	0.8±0.1	0.14±0.02	0.15±0.02	0.9±0.1	0.15±0.02
his	0.15±0.07	0.4±2	0.15±0.07	0.12±0.01	0.36±0.04	0.12±0.01	0.14±0.02	0.42±0.05	0.14±0.02
gly/thr	0.3±0.1	1.1±0.4	0.3±0.1	0.26±0.03	0.9±0.1	0.26±0.03	0.37±0.05	1.3±0.2	0.37±0.05
arg	0.022±0.006	0.07±0.02	0.09±0.02	0.028±0.003	0.08±0.01	0.11±0.1	0.0190±0.0005	0.057±0.001	0.076±0.002
ala	0.13±0.05	0.4±0.1	0.13±0.05	0.12±0.01	0.36±0.04	0.12±0.01	0.16±0.03	0.5±0.1	0.16±0.03
tyr	0.019±0.006	0.08±0.02	0.019±0.006	0.020±0.003	0.08±0.01	0.020±0.003	0.04±0.01	0.14±0.03	0.04±0.01
met	0.02±0.03	0.09±0.1	0.02±0.03	0.04±0.01	0.19±0.07	0.04±0.01	0.03±0.01	0.13±0.04	0.03±0.01
val	0.05±0.02	0.23±0.09	0.05±0.02	0.05±0.01	0.25±0.06	0.05±0.01	0.08±0.01	0.40±0.05	0.08±0.01
phe	0.04±0.01	0.3±0.1	0.04±0.01	0.034±0.004	0.31±0.03	0.034±0.004	0.04±0.01	0.37±0.07	0.04±0.01
ile	0.03±0.01	0.16±0.07	0.03±0.01	0.03±0.01	0.19±0.05	0.03±0.01	0.05±0.01	0.30±0.07	0.05±0.01
leu	0.06±0.02	0.3±0.1	0.06±0.02	0.06±0.01	0.38±0.05	0.06±0.01	0.08±0.01	0.49±0.09	0.08±0.01
lys	0.025±0.007	0.15±0.04	0.05±0.01	0.025±0.004	0.15±0.02	0.05±0.01	0.04±0.01	0.23±0.07	0.08±0.02
total	1.1±0.3	5±2	1.2±0.2	1.1±0.1	4.9±0.7	1.2±0.2	1.4±0.2	6.1±0.9	1.5±0.2

Table 4.5D: 10 times virus incubation

amino acid	uM amino acid	T0 uM C	uM N	uM amino acid	T1 uM C	uM N	uM amino acid	T2 uM C	uM N	uM amino acid	T3 uM C	uM N
asp	0.117±0.003	0.47±0.01	0.117±0.003	0.15±0.01	0.58±0.05	0.15±0.01	0.13±0.05	0.5±0.2	0.13±0.05	0.16±0.02	0.66±0.07	0.16±0.02
glu	0.100±0.004	0.50±0.02	0.100±0.004	0.14±0.01	0.69±0.04	0.14±0.01	0.17±0.03	0.9±0.2	0.17±0.03	0.13±0.02	0.66±0.08	0.13±0.02
ser	0.21±0.06	1.2±0.3	0.21±0.06	0.30±0.09	1.8±0.5	0.30±0.09	0.12±0.03	0.7±0.2	0.12±0.03	0.30±0.03	1.8±0.2	0.30±0.03
his	0.2±0.1	0.5±0.3	0.2±0.1	0.3±0.3	0.8±0.8	0.3±0.3	0.13±0.04	0.4±0.1	0.13±0.04	0.21±0.02	0.63±0.06	0.21±0.02
gly/thr	0.5±0.1	1.8±0.5	0.5±0.1	0.7±0.1	1.5±0.4	0.7±0.1	0.39±0.05	1.3±0.2	0.39±0.05	0.78±0.06	2.7±0.2	0.78±0.06
arg	0.10±0.09	0.3±0.3	0.4±0.4	0.02±0.01	0.06±0.04	0.08±0.05	0.06±0.02	0.19±0.06	0.26±0.08	0.04±0.01	0.13±0.02	0.04±0.01
ala	0.04±0.04	0.1±0.1	0.04±0.04	0.29±0.06	0.9±0.2	0.29±0.06	0.12±0.01	0.35±0.03	0.12±0.01	0.41±0.06	1.2±0.2	0.18±0.03
tyr	0.03±0.02	0.11±0.07	0.03±0.02	0.06±0.01	0.24±0.06	0.06±0.01	0.020±0.002	0.08±0.01	0.020±0.002	0.08±0.02	0.3±0.1	0.08±0.02
met	0.02±0.02	0.1±0.1	0.02±0.02	0.01±0.01	0.07±0.04	0.01±0.01	0.07±0.07	0.4±0.03	0.07±0.07	0.008±0.003	0.04±0.01	0.008±0.003
val	0.10±0.02	0.5±0.1	0.10±0.02	0.12±0.03	0.6±0.2	0.12±0.03	0.2±0.1	0.8±0.6	0.2±0.1	0.17±0.03	0.8±0.02	0.17±0.03
phe	0.047±0.006	0.43±0.06	0.047±0.006	0.09±0.02	0.9±0.2	0.09±0.02	0.04±0.01	0.32±0.07	0.04±0.01	0.06±0.01	0.56±0.06	0.06±0.01
ile	0.067±0.007	0.40±0.04	0.067±0.007	0.07±0.01	0.40±0.08	0.07±0.01	0.03±0.02	0.2±0.1	0.03±0.02	0.09±0.01	0.57±0.06	0.09±0.01
leu	0.08±0.04	0.5±0.2	0.08±0.04	0.15±0.03	0.9±0.2	0.15±0.03	0.05±0.02	0.3±0.1	0.05±0.02	0.15±0.01	0.88±0.08	0.15±0.01
lys	0.049±0.008	0.29±0.05	0.10±0.02	0.10±0.03	0.6±0.2	0.19±0.07	0.06±0.03	0.4±0.2	0.12±0.05	0.066±0.004	0.40±0.03	0.13±0.01
total	1.6±0.2	7±1	2.0±0.3	2.5±0.6	11±3	2.6±0.8	1.57±0.01	6.90±0.05	1.83±0.01	2.7±0.2	11±1	2.9±0.3

amino acid	uM amino acid	T4 uM C	uM N	uM amino acid	T5 uM C	uM N	uM amino acid	T6 uM C	uM N
asp	0.073±0.006	0.29±0.03	0.073±0.006	0.087±0.006	0.35±0.03	0.087±0.006	0.091±0.006	0.36±0.02	0.091±0.006
glu	0.068±0.002	0.34±0.01	0.068±0.002	0.087±0.006	0.43±0.03	0.087±0.006	0.071±0.006	0.36±0.03	0.071±0.006
ser	0.141±0.006	0.85±0.04	0.141±0.006	0.2±0.1	1.2±0.6	0.2±0.1	0.17±0.05	1.0±0.3	0.17±0.05
his	0.26±0.05	0.8±0.1	0.26±0.05	0.3±0.2	0.8±0.5	0.3±0.2	0.21±0.06	0.6±0.2	0.21±0.06
gly/thr	0.30±0.03	1.0±0.1	0.30±0.03	0.3±0.1	1.2±0.4	0.3±0.1	0.36±0.09	1.3±0.3	0.36±0.09
arg	0.027±0.003	0.08±0.01	0.11±0.01	0.03±0.02	0.10±0.05	0.13±0.06	0.02±0.01	0.07±0.04	0.10±0.05
ala	0.15±0.01	0.46±0.04	0.15±0.01	0.16±0.07	0.5±0.2	0.16±0.07	0.21±0.05	0.6±0.2	0.21±0.05
tyr	0.019±0.003	0.08±0.01	0.019±0.003	0.02±0.01	0.08±0.04	0.02±0.01	0.04±0.01	0.17±0.05	0.04±0.01
met	0.03±0.03	0.2±0.2	0.03±0.03	0.044±0.006	0.22±0.03	0.044±0.006	0.010±0.007	0.05±0.04	0.010±0.007
val	0.056±0.003	0.3±0.2	0.056±0.003	0.07±0.03	0.3±0.1	0.07±0.03	0.07±0.02	0.34±0.09	0.07±0.02
phe	0.034±0.002	0.31±0.02	0.034±0.002	0.04±0.02	0.4±0.2	0.04±0.02	0.04±0.01	0.33±0.09	0.04±0.01
ile	0.031±0.001	0.18±0.01	0.031±0.001	0.04±0.02	0.24±0.09	0.04±0.02	0.04±0.01	0.24±0.08	0.04±0.01
leu	0.061±0.005	0.36±0.03	0.061±0.005	0.09±0.04	0.5±0.2	0.09±0.04	0.08±0.02	0.5±0.1	0.08±0.02
lys	0.021±0.002	0.13±0.01	0.042±0.003	0.03±0.01	0.20±0.08	0.07±0.03	0.030±0.008	0.18±0.05	0.06±0.02
total	1.3±0.1	5.3±0.6	1.4±0.2	1.5±0.6	6±3	1.6±0.7	1.4±0.3	6±2	1.6±0.4

Table 4.6: Amino acids as percent of the DOC and TDN for the control, 0 virus (0V), grazer and 10 times virus (10V) culture treatments. DOC and TDN measurements obtained from Aubrey Cano/Craig Carlson, UCSB.

A: control incubation

timepoints	DOC ($\mu\text{M C}$)	amino acid $\mu\text{M C}$	% C as amino acids	TDN ($\mu\text{M N}$)	amino acid $\mu\text{M N}$	% N as amino acids
T0	188	6	3.2	18.8	1.6	8.5
T1	188	7	3.7	16.94	1.8	10.6
T2	190	6	3.2	14.7	1.4	9.5
T3	180	8.5	4.7	12	2.12	17.7
T4	189	4.4	2.3	13.2	1.1	8.3
T5	194	4.1	2.1	13.5	1.03	7.6
T6	190	6.2	3.3	13.6	1.5	11.0

B: 0V incubation

timepoints	DOC ($\mu\text{M C}$)	amino acid $\mu\text{M C}$	% C as amino acids	TDN ($\mu\text{M N}$)	amino acid $\mu\text{M N}$	% N as amino acids
T0	177	5.9	3.3	19.8	1.4	7.1
T1	174	6.4	3.7	20.3	1.5	7.4
T2	176	3	1.7	20.0	1	5.0
T3	169	7	4.1	18	1.8	10.0
T4	169	4	2.4	16.3	1	6.1
T5	165.9	2.5	1.5	13.7	0.6	4.4
T6	169	3.3	2.0	12.6	0.82	6.5

C: grazer incubation

timepoints	DOC ($\mu\text{M C}$)	amino acid $\mu\text{M C}$	% C as amino acids	TDN ($\mu\text{M N}$)	amino acid $\mu\text{M N}$	% N as amino acids
T0	188	2.7	1.4	18.7	0.71	3.8
T1	185	10	5.4	16.9	2.4	14.2
T2	188.7	8	4.2	14.5	2	13.8
T3	190	9.6	5.1	13.4	2.5	18.7
T4	190	5	2.6	13.45	1.2	8.9
T5	191	4.9	2.6	13.2	1.2	9.1
T6	192.5	6.1	3.2	13.7	1.5	10.9

D: 10V incubation

timepoints	DOC ($\mu\text{M C}$)	amino acid $\mu\text{M C}$	% C as amino acids	TDN ($\mu\text{M N}$)	amino acid $\mu\text{M N}$	% N as amino acids
T0	223	7	3.1	21.9	2	9.1
T1	222	11	5.0	20	2.6	13.0
T2	208	6.9	3.3	16.2	1.83	11.3
T3	250	11	4.4	18	2.9	16.1
T4	209	5.3	2.5	14.7	1.4	9.5
T5	216.1	6	2.8	14.90	1.6	10.7
T6	220	6	2.7	15.2	1.6	10.5

In contrast, the THAA concentration for the grazer added incubation was much lower than the control and 0 virus treatments at timepoint T0 ($0.6 \pm 0.06 \mu\text{M}$), but was much higher for the remainder of the experiment (1.1 ± 0.1 - $2.2 \pm 0.6 \mu\text{M}$), resulting in a wider concentration range than the other incubations. This translated to an amino acid

carbon concentration of 2.7 ± 0.3 - 10 ± 3 $\mu\text{M C}$, which was 1.4-5.4% of the DOC (Table 4.6C). The percent of the total nitrogen present as amino acid was larger than the control and 0 virus treatments, ranging from 3.8-18.7% of the TDN (0.71 ± 0.07 - 2.4 ± 0.8 $\mu\text{M N}$). As with the other incubations, hydrolyzable amino acids made up the largest percent of the DOC and TDN after 48 hours, though the maximum amino acid concentration occurred at the T1 timepoint.

The 10 times virus culture contained the highest concentration of THAA of all the treatments, ranging from 1.3 ± 0.1 μM to 2.7 ± 0.2 μM , with the maxima at T3. This higher amino acid concentration was reflected in the higher percent of the DOC represented by the amino acid fraction (5.3-11%) and the higher concentration of amino acid carbon (5.3 ± 0.6 - 11 ± 1 $\mu\text{M C}$) (Table 4.6D). The concentration of amino acid nitrogen was also higher than the other incubations, ranging from 1.4 ± 0.2 - 2.9 ± 0.3 $\mu\text{M N}$. Amino acid nitrogen also was a larger percentage of the total dissolved nitrogen, 9.1-16%. Again, amino acids represented the largest percent of the DOC and TDN at the T3 timepoint, 48 hours after the start of the experiment.

The mole fractions for the individual amino acids released by hydrolysis is listed in Table 4.7. In general, the replication between both duplicate analyses and duplicate carboy incubations was good, except for those amino acids that have a particularly low mole fraction, which were therefore present in only small amounts in the samples. Most of the hydrolyzed amino acids had a mole fraction of less than 0.1. With the exception of glycine and threonine, which co-elute, the mole fraction of any individual amino acid from any treatment was not greater than 0.2. The mole fraction for the glycine/threonine pair was generally between 0.25 and 0.3.

With some exceptions, the mole fractions of individual amino acids within each incubation were usually constant during the course of the experiment, even when the concentration of the total amino acids varied between timepoints. The mole fraction of the glycine/threonine pair in the 10 times virus culture decreased from 0.31 ± 0.05 to 0.23 ± 0.02 within the first 72 hours of the experiment, then remained constant until the end of the incubation (Table 4.7D). The grazer added incubation seemed to be the most variant in terms of amino acid mole fractions between timepoints (Table 4.7C). Both the aspartic and glutamic acid mole fractions dropped rapidly within the first 12 hours, from 0.2 ± 0.1 and 0.18 ± 0.06 respectively down to approximately 0.07 for both amino acids. In addition, the arginine mole fraction also declined from 0.05 ± 0.01 down to 0.014 ± 0.002 by the end of the incubation. Histidine and alanine had opposite trends; the mole fraction for histidine increased from 0.012 ± 0.004 at T0 to 0.10 ± 0.03 at T6, while the alanine mole fraction rose from 0.03 ± 0.03 to 0.12 ± 0.01 within the same time period. A sharp increase in the mole fraction for valine appeared at timepoint T2. Decreases in aspartic acid (0.106 ± 0.001 to 0.08 ± 0.01) and glutamic acid (0.10 ± 0.02 to 0.06 ± 0.01) mole fractions were also seen in the control incubations (Table 4.7A). The mole fraction for histidine increased from 0.05 ± 0.01 at the initial T0 timepoint to a maxima of 0.18 ± 0.02 at T5, then dropped again to 0.091 ± 0.003 . The zero virus incubation had the most consistent amino acid mole fractions during the experiment (Table 4.7B).

The mole fractions for the hydrolyzed amino acids were also generally similar between carboy treatments. In general, aspartic and glutamic acids had matching mole fractions of approximately 0.7. Serine and alanine had mole fractions ranging from 0.1-0.15, and histidine between 0.05 and 0.1. The remaining amino acids, arginine, tyrosine,

Table 4.7: Mole fraction of individual hydrolyzed amino acids for the control (A), 0 virus (0V, B), grazer added (C), and 10 times virus (10V, D) incubation treatments. The sum of the mole fraction for all amino acids at each timepoint was 1.

A: control incubation							
Amino acid	mol fraction						
	T0	T1	T2	T3	T4	T5	T6
asp	0.106±0.001	0.07±0.01	0.09±0.02	0.08±0.01	0.07±0.02	0.075±0.002	0.08±0.01
glu	0.10±0.02	0.07±0.01	0.09±0.03	0.07±0.01	0.06±0.02	0.067±0.009	0.06±0.01
ser	0.10±0.03	0.12±0.01	0.10±0.01	0.12±0.01	0.11±0.01	0.12±0.01	0.122±0.005
his	0.05±0.04	0.07±0.01	0.05±0.02	0.12±0.01	0.16±0.05	0.18±0.02	0.091±0.003
gly/thr	0.34±0.02	0.30±0.02	0.29±0.02	0.27±0.01	0.25±0.02	0.20±0.03	0.28±0.02
arg	0.05±0.03	0.02±0.02	0.01±0.01	0.0139±0.0004	0.018±0.004	0.020±0.001	0.014±0.001
ala	0.07±0.03	0.12±0.03	0.12±0.04	0.129±0.002	0.122±0.003	0.11±0.01	0.124±0.005
tyr	0.016±0.002	0.02±0.01	0.012±0.001	0.034±0.001	0.02±0.01	0.019±0.001	0.028±0.005
met	0.01±0.01	0.003±0.001	0.01±0.01	0.0010±0.0002	0.01±0.01	0.04±0.04	0.003±0.003
val	0.03±0.03	0.05±0.01	0.07±0.01	0.048±0.002	0.05±0.01	0.040±0.005	0.06±0.01
phe	0.02±0.01	0.029±0.002	0.03±0.01	0.024±0.003	0.029±0.002	0.029±0.002	0.029±0.001
ile	0.03±0.02	0.029±0.001	0.03±0.01	0.020±0.001	0.03±0.01	0.024±0.003	0.0322±0.0005
leu	0.02±0.02	0.054±0.003	0.06±0.01	0.049±0.001	0.05±0.01	0.053±0.006	0.064±0.004
lys	0.044±0.001	0.034±0.002	0.037±0.003	0.0226±0.0005	0.019±0.005	0.020±0.001	0.026±0.005

B: 0V incubation							
Amino acid	mol fraction						
	T0	T1	T2	T3	T4	T5	T6
asp	0.07±0.01	0.06±0.01	0.0828±0.0002	0.06±0.01	0.11±0.01	0.08±0.02	0.073±0.004
glu	0.08±0.01	0.07±0.01	0.10±0.01	0.06±0.01	0.10±0.01	0.09±0.03	0.070±0.004
ser	0.14±0.01	0.124±0.004	0.08±0.03	0.12±0.02	0.12±0.01	0.12±0.01	0.13±0.01
his	0.04±0.02	0.03±0.02	0.06±0.04	0.0665±0.0004	0.07±0.01	0.08±0.02	0.061±0.006
gly/thr	0.33±0.02	0.36±0.05	0.3±0.1	0.33±0.01	0.28±0.03	0.30±0.03	0.32±0.02
arg	0.01±0.01	0.008±0.002	0.06±0.04	0.02±0.01	0.022±0.003	0.027±0.002	0.020±0.003
ala	0.09±0.01	0.12±0.03	0.03±0.03	0.15±0.01	0.11±0.02	0.11±0.02	0.106±0.008
tyr	0.03±0.02	0.03±0.01	0.01±0.02	0.018±0.001	0.018±0.005	0.020±0.003	0.032±0.003
met	0.01±0.01	0.01±0.01	0.1±0.1	0.02±0.02	0.004±0.001	0.02±0.01	0.0048±0.0004
val	0.05±0.03	0.036±0.003	0.043±0.005	0.039±0.005	0.05±0.02	0.04±0.01	0.043±0.006
phe	0.03±0.01	0.029±0.001	0.018±0.004	0.018±0.004	0.018±0.004	0.026±0.004	0.021±0.002
ile	0.022±0.005	0.030±0.002	0.02±0.01	0.04±0.02	0.023±0.003	0.02±0.01	0.032±0.002
leu	0.05±0.01	0.054±0.001	0.028±0.007	0.04±0.01	0.050±0.003	0.05±0.01	0.053±0.002
lys	0.04±0.01	0.03±0.01	0.031±0.005	0.03±0.01	0.02±0.01	0.03±0.01	0.03±0.01

C: grazer incubation							
Amino acid	mol fraction						
	T0	T1	T2	T3	T4	T5	T6
asp	0.2±0.1	0.064±0.004	0.07±0.02	0.07±0.01	0.06±0.02	0.08±0.02	0.073±0.004
glu	0.18±0.06	0.068±0.004	0.09±0.02	0.07±0.02	0.06±0.02	0.08±0.01	0.06±0.01
ser	0.11±0.05	0.12±0.01	0.09±0.01	0.10±0.01	0.12±0.01	0.12±0.01	0.111±0.003
his	0.012±0.004	0.06±0.04	0.048±0.005	0.10±0.02	0.13±0.02	0.11±0.01	0.10±0.03
gly/thr	0.28±0.07	0.31±0.01	0.21±0.08	0.25±0.02	0.29±0.03	0.23±0.02	0.27±0.01
arg	0.05±0.01	0.02±0.01	0.04±0.05	0.03±0.01	0.021±0.006	0.025±0.002	0.014±0.002
ala	0.03±0.03	0.11±0.01	0.05±0.04	0.13±0.01	0.113±0.009	0.108±0.004	0.12±0.01
tyr	0.03±0.01	0.018±0.002	0.013±0.002	0.024±0.002	0.018±0.002	0.018±0.002	0.03±0.01
met	0.02±0.01	0.02±0.02	0.02±0.02	0.01±0.01	0.02±0.02	0.03±0.01	0.019±0.003
val	0.01±0.01	0.0451±0.0005	0.2±0.1	0.06±0.01	0.041±0.006	0.04±0.01	0.058±0.002
phe	0.0286±0.0004	0.029±0.002	0.029±0.002	0.025±0.005	0.033±0.003	0.031±0.002	0.030±0.001
ile	0.04±0.02	0.04±0.01	0.03±0.01	0.03±0.01	0.024±0.003	0.03±0.01	0.035±0.003
leu	0.007±0.002	0.06±0.01	0.044±0.003	0.058±0.002	0.051±0.004	0.058±0.005	0.059±0.003
lys	0.03±0.02	0.034±0.002	0.047±0.004	0.032±0.002	0.023±0.002	0.022±0.002	0.03±0.01

D: 10V incubation							
Amino acid	mol fraction						
	T0	T1	T2	T3	T4	T5	T6
asp	0.07±0.01	0.06±0.02	0.08±0.03	0.06±0.01	0.06±0.01	0.07±0.03	0.07±0.01
glu	0.06±0.01	0.06±0.01	0.11±0.02	0.05±0.01	0.054±0.007	0.07±0.02	0.05±0.02
ser	0.13±0.02	0.12±0.01	0.08±0.02	0.112±0.002	0.112±0.007	0.12±0.02	0.119±0.006
his	0.10±0.07	0.09±0.09	0.09±0.02	0.08±0.01	0.20±0.02	0.17±0.05	0.14±0.01
gly/thr	0.31±0.05	0.29±0.03	0.25±0.04	0.293±0.003	0.23±0.02	0.23±0.03	0.246±0.005
arg	0.06±0.05	0.007±0.004	0.04±0.01	0.017±0.001	0.021±0.001	0.022±0.002	0.016±0.005
ala	0.02±0.02	0.12±0.01	0.07±0.01	0.15±0.01	0.122±0.003	0.102±0.008	0.148±0.009
tyr	0.016±0.008	0.03±0.01	0.013±0.002	0.03±0.01	0.015±0.001	0.014±0.005	0.029±0.007
met	0.01±0.01	0.01±0.01	0.05±0.04	0.003±0.001	0.02±0.02	0.03±0.02	0.007±0.005
val	0.06±0.02	0.047±0.002	0.11±0.08	0.06±0.01	0.044±0.002	0.044±0.001	0.047±0.002
phe	0.030±0.006	0.04±0.02	0.02±0.01	0.023±0.004	0.027±0.002	0.030±0.001	0.026±0.001
ile	0.041±0.002	0.027±0.002	0.02±0.01	0.035±0.002	0.024±0.002	0.027±0.001	0.028±0.004
leu	0.05±0.03	0.060±0.003	0.03±0.01	0.055±0.001	0.048±0.003	0.056±0.005	0.053±0.003
lys	0.030±0.002	0.038±0.005	0.04±0.02	0.025±0.003	0.017±0.002	0.023±0.001	0.021±0.001

methionine, valine, phenylalanine, isoleucine, leucine and lysine generally had small mole fractions of less than 0.05.

THAA yields for all carboys ranged between 0.6-2.7 μM amino acids (Figure 4.4), and constituted less than 19% of the TDN. The concentration range for the untreated control incubation (0.95-1.99 μM) was similar to literature values for other coastal and bay waters (Jørgensen et al., 1993; Kuznetsova and Lee, 2002; Yamashita and Tanoue, 2003). The mole fraction distribution of the individual amino acids for the control incubation were also very similar to those measured in similar locations, with the exception of histidine, which had a higher mole fraction in this study (Kuznetsova and Lee, 2002; Yamashita and Tanoue, 2003).

Since the control incubation had an unaltered distribution of phytoplankton, microzooplankton, bacteria, and viruses, the effect of the alterations performed on the other carboys can be determined by comparing the results with the control data. Statistical analysis of the experimental means for the control carboy versus the other treatment carboys was performed using Student's T test. This was used to determine whether the treatments had a significant effect on the measured compounds by determining the percent confidence that any value from the zero virus, 10 times virus or grazer added incubations were different from that of the control incubation. Comparisons that had a percent confidence of less than 75% were not considered to be significantly different.

The data shown in Figure 4.4 indicates that the THAA concentration for the zero virus sample was less than the THAA concentration of the control incubation for all timepoints. On average, the concentration of THAA for the control incubation over the

120 h experiment was $1.4 \pm 0.1 \mu\text{M}$. When the mean concentration for THAA for the zero virus incubation ($1.1 \pm 0.2 \mu\text{M}$) was compared to that of the control, it was determined that the THAA concentration of the zero virus treatment was different from the control within a 75-90% confidence interval. This indicates that the absence of viruses had a significant, negative effect on the THAA concentration by reducing the amount of THAA in the culture. The role of viruses in THAA concentration is confirmed by comparing the 10 times virus incubation to the control. Comparing the average concentration of THAA for the 10 times virus incubation ($1.8 \pm 0.2 \mu\text{M}$) with the control culture, the statistical analysis also finds that the average THAA concentration during the experiment for these two cultures were significantly different, within a 75-90% confidence level. In this case, the concentration of THAA in the 10 times virus incubation was greater than that for the control, indicating that the addition of extra viruses causes an increase in the amount of THAA. The relatively low amount of THAA increase compared to the amount of viruses added to the culture indicates that the concentration of THAA present is not directly scaled to the amount of virus in the carboy. Unfortunately, the viral counts for this carboy experiment have not been processed, so it is unknown whether the amount of viruses present stayed at the initial 10 times ambient concentration. By comparing the zero virus, the control (ambient concentrations of virus) and the 10 times virus incubations, the role of viruses in the release of THAA can be determined. While the presence of viruses is not the sole factor in determining the concentration of THAA in culture, viruses do have a positive effect on THAA levels in these incubations.

In contrast, the grazer added carboy has a THAA concentration of $1.5 \pm 0.3 \mu\text{M}$, which is not statistically different (>75% confidence) from the control carboy. While the

THAA curves shown in Figure 4.4 seem to indicate that the grazer added incubation has a higher concentration of THAA relative to the control, the average concentration of THAA over the course of the experiment is the same as the control. It can be concluded from this data that the addition of grazers had no effect on the concentration of THAA in the incubations.

The differences in DON between the control incubation and the zero virus, 10 times virus and grazer added incubation can also be examined on an individual amino acid basis. The average mole fraction of each amino acid throughout the course of the experiment was calculated for the zero virus, 10 times virus, and grazer added incubations and compared to the average amino acid mole fraction for the control incubation using Student's T test. Comparison of the zero virus incubation amino acids with the control resulted in five amino acids exhibiting significant ($\geq 75\%$ confidence) differences: histidine, valine, phenylalanine, and the glycine/threonine pair. Compared to the control, the zero virus incubation had, on average, a decrease in mole fraction of 0.04 for histidine, 0.01 for valine, and 0.01 for phenylalanine. In contrast, the average glycine/threonine mole fraction was increased by 0.03. The 10 times virus incubation had four amino acids (aspartic acid, glutamic acid, and valine) with significantly different mole fractions relative to the control culture. The aspartic acid and glutamic acid mole fractions were smaller by 0.01, while the valine mole fraction was greater by 0.04. In the grazer added incubation, alanine and isoleucine had significantly different mole fractions compared to the control; alanine was greater by 0.01, and isoleucine was 0.01 smaller. Given that 15 amino acids were measured in these samples, the majority of the amino acid mole fractions were not significantly different between the four cultures, in spite of

differences in THAA. This implies that viruses and grazers do not effect the distribution of individual amino acids in culture.

4.3.3 Nucleic Acid Measurements

The ethanol precipitation method used for DNA and RNA analysis of the four carboys was adapted from Matsui, et al., 2004. Due to the amount of water needed, only one DNA and one RNA measurement could be made per sample. Replicate analysis of a standard seawater sample had an error of 20%, which was assumed to be the same for the culture samples. While the regression lines used to calculate the concentration of DNA in all the measured samples had r^2 values of greater than 0.84 (Table 4.8), the regression lines for RNA were much less accurate, indicating that the measured values deviated greatly from straight line. This deviation from a linear regression line seemed to be an artifact of the DNase used to eliminate the DNA in the sample prior to RNA analysis, since both nucleic acids could not be measured together. This conclusion was based on the fact that the 0 virus samples, which contained the smallest concentrations of DNA and therefore required the least amount of DNase had better r^2 values for regression lines than the other samples. For samples with r^2 values less than 0.80, one data point out of the four was eliminated, and the r^2 was recalculated. In most cases the outlying data point was obvious; for others the datapoint which resulted in the maximum recalculated r^2 was removed. The whole RNA sample was usually incubated with the DNase in one tube, then apportioned out to three other tubes to make 4 identical tubes prior to RNA spiking and ethanol precipitation. Usually, the sample and DNase were incubated in the

Table 4.8: DNA and RNA concentrations for the control (A), 0 virus (B), grazer added (C), and 10 times virus (D) incubation treatments. Calculation of nucleic acids in μM was based on an average DNA base molecular weight of 325g/mol, and an average RNA base molecular weight of 340g/mol. It was also assumed that both DNA and RNA contained an equal distribution of nucleic acid base molecules.

A: control incubation

time points	DNA $\mu\text{g/L}$	R ²	μM N DNA	μM C DNA	RNA $\mu\text{g/L}$	R ²	μM N RNA	μM C RNA	μM nucleic acid N	μM nucleic acid C	% TDN as nucleic acid	% DOC as nucleic acid
T0	92.2	0.86	1.06	2.77	88.9	0.88	0.98	2.48	2.04	5.25	10.9	2.8
T1	109.0	0.86	1.26	3.27	91.3	0.98	1.01	2.55	2.26	5.82	13.4	3.1
T2	139.5	0.94	1.61	4.18	55.3	0.90	0.61	1.54	2.22	5.73	15.1	3.0
T3	36.3	0.99	0.42	1.09	46.9	0.95	0.52	1.31	0.94	2.40	7.8	1.3
T4	59.3	0.98	0.68	1.78	36.9	0.96	0.41	1.03	1.09	2.81	8.3	1.5
T5	104.7	0.96	1.21	3.14	37.9	0.99	0.42	1.06	1.63	4.20	12.0	2.2
T6	63.9	0.99	0.74	1.92	50.0	1.00	0.55	1.40	1.29	3.31	9.5	1.7

B: 0V incubation

time points	DNA $\mu\text{g/L}$	R ²	μM N DNA	μM C DNA	RNA $\mu\text{g/L}$	R ²	μM N RNA	μM C RNA	μM nucleic acid N	μM nucleic acid C	% TDN as nucleic acid	% DOC as nucleic acid
T0	5.7	1.00	0.07	0.17	15.0	0.98	0.17	0.42	0.23	0.59	1.2	0.3
T1	10.1	0.99	0.12	0.30	3.5	1.00	0.04	0.10	0.16	0.40	0.8	0.2
T2	3.5	1.00	0.04	0.11	3.7	1.00	0.04	0.10	0.08	0.21	0.4	0.1
T3	7.5	1.00	0.09	0.22	4.2	1.00	0.05	0.12	0.13	0.34	0.7	0.2
T4	1.8	1.00	0.02	0.06	1.3	0.99	0.01	0.04	0.04	0.09	0.2	0.1
T5	5.1	1.00	0.06	0.15	8.2	0.98	0.09	0.23	0.15	0.38	1.1	0.2
T6	5.2	1.00	0.06	0.16	8.5	1.00	0.09	0.24	0.15	0.39	1.2	0.2

C: grazer incubation

time points	DNA $\mu\text{g/L}$	R ²	μM N DNA	μM C DNA	RNA $\mu\text{g/L}$	R ²	μM N RNA	μM C RNA	μM nucleic acid N	μM nucleic acid C	% TDN as nucleic acid	% DOC as nucleic acid
T0	69.5	0.95	0.80	2.08	112.0	0.68	1.24	3.13	2.04	5.21	10.9	2.8
T1	142.9	1.00	1.65	4.29	57.1	0.92	0.63	1.60	2.28	5.88	13.5	3.2
T2	123.7	0.96	1.43	3.71	47.6	0.94	0.53	1.33	1.95	5.04	13.5	2.7
T3	114.0	0.96	1.32	3.42	37.1	0.98	0.41	1.04	1.72	4.46	12.9	2.3
T4	92.6	0.84	1.07	2.78	149.3	0.96	1.65	4.17	2.72	6.95	20.2	3.7
T5	57.6	0.90	0.66	1.73	34.7	0.97	0.38	0.97	1.05	2.70	7.9	1.4
T6	44.7	0.87	0.52	1.34	67.7	0.97	0.75	1.89	1.26	3.24	9.2	1.7

D: 10V incubation

time points	DNA $\mu\text{g/L}$	R ²	μM N DNA	μM C DNA	RNA $\mu\text{g/L}$	R ²	μM N RNA	μM C RNA	μM nucleic acid N	μM nucleic acid C	% TDN as nucleic acid	% DOC as nucleic acid
T0	150.4	0.88	1.74	4.51	52.0	0.92	0.57	1.45	2.31	5.97	10.5	2.7
T1	80.3	0.84	0.93	2.41	67.3	0.78	0.74	1.88	1.67	4.29	8.3	1.9
T2	62.7	0.89	0.72	1.88	34.5	0.96	0.38	0.96	1.10	2.85	6.8	1.4
T3	50.0	0.98	0.58	1.50	40.0	1.00	0.44	1.12	1.02	2.62	5.7	1.0
T4	73.1	0.96	0.84	2.19	49.5	0.96	0.55	1.38	1.39	3.57	9.4	1.7
T5	69.2	0.99	0.80	2.08	35.2	0.92	0.39	0.98	1.19	3.06	8.0	1.4
T6	72.7	0.96	0.84	2.18	20.7	0.99	0.23	0.58	1.07	2.76	7.0	1.3

same tube that was later eliminated as an outlier, indicating that some residue from the DNase process had altered the measurement. This may be a due to the presence of non-DNase digestible DNA (Maruyama et al., 1993), though this problem did not occur after the DNase incubation of the test seawater samples.

Nucleic acid concentrations in $\mu\text{g/L}$ were converted to μM by assuming that the average molecular weight for a DNA base was 325 g/mol, and a RNA base was 340 g/mol. To calculate the carbon and nitrogen content of DNA and RNA it was assumed that there was an average of 3.75 moles of N and 9.75 moles of C per mole of DNA

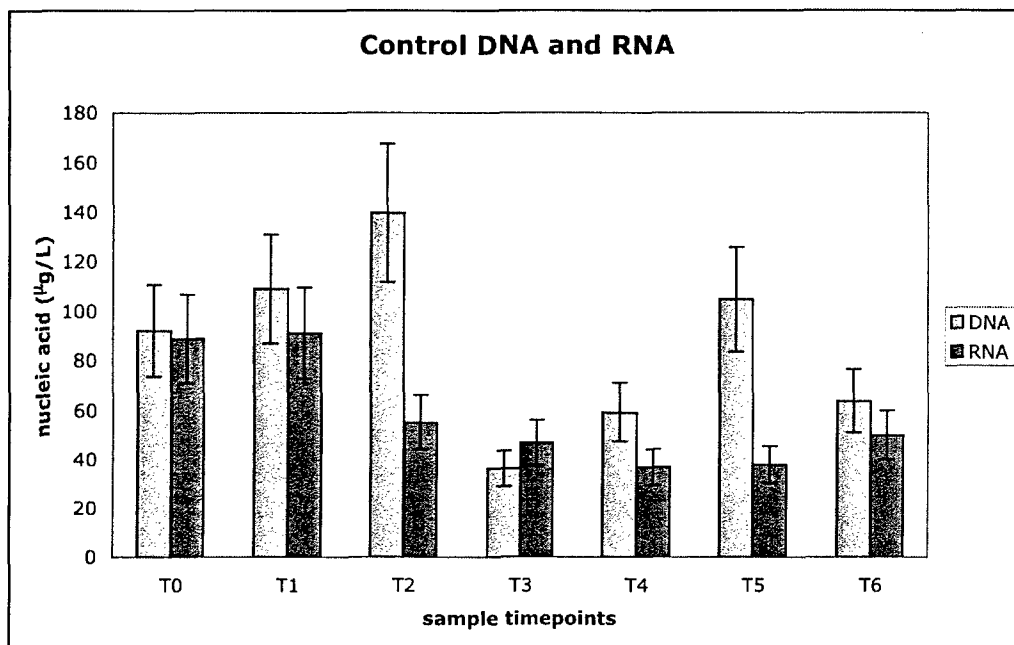
base, and an average of 3.75 moles of N and 9.5 moles of C per mole of RNA base. The contribution of total nucleic acids to the DOC and TDN pools could then be calculated (Table 4.8). Table 4.8 also shows the r^2 value for the regression lines used in the standard addition method to calculate the concentration of DNA and RNA in the water samples.

For the control incubation (Figure 4.5A), DNA concentrations ranged from 36.3 $\mu\text{g/L}$ to 139 $\mu\text{g/L}$, and were in general slightly larger than the RNA concentrations (36.9-91.3 $\mu\text{g/L}$) at each timepoint. DNA concentrations increased from the initial value of 92.2 $\mu\text{g/L}$ to 139 $\mu\text{g/L}$ within 24 hours, dropped to 63.9 $\mu\text{g/L}$ at timepoint T3, then rose again to 104.7 $\mu\text{g/L}$ by timepoint T5. The final concentration was 63.9 $\mu\text{g/L}$. RNA concentrations decreased gradually from the initial T0 value of 88.9 $\mu\text{g/L}$ down to a minimum of 36.9 $\mu\text{g/L}$ at timepoint T4, then increased slightly to a final concentration of 50.0 $\mu\text{g/L}$. The total nucleic acids constituted 1.3-3.1% of the DOC pool, and 7.8-15.1% of the total dissolved nitrogen (Table 4.8A).

Nucleic acid concentrations for the zero virus incubation were the lowest of all the culture treatments. The DNA concentrations ranged from 1.8-10.1 $\mu\text{g/L}$, and RNA concentrations ranging from 1.3-15.0 $\mu\text{g/L}$, with little relationship between the two (Figure 4.5B). The total nucleic acids contribute 0.1-0.3% to the DOC in the incubation, and 0.2-1.2% to the total dissolved nitrogen (Table 4.8B). The nucleic acid contribution to the carbon and nitrogen pools of the zero virus incubation was approximately 10% of the other culture treatments.

Figure 4.5: DNA and RNA concentrations for the control (A), 0 virus (B), grazer added (C), and 10 times virus (D) culture treatments.

A: Control incubation



B: 0V incubation

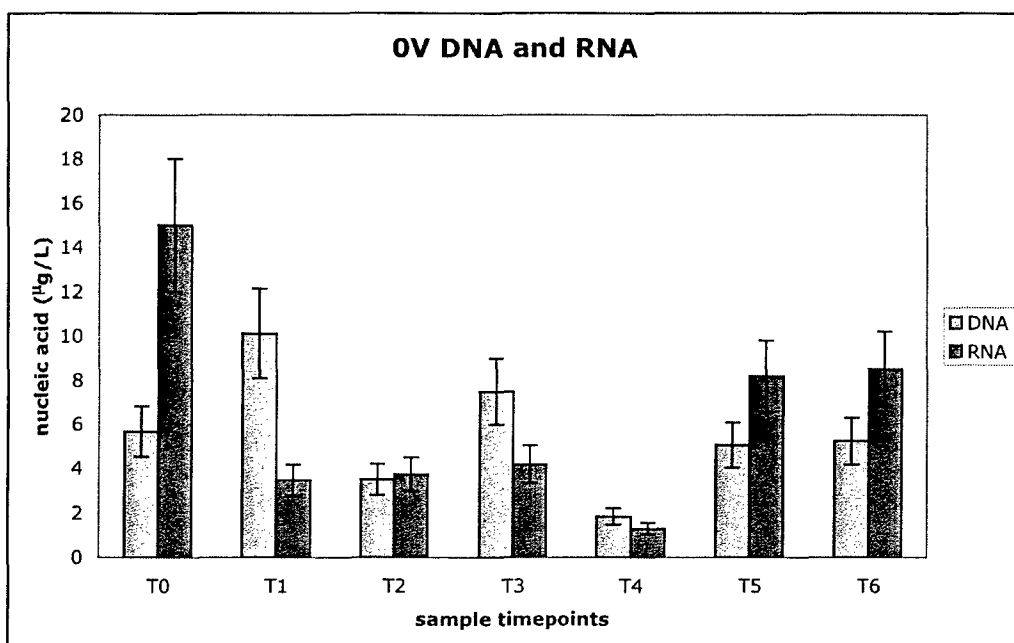
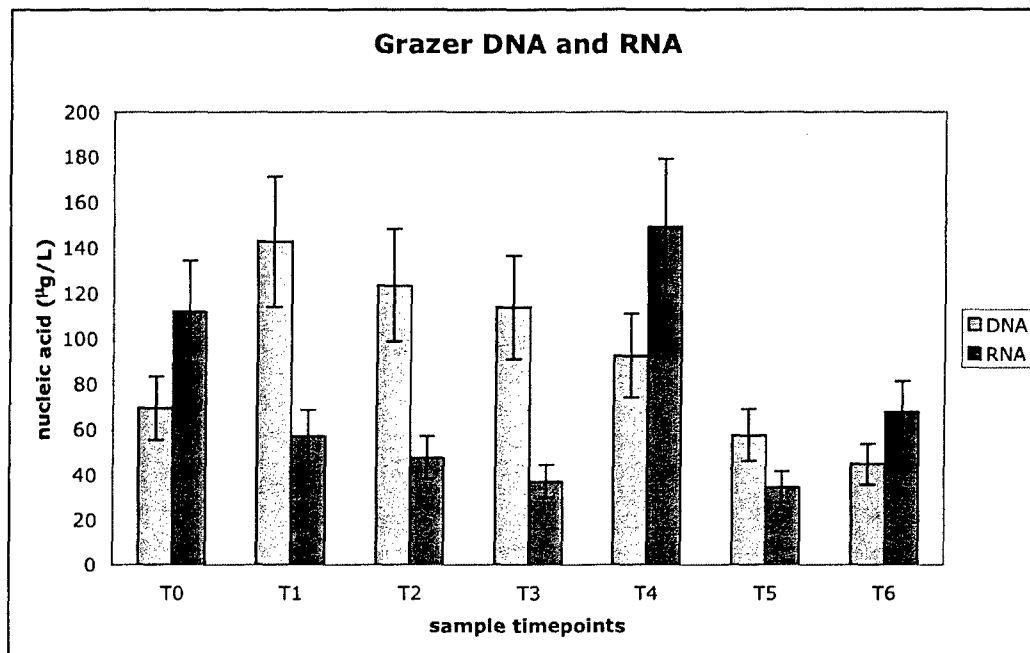


Figure 4.5C: grazer incubation



D: 10V incubation

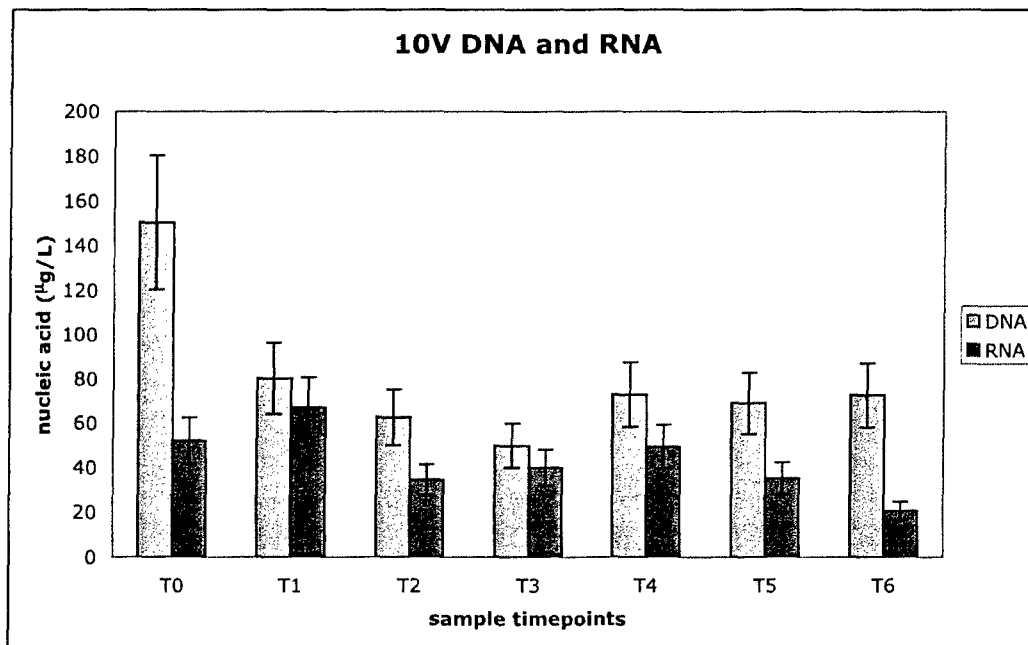


Figure 4.5C shows that the DNA concentration for the grazer added treatment ranged from 57.6 $\mu\text{g/L}$ to 142.9 $\mu\text{g/L}$, with the maximum value at timepoint T1. RNA concentrations were between 34.7-149.3 $\mu\text{g/L}$, with the maximum value occurring after

72 hours (timepoint T4). The contribution of the total nucleic acids to the total nitrogen pool was higher for this culture than the control incubation (7.9-20.2%), while the contribution to the DOC pool was more similar to the control experiment (1.4-3.2%) (Table 4.8C).

DNA levels in the 10 times virus incubation started at a maximum value of 150.4 $\mu\text{g/L}$, which decreased rapidly by half, ranging from 80.3-50.0 $\mu\text{g/L}$ for the rest of the experiment. The RNA concentrations remained fairly constant between 20.7-52.0 $\mu\text{g/L}$ throughout the incubation time, and were always lower than the accompanying DNA levels (Figure 4.5D). Contributions of the nucleic acids in the 10V sample were lower than for the grazer added and control incubations with a much narrower range, representing 1.0-2.7% of the DOC and 5.7-10.5% of the total dissolved nitrogen (Table 4.8D).

The concentration of both DNA (36.3-139.5 $\mu\text{g/L}$) and RNA (36.9-91.3 $\mu\text{g/L}$) for the control incubation were higher than the majority of other measured values for various coastal seawater locations, which generally ranged from 2.66-80.6 $\mu\text{g/L}$ for DNA and 6.67-51.1 $\mu\text{g/L}$ for RNA (Paul and Myers, 1982; DeFlaun et al., 1986; Karl and Bailiff, 1989; Sakano and Kamatani, 1992). However, one measurement at 140 $\mu\text{g/L}$ DNA was obtained for a Chesapeake Bay sample (Paul and Myers, 1982). The differences between the DNA and RNA concentrations measured for this experiment and the lower literature values may be a result of both the different locations and the different techniques used for nucleic acid measurement. In terms of nitrogen, amino acids and nucleic acids for all incubation treatments were generally the same. The concentrations combined DNA and RNA never exceeded 3 $\mu\text{M N}$ in concentration, and constituted less than 20% of the total

dissolved nitrogen (TDN) for all carboy incubations. With the exception of the zero virus incubation, THAA and total nucleic acids were approximately equal in concentration with respect to nitrogen.

The differences in the average DNA and RNA concentration during the course of the experiment between the zero virus, 10 times virus and grazer added treated incubations compared to the control was analyzed using Student's T test. The average DNA concentration in the control during the 120 h experiment was $90 \pm 10 \mu\text{g/L}$. The average concentrations for the 10 times virus ($80 \pm 10 \mu\text{g/L}$) and grazer added ($90 \pm 10 \mu\text{g/L}$) were not significantly ($>75\%$ confidence) different from the control. In contrast, the zero virus incubation had a DNA concentration of $6 \pm 1 \mu\text{g/L}$, which was significantly ($>90\%$ confidence) different than that of the control incubation, indicating that phytoplankton and zooplankton alone do not release large amounts of DNA. These results imply that either the presence of grazers or viruses was necessary to mediate the release of phytoplankton DNA into the carboys by cell lysis or breakage, or that the majority of the additional DNA seen in the control was originally from the viruses or grazers themselves. While the contribution of grazer-derived DNA is undetermined, an estimate of the release of DNA from viruses indicate that viral DNA could contribute up to 17.1% to the total DNA (Weinbauer et al., 1993). The types of DNA present in the incubations would need to be determined in order to differentiate between the two explanations for the DNA concentrations.

The average RNA concentrations for the zero virus, 10 times virus, and grazer added incubations was also statistically compared to the control culture. The control carboy had an average RNA concentration of $58 \pm 9 \mu\text{g/L}$ throughout the experiment. The

concentration of RNA in the grazer added carboy was 70 ± 20 $\mu\text{g/L}$, and was not significantly different from the control. The average 10 times virus RNA concentration of 43 ± 6 $\mu\text{g/L}$ was determined to be different from the control, but only with a 75% confidence level. As with the DNA concentrations, the average RNA concentration for the zero virus incubation (6 ± 2 $\mu\text{g/L}$) was significantly lower than the control concentration. Again, the source of the RNA would have to be identified before the roles that viruses and/or grazers play in RNA release could be determined.

4.4 Conclusions

A set of four incubations with different biological treatments was set up to analyze the effect of different types of biology on the DON concentration of the cultures. A control culture, containing the ambient levels of phytoplankton, zooplankton, bacteria and viruses was used as a baseline to compare to the treatments for the other three cultures: a zero virus culture, a grazer added culture, and a 10 times virus culture. The concentrations of THAA and total nucleic acids were approximately equal in terms of nitrogen concentration, and both compound classes constituted less than 20% of the TDN. Analyses of the total hydrolyzable amino acids in these incubations show that the presence of viruses has a positive effect on the THAA concentration, while grazers do not have a significant influence. Neither viruses nor grazers alter the mole fraction distribution of a majority of the individual amino acids compared to the control incubation. Compared to the control, only the zero virus incubation had significantly different DNA and RNA concentrations; the DNA and RNA concentrations for the 10 times virus and grazer added incubations were statistically equal to the control. It is unknown whether the viruses and grazers mediate nucleic acid release due to cell lysis or

breakage, or whether the higher concentrations of DNA and RNA are due to direct release of nucleic acids originating from the viruses or grazers. As a result, the exact role that these organisms play in the release of DNA and RNA still needs to be investigated.

4.5 References

- Abell, J., S. Emerson and P. Renaud (2000). Distributions of TOP, TON, TOC in the North Pacific subtropical gyre: Implications for nutrient supply in the surface ocean and remineralization in the upper thermocline. Journal of Marine Research **58**: 203-222.
- Aluwihare, L. I. (1999). High molecular weight (HMW) dissolved organic matter (DOM) in seawater: chemical structure, sources and cycling, MIT/WHOI: 224.
- Aluwihare, L. I., D. J. Repeta and R. F. Chen (2002). Chemical composition and cycling of dissolved organic matter in the Mid-Atlantic Bight. Deep-Sea Research II **49**: 4421-4437.
- Baines, S. B. and M. L. Pace (1991). The production of dissolved organic matter by phytoplankton and its importance to bacteria: Patterns across marine and freshwater systems. Limnology and Oceanography **36**(6): 1078-1090.
- Berg, G. M., P. M. Glibert, M. W. Lomas and M. A. Burford (1997). Organic nitrogen uptake and growth by the chrysophyte *Aureococcus anophagefferens* during a brown tide event. Marine Biology **129**: 377-387.
- Biddanda, B. and R. Benner (1997). Carbon, nitrogen and carbohydrate fluxes during the production of particulate and dissolved organic matter by marine phytoplankton. Limnology and Oceanography **42**(3): 506-518.
- Björnson, P. K. (1988). Phytoplankton exudation of organic matter: Why do healthy cells do it? Limnology and Oceanography **33**: 151-155.
- Bronk, D. A. (1999). Rates of NH_4^+ uptake, intracellular transformation and dissolved organic nitrogen release in two clones of marine *Synechococcus* spp. Journal of Plankton Research **21**(7): 1337-1353.
- Bronk, D. A. (2002). Dynamics of DON. Biogeochemistry of Marine Dissolved Organic Matter. D. A. Hansell and C. A. Carlson. San Diego, Academic Press: 153-247.
- Bronk, D. A. and P. M. Glibert (1991). A ^{15}N tracer method for the measurement of dissolved organic nitrogen release by phytoplankton. Marine Ecology Progress Series **77**: 171-182.
- Bronk, D. A. and B. B. Ward (2000). Magnitude of dissolved organic nitrogen release relative to gross nitrogen uptake in marine systems. Limnology and Oceanography **45**(8): 1879-1883.

Capone, D. G., M. D. Ferrier and E. J. Carpenter (1994). Amino acid cycling in colonies of the planktonic marine cyanobacterium *Trichodesmium thiebautii*. Applied and Environmental Microbiology **60**(11): 3989-3995.

Cowie, G. L. and J. I. Hedges (1992). Improved amino acid quantification in environmental samples: charge-matched recovery standards and reduced analysis time. Marine Chemistry **37**: 223-238.

DeFlaun, M. F., J. H. Paul and D. Davis (1986). Simplified method for dissolved DNA determination in aquatic environments. Applied and Environmental Microbiology **52**(4): 654-659.

Flynn, K. J. and I. Butler (1986). Nitrogen sources for the growth of marine microalgae: role of dissolved free amino acids. Marine Ecology Progress Series **34**: 281-304.

Fuhrman, J. (1999). Marine viruses and their biogeochemical and ecological effects. Nature **399**: 541-548.

Glibert, P. M. and D. A. Bronk (1994). Release of dissolved organic nitrogen by marine diazotrophic cyanobacteria, *Trichodesmium* spp. Applied and Environmental Microbiology **60**(11): 3996-4000.

Hansell, D. and T. Waterhouse (1997). Controls on the distributions of organic carbon and nitrogen in the eastern Pacific Ocean. Deep-Sea Research **44**: 843-857.

Hansell, D. A., C. A. Carlson and Y. Suzuki (2002). Dissolved organic carbon export with North Pacific Intermediate Water formation. Global Biogeochemical Cycles **16**(1): 10.1029/2000GB001361.

Hasegawa, T., I. Koike and H. Mukai (2000). Dissolved organic nitrogen dynamics in coastal waters and the effect of copepods. Journal of Experimental Marine Biology and Ecology **244**: 219-238.

Jørgensen, N. O. G., N. Kroer and R. B. Coffin (1994). Utilization of dissolved organic nitrogen by heterotrophic bacterioplankton: Effect of substrate C/N ratio. Applied and Environmental Microbiology **60**(11): 4124-4133.

Jørgensen, N. O. G., N. Kroer, R. B. Coffin, X.-H. Yang and C. Lee (1993). Dissolved free amino acids, combined amino acids, and DNA as sources of carbon and nitrogen to marine bacteria. Marine Ecology Progress Series **98**: 135-148.

Kahler, P., P. K. Bjørnsen, K. Lochte and A. Antia (1997). Dissolved organic matter and its utilization by bacteria during the spring in the Southern Ocean. Deep-Sea Research II **44**(1-2): 341-353.

- Karl, D. M. and M. D. Bailiff (1989). The measurement and distribution of dissolved nucleic acids in aquatic environments. Limnology and Oceanography **34**(3): 543-558.
- Keller, A. A. and R. L. Rice (1989). Effects of nutrient enrichment on natural populations of the brown tide phytoplankton *Aureococcus anophagefferens* (crrysophyceae). Journal of Phycology **25**: 636-646.
- Kuznetsova, M. and C. Lee (2002). Dissolved free and combined amino acid in nearshore seawater, sea surface microlayers and foams: Influence of extracellular hydrolysis. Aquatic Sciences **64**: 252-268.
- Maruyama, A., M. Oda and T. Higashihara (1993). Abundance of virus-sized non-DNase-digestible coated DNA in eutropic seawater. Applied and Environmental Microbiology **59**: 712-717.
- Matsui, K., N. Ishii, M. Honjo and Z. i. Kawabata (2004). Use of SYBR Green I fluorescent dye and a centrifugal filter device for rapid determination of dissolved DNA concentration in fresh water. Aquatic Microbial Ecology **36**: 99-105.
- McCarthy, M., T. Pratum, J. Hedges and R. Benner (1997). Chemical composition of dissolved organic nitrogen in the ocean. Nature **390**: 150-154.
- McCarthy, M. D., J. I. Hedges and R. Benner (1998). Major bacterial contribution to marine dissolved organic nitrogen. Science **281**: 231-234.
- Nixon, S. W., S. L. Granger, D. I. Taylor, P. W. Johnson and B. A. Buckley (1994). Subtidal volume fluxes, nutrient inputs and the brown tide-an alternatice hypothesis. Estuarine, Coastal and Shelf Science **39**: 303-312.
- Norrman, B., U. L. Zweifel, C. S. Hopkinson and B. Fry (1995). Production and utilization of dissolved organic carbon during an experimental diatom bloom. Limnology and Oceanography **40**(5): 898-907.
- Palenik, B. and S. E. Henson (1997). The use of amides and other organic nitrogen sources by the phytoplankton *Emiliana huxleyi*. Limnology and Oceanography **42**(7): 1544-1551.
- Palenik, B. and F. M. M. Morel (1990). Amino acid utilization by marine phytoplankton: a novel mechanism. Limnology and Oceanography **35**(2): 260-269.
- Palenik, B. and F. M. M. Morel (1990). Comparison of cell-surface L-amino acid oxidases from several marine phytoplankton. Marine Ecology Progress Series **59**: 159-201.
- Palenik, B. and F. M. M. Morel (1991). Amine oxidases of marine phytoplankton. Applied and Environmental Microbiology **57**(8): 2440-2443.

Paul, J. H. and B. Myers (1982). Fluorometric determination of DNA in aquatic microorganisms by use of Hoechst 33258. Applied and Environmental Microbiology **43**(6): 1393-1399.

Pérez, M. T., C. Pausz and G. J. Herndl (2003). Major shift in bacterioplankton utilization of enantiomeric amino acids between surface waters and the ocean's interior. Limnology and Oceanography **48**(2): 755-763.

Sakano, S. and A. Kamatani (1992). Determination of dissolved nucleic acids in seawater by the fluorescence dye, ethidium bromide. Marine Chemistry **37**: 239-255.

Steinberg, D. K., C. A. Carlson, N. R. Bates, S. A. Goldthwait, L. P. Madin and Michale (2000). Zooplankton vertical migration and the active transport of dissolved organic and inorganic carbon in the Sargasso Sea. Deep-Sea Research I **47**: 137-158.

Steinberg, D. K., S. A. Goldthwait and D. A. Hansell (2002). Zooplankton vertical migration and the active transport of dissolved organic and inorganic nitrogen in the Sargasso Sea. Deep-Sea Research II **49**: 1445-1461.

Tanoue, E. (1995). Detection of dissolved protein molecules in oceanic waters. Marine Chemistry **51**: 239-252.

Urban-Rich, J. (1999). Release of dissolved organic carbon from copepod fecal pellets in the Greenland Sea. Journal of Experimental Marine Biology and Ecology **232**: 107-124.

Varela, M. M., S. Barquero, A. Bose, E. Fernández, N. González, E. Teira and M. Varela (2003). Microplanktonic regeneration of ammonium and dissolved organic nitrogen in the upwelling area of the NW of Spain: relationships with dissolved organic carbon production and phytoplankton size-structure. Journal of Plankton Research **25**(7): 719-736.

Ward, B. B. and D. A. Bronk (2001). Net nitrogen uptake and DON release in surface waters: importance of trophic interactions implied from size fractionation experiments. Marine Ecology Progress Series **219**: 11-24.

Weinbauer, M. G., D. Fuks and P. Peduzzi (1993). Distribution of viruses and dissolved DNA along a coastal trophic gradient in the Northern Adriatic Sea. Applied and Environmental Microbiology **59**(12): 4074-4082.

Wheeler, P. and D. L. Kirchman (1986). Utilization of inorganic and organic nitrogen by bacteria in marine systems. Limnology and Oceanography **31**(5): 998-1009.

Wheeler, P. A., B. B. North and G. C. Stephens (1974). Amino acid uptake by marine phytoplankters. Limnology and Oceanography **19**(2): 249-259.

Xu, Y. and W.-X. Wang (2003). Fates of diatom carbon and trace elements by the grazing of marine copepod. Marine Ecology Progress Series **254**: 225-238.

Yamada, N., S. Suzuki and E. Tanoue (2000). Detection of *Vibrio (Listonella) anguillarum* porin homologue proteins and their source bacteria from coastal seawater. Journal of Oceanography **56**: 583-590.

Yamada, N. and E. Tanoue (2003). Detection and partial characterization of dissolved glycoproteins in oceanic waters. Limnology and Oceanography **48**(3): 1037-1048.

Yamashita, Y. and E. Tanoue (2003). Distribution and alteration of amino acids in bulk DOM along a transect from bay to oceanic waters. Marine Chemistry **82**: 145-160.

5. Conclusions

5.1 General Conclusions

Dissolved organic matter (DOM) is the major reservoir of oceanic organic carbon and nitrogen, and as a result has a large impact on the oceanic and global carbon and nitrogen cycles. Analyses of this pool of organic matter has been limited by the low concentration and dissolved or colloidal state of the samples, along with the difficulty in removing interfering salts. The development of ultrafiltration techniques to isolate a high molecular weight (HMW) fraction of the DOM has helped facilitate structural analysis, as well as helping to determine sources and cycling times for different fractions within the DOM pool. However, many questions remain about the identification of compounds within DOM, their turnover times, and the influence of different organisms on the input and uptake of DOM. The goal of this thesis was to obtain a better understanding of these aspects of DOM. To facilitate this, a variety of different methods were developed to identify new compounds within the HMWDOM fraction, to measure the radiocarbon age of amino acids from surface HMWDOM, and to determine the biological contribution to the dissolved organic nitrogen (DON) pool.

Chapter 2 of this thesis focused on the discrepancy between the large amount of carbohydrate determined by spectroscopic methods and the much smaller concentration actually measured by molecular analysis of hydrolyzate the HMWDOM fraction. Nuclear magnetic resonance spectroscopy (NMR) spectra indicated that 60-70% of the high molecular weight dissolved organic carbon (HMWDOC) is in the form of carbohydrates, but less than 20% has been isolated using chemical hydrolysis techniques

(McCarthy et al., 1996; Aluwihare et al., 1997; Aluwihare et al., 2002). Periodate over-oxidation was used to determine that the majority of HMWDOM from surface and deep water samples was periodate oxidizable in nature. The periodate demand for HMWDOM was greater than that measured for linear glucopolysaccharide standards, indicating that HMWDOM has a more highly branched and heterogeneous structure. In addition to the oxidation of carbohydrate-type carbon, periodate oxidation also removed 70% of the aliphatic proton NMR signal. *This experiment concluded that the remaining carbohydrate in both the surface and deep water HMWDOM samples consists of 6-deoxy and methyl sugars, and that no significant amounts of lipid-like compounds are present in HMWDOM.* In addition, the deep water HMWDOM contains a higher concentration of 6-deoxysugars compared to the surface sample.

Hydrolyzed amino acids compose approximately 4-5% of the total HMWDOC, and less than 20% of the total HMWDON (McCarthy et al., 1996; McCarthy et al., 1997; Aluwihare, 1999). Sources of proteins, and therefore amino acids, are thought to be bacterial in nature, based on isolation of complete proteins and studies of amino acid enantiomers (McCarthy et al., 1998; Yamada et al., 2000). Amino acids can also serve as nitrogen sources for phytoplankton and bacteria, and may be used as indicators of microbial degradation (Dauwe et al., 1999; Amon et al., 2001). Radiocarbon measurements of the total protein fraction taken from HMWDOM indicates that amino acids are modern in age at the surface, and are younger than the bulk HMWDOM throughout the water column (Loh et al., 2004). In Chapter 3 of this thesis, *a new method for isolating and purifying underivatized amino acids was developed, and the first radiocarbon measurements of individual amino acids reported.*

Three different steps were necessary to remove the amino acids from the rest of the HMWDOM compounds. First, the bulk amino acid fraction using was collected using cation exchange resin column chromatography. A reverse-phase C18 and a strong cation exchange (SCX) high pressure liquid chromatography (HPLC) purification steps were then used to yield six amino acid samples for radiocarbon analysis. Since the final SCX HPLC purification step required the use of buffer salts, the amino acid samples were sealed in pyrex tubes and converted to CO₂ using low temperature combustion. In general, this newly developed method provided amino acid samples with excellent purity, though some loss of sample was evident, and not all the amino acids were pure. $\Delta^{14}\text{C}$ values for the six amino acid samples ranged from 121‰ to -454‰, indicating that individual amino acids have different turnover times.

A set of cultures with different biological treatments was used to determine the role of biology on the hydrolyzable amino acid, RNA, and DNA concentrations over time. Four different incubations were measured, each starting with a aliquot of Chesapeake Bay water: a control containing the ambient populations of phytoplankton, zooplankton, viruses, and bacteria; a zero virus incubation from which all viruses and bacteria were removed; a grazer added culture to which copepod grazers were added; and a 10 times virus treatment, where 10 times the ambient level of viruses were added to the system. Hydrolyzable amino acids were measured by using charge-matched standards and HPLC separation, and RNA and DNA were concentrated by ethanol precipitation and centrifuge filtration, measured using fluorometry, then quantified by a standard addition method (Cowie and Hedges, 1992; Matsui et al., 2004). Using these parameters, the effect of the different biological treatments was compared and quantified. *Compared*

to the control incubation, the 10 times virus treatments produced a higher concentration of total hydrolyzable amino acids and total nucleic acids, while the zero virus culture had lower concentrations of these components. The grazer added incubation did not show any significant difference in amino acid or nucleic acid concentrations. As a result, it was concluded that both viruses stimulate the release of these compounds into the surrounding water.

5.2 Future Research Directions

One of the limiting factors in the analysis of DOM and HMWDOM is the lack of structural knowledge. Without knowledge of the chemical compounds that constitute DOM, it is impossible to determine whether compounds released by phytoplankton can accumulate in the ocean or to identify the composition of the fraction of DON used by bacteria. The experiments described in chapter 2 have shown that the majority of HMWDOC consists of periodate over-oxidizable compounds. Based on the NMR spectra taken during the course of oxidation, it was concluded that these compounds were 6-deoxy and methyl sugars. However, because periodate over-oxidation completely disintegrates carbohydrates into a variety of products, the 6-deoxy and methyl sugars could not be isolated intact for absolute identification. The first step would be to try to isolate these compounds from HMWDOM as intact monomers in order to confirm their identity, and to determine their actual structure. This is complicated by the fact that these 6-deoxy and methyl sugars may not be released with conventional acid hydrolysis, which may be a result of the chemical bonding of these compounds within HMWDOM, or due to steric hindrance. Quenching the periodate oxidation in the middle of the experiment

and analyzing the reaction intermediates could supply additional information about the overall structure of HMWDOM, which may help to determine why acid hydrolysis fails to release these compounds.

Another aspect of future research on the 6-deoxy and methyl sugar fraction of HMWDOM would be compound specific radiocarbon measurements. Bulk HMWDOM is slightly depleted in radiocarbon compared to the concurrent DIC by approximately 60‰ at the surface to over 250‰ at deeper depths (Aluwihare et al., 2002; Loh et al., 2004). This difference in radiocarbon means that there is a fraction of HMWDOM that is older than the compounds produced from the modern DIC. A quick isotopic mass balance calculation can be used to determine what the $\Delta^{14}\text{C}$ of this unknown fraction must be. Neutral monosaccharides constitute approximately 20% of the total HMWDOC, and have an average $\Delta^{14}\text{C}$ of 71‰, based on the average $\Delta^{14}\text{C}$ of individual monosaccharide radiocarbon measurements (Aluwihare et al., 2002). Similarly, amino acids contribute approximately 5% of the HMWDOC, with an average $\Delta^{14}\text{C}$ of 90‰. The lipid fraction has been shown to have a $\Delta^{14}\text{C}$ of -600‰, but constitutes 0.1% of the total HMWDOC (Loh et al., 2004). If it is assumed that the bulk HMWDOM fraction has a $\Delta^{14}\text{C}$ of -10‰, then the remaining 75% of the HMWDOC has a $\Delta^{14}\text{C}$ of -37.5‰. The amount of 6-deoxy and methyl sugars determined by periodate over-oxidation is approximately 20% of the total HMWDOC and falls within the remaining 75%. In addition, the amount of 6-deoxysugars is higher in the deep ocean than in the surface, supporting the hypothesis that this fraction is depleted in ^{14}C . While it may be that the 6-deoxy and methyl sugars are similar in age to the neutral monosaccharides, this fraction also seems to be impervious to acid hydrolysis. This factor may make them more resistant to degradation

and more likely to contain older carbon. Compound specific radiocarbon measurements of the HMWDOM fraction that oxidized by periodate but not released with acid, or the actual deoxysugars, would help to determine their labilities, as well as whether they were formed using modern DIC or whether they are altered from other compounds.

The sources of these 6-deoxy and methyl sugars are also unknown. Since these are newly identified compounds in the HMWDOM fraction, they have not been measured in phytoplankton culture incubations. Such incubations have been shown to produce a high molecular weight organic exudate similar to oceanic HMWDOM, with similar carbohydrate-rich proton NMR spectra (Aluwihare and Repeta, 1999). While neutral monosaccharides isolated via acid hydrolysis constitute a larger fraction of the total HMWDOC than the same fraction in seawater samples, these monosaccharides still cannot account for all the carbohydrate in the sample. The remaining carbohydrate may be 6-deoxy and methyl sugars. There is also the possibility that other processes may contribute to the generation of these compounds, or preferentially protect them from remineralization. If 6-deoxy and methyl sugars are determined to be alteration products, they could be used as biomarkers for microbial degradation.

While the method to isolate and purify amino acids for compound specific radiocarbon analysis outlined in chapter 3 was successful in obtaining 6 amino acids of sufficient purity and concentration to be measured, it can definitely be improved. Issues to be addressed are the sample loss during the procedure, and the lack of clean separation for some amino acids, even after 2 HPLC steps. Optimization of this method could allow for amino acids to be isolated more easily, and from other HMWDOM samples with lower amino acid concentrations, including deep water samples. Measuring

the radiocarbon age of amino acids at various points in the water column would allow determination of whether modern radiocarbon signatures can be found in deeper waters, indicating preferential transport of amino acids. The more unusual $\Delta^{14}\text{C}$ values measured for phenylalanine and threonine could also be confirmed with additional samples, providing additional information about the cycling of these two amino acids. It would be especially interesting to analyze phenylalanine and threonine in deep water samples, to see if the $\Delta^{14}\text{C}$ values remain the same, or decrease even more. Enantiomeric ratios for amino acids along with the radiocarbon data can help determine potential sources, and whether both enantiomers are utilized at the same rate.

Another aspect of this method that could be improved is the process of combusting the amino acids to CO_2 in preparation for radiocarbon measurement. Due to the interference of the buffer salts used in the second HPLC separation, the amino acid samples could not be combusted at 850°C in quartz tubes, the standard procedure for organic sample analysis. Instead, the samples were heated to 550°C in pyrex. It was assumed that since amino acids are relatively small molecules, and since measured standard solutions resulted in good CO_2 yields after combustion, that this low temperature combustion method was adequate for radiocarbon analysis. The use of a non-conventional combustion procedure adds another complication when comparing the low temperature combustion values with other samples measured using high temperature combustion, as can be seen in the difference in $\Delta^{14}\text{C}$ values between the unhydrolyzed HMWDOM combusted at 850°C and the hydrolyzed HMWDOM sample combusted at 550°C . It is still not known whether the presence of the buffer salts included with the

organic samples results in the production of interfering byproducts or fractionation of the isotopic signal during combustion.

Repetition of the compound specific amino acid measurements can also confirm or refute the $\Delta^{14}\text{C}$ values measured in this thesis. While it is evident that there was at least one instance of an unknown point source contamination, some of the other $\delta^{13}\text{C}$ and $\Delta^{14}\text{C}$ values may be either due to contamination, or evidence of interesting and previously unknown processes. Of particular interest are the much older radiocarbon ages for threonine and phenylalanine, and the very enriched $\delta^{13}\text{C}$ value for glycine. If these measurements are confirmed by additional analyses, they may provide interesting information about the behavior of amino acids and their degradation and uptake patterns. For example, the lower phenylalanine and threonine $\Delta^{14}\text{C}$ values may be due to a mixture of modern and older amino acids, or may represent a single age fraction. Comparison of the HMWDOM amino acids values from this thesis with those of other locations with different radiocarbon concentrations or productivity levels and from cultures can determine whether there are any unique patterns depending on the amino acid sources, the organisms present or the nutrient levels. For example, the isotopic signatures of the amino acids may be altered during phytoplankton blooms, or in places where DON utilization occurs.

The biocomplexity experiments were just a part of a larger investigation about the impact of different organisms on the carbon and nitrogen cycling in the Chesapeake Bay. In order to do so, the contributions of each type of organism must be identified, as well as how they are affected by outside factors. Other avenues being investigated were the effect of different nitrogen sources (NO_3 versus NH_4), different water depths, and

different ratios of viruses, zooplankton and phytoplankton. This research will be able to identify the response of the organisms under different conditions. Unfortunately, the analysis of the data in chapter 4 was limited due to the lack of DON and virus population numbers, which were unavailable at the time. Does the presence of viruses always stimulate DON release, and is the amount of DON released dependant on the virus population? Is there a relationship between the type of nitrogen available for uptake and the types of compounds released? Do any conditions preferentially favor bloom conditions? From these experiments it is hoped that the role of different types of organisms and environments upon the release of DON and DOC will be better constrained. With a better understanding of the nitrogen and carbon release and export, improved models of nutrient cycling and the effect of different organisms can be developed.

Another possible area of further research is to take the measurement and identification of different compounds one step further by using them as biomarkers. The presence of viruses seems to stimulate the release of DNA and RNA, but the origin of these nucleic acids, whether from phytoplankton or viruses themselves is still unknown. If the DNA and RNA could be determined to be from phytoplankton, then the argument for viral cell lysis, and the amount of carbon and nitrogen released into the nutrient cycle by this process can be determined. Similarly, the impact of grazers may be the result of sloppy feeding or dissolution of DON and DOC from fecal pellets. By identifying the source of the dissolved compounds, the identification of which process was dominant under which conditions could be determined. It would also be interesting to investigate whether any of the dissolved amino acids or nucleic acids are re-used as nitrogen sources,

the conditions under which this uptake occurs, along with identifying which compounds are preferentially used. The bacterial input into the amino acid and nucleic acid pools might also be determined by using enantiomeric ratios and specific DNA or RNA sequence identification.

5.3 References

- Aluwihare, L. I. (1999). High molecular weight (HMW) dissolved organic matter (DOM) in seawater: chemical structure, sources and cycling, MIT/WHOI: 224.
- Aluwihare, L. I. and D. J. Repeta (1999). A comparison of the chemical characteristics of oceanic DOM and extracellular DOM produced by marine algae. Marine Ecology Progress Series **186**: 105-117.
- Aluwihare, L. I., D. J. Repeta and R. F. Chen (1997). A major biopolymeric component to dissolved organic carbon in surface seawater. Nature **387**: 166-169.
- Aluwihare, L. I., D. J. Repeta and R. F. Chen (2002). Chemical composition and cycling of dissolved organic matter in the Mid-Atlantic Bight. Deep-Sea Research II **49**: 4421-4437.
- Amon, R. M. W., H.-P. Fitznar and R. Benner (2001). Linkages among the bioreactivity, chemical composition, and diagenetic state of marine dissolved organic matter. Limnology and Oceanography **46**(2): 287-297.
- Cowie, G. L. and J. I. Hedges (1992). Improved amino acid quantification in environmental samples: charge-matched recovery standards and reduced analysis time. Marine Chemistry **37**: 223-238.
- Dauwe, B., J. J. Middelburg, P. M. J. Herman and C. H. R. Heip (1999). Linking diagenetic alteration of amino acids and bulk organic matter reactivity. Limnology and Oceanography **44**(7): 1809-1814.
- Loh, A. N., J. E. Bauer and E. R. M. Druffel (2004). Variable ageing and storage of dissolved organic components in the open ocean. Nature **430**: 877-881.
- Matsui, K., N. Ishii, M. Honjo and Z. i. Kawabata (2004). Use of SYBR Green I fluorescent dye and a centrifugal filter device for rapid determination of dissolved DNA concentration in fresh water. Aquatic Microbial Ecology **36**: 99-105.
- McCarthy, M., J. Hedges and R. Benner (1996). Major biochemical composition of dissolved high molecular weight organic matter in seawater. Marine Chemistry **55**: 281-297.
- McCarthy, M., T. Pratum, J. Hedges and R. Benner (1997). Chemical composition of dissolved organic nitrogen in the ocean. Nature **390**: 150-154.
- McCarthy, M. D., J. I. Hedges and R. Benner (1998). Major bacterial contribution to marine dissolved organic nitrogen. Science **281**: 231-234.

Yamada, N., S. Suzuki and E. Tanoue (2000). Detection of *Vibrio (Listonella) anguillarum* porin homologue proteins and their source bacteria from coastal seawater. Journal of Oceanography **56**: 583-590.

REPORT DOCUMENTATION PAGE	1. REPORT NO. MIT/WHOI 2005-05	2.	3. Recipient's Accession No.
4. Title and Subtitle Chemical Characterization of Dissolved Organic Matter (DOM) in Seawater: Structure, Cycling, and the Role of Biology			5. Report Date February 2005
7. Author(s) Tracy M. Quan			6.
9. Performing Organization Name and Address MIT/WHOI Joint Program in Oceanography/Applied Ocean Science & Engineering			8. Performing Organization Rept. No.
12. Sponsoring Organization Name and Address National Science Foundation Department of Energy			10. Project/Task/Work Unit No. MIT/WHOI 2005-05
			11. Contract(C) or Grant(G) No. (C) OCE-9818654; (G) DEFG0200ERG62999
15. Supplementary Notes This thesis should be cited as: Tracy M. Quan, 2004. Chemical Characterization of Dissolved Organic Matter (DOM) in Seawater: Structure, Cycling, and the Role of Biology. Ph.D. Thesis. MIT/WHOI, 2005-05.			13. Type of Report & Period Covered Ph.D. Thesis
			14.
16. Abstract (Limit: 200 words) <p>The goal of this thesis is to investigate three different areas relating to the characterization of dissolved organic matter (DOM).</p> <p>The first section used periodate over-oxidation to analyze the previously unidentified fraction of HMWDOM. The majority of the carbon in two HMWDOM samples was over-oxidizable, including 70% of the aliphatic NMR signal, with a high degree of branching. Based on the ¹H NMR spectra data, it was concluded that 6-deoxysugars were the primary compounds in the unidentified fraction of HMWDOM.</p> <p>In the second section, a new method was presented for the purification of individual underivatized amino acids hydrolyzed from HMWDOM, using cation exchange chromatography and high-pressure liquid chromatography (HPLC) with C18 and strong cation exchange (SCX) columns. Six amino acids were isolated from HMWDOM with sufficient purity and quantity for radiocarbon analysis. These amino acids had a range of $\Delta^{14}\text{C}$ values, from 121‰ to -454‰.</p> <p>The final section investigates biological controls on dissolved organic nitrogen (DON). Total hydrolyzable amino acids (THAA), and nucleic acids were measured for four incubations: a control, a grazer added, a zero virus, and a 10 times virus. Comparison to the control showed THAA and nucleic acid release were influenced by viruses but not grazers.</p>			
17. Document Analysis			
a. Descriptors DOM HMWDOM DON			
b. Identifiers/Open-Ended Terms			
c. COSATI Field/Group			
18. Availability Statement Approved for publication; distribution unlimited.		19. Security Class (This Report) UNCLASSIFIED	21. No. of Pages 212
		20. Security Class (This Page)	22. Price